

**Molecular investigation of Keap1-
dependent regulation of the Nrf2 cell
defence pathway**

Thesis submitted in accordance with the requirements of the
University of Liverpool for the degree of Doctor of Philosophy

Holly Katherine Bryan

October 2014

DECLARATION

This thesis is the result of my own work. The material contained within this thesis has not been presented, nor is currently being presented, either wholly or in part for any other degree qualification.

Holly Katherine Bryan

This research was carried out in the Department of Clinical and Molecular
Pharmacology, Institute of Translational Medicine, at the University of
Liverpool

CONTENTS

	PAGE
ABSTRACT	i
ACKNOWLEDGEMENTS	iii
PUBLICATIONS	iv
ABBREVIATIONS	v

CHAPTER 1: GENERAL INTRODUCTION

1.1 INTRODUCTION	- 4 -
1.2 CELL DEFENCE	- 6 -
Figure 1.1. The tiers of cell defence	- 7 -
1.2.1 Tier I of cell defence- basal	- 7 -
1.2.2 Tier II of cell defence- adaptive response	- 8 -
1.2.3 Tier III of cell defence-toxicity and apoptosis	- 9 -
1.3 REDOX REGULATION OF CELL DEFENCE	- 10 -
Figure 1.2. Overview of the states of cysteine oxidation	- 11 -
1.4 THE ANTIOXIDANT RESPONSE PATHWAY	- 12 -
1.4.1 Nuclear Factor Erythroid 2 (NF-E2) -Related Factor 2 (Nrf2)	- 12 -
Figure. 1.3. Structure and Functional domains of Nrf2.	- 14 -
Table 1.1. Functional domains of Nrf2.	- 14 -
Table 1.2 Cell defence proteins encoded by Nrf2-regulated genes.	- 16 -
1.4.2 Glutathione (GSH)	- 17 -
Figure 1.4. Chemical structure of GSH (A) and the recycling of oxidised glutathione (GSSG) to reduced glutathione (GSH) (B).	- 18 -
1.4.3 Detoxification enzymes	- 18 -
Figure 1.5. The recycling of oxidised peroxiredoxin via thioredoxin.	- 19 -
1.4.4 Kelch-like ECH Associated Protein 1 (Keap1)	- 20 -
Table 1.3. The functional domains of Keap1.	- 21 -
1.4.5 The hinge and latch hypothesis	- 22 -
Figure 1.7. Schematic of the hinge and latch hypothesis of Nrf2 regulation	- 24 -
1.5 KEAP1-DEPENDENT REGULATION OF NRF2	- 25 -
1.5.1 Keap1 as a sensor of stress	- 25 -
Figure 1.8. Cysteine residues in Keap1 with low predicted pKa values.	- 26 -
1.5.2 Evidence for chemical modification of Keap1	- 27 -
Table 1.4. Common classes of Nrf2-inducing compounds.	- 29 -
Figure 1.9 Schematic overview of Keap1 cysteine residues and their modification by electrophiles.	- 32 -
1.5.3 Binding partners of Keap1	- 33 -
Figure 1.10. Table showing the conservation of the Keap1 binding ETGE-like domain across a number of known Keap1 binding partners	- 33 -
1.6 KEAP1-INDEPENDENT REGULATION OF NRF2	- 37 -
1.6.1 Phosphorylation of Nrf2	- 37 -
1.6.2 Alternative post-translational modification of Nrf2	- 39 -
1.6.3 MicroRNAs	- 42 -
1.7 NRF2/KEAP1 IN HEALTH AND DISEASE	- 43 -
1.7.1 Nrf2 and cancer	- 43 -
1.7.2 Nrf2 and diseases associated with oxidative stress	- 45 -
1.7.3 Adverse drug reactions and drug-induced liver injury	- 47 -
1.7.4 Potential therapeutic strategies related to Nrf2	- 49 -
1.8 THESIS AIMS	- 52 -

CHAPTER 2: COVALENT AND OXIDATIVE MODIFICATION OF KEAP1 CYSTEINE RESIDUES AS A MECHANISM OF NRF2 ACTIVATION

2.1. INTRODUCTION	- 56 -
Figure 2.1. Schematic diagram of protein cysteine oxidation.	- 58 -

Figure 2.2 Chemical structures of the Nrf2 inducing compounds under investigation in this chapter.....	- 59 -
2.2 MATERIALS AND METHODS	- 60 -
2.2.1 Materials and reagents	- 60 -
2.2.2 Cell culture	- 61 -
2.2.3 Mouse Keap1-V5 plasmid purification	- 62 -
2.2.4 Transfection of cells with Keap1-V5	- 63 -
2.2.5 Cell treatment	- 64 -
2.2.6 Immunopurification of Keap1-V5	- 64 -
2.2.7 Measurement of protein content	- 65 -
2.2.8 Quantification of glutathione levels	- 65 -
2.2.9 Western Immunoblotting- whole cell lysates	- 67 -
2.2.10 Western Immunoblotting- immunopurified Keap1-V5	- 69 -
2.2.11 Preparation of Keap1-V5 for LC-ESI-MS/MS	- 69 -
2.2.12 MALDI-TOF mass spectrometry	- 70 -
2.2.13 LC-ESI-MS/MS methods.....	- 70 -
2.3 RESULTS	- 72 -
2.3.1 Optimisation of Keap1-V5 transfection in HEK293T cells	- 72 -
2.3.2 MALDI validation of Keap1-V5.....	- 72 -
Figure 2.3. Optimisation of Keap1-V5 transfection in HEK293T cells.....	- 73 -
2.3.3 LC-ESI-MS/MS validation of Keap1-V5.....	- 73 -
Figure 2.4. Validation of Keap1-V5 Immunopurification.....	- 74 -
2.3.4 Effect of chosen compounds on Nrf2 and GSH in cells	- 75 -
Figure 2.5. Nrf2 induction and GSH quantification by Nrf2-inducing compounds..	- 75 -
2.3.5 Determining susceptibility of cysteine residues to modification	- 76 -
Figure 2.6. Schematic overview of the experimental protocol.....	- 76 -
2.3.6 Modification of cysteines in Keap1-V5 by DNCB	- 77 -
Figure 2.7. Labelling of Keap1-V5 cysteine residues by NEM and IAA following exposure of HEK293T cells to DNCB.....	- 78 -
2.3.7 Modification of cysteines in Keap1-V5 by Dex-mes.....	- 79 -
Figure 2.8. Labelling of Keap1-V5 cysteine residues by NEM and IAA following exposure of HEK293T cells to Dex Mes.....	- 80 -
2.3.8 Modification of cysteines in Keap1-V5 by H ₂ O ₂	- 81 -
Figure 2.9. Labelling of Keap1-V5 cysteine residues by NEM and IAA following exposure of HEK293T cells to H ₂ O ₂	- 82 -
2.3.9 Modification of cysteines in Keap1-V5 by BSO.....	- 83 -
Figure 2.10. Labelling of Keap1-V5 cysteine residues by NEM and IAA following exposure of HEK293T cells to BSO.....	- 84 -
2.3.10 Modification of cysteines in Keap1-V5 by CDDO-Me	- 85 -
Figure 2.11. Labelling of Keap1-V5 cysteine residues by NEM and IAA following exposure of HEK293T cells to CDDO-Me.....	- 86 -
2.4 DISCUSSION	- 87 -

CHAPTER 3: CHARACTERISING THE COVALENT MODIFICATION OF KEAP1 BY TRITERPENOID, POTENT INDUCERS OF NRF2 SIGNALLING

3.1 INTRODUCTION	- 95 -
Table 3.1 Chemical structure and properties of the semi-synthetic TPs used in this study.	- 98 -
3.2 MATERIALS AND METHODS	- 99 -
3.2.1 Materials and reagents	- 99 -
3.2.2 Cell culture	- 99 -
3.2.3 H4IIE ARE-reporter cell luciferase assay.....	- 100 -
Figure 3.1. Schematic of ARE-reporter luciferase assay.....	- 100 -
3.2.4 Western blotting- whole cell lysates	- 101 -

3.2.5.	Quantification of glutathione levels	- 101 -
3.2.6.	Expression and purification of recombinant proteins	- 102 -
3.2.7.	Determination of on-bead protein content	- 103 -
3.2.8.	Treatment of recombinant protein	- 104 -
3.2.9.	Preparation of recombinant protein for LC-ESI-MS/MS	- 105 -
3.2.10.	LC-ESI-MS-MS methods	- 105 -
3.2.11.	Mouse Keap1-V5 plasmid purification	- 106 -
3.2.12.	Transfection of cells with Keap1-V5	- 106 -
3.2.13.	Cell treatment	- 106 -
3.2.14.	Immunopurification of Keap1-V5	- 106 -
3.2.15.	Preparation of Keap1-V5 for LC-ESI-MS/MS	- 107 -
3.2.16.	<i>In silico</i> modelling	- 107 -
3.2.17.	Data analysis	- 108 -
3.3.	RESULTS	- 109 -
3.3.1.	Effect of chemically tuned TPs on the Nrf2 pathway in cells	- 109 -
	Figure 3.2. Effect of TPs on Nrf2 cell defence pathway in cells.....	- 110 -
3.3.2	LC-ESI-MS/MS validation of recombinant protein	- 111 -
	Table 3.2. Sequence coverage of recombinant His tagged GSTP1 and Keap1 following LC-ESI-MS/MS, as determined by a ProteinPilot search.	- 111 -
3.3.3	LC-ESI-MS/MS evidence for TP modification of GSTP1-His	- 111 -
	Figure 3.3. Schematic of the procedure to identify covalently modified cysteine residues.....	- 112 -
	Figure 3.4. Mass spectrometry spectra showing GSTP1 cysteine-47 modified by (A) CDDO-Me and (B) CDDO-Epoxyde	- 113 -
3.3.4	LC-ESI-MS/MS evidence for TP modification of Keap1-His	- 114 -
	Table 3.3. Recombinant Keap1-V5 cysteines modified by IAA <i>in vitro</i>	- 115 -
	Figure 3.5. Mass spectra showing Keap1 cysteine residues modified by CDDO- Epoxyde..	- 116 -
	Figure 3.6. Concentration-dependent changes in Keap1-His cysteine modification by CDDO-Epoxyde.	- 118 -
3.3.5	Investigating the ability of CDDO-Me to compete with CDDO- Epoxyde to covalently modify protein thiols	- 119 -
	Figure 3.7. Variation in CDDO-Me competing with CDDO-Epoxyde to bind to Keap1.....	- 120 -
	Table 3.4. Total ion count (TIC) of four Keap1 samples treated with CDDO- Epoxyde..	- 121 -
	Figure 3.8. Variation in CDDO-Epoxyde modification of Keap1.....	- 121 -
	Figure 3.9. CDDO-Me competes with CDDO-Epoxyde to bind to GSTP1 Cys-47- 122 -	- 122 -
3.3.6	CDDO-Epoxyde forms covalent adducts with Keap1-V5 in cells-	123 -
	Table 3.5. Keap1-V5 cysteines modified by IAA in cells.....	- 124 -
	Figure 3.10. Mass spectra showing Keap1-V5 cysteine containing peptides modified by CDDO-Epoxyde in cells..	- 125 -
	Table 3.6. Keap1-V5 cysteine residues modified by CDDO-Epoxyde in cells.....	- 126 -
	Figure. 3.11. Correlation between CDDO-Epoxyde modification of recombinant Keap1 and Keap1-V5 expressed in cells..	- 126 -
3.3.7	Molecular modelling of CDDO-Epoxyde modification of Keap1 -	127 -
	Figure 3.12. Molecular modelling of CDDO-Epoxyde bound to Keap1 cysteine residues identified in this study	- 128 -
3.3.8	Correlation of TP potency towards Nqo1 activity and Keap1 covalent binding score	- 129 -
	Figure. 3.13. Correlation between TP <i>in silico</i> covalent binding score and potency as inducers of Nqo1 activity.....	- 130 -

Figure. 3.14. Correlation between TP <i>in silico</i> covalent binding score and potency as inducers of Nqo1 activity.....	- 131 -
3.3.9 Correlation of TP potency towards Nqo1 activity and Keap1 non-covalent binding score	- 132 -
Figure. 3.16. Correlation between TP <i>in silico</i> free binding score and potency as inducers of Nqo1 activity.....	- 134 -
3.4 DISCUSSION	- 135 -

CHAPTER 4: THE IDENTIFICATION OF NOVEL KEAP1 BINDING PARTNERS

4.1 INTRODUCTION	- 143 -
Figure 4.1. Flow diagram of the methods used in this study.....	- 146 -
4.2 MATERIALS AND METHODS	- 147 -
4.2.1 Materials and reagents	- 147 -
4.2.2 Cell culture	- 147 -
4.2.3 Mouse Keap1-V5 plasmid purification	- 148 -
4.2.4 Transfection of cells with Keap1-V5	- 148 -
4.2.5 Immunopurification of Keap1-V5	- 148 -
4.2.6 Preparation of Keap1-V5 for LC-ESI-MS/MS	- 148 -
4.2.7 LC-ESI-MS/MS methods	- 148 -
4.2.8 Western immunoblotting of immunopurified Keap1-V5	- 149 -
4.2.9 Network analysis	- 149 -
4.2.10 Amplification of PCR product from pDONR DNA plasmid	- 149 -
Table 4.1. Steps and cycles for Hot-Start KOD Polymerase amplification of sequence verified cDNA clones	- 150 -
4.2.11 DNA electrophoresis	- 150 -
4.2.12 GAP repair of PCR product	- 151 -
Figure 4.2. Flow diagram of the experimental procedure	- 152 -
4.2.13 Diagnostic yeast colony PCR (YCPCR)	- 153 -
Table 4.2. Steps and cycles for Taq DNA polymerase yeast colony PCR .	- 154 -
4.2.14 Determination of auto-activating clones	- 154 -
Table 4.3. Table describing selective media for determining auto-activation of clones.....	- 155 -
4.2.15 Yeast 2-Hybrid (Y2H) matrix style mating	- 156 -
Figure 4.3. Schematic of the classical Y2H system.....	- 157 -
4.2.16 β-Galactosidase enzymatic assay	- 158 -
Figure 4.4. Flow diagram of the experimental procedure used for determining binary protein interactions.....	- 160 -
4.3 RESULTS	- 161 -
4.3.1 Validation of LC-MS/MS assay	- 161 -
Table 4.4. Proteins chosen for validation of MS data.	- 161 -
Figure 4.5. Western blot validation of Keap1 binding proteins identified by mass spectrometry.....	- 163 -
4.3.2 LC-MS/MS analysis of putative Keap1-V5 binding partners	- 163 -
Figure 4.6. Flow diagram highlighting the number of proteins retained for further analysis of potential Keap1-interacting partners.....	- 164 -
4.3.3 Identification of proteins with Keap1 binding motif	- 165 -
Figure 4.7. Venn diagram	- 166 -
4.3.4 Network and pathway analysis	- 166 -
Table 4.5. Network analysis of putative Keap1 interacting proteins containing ETGE-like Keap1 binding motif.	- 168 -
Figure 4.8. Network 1 identified through Ingenuity network analysis of putative Keap1 interacting partners.....	- 169 -
Figure 4.9. Network 2 identified through Ingenuity network analysis of putative Keap1 interacting partners.....	- 170 -

Figure 4.10. Network 3 identified through Ingenuity network analysis of putative Keap1 interacting partners.....	- 171 -
Table 4.6. Pathway analysis of putative Keap1-interacting proteins containing an ETGE-like Keap1 binding motif.....	- 173 -
4.3.5 Validation of Keap1-interacting partners using Y2H	- 174 -
Table 4.7. Details of clones obtained for Y2H screen against Keap1.....	- 176 -
Table 4.8. Proteins identified as positive binding partners in Y2H screen from two biological repeats.	- 177 -
Figure 4.11. Y2H matrix style mating.	- 178 -
Table 4.9. Function of proteins identified as novel Keap1-binding partners in Y2H screen.....	- 180 -
4.3.6 β-Galactosidase Reporter Assay	- 180 -
Figure 4.12. β -Gal Reporter assay.....	- 181 -
4.3.7 Comparison of Keap1 interactome composition following exposure of cells to selected Nrf2 inducers	- 182 -
Figure 4.13. Venn diagram comparison of proteins co-purified with Keap1-V5 following treatment of cells with Nrf2 inducing electrophiles.....	- 183 -
Table 4.10. Pathway analysis proteins co-purified with Keap1-V5 following treatment of cells with Nrf2 inducers.	- 185 -
Table 4.11. Network analysis of proteins co-purified with Keap1-V5 from cells following DNCB treatment only	- 186 -
Table 4.12. Network analysis of proteins co-purified with Keap1-V5 from cells following dex-mes treatment only.....	- 187 -
Table 4.13. Network analysis of proteins co-purified with Keap1-V5 from cells following CDDO-Me treatment only.....	- 187 -
4.4 DISCUSSION	- 189 -
 <u>CHAPTER 5: CONCLUDING DISCUSSION</u>	
5.1 INTRODUCTION	- 198 -
5.2 SUMMARY OF THE WORK PRESENTED IN THIS THESIS	- 198 -
5.3 FUTURE DIRECTIONS	- 200 -
5.4 CONCLUDING REMARKS	- 203 -
 <u>APPENDIX</u>	-206-
<u>BIBLIOGRAPHY</u>	-220-

ABSTRACT

Mammalian cells have evolved highly regulated defence pathways, which are activated in response to stress. The transcription factor Nrf2 is activated in response to chemical and oxidative stress and induces the expression of antioxidants and detoxification enzymes. Nrf2 activity is regulated by its cysteine-rich repressor protein Keap1, which facilitates Nrf2 degradation. In the presence of electrophilic compounds and/or oxidative stress, Keap1-mediated repression of Nrf2 is hindered, allowing the nuclear localisation of Nrf2 and the up-regulation of cell defence gene expression. The dysregulation of the Nrf2 pathway has been associated with many disease pathologies, and is a promising therapeutic target. Furthering our understanding of the chemico-biological triggers for Nrf2 activation may inform the design of novel Nrf2-inducers with increased efficacy and reduced toxicity. The modification of one or more cysteine residues in Keap1 by electrophiles is believed to be central to Nrf2 activation. Therefore, the aims of the studies in this thesis were to investigate the chemical modification of Keap1 cysteine residues by Nrf2-inducers and identify novel Keap1 binding proteins, which may play a role in the regulation of Nrf2 activity.

Previous work carried out in this lab identified cysteine residues in Keap1 that are covalently modified by a panel of Nrf2-inducing compounds in recombinant Keap1 protein and in cells. Additionally, Nrf2 can be induced by glutathione (GSH) depletion in the absence of Keap1 adduct formation. We hypothesised that GSH depletion permits reactive oxygen species (ROS) to accumulate and oxidise Keap1 cysteine residues, thereby inducing Nrf2. To address this, we treated Keap1-V5 expressing HEK293T cells with Nrf2-inducing compounds. We used liquid chromatography tandem mass spectrometry (LC-MS/MS) to investigate the ability of these compounds to form adducts with Keap1 cysteine residues, or induce reversible/irreversible redox modifications of these residues. We show that compounds which form covalent adducts with Keap1 and deplete GSH (i.e. 2,4-dinitrochlorobenzene) or do not deplete GSH (i.e. dexamethasone 2,1-mesylate) induce modifications of Keap1 that could be representative of oxidation. However compounds which do not form covalent adducts with Keap1 but cause oxidative stress (i.e. hydrogen peroxide), or GSH depletion (i.e. L-buthionine-sulfoximine), do not appear to cause oxidative-like modification of Keap1 cysteines. We therefore show that some Nrf2 inducers promote the formation of reversible and/or irreversible redox modifications of Keap1 which could be due to thiol oxidation, although this is not dependent on GSH depletion.

To further explore the modification of Keap1 cysteine residues by Nrf2 inducers, we investigated the ability of triterpenoids (TPs) to modify Keap1. TPs, in particular methyl 2-cyano-3,12-dioxooleana-1,9(11)dien-28-oate (CDDO-Me), are potent inducers of Nrf2 and are potential therapeutic agents.

However, the mechanism of Nrf2 activation by TPs has not been fully elucidated using LC-MS/MS. We identify key cysteine residues in Keap1 which are adducted by a chemically-tuned TP (CDDO-Epoxyde) in recombinant Keap1 and in cells expressing Keap1-V5. Additionally, we use an *in silico* modelling approach to visualise the binding orientations of CDDO-Epoxyde with key Keap1 cysteine residues. Correlating the potency of a panel of TPs towards the Nrf2 pathway with their *in silico* propensity to bind covalently to the identified residues showed no relationship. However, we show significant positive correlation between the potency of these TPs towards Nrf2 and their *in silico* propensity to bind non-covalently in two cysteine-containing pockets (Cys-273, -288) in Keap1. These data reveal the specific sites of interactions between potent TP Nrf2 inducers and Keap1, and highlight the non-covalent binding of Keap1 by electrophiles as a potential mechanism of Nrf2 activation.

The function of Keap1 is regulated by interactions with binding partners, such as sequestosome1 (p62) which targets it for autophagic degradation, or PGAM5 which localises Keap1 to the mitochondria. We previously used an LC-MS/MS approach to identify p62 as a novel Keap1-binding partner in cells. Therefore, we reasoned that using the same experimental approach with a more sensitive MS system, we could identify additional Keap1-binding proteins. Specifically, we identified a large number of proteins that co-purified with Keap1-V5 from HEK293T cell lysates, of which 55 were found to contain a known Keap1 binding motif, such as the one found in Nrf2, p62 and PGAM5. Network analysis highlighted the potential link between Keap1/Nrf2 and the p53 cell survival pathway. We validated the LC-MS/MS data using a yeast 2-hybrid screen, which reveals HBS1L, RIC8A and PSMD3 as novel Keap1 binding partners, although the functional relevance of the interaction of these proteins with Keap1 requires further investigation.

In summary, the data presented in this thesis demonstrates that whilst the covalent modification of Keap1 cysteines is an important aspect of Nrf2 induction, the oxidation of Keap1 thiols may be an alternative mechanism. We identify key cysteine residues in Keap1 covalently modified by a potent TP Nrf2 inducer in recombinant protein and cells, but show that non-covalent modification of Keap1 may be involved in the process of Nrf2 activation by this class of compound. It will be important in future studies to determine how the modification of Keap1 cysteine residues is translated to the activation of Nrf2. Additionally, we identify putative novel Keap1 binding partners which may serve to regulate the activity of the Nrf2 pathway. Overall, these findings expand our understanding of the chemical and molecular interactions that govern the activity of Nrf2, and will therefore contribute to the ongoing efforts to target this pathway as a novel therapeutic strategy in numerous diseases.

ACKNOWLEDGEMENTS

I must first thank my supervisors- Prof. Kevin Park, Prof. Chris Sanderson, Dr. Neil Kitteringham, and in particular Dr. Chris Goldring for their ideas, continuous guidance and enthusiasm. Thank you also to the BBSRC for funding the work in this thesis.

I would like to extend this thanks to Dr. Ian Copple. I will be eternally grateful for your help. Your unrelenting quest for knowledge is contagious and without your help and motivational pep-talks, I probably would have quit!

Dr. Roz Jenkins, thank you sharing with me your never-ending proteomics knowledge. Your patience with me as I asked silly questions and begged you to run my samples on a Friday afternoon will not be forgotten.

Thanks to those in the lab, in particular Dammy, Luke, Jo, James, Rob, Row and Row (thanks for the hugs!). And Mike Wong for his chemistry skills! Thank you to Chris Sanderson's group, in particular Amy, for your invaluable help with all things yeasty! And thank you to everyone else for your support in science and, more importantly, non-science related activities, particularly Agnès, Áine, Ali, Alix, Fiazia, Hannah, Harriet, Jo, Jon, Junnat, Lister, Liz, Peeney, Pika, Rach and Swale.

Thank you to everyone in London who have supported me from afar (Hannah, Lakshmi and The Streets). Also my UBF, Mel, thank you for always knowing the right thing to say, and sharing one too many sauvignon blancs with me, and for being my comma queen. And thanks Seb- because you thanked me!

Thank you also to my Mum, without whom this thesis would never have been written. You inspire me. Rosie, without you it would have been written quicker but the allure of home, horror films and Haribo were too tempting. Edward, thank you for putting up with science tantrums, driving me to the lab on rainy Sundays, and always reminding me of why I wanted to do this in the first place!

Lastly, this thesis is dedicated to the man who taught me to embrace my inner geek, and the only person who would have read this thesis for fun- even though it would have taken him longer to read than it took me to write. To my Dad, Peter Bryan, Popsicle, the original bean, and one half of the Mahafaja, who I hope would be proud. This is all for you.

PUBLICATIONS

Papers(*Joint first author)

Olayanju, A, Copple, IM, **Bryan, HK**, Edge, GT, Sison, RL, Lai, ZQ, Lin, ZX, Dunn, K, Sanderson, CM, Alghanem, AF, Cross, MJ, Ellis, EC, Ingelman-Sundberg, M, Malik, HZ, Kitteringham, NR, Goldring, CE, Park, BK(2014) Brusatol provokes a rapid and transient inhibition of Nrf2 signalling and sensitizes mammalian cells to chemical toxicity – Implications for therapeutic targeting of Nrf2 (2014). *Free Radic Biol Med*, 79, 202-21

Bryan, H.K.*, Olayanju, A.*, Goldring, C.E., Park, B.K. The Nrf2 cell defence pathway: Keap1-dependent and -independent mechanisms of regulation (2013). *Biochemical Pharmacology*, 85, 705-717

Copple, IM*, **Bryan, HK***, Wong, MHL*, Jenkins, RE, Chia, A JL, Bibby, J, Berry, NG, Kitteringham, NR, Goldring, CE, O'Neill, PM, Park, BK. Chemical Tuning of the Potent Nrf2 Inducer Bardoxolone Methyl Reveals Sites of Interaction with Keap1. (*Manuscript in preparation*)

Bryan, HK, Copple, IM, Chia, AJL, Jenkins, RE, Goldring, CE Kitteringham, NR, Park, BK. Investigating the interplay between covalent and oxidative modification of Keap1 as a mechanism of the regulation of the Nrf2 cell defence pathway. (*Manuscript in preparation*)

Abstracts

Bryan, H. K., Wong, M. H. L., Jenkins, R. E., Copple, I. M., Goldring, C. E., O'Neill, P., Park, B. K. Towards the Chemical Mechanism of Action of CDDO-Me - a Potent Inducer of the Nrf2 Cell Defence Pathway (2014). *pA₂ Online*, E-journal of the BPS

ABBREVIATIONS

α CHCA;	α -cyano-4-hydroxy-cinnamic acid
ABC;	ATP-binding cassette transporter
AD;	activation domain
Ade;	adenine
ADR;	adverse drug reaction
ACN;	acetonitrile
AIR;	P-ribosylamino imidazole
Ala;	alanine
Arg;	arginine
AKR;	aldo-keto reductase
AMP;	adenoside monophosphate
amu;	atomic mass units
AP-1;	activator protein 1
APAP;	Acetaminophen/paracetamol
ARE;	antioxidant response element
ATP;	adenosine triphosphate
ATRA;	<i>all-trans</i> retinoic acid
β -gal;	β -galactosidase
β -Trcp;	β -transducing repeat containing protein
BCA;	bicinchoninic acid
BHA;	butylatedhydroxyanisole
BD;	DNA binding domain
bp;	base pair
BSA;	bovine serum albumin
BSO;	buthionine (S-R)-sulfoximine
BTB;	bric-a-brac/tram-track/broad complex
bZip;	basic leucine zipper
CBP;	CREB-binding protein
CDDO;	cyano 3,13-dioxooleano-1,9-dien-28-oate
CDDO-Me;	methyl-2-cyano 3,13-dioxooleano-1,9-dien-28-oate
cDNA;	complementary DNA
CN;	cyano group
CO ₂ ;	carbon dioxide
COOH;	carboxyl
CRE;	cAMP-responsive element
CREB;	cAMP responsive element binding protein
CUL3;	Cullin 3
CYP450;	cytochrome P450
cys;	cysteine
DEM;	diethyl maleate
dex-mes;	dexamethasone 21-mesylate
DGR;	double glycine repeat
dH ₂ O;	distilled H ₂ O
DILI;	drug-induced liver injury
DMEM;	Dulbecco's modified Eagle's medium
DMSO;	dimethyl sulphoxide
DNA;	deoxyribonucleic acid
DNCB;	2,4-dinitrochlorobenzene

DNP;	dinitrophenol
dNTP;	deoxyribonucleotide triphosphate
15d-PGJ ₂ ;	15-deoxy- $\Delta^{12,14}$ -prostaglandin J ₂
DPP3;	dipeptidyl-peptidase 3
DTNB;	5,5'-dithiobis(2-nitrobenzoic acid)
DTT;	dithiothrietol
ECH;	erythroid cell-derived protein with CNC homology
ECN1;	ectodermal-neural cortex protein
EDTA;	ethylenediaminetetraacetic acid
ERK-1;	extracellular signal-regulated kinase 1
FDA;	Food and Drug Administration
FBS;	fetal bovine serum
GCL;	γ -glutamylcysteine ligase
GCLC;	GCL, catalytic subunit
GCLM;	GCL, regulatory subunit
GPX;	GSH peroxidase
GS;	GSH synthetase
GSH;	glutathione
GSK3 β ;	glycogen synthase kinase 3 β
GSR;	GSH reductase
GSSG;	oxidised GSH
GST;	GSH S-transferase
GSTP1;	GST subunit P1-1
H ₂ O;	water
H ₂ O ₂ ;	hydrogen peroxide
HEK293T;	human embryonic kidney cell line 293T
HEPES;	4-(2-hydroxyethyl)-1-piperazineethanesulfonic acid
HIF-1;	hypoxia-inducible factor 1
His;	histidine
6xHis;	polyhistidine
HO-1;	hemeoxygenase 1
HRP;	horseradish peroxidase
HSF;	heat shock factor
HSP;	heat shock protein
IAA;	iodoacetamide
I κ B;	inhibitor of κ B
IKK;	I κ B kinase
iNOS;	inducible nitric oxide synthase
IP;	immunopirification
IPTG;	isopropyl- β -D-thiogalactopyranoside
IVR;	intervening region
JNK;	c-jun N-terminal kinase
kDa;	kiloDalton
Keap1;	Kelch-like ECH-associated protein 1
LC3;	microtubule-associated protein 1 light chain 3
LC-ESI-MS/MS;	liquid chromatography electrospray ionisation MS/MS
LiOAC;	lithium acetate
Lys;	lysine

MALDI-TOF MS;	matrix-assisted laser desorption ionisation time-of-flight mass spectrometry
MAPK;	mitogen-activated protein kinase
MOPS;	3-(N-morpholino)propanesulfonic acid
MRM;	multiple reaction monitoring
mRNA;	messenger RNA
miR;	micro RNA
MS	mass spectrometry
MS/MS;	tandem mass spectrometry
m/z;	mass-to-charge ratio
NADPH;	nicotinamide adenine dinucleotide phosphate
NaOH;	sodium hydroxide
NAPQI;	N-acetyl- <i>p</i> -benzoquinoneimine
Neh;	Nrf2-ECH homology
NEM;	N-ethylmaleimide
NES;	nuclear export signal
NF-E2;	nuclear factor erythroid 2
NF-κB;	nuclear factor κB
Ni ²⁺ ;	nickel
NO;	nitric oxide
NLS;	nuclear localisation signal
NQO1;	NAD(P)H:quinoneoxidoreductase 1
Nrf2;	Nuclear Factor Erythroid 2-Related Factor 2
OD _{600nm} ;	optical density at 600 nm
OH;	hydroxyl
ORF;	open reading frame
O ₂ ;	molecular oxygen
O ₂ ⁻ ;	superoxide anion radical
PARP;	poly (adenosine diphosphate-ribose) polymerase
PCR;	polymerase chain reaction
PPi;	inorganic phosphate
pKa;	acid dissociation constant
PKC;	protein kinase C
PRX;	peroxiredoxin
Rcf;	relative centrifugal force
RIPA;	radioimmunoprecipitation assay
RNA;	ribonucleic acid
ROS;	reactive oxygen species
rpm;	revolutions per minute
S-;	thiolate
SD;	standard deviation of the mean
SDS;	sodium dodecyl sulphate
SH;	sulphydryl
siRNA;	short interfering RNA
SNO;	S-nitrosothiol
SNO ₂ ;	S-nitrothiol
SNP;	single nucleotide polymorphism
SOD;	superoxide dismutase
S-OH;	sulphenic acid

S-O ₂ H;	sulphinic acid
S-O ₃ H;	sulphonic acid
SRXN1;	sulphiredoxin
S-S;	disulphide
SSA;	sulphopalicylic acid
Std;	standard
Sul;	sulforaphane
TBE;	tris-borate-EDTE buffer
tBHQ;	<i>tert</i> -butylhydroquinone
TIC;	total ion count
TBS;	tris-buffered saline
TFA;	trifluoroacetic acid
TNF α ;	tumour necrosis factor α
TP	triterpenoid
TRX;	thioredoxin
TRX-R;	TRX reductase
Tyr;	tyrosine
U;	unit
UK;	United Kingdom
USA;	United States of America
v/v;	volume/volume
w/v;	weight/volume
X-Gal;	5-bromo-4-chloro-3-indolyl-beta-D-galactopyranoside
XIC;	extracted ion count
Y2H;	yeast two-hybrid
YCPCR;	yeast colony polymerase chain reaction

CHAPTER 1

GENERAL INTRODUCTION

CONTENTS

1.1	INTRODUCTION	- 4 -
1.2	CELL DEFENCE	- 6 -
1.2.1	Tier I of cell defence- basal	- 7 -
1.2.2	Tier II of cell defence- adaptive response	- 8 -
1.2.3	Tier III of cell defence- toxicity and apoptosis.....	- 9 -
1.3	REDOX REGULATION OF CELL DEFENCE	- 10 -
1.4	THE ANTIOXIDANT RESPONSE PATHWAY	- 12 -
1.4.1	Nuclear Factor Erythroid 2 (NF-E2) -Related Factor 2 (Nrf2) ...	- 12 -
1.4.2	Glutathione (GSH)	- 17 -
1.4.3	Detoxification enzymes	- 18 -
1.4.4	Kelch-like ECH Associated Protein 1 (Keap1).....	- 20 -
1.4.5	The hinge and latch hypothesis	- 22 -
1.5	KEAP1-DEPENDENT REGULATION OF NRF2	- 25 -
1.5.1	Keap1 as a sensor of stress	- 25 -
1.5.2	Evidence for chemical modification of Keap1	- 27 -
1.5.3	Binding partners of Keap1	- 33 -
1.6	KEAP1-INDEPENDENT REGULATION OF NRF2	- 37 -
1.6.1	Phosphorylation of Nrf2	- 37 -
1.6.2	Alternative post-translational modification of Nrf2	- 39 -
1.6.3	MicroRNAs	- 42 -

1.7	NRF2/KEAP1 IN HEALTH AND DISEASE	- 43 -
1.7.1	Nrf2 and cancer	- 43 -
1.7.2	Nrf2 and diseases associated with oxidative stress.....	- 45 -
1.7.3	Adverse drug reactions and drug-induced liver injury.....	- 47 -
1.7.4	Potential therapeutic strategies related to Nrf2	- 49 -
1.8	THESIS AIMS	- 52 -

1.1 INTRODUCTION

In order for cells to function efficiently and synergistically, they must be maintained in a homeostatic state. Deviation from this homeostatic state may lead to an increase in the susceptibility of the cells to damage. The loss of homeostatic conditions can be brought about by chemical and/or oxidative stress, which can originate from external sources (i.e. via the ingestion of a pharmacological agent), or internal sources, such as the accumulation of reactive oxygen species (ROS). To adapt to the stress and limit damage, cells have evolved multi-faceted, highly-regulated defence mechanisms to respond to varying levels and types of stress, and initiate defence pathways accordingly. Indeed, numerous pathways are activated simultaneously to confer survival and limit the spread of stress or damage to neighbouring cells and surrounding tissue. If these defence mechanisms become defective, cells can be vulnerable to damage and disease pathologies. These defence pathways are often regulated by transcription factors which activate the transcription of genes involved in cell defence.

The most important defence pathway employed by cells to defend against chemical and oxidative stress is coordinated by the transcription factor Nuclear Factor Erythroid 2-Related Factor 2 (Nrf2) (Park *et al.* 2010, Motohashi and Yamamoto 2004, Lewis *et al.* 2010, Ishii *et al.* 2000). Nrf2 mediates the basal and inducible expression of cytoprotective genes including detoxification enzymes and antioxidants. The up-regulation of this pathway enhances the removal of stressors from the cell, limiting the potential for damage and reducing the risk of toxicity. Nrf2 is ubiquitously

expressed, however, it is more prominent in organs of the body that are exposed to the environment, such as the skin, the gastrointestinal tract, and the liver, the main drug metabolising organ of the body (J. M. Lee *et al.* 2005). The regulation of this pathway has been attributed to Keap1 (Kelch-like ECH-associated Protein 1), a cysteine rich protein which can “sense” the presence of chemical or oxidative stress such as electrophilic activators of Nrf2 (Wakabayashi *et al.* 2004). This pathway is activated by many compounds, including naturally occurring phytochemicals (Jaramillo and Zhang 2013) and reactive metabolites generated by drug metabolism processes, many of which activate Nrf2 via the modification of cysteine residues in Keap1 (Jaramillo and Zhang 2013, Copple *et al.* 2008a).

The Nrf2 pathway is protective against drug-induced toxicities (Copple *et al.* 2008b) and its dysregulation has been linked to a variety of diseases (Hybertson *et al.* 2011, Jaramillo and Zhang 2013, Ramsey *et al.* 2007), thus, Nrf2 is a promising therapeutic target. Increasing our knowledge regarding the mechanism of action of Nrf2 inducers, and furthering our understanding of Keap1 as the point of interaction between a cell’s chemical environment and Nrf2 activation will be important for developing therapeutic agents that target this pathway in a safe and efficacious manner. Therefore, the focus of this thesis is to investigate the mechanisms whereby molecular interactions with Keap1 are capable of regulating the activity of Nrf2, in particular via the modification of its redox-sensing cysteine residues.

1.2 CELL DEFENCE

Cells can respond to stress in numerous ways, from activating survival pathways, to the initiation of cell death. The path taken by the cell often depends on the nature and severity of the stress being encountered. Often, there is interplay between the pathways activated, to ensure cell survival and limit damage. Upon initial exposure to stress, the cell will activate pathways which aim to defend against the stress being encountered, thus encouraging cell survival. However, if the stress is sustained or the initial cell defence mechanisms become overwhelmed, cell death may be initiated. Under conditions whereby cells are exposed to chemical or oxidative stress, such as in the presence of reactive drug metabolites in the liver, a carefully regulated set of protective pathways function synergistically to couple the bioactivation and bioinactivation of compounds which allows a therapeutic effect to occur, whilst limiting exposure and the potential for damage. These cell defence mechanisms can be grouped into three tiers (Figure 1.1). The first is the basal, constitutive expression of detoxification enzymes and antioxidants, and the second is the activation of cytoprotective genes by transcription factors to enhance basal defences. The third tier is the activation of programmed cell death (apoptosis), in an attempt to limit the spread of damage to neighbouring cells.

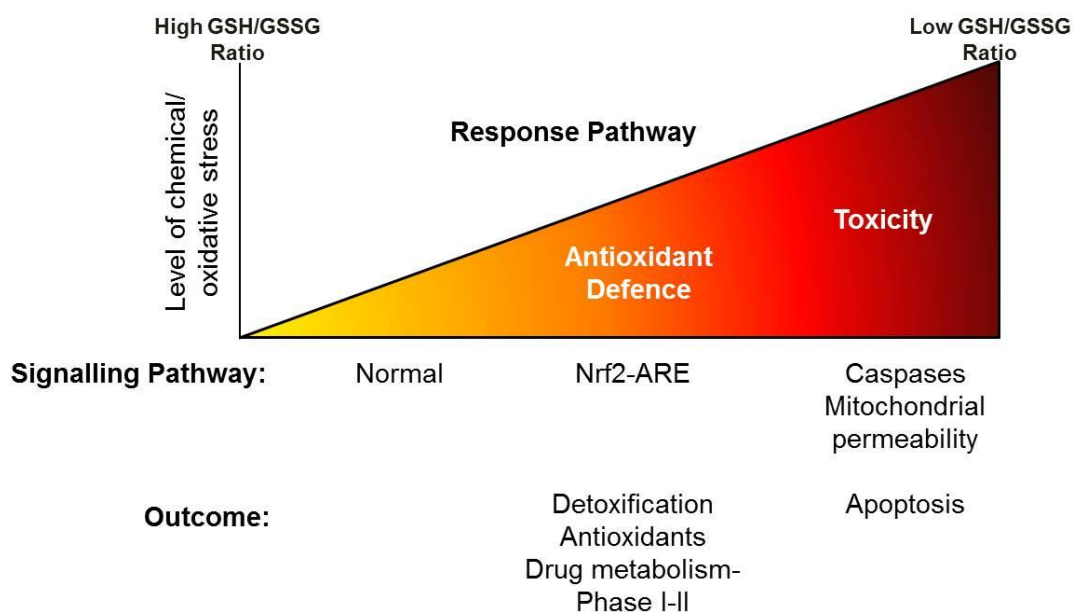


Figure 1.1. The tiers of cell defence. Cell defence consists of 3 main tiers, their activity determined by the level of stress in the cell. Basally, cells express constitutive levels of non-protein antioxidants and detoxification enzymes. The second tier is activated by transcription factors such as Nrf2 to up-regulate the expression of antioxidants and detoxification enzymes. If these defence mechanisms are overwhelmed, toxicity occurs and apoptosis is activated to limit the spread of damage. (Adapted from Nel *et al.* (2006))

1.2.1 Tier I of cell defence- basal

Under basal conditions, there are constitutive levels of non-protein antioxidants and enzymes present in the cell. These are capable of detoxifying a range of reactive species including electrophiles and free radicals, generated via aerobic metabolic transformations (Yu 1994). This tier also includes drug metabolising enzymes which facilitate the bioactivation of xenobiotics. Non-protein antioxidants include α -Tocopherol, ascorbic acid, β -carotene, bilirubin and glutathione (GSH). α -Tocopherol is a

potent antioxidant found in vegetable oils, and is primarily involved in breaking chain reactions involving oxygen and lipid peroxy free radicals, resulting in a relatively stable form of vitamin E (Engin 2009). Thus, it protects against membrane lipid peroxidation (Yu 1994). Ascorbic acid (vitamin C), is a naturally occurring compound which can recycle oxidised vitamin E and scavenge ROS (Yu 1994). β -Carotene, the pre-cursor of retinol (Vitamin A) found in plants and fruits, scavenges ROS and protects lipids against peroxidation (Yu 1994). Additionally, bilirubin, the breakdown product of heme, scavenges peroxy radicals, protecting from lipid peroxidation (Sedlak *et al.* 2009). The most vital non-protein thiol is GSH, discussed in Section 1.4.2.

1.2.2 Tier II of cell defence- adaptive response

The second tier of cell defence involves the up-regulation of cytoprotective pathways via the induction of cell defence genes, such as antioxidants and drug-metabolising enzymes. This up-regulation is facilitated by redox-sensitive transcription factors which recognise and bind to distinct, specific deoxyribonucleic acid (DNA) regions, recruiting co-factors and ribonucleic acid (RNA) polymerase to facilitate the transcription and translation of target genes. One of the key transcription factors involved in the adaptive response to cell defence is Nrf2, which aims to restore cellular redox homeostasis, and is activated by the presence of chemical and oxidative stress in the cell. At higher levels of oxidative stress, the pro-inflammatory signalling pathways take over, facilitated by the activation of the mitogen-activated protein kinase

(MAPK) and the nuclear factor κ B (NF- κ B) pathways (Nel *et al.* 2006). When cells are exposed to low levels of ROS, NF- κ B encourages cell survival, however when higher levels of ROS are encountered, NF- κ B is inhibited, promoting cell death (Trachootham *et al.* 2008). Additionally, the redox sensitive transcription factor activator protein 1 (AP-1) promotes either cell survival or cell death dependent on the tissue type or developmental stage (Trachootham *et al.* 2008). Under conditions of increased temperature and other stresses, heat shock factor protein 1 (HSF1) transcription factors induce the expression of heat-shock proteins (HSP), which act as molecular chaperones to restore protein function or facilitate the degradation of irreparably damaged proteins (Kiang and Tsokos 1998).

1.2.3 Tier III of cell defence-toxicity and apoptosis

Should efforts to detoxify and eliminate a stress be overcome, toxicity ensues and the cell will initiate the apoptotic pathway. This can be considered a “breaking point”, i.e. sufficient damage has accumulated in the cell so much that it will no longer be able to return to a homeostatic state. Apoptosis, or programmed cell death, is a mechanism whereby the cell can prevent the spread of damage to neighbouring cells by facilitating its own death. Oxidative stress-induced apoptosis often stems from damage to the mitochondria, such as the loss of mitochondrial membrane potential, the release of cytochrome c into the cytosol, and the degradation of mitochondrial encoded DNA (Davies 2000). The characteristics of apoptosis include cell shrinkage and membrane blebbing, although the integrity of the membrane is maintained (Elmore 2007). Components of the cell are formed into membrane bound apoptotic bodies which are engulfed by neighbouring

phagocytic cells(Elmore 2007), thus there is no release of cellular contents into the surrounding tissue, and no inflammatory response (Elmore 2007). Apoptosis is characteristically distinct from necrosis as in the latter, cells swell, resulting in a loss of membrane integrity and leaking of cellular contents, inducing an inflammatory response (Elmore 2007). Apoptosis, rather than necrosis, is considered a cell defence mechanism as it is induced to protect the tissue, whilst necrosis is an uncontrollable consequence of cellular damage (Davies 2000). Apoptosis is partly regulated by the cellular redox state, and oxidative stress is central to apoptotic pathways induced by toxicity (Franco *et al.* 2009).

1.3 REDOX REGULATION OF CELL DEFENCE

ROS play an important role in cell survival, and many cell defence mechanisms are redox-sensitive (Trachootham *et al.* 2008). Whilst moderate levels of ROS can encourage cell proliferation and survival, severe ROS accumulation can trigger cell death. Thus, the balance between the generation and elimination of ROS maintains cellular homeostasis and the function of redox sensitive proteins (Trachootham *et al.* 2008). Redox-sensitivity is commonly conferred by the presence of sulphhydryl groups found in cysteine residues. These groups can regulate protein function via reversible or irreversible redox reactions such as the loss of electrons (oxidation), or the gain of electrons (reduction). The possible redox changes of sulphhydryl groups are outlined in Fig 1.2. If a cysteine residue is located adjacent to a basic amino acid (arginine, lysine, histidine), it can be stabilised in a thiolate form ($-S^-$), which is more nucleophilic and reacts more readily with oxidants and nucleophiles than a protonated thiol ($-SH$; a) (Snyder *et al.*

1981). The thiol can undergo oxidation to yield sulphenic acid (-SOH; b), which can be further oxidised to sulphinic acid (-SO₂H; c) and subsequently the terminal oxidation state, sulphonic acid (SO₃H; d)(Paget and Buttner 2003). Primary oxidation can also lead to the formation of disulphide bonds (S-S), either intramolecular (e), intermolecular (f), or with non-protein thiols such as GSH via S-glutathiolation (g) (Paget and Buttner 2003). Furthermore, thiol-disulphide exchange reactions occur between thiols and disulphides (h), and thiols can be modified by reactive nitrogen species (NO) or peroxynitrite (ONOO⁻), yielding S-nitrothiols (-SNO; i /-SNO₂; j) (Cooper *et al.* 2002).

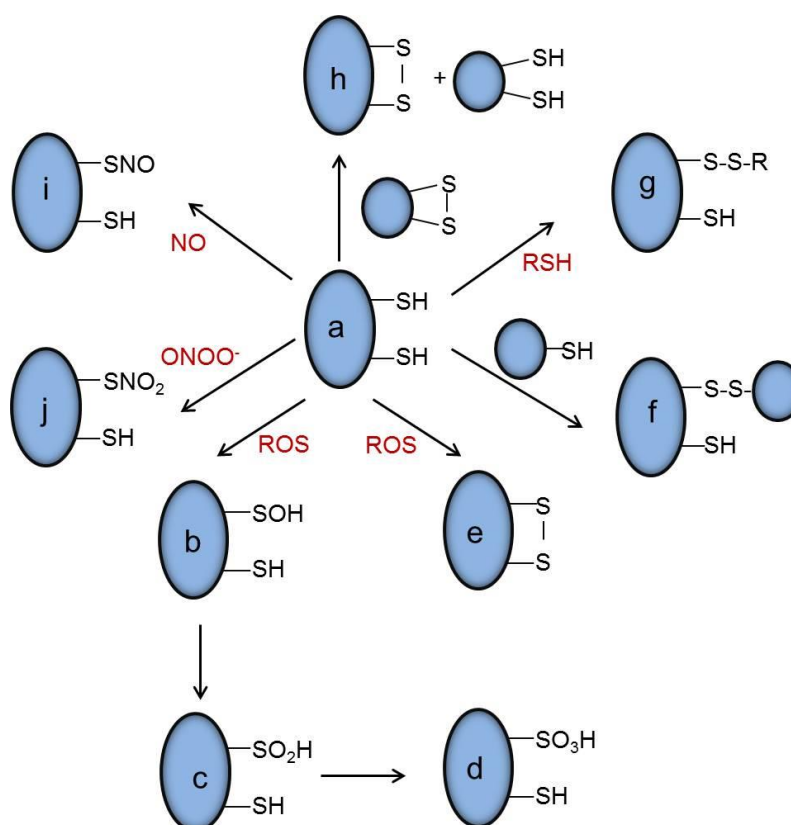


Figure 1.2. Overview of the states of cysteine oxidation. Details of each oxidation state are in the main text. Adapted from Paget and Buttner (2003).

1.4 THE ANTIOXIDANT RESPONSE PATHWAY

Mammalian cells have evolved numerous cell defence pathways in order to maintain cellular homeostasis. One such pathway is termed the antioxidant response pathway. This pathway facilitates the up-regulation of an array of cytoprotective enzymes which enhance the metabolism of electrophilic moieties and oxidants in the cell, thus reducing the presence of stress. This pathway is comprised of three main components, which are; a) the antioxidant response element (ARE), a DNA sequence within the promoter region of cytoprotective genes, b) Nrf2, the transcription protein that binds to the ARE and c) Keap1, the cysteine-rich, redox-sensitive repressor of Nrf2.

1.4.1 Nuclear Factor Erythroid 2 (NF-E2) -Related Factor 2 (Nrf2)

Nrf2 was first isolated in a screen of a hemin-induced complimentary DNA (cDNA) library for proteins which could bind to the AP1-nuclear factor erythroid 2 (NF-E2) repeat promoter sequence (Moi *et al.* 1994). It is a cap'n'collar bZip transcription factor primarily responsible for the adaptive response to chemical and oxidative stress by up-regulating the expression of ARE-containing genes which are involved in drug metabolism, the oxidative stress response and cytoprotection (Miao *et al.* 2005). Nrf2 is ubiquitously expressed, both in humans and mice, and is highly expressed in organs which are involved in detoxification (the liver and kidneys), and those exposed to the external environment (the skin, gastrointestinal tract, and lungs) (Motohashi *et al.* 2002, Moi *et al.* 1994).

Nrf2 was shown to up-regulate the expression of target genes by binding to the ARE (Venugopal and Jaiswal 1996, Nguyen *et al.* 2000), a *cis*-acting DNA enhancer motif, as identified in with a consensus sequence as follows:

5'-gagTcACa**GTgAGtCggC**Aaaatt-3'

(Essential nucleotides in capitals and the core in bold) (Nioi *et al.* 2003).

Nrf2 binds to this consensus sequence with high affinity only when in a homodimer with small Maf proteins (MafF, MafK, MafG) (Itoh *et al.* 1997). Maf proteins interact with other bZip proteins, however lack transactivation domains, therefore are reliant on Nrf2 to promote transcription (Kataoka *et al.* 1993, Motohashi *et al.* 2002). The comparison of the human Nrf2 amino acid sequence with that of the chicken Nrf2 sequence revealed six highly-conserved regions, the Nrf2-ECH (erythroid-derived CNC homology protein) homology (Neh) domains, which are important for Nrf2 function (Itoh *et al.* 1999) (Fig 1.3, Table 1.1). The binding of Nrf2 to the ARE is reliant on a conserved cysteine residue (Cys-506) within the Neh1 domain (Bloom *et al.* 2002). Co-activator proteins, such as cAMP responsive element binding protein (CREB)-binding protein (CBP) are recruited to enhance transcriptional activity (Kalkhoven 2004, Katoh *et al.* 2001).

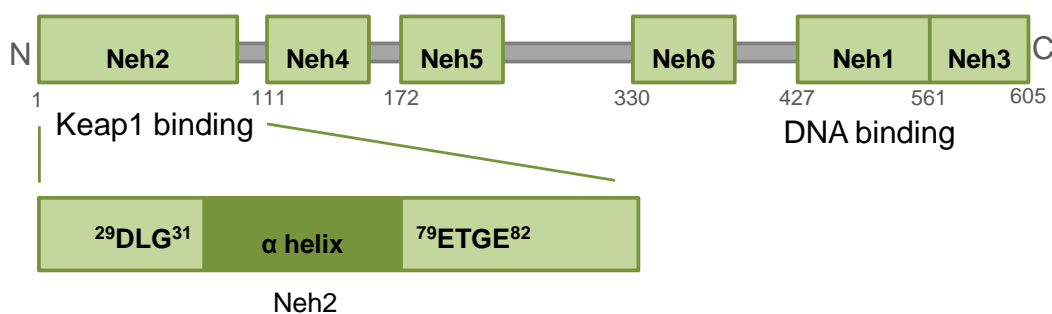


Figure. 1.3. Structure and Functional domains of Nrf2. Schematic overview of the six Neh domains of Nrf2. See table 1.1 for the functions of each domain. The names of the domains are shown in the green boxes, with the amino acid residue at the beginning of each domain shown below.

Domain	Residues	Function	Reference(s)
Neh2	1-96	Facilitates interaction with Keap1 via DLG/ETGE motif. Point of lysine ubiquitination Point of serine phosphorylation by PKC	Itoh <i>et al.</i> (1999) Katoh <i>et al.</i> (2005) McMahon <i>et al.</i> (2006) McMahon <i>et al.</i> (2004) Tong <i>et al.</i> (2006) (Numazawa <i>et al.</i> 2003)
Neh4	111-141	Transactivation domain Interaction with CBP Point of phosphorylation by CK2 <i>in vitro</i>	Katoh <i>et al.</i> (2001) Apopa <i>et al.</i> (2008)
Neh5	172-201	As Neh4 Contains nuclear export signal Interacts with caveolin-1	Katoh <i>et al.</i> (2001) Li <i>et al.</i> (2006) Zhang <i>et al.</i> (2007) (W. Li <i>et al.</i> 2012)
Neh6	330-380	Facilitates Nrf2 regulation under stress conditions Facilitates interaction with β -TrCp	McMahon <i>et al.</i> (2004) Chowdhry <i>et al.</i> (2013)
Neh1	427-560	Facilitates binding to ARE and small Maf proteins Contains nuclear localisation/export signals Point of acetylation by p300/CBP	Bloom <i>et al.</i> (2002) Itoh <i>et al.</i> (1999) Sun <i>et al.</i> (2009)
Neh3	561-597	Transactivation Interaction with other co-activator proteins	Nioi <i>et al.</i> (2005)

Table 1.1. Functional domains of Nrf2.

The genes regulated by Nrf2 can be categorised as; drug-metabolizing enzymes; antioxidants; molecular chaperones; DNA repair enzymes; and anti-inflammatory proteins (Table 1.2) (Hayes and McLellan 1999, Nguyen *et al.* 2003b). Their co-ordinated up-regulation by Nrf2 enhances removal of the insult, thereby restoring the cell to a basal state and conferring resistance to stress. This prevents damage to cellular components which are sensitive to changes in the redox state of the cell, such as proteins, lipids and DNA, which, if damaged, can promote cell death.

Nrf2 has been linked to a diverse array of cellular mechanisms including, but not limited to differentiation, proliferation, apoptosis (Y. Li *et al.* 2012) and lipid metabolism in the liver (Kitteringham *et al.* 2010). As expected, Nrf2 knockout (*Nrf2*^{-/-}) animals show reduced basal and/or inducible expression of detoxification and antioxidant genes across tissues (liver, lung, skin) (Ramos-Gomez *et al.* 2001, Rangasamy *et al.* 2005, Xu *et al.* 2006, Walsh *et al.* 2014). This has knock-on effects, in that the animals are more susceptible to toxicity by xenobiotics and environmental stresses (Copples *et al.* 2008b). The *Nrf2*^{-/-} animals exhibit no characteristic phenotype, in that they exhibit no growth or developmental issues (Chan *et al.* 1996). However, these mice do develop vacuolar leukoencephalopathy characterised by myelin degeneration and the presence of cavities in the brain (Hubbs *et al.* 2007). Moreover, these animals develop lupus-like symptoms including nephritis (inflammation of the kidney) (Yoh *et al.* 2001). Ultimately this indicates that whilst Nrf2 is not essential for the growth and development of mice, it is vital for survival following insult.

Protein	Function	Reference(s)
ATP-binding cassette transporters (ABC)	Drug transporters	Malhotra <i>et al.</i> (2010) Hirotsu <i>et al.</i> (2012) Maher <i>et al.</i> (2007)
Aldo-keto reductases (AKR)	Reduces aldehydes and ketones to primary and secondary alcohols	Lou <i>et al.</i> (2006) Nishinaka and Yabe-Nishimura (2005)
Cytochrome p450 enzymes (CYP)	Phase I drug metabolism	Malhotra <i>et al.</i> (2010) Yates <i>et al.</i> (2009)
Glutamate cysteine ligase, catalytic subunit (GCLC)	Catalyses the conjugation of cysteine with L-glutamate yielding γ -glutamylcysteine (γ -GC)	Chan and Kwong (2000) Jeyapaul and Jaiswal (2000)
Glutamate cysteine ligase, modifier subunit (GCLM)	Increases kinetic efficiency of GCLC-mediated reaction	Chan and Kwong (2000) Moinova and Mulcahy (1999)
Glutathione peroxidases (GPX)	Catalyse reduction of peroxides (e.g. H_2O_2), uses GSH as a substrate	Banning <i>et al.</i> (2005), Singh <i>et al.</i> (2006)
Glutathione Reductase (GSR)	Catalyses reduction of oxidised glutathione (GSSG) to GSH	Thimmulappa <i>et al.</i> (2002)
Glutathione Synthetase (GS)	Catalyses conjugation of glycine with γ -GC to give GSH	T. D. Lee <i>et al.</i> (2005)
Glutathione-S-transferase (GST)	Catalyses conjugation of GSH to electrophiles	Chanas <i>et al.</i> (2002) Hayes <i>et al.</i> (2000), McMahon <i>et al.</i> (2001)
Heme-oxygenase 1 (HO-1)	Catabolises heme degradation	Alam <i>et al.</i> (1999) Ishii <i>et al.</i> (2000)
NAD(P)H:quinone oxidoreductases (NQO)	Catalyses reduction and detoxification of quinones	Venugopal and Jaiswal (1996) Wang and Jaiswal (2006)
Peroxiredoxin 1 (PRX1)	Reduces peroxides	Y. J. Kim <i>et al.</i> (2007)
Superoxide Dismutase (SOD)	Converts superoxide radicals into H_2O_2 and oxygen (O_2)	Park and Rho (2002)
Sulfiredoxin (SRXN1)	Catalyses reduction of PRX	Abbas <i>et al.</i> (2011), Jeong <i>et al.</i> (2012)
Thioredoxins (TRX)	Catalyses reduction of disulphides to sulphydryl groups	Kim <i>et al.</i> (2001) Kim <i>et al.</i> (2003)

Table 1.2 Cell defence proteins encoded by Nrf2-regulated genes.

1.4.2 Glutathione (GSH)

Upon activation of Nrf2, the synthesis of the abundant non-protein antioxidant GSH is up-regulated. GSH is a tripeptide comprised of glycine, cysteine and glutamic acid expressed in virtually all mammalian cells (Yu 1994), with roles in many aspects of homeostasis (Pompella *et al.* 2003). GSH can act as both a nucleophile and a reductant, and can detoxify oxidising agents and electrophiles via its reactive thiol group (Pompella *et al.* 2003). GSH is synthesised in two ATP dependent steps; 1) the rate limiting conjugation of cysteine with L-glutamate via γ -glutamate cysteine ligase (GLC) resulting in γ -glutamylcysteine and; 2) the addition of glycine to the C-terminal of γ -glutamylcysteine via glutathione synthetase (GS) yielding γ -glutamylcysteinylglycine (GSH) (Fig. 1.4A) (Kaplowitz *et al.* 1985).

During GSH-mediated detoxification of peroxides, reduced GSH donates a reducing equivalent via glutathione peroxidase forming the oxidised form GSSG, a glutathione disulphide. This is recycled back to GSH in a nicotinamide adenine dinucleotide phosphate (NADPH)-dependent manner via glutathione reductase (Fig 1.4B). In a healthy cell, the ratio of GSH:GSSG is upwards of 9:1, with an increase in GSSG:GSH ratio indicative of oxidative stress (DeLeve and Kaplowitz 1991). If GSSG accumulates, it can be actively transported out of the cell to protect from a shift in the redox equilibrium (DeLeve and Kaplowitz 1991). The ability of GSH to conjugate with electrophiles is facilitated by its nucleophilic cysteine residue and can occur spontaneously or enzymatically, forming thioether conjugates (DeLeve and Kaplowitz 1991). The GSH conjugates are cleaved to remove the γ -glutamyl,

and dissociate the cysteinyl-glycine conjugate leaving a simple cysteinyl conjugate which is acetylated to form mercapturic acid (DeLeve and Kaplowitz 1991). The breakdown products are normally excreted or recycled.

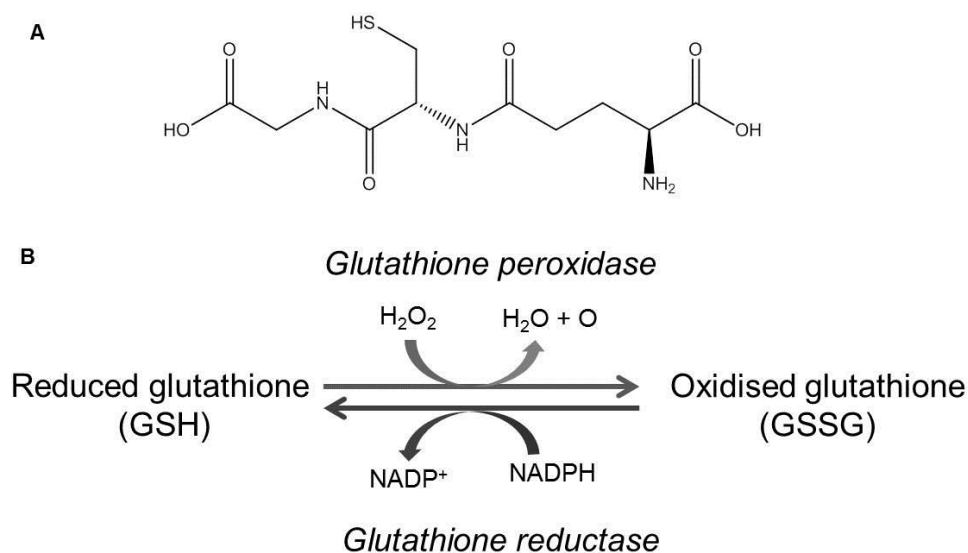


Figure 1.4. Chemical structure of GSH (A) and the recycling of oxidised glutathione (GSSG) to reduced glutathione (GSH) (B).

1.4.3 Detoxification enzymes

Other mechanisms of detoxification activated by Nrf2 include those facilitated by enzymatic reactions. The superoxide dismutase (SOD) family catalyse the dismutation of two superoxide anion radicals (O_2^-) to H_2O_2 and O_2 (Nordberg and Arner 2001). H_2O_2 can be further reduced to H_2O and O_2 by catalase, glutathione peroxidases (GRX) or peroxiredoxins (PRX) (Nordberg and Arner 2001). Catalase is a heme-containing enzyme which catalyses the conversion of H_2O_2 to H_2O and molecular oxygen, as well as detoxifying phenols and alcohols (Nordberg and Arner 2001). Peroxiredoxins (PRX) are

involved in the reduction of peroxides via a conserved cysteine residue (the peroxidatic cysteine), which can be oxidised to a sulphenic acid (Wood *et al.* 2003). Typical PRXs form homodimers and the resolving cysteine in one PRX facilitates the recycling of the peroxidatic cysteine in another, forming a stable intermolecular disulphide bond (Wood *et al.* 2003). The atypical PRXs contain both cysteine residues in one peptide forming an intra-molecular disulphide bond upon reduction (Wood *et al.* 2003). These dipeptides can be reduced by thioredoxins (TRX) to re-establish PRX function (Wood *et al.* 2003). In turn, the oxidised TRX is reduced by TRX reductase (TRXR) at the expense of NADPH (Collet and Messens 2010) (Fig 1.5).

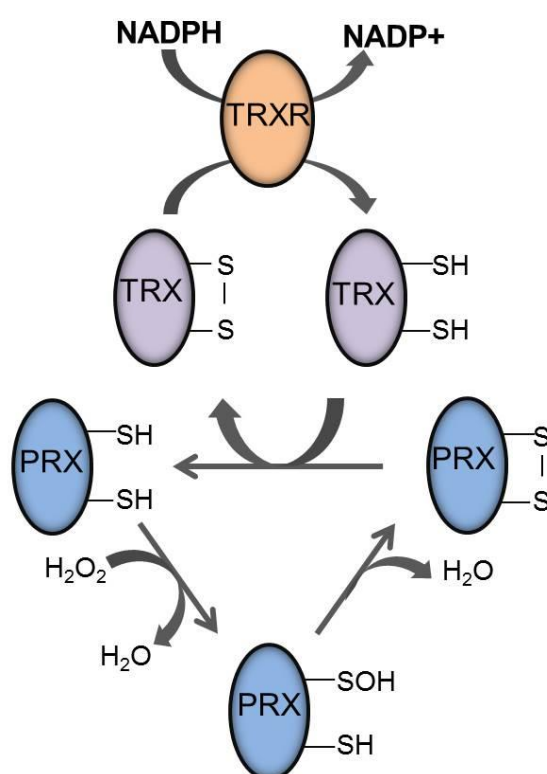


Figure 1.5. The recycling of oxidised peroxiredoxin via thioredoxin. Peroxiredoxin (PRX) is oxidised by hydrogen peroxide (H_2O_2) to a sulphenic acid intermediate. Further oxidation results in disulphide bond formation which can be reduced by thioredoxin (TRX) to re-establish PRX function. TRX is reduced by thioredoxin reductase (TRXR) at the expense of NADPH.

1.4.4 Kelch-like ECH Associated Protein 1 (Keap1)

The activation of Nrf2 must be tightly regulated to prevent its constitutive activation, and this is facilitated by its repressor protein Keap1. Initial observations showed that in the absence of cellular stress, Nrf2 is sequestered in the cytosol by an inhibitor protein which it binds via the Neh2 domain (Itoh *et al.* 1999). Keap1 was identified as this inhibitor following the observation that the deletion of the Neh2 domain of Nrf2 results in a significant increase in basal Nrf2 activity in erythroblasts (Itoh *et al.* 1999). Keap1 is regarded as the regulator of Nrf2 as when transfected into cells, recombinant Nrf2 accumulates in the nucleus however, when co-transfected with Keap1 the two co-localise in the cytoplasm (Itoh *et al.* 1999). In the presence of electrophiles such as diethyl maleate, this co-localisation is lost and Nrf2 localises in the nucleus (Itoh *et al.* 1999). Additionally, the over-expression of Keap1 in cells reduces the activation of ARE-regulated genes (Dhakshinamoorthy and Jaiswal 2001, Itoh *et al.* 1999), whilst siRNA mediated knockdown of Keap1 results in increased Nrf2 levels in the cell (Williamson *et al.* 2012). Keap1 was named due to sequence similarities to the *Drosophila* cytoskeleton-binding protein Kelch (Xue *et al.* 1993) (Figure 1.6, Table 1.3). Keap1 is primarily located in the cytosol of the cell and interacts with the actin cytoskeleton and the mitochondria (Kang *et al.* 2004, Lo and Hannink 2008). Two Keap1 molecules are responsible for binding and sequestering one Nrf2 molecule (Tong *et al.* 2006). A more detailed explanation of how Keap1 regulates Nrf2 localisation and activity is provided in Section 1.5.

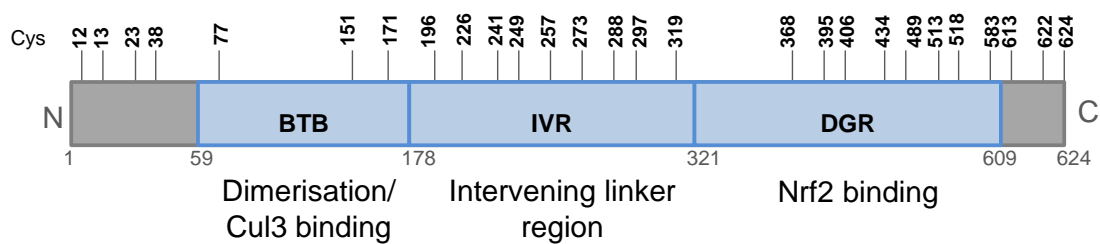


Figure 1.6. The functional domains of Keap1. Schematic of the three main functional domains of Keap1. BTB- bric-a-brac/tram-track/broad complex; IVR- intervening linker region; DGR- double glycine repeats. The positions of the cysteine residues in human Keap1 are indicated. See table 1.3 for details of the functions of each domain

Domain	Residues	Function	Reference(s)
BTB	59-178	Facilitates homodimerisation and interaction with Cul3 / ubiquitination machinery	Zipper and Mulcahy (2002)
IVR	178-321	Contains many reactive cysteine residues	Bryan <i>et al.</i> (2013)
DGR	321-609	Kelch repeats Facilitates interaction with Nrf2 and other binding partners such as actin cytoskeleton	Dhakshinamoorthy and Jaiswal (2001) Itoh <i>et al.</i> (1999) McMahon <i>et al.</i> (2006) Kang <i>et al.</i> (2004)

Table 1.3. The functional domains of Keap1.

Keap1-deficient mice (*Keap1*^{-/-}) do not survive longer than 3 weeks post natively, and suffer from severe malnutrition due to hyperkeratosis of the digestive system, leading to ulcers in the oesophagus and stomach (Wakabayashi *et al.* 2003). This phenotype is rescued by synchronous knockout of Nrf2 and Keap1 (*Keap1*^{-/-}::*Nrf2*^{-/-}) indicating that this phenotype is due to Nrf2 accumulation, and that Nrf2 is likely to be the only down-stream

effector of Keap1 (Wakabayashi *et al.* 2003). This made studying the role of Keap1 in the *in vivo* regulation of Nrf2 difficult, until the development of a hepatocyte-specific Keap1 knockout using a Cre-LoxP system (Okawa *et al.* 2006). These mice show resistance to APAP doses which would be toxic to WT mice. Ultimately, this indicates that Keap1 is the main regulator of Nrf2.

1.4.5 The hinge and latch hypothesis

In the absence of cellular stress, the half-life of Nrf2 protein is approximately 10-30 minutes (Itoh *et al.* 2003, Alam *et al.* 2003). This observation cannot be explained purely by the ability of Keap1 to tether Nrf2 in the cytosol. The inhibition of the proteasome results in the accumulation of Nrf2 protein in the cell, in particular in the nucleus, and an increase in the activation of ARE-dependent gene expression (Sekhar *et al.* 2000, McMahon *et al.* 2003, Yamamoto *et al.* 2007). Under these conditions, ubiquitinated Nrf2 has been detected, suggesting that Keap1 is not simply a cytosolic anchor, but it also directs the poly-ubiquitination of Nrf2, leading to its proteasomal degradation (Cullinan *et al.* 2004, McMahon *et al.* 2003). This ubiquitination is facilitated by a Cullin-dependent E3 ubiquitin ligase complex which interacts directly with Keap1 and is crucial for Nrf2 proteasomal degradation (Kobayashi *et al.* 2004, Cullinan *et al.* 2004). The mutation of seven lysine residues within the Neh2 domain of Nrf2 inhibits the Keap1-mediated ubiquitination of Nrf2, thus preventing its proteasomal degradation and increasing its half-life (Zhang *et al.* 2004). Nrf2 must be appropriately positioned in order for the Keap1/Cul3 complex to ubiquitinate the lysine residues, and this has led to the development of the “hinge and latch” hypothesis of Nrf2 regulation by Keap1.

In the absence of cellular stress, Nrf2 is sequestered in the cytosol, with a Keap1 homodimer acting as a substrate adaptor for the ubiquitination of Nrf2, in a Cul3 dependent manner (Kobayashi *et al.* 2004). Nrf2 binds to the DGR site of each Keap1 subunit in the homodimer via two motifs within the Neh2 domain, one high affinity, ⁷⁹ETGE⁸², and one low affinity, ²⁹DLG³¹ (Tong *et al.* 2006). The “hinge and latch” hypothesis proposes that the ETGE binding site acts as a hinge, permitting Nrf2 to bind to Keap1 but able to move freely. On the other hand, the DLG site acts as a latch hindering the movement of Nrf2. When bound via both binding sites, target lysine residues within the Neh2 region of Nrf2 are positioned to undergo poly-ubiquitination via the Cul3 E3 ligase, and Nrf2 is consequently degraded by the 26S proteasome (Fig 1.7A).

Under conditions of chemical or oxidative stress, a conformational change in Keap1 renders it unable to bind to Nrf2 via the DLG site, disrupting the transfer of ubiquitin molecules to Nrf2. As Nrf2 is no longer degraded, Keap1 molecules become saturated with Nrf2 and newly synthesised Nrf2 accumulates in the cytosol. This free Nrf2 is able to translocate to the nucleus and bind the ARE (Fig 1.7B). In this situation, the half-life of Nrf2 increases, however the time varies between cell types due to differences in detectable basal levels of the Nrf2 (Kwak *et al.* 2001b, Nguyen *et al.* 2003a, Kwak *et al.* 2002). There is conflicting evidence on whether Nrf2 becomes free in the cell in the presence of stress, with evidence supporting the full or partial dissociation of the Keap1-Nrf2 complex (Levonen *et al.* 2004, Niture *et*

al. 2009) or the dissociation of Cul3 and Keap1 (Egler *et al.* 2009, Gao *et al.* 2007, Rachakonda *et al.* 2008), thus impeding the ubiquitination of Nrf2.

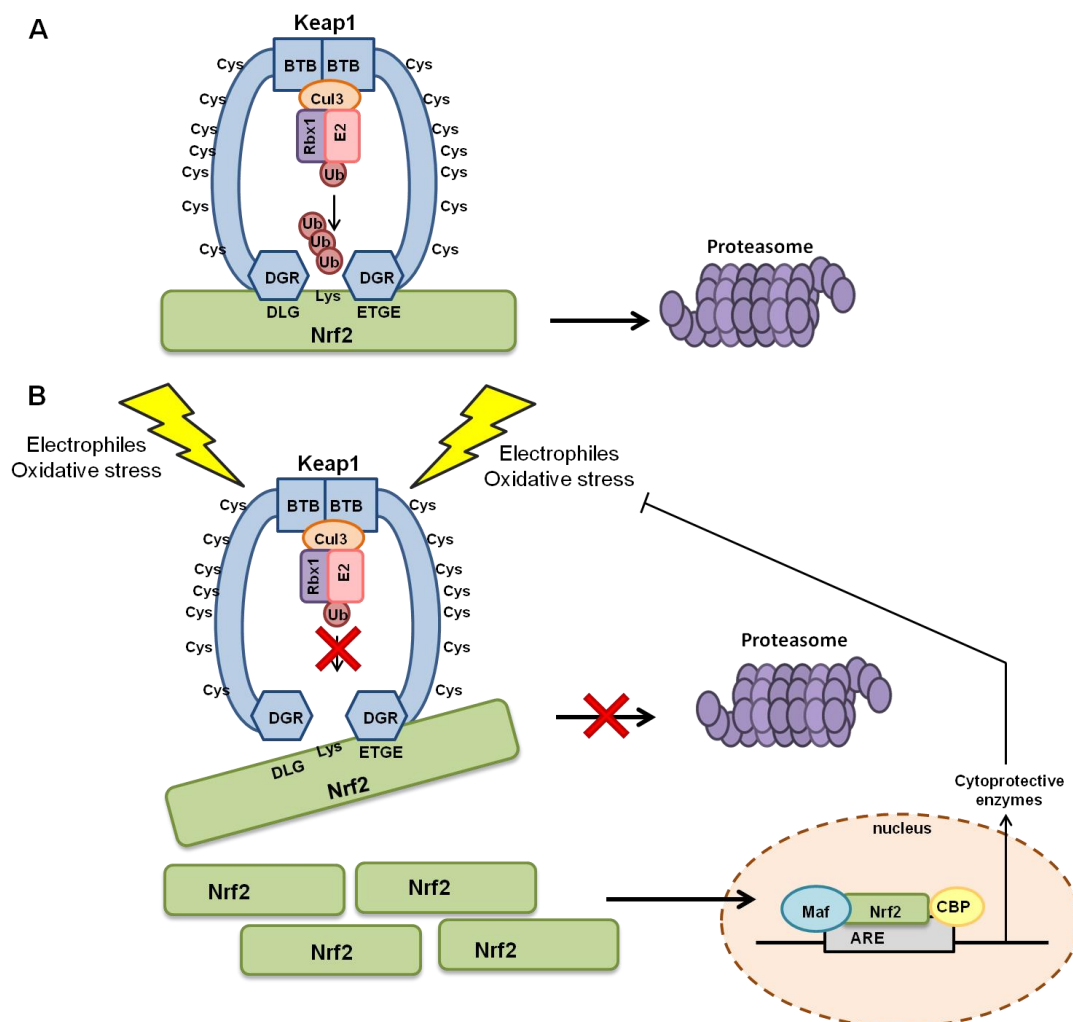


Figure 1.7. Schematic of the hinge and latch hypothesis of Nrf2 regulation. (A) Under basal conditions, a Keap1 homodimer binds a single Nrf2 molecule via two motifs- ETGE and DLG. This positions Nrf2 for lysine ubiquitination, targeting it for proteasomal degradation. (B) Under conditions of chemical or oxidative stress, binding via the low affinity DLG 'latch' is hindered due to a conformational change in Keap1, likely due to modification of one or more of Keap1's cysteine residues. The ETGE domain remains bound to Keap1 acting as the "hinge". Nrf2 is no longer located ideally for ubiquitination and Keap1 becomes saturated with Nrf2 molecules. Newly synthesised Nrf2 is free to accumulate in the cytosol and nucleus and thus activate the transcription of cytoprotective genes. Adapted from Bryan *et al.* (2013), based on work by Tong *et al.* (2006), McMahon *et al.* (2006).

1.5 KEAP1-DEPENDENT REGULATION OF NRF2

1.5.1 Keap1 as a sensor of stress

Keap1 is a cysteine rich protein with 4.3% of all its residues being cysteines (27 of 624 residues in human Keap1), approximately double the number of cysteine residues in the average protein (Miseta and Csutora 2000). Cysteine residues are commonly located within the functional domains of proteins and their thiol side chains (-SH) are nucleophilic and redox-sensitive, thus responsive to the local environment (Fig 1.5) (Marino and Gladyshev 2012). It is these reactive cysteine residues that are purported to afford Keap1 the ability to sense electrophilic or oxidative stress (Holland and Fishbein 2010). A number of Keap1 cysteine residues are considered to be highly reactive as they are flanked by basic amino acids, lowering the predicted pK_a value of the residue, thus increasing its reactivity with electrophiles (Fig. 1.8)(Snyder *et al.* 1981). Both Cys-273 and -297 are immediately preceded and followed by basic residues, whilst Cys-151, -257, -434 and -613 have two or more basic residues in their proximity, in the primary structure of the protein. Thus, these residues are predicted to be highly reactive towards electrophiles. A vast number of Nrf2-inducing compounds are electrophilic and capable of reacting with cysteine thiol groups, forming direct covalent adducts. The ability of Nrf2-inducing compounds to form adducts with cysteine residues in Keap1 is considered to be the underlying mechanism of Nrf2-induction by electrophiles, and there is a considerable amount of literature supporting this (Chia *et al.* 2010, Copple *et al.* 2008a, Yamamoto *et al.* 2008, Dinkova-Kostova *et al.* 2002). Other Nrf2-inducing compounds are oxidants which can

cause the addition of molecular oxygen to the SH group of cysteines. However, there is no concrete evidence demonstrating that Keap1 cysteine residues are sensitive to oxidation *in vivo*. Even so, Keap1 is considered a sensor of both chemical and oxidative stress within the cell, and it is postulated that the modification of specific cysteine residues disrupts the ability of Keap1 to repress Nrf2 (Eggler *et al.* 2005).

```

1  MQPEPKLSGA  PRSSQFLPLW  SK23PEGAGDA  VMYASTE38CKA  EVTPSQDGNR  TFSYTLLEDHT

61  KQAFGVMNEL  RLSQQL77CDVT  LQVKYEDIPA  AQFMAHKVVL  ASSSPVFKAM  FTNGLREQGM

121  EVSIEGIHP  KVMERLIEFA  YTASISVGE151K  171C151VLHVMNGAV  MYQIDSV171RA  171C171SDFLVQQLD

181  PSNAIGIANF  AEQIG196CTELH  QRAREYIMH  FGEVAKQEEF  FNLS226HCQLAT  LISRDDLN226VR

241  241C241ESEVFH249AC249I  DWVK257YDC257PC257QR  RFYVQALL273RA  273VR273CH273ALTPRF  LQTQLQ288K288CEI  LQADAR297C297K297LDY

301  LVQIFQELTL  HKPTQAVP319CR  APKVGRLIYT  AGGYFRQSLS  YLEAYNPSNG  SWLRLADLQV

361  PRSGLAG368CVV  GLLLYAVGGR  NNSPDGNTDS  SALD395CYNPMT  NQWSP406CASMS  VPRNRIGVGV

421  IDGHYAVGG  SH434GC434IHH434SSV  ERYEPERDEW  HLVPMLTRR  IGVGVAVLNR  LLYAVGGFDG

481  TNRLNSAE489CY  YPERNEWRFMI  TPMNTIRSGA  GVC513V513L513H518NC518IY  AAGGYDGQDQ  LNSVERYDVE

541  TETWTFVAPM  RHRSALGIT  VHQGKIYVLG  GYDGHTFLDS  VEC583YDPDSDT  WSEVTRMTSG

601  RSGVGVAVTM  EPC613CR613K613QIDQQ  N622C622T624C624

```

Figure 1.8. Cysteine residues in mouse Keap1 with low predicted pKa values. Full length sequence of Keap1 with cysteine residues highlighted in pink and labelled with their residue number. Basic amino acids (arginine (R), lysine (K), histidine (H)) flanking cysteine residues are highlighted in blue.

1.5.2 Evidence for chemical modification of Keap1

The first proposal that Keap1 cysteine modification may play a role in Nrf2 regulation was made by Dinkova-Kostova *et al.* (2002), who showed that a number of structurally dissimilar Nrf2 inducers were all reactive with Keap1 cysteine residues at rates that correlated with their potency towards Nrf2. These Nrf2 inducers were capable of dissociating Keap1 from the Neh2 region of Nrf2 *in vitro* (Dinkova-Kostova *et al.* 2002), implying that the thiol sensing mechanism is afforded by Keap1, as the Nrf2 Neh2 region contains no cysteine residues. Cysteine residues that lie in the IVR domain of Keap1; Cys-257, -273, -288 and -297 were shown to be particularly reactive (Dinkova-Kostova *et al.* 2002). Following this, it was shown in cells that Cys-273 and -288 are required for the basal repression of Nrf2 (Zhang and Hannink 2003). The expression of serine mutants of these Keap1 cysteines in cells results in constitutively increased Nrf2 levels, and no further increase in Nrf2-mediated gene expression following treatment of the cells with known Nrf2 inducers (Zhang and Hannink 2003). This study also identified a residue within the BTB region of Keap1 (Cys-151), required for Nrf2 regulation (Zhang and Hannink 2003). This cysteine is required for the stabilisation of Nrf2 following treatment with sulforaphane and tBHQ, and following its mutation to alanine (Keap1^{C151A}), no Nrf2 induction is observed (Zhang and Hannink 2003). Zhang and Hannink (2003) also identified a stably-modified form of Keap1 which accumulates only following treatment with Nrf2-inducing compounds. This was the first evidence for electrophilic Nrf2-inducers modifying Keap1 and resulting in Nrf2 accumulation in cells.

There has been a vast quantity of literature published regarding the modification of Keap1 cysteine residues by Nrf2-inducing compounds. There does not appear to be a single cysteine or selection of cysteines that are reactive to all electrophilic Nrf2 inducers. Rather, some cysteine residues, spanning the Keap1 sequence, are more reactive than others (Holland *et al.* 2008). The formation of direct adducts between a subset of cysteine residues in Keap1 and Nrf2-inducing electrophiles with similar structures, supports the hypothesis of a “cysteine code” and underlies the ability of Nrf2 to respond to such a diverse array of compounds (Kobayashi *et al.* 2009) (see Table 1.4 for the classes of Nrf2-inducing compounds). In support of the work performed by Zhang and Hannink (2003), the three cysteine residues which are most commonly adducted by Nrf2-inducing compounds are Cys-151, -273 and -288. Work carried out *in vivo* shows that the expression of mutant Keap1 (Keap1^{C273A}/Keap1^{C288A}) in Keap1^{-/-} mice does not rescue Keap1’s ability to repress Nrf2, and results in constitutive activation of Nrf2, as seen in Keap1-null cells (Yamamoto *et al.* 2008). On the other hand, mutant Keap1^{C151S} retains the ability to suppress Nrf2, although it confers decreased expression of Nrf2-regulated genes both in the absence and presence of electrophilic insult (Yamamoto *et al.* 2008). Interestingly, the mutation of Cys-151 results in reduced Nrf2 activation in cells exposed to some inducers (tBHQ, DEM, sulforaphane) but not to others (CDDO-Im, nitro-oleic acid, cadmium chloride), compared to wild type cells (Takaya *et al.* 2012). These observations support the concept that Cys-273 and Cys-288 are required for basal Nrf2 repression, whilst Cys-151 is required for Nrf2 up-regulation in response to some Nrf2 inducers.

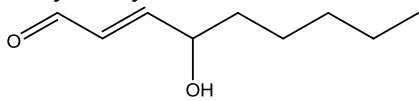
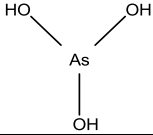
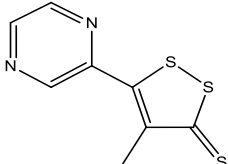
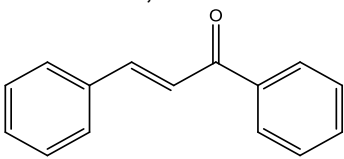
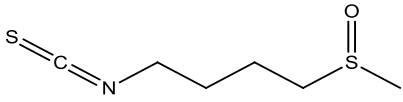
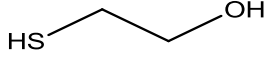
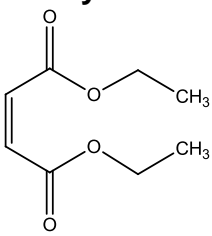
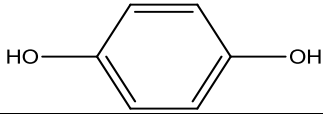
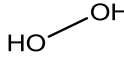
Class	Example(s)	Reference(s)
Alkenes	4-Hydroxynonenal 	Chen <i>et al.</i> (2005) Ishii <i>et al.</i> (2004) Zhang <i>et al.</i> (2006)
Arsenicals	Arsenite, Arsenate 	Pretera <i>et al.</i> (1993) Aono <i>et al.</i> (2003) Pi <i>et al.</i> (2003)
Dithiolethiones	Oltipraz, Anetholedithione 	Kensler <i>et al.</i> (2000) Ramos-Gomez <i>et al.</i> (2001) Petzer <i>et al.</i> (2003)
Enones	Chalcone, Acrolein 	Kumar <i>et al.</i> (2011) Tirumalai <i>et al.</i> (2002)
Isothiocyanites	Sulforaphane 	Pretera <i>et al.</i> (1993), Thimmulappa <i>et al.</i> (2002) Jakubikova <i>et al.</i> (2006)
Mercaptans / disulphides	2-Mercaptoethanol 	Pretera <i>et al.</i> (1993) Chen <i>et al.</i> (2004) Fisher <i>et al.</i> (2007)
Michael acceptors	Diethylmaleate, CDDO-Me 	Pretera <i>et al.</i> (1993) Copple <i>et al.</i> (2014)
Diphenols / quinones	Hydroquinone, tBHQ 	Pretera <i>et al.</i> (1993) Lee <i>et al.</i> (2001) Li <i>et al.</i> (2005)
Reactive oxygen / nitrogen species	Hydrogen peroxide 	Pretera <i>et al.</i> (1993) Buckley <i>et al.</i> (2003) Ding <i>et al.</i> (2008)

Table 1.4. Common classes of Nrf2-inducing compounds. Where more than one example is given, the structure shown is that of the example in bold type.

McMahon *et al.* (2010) propose that Keap1 can respond to endogenous stress by monitoring levels of cellular messengers NO, Zn⁺ and alkenals (which imply the presence of stress), using three unique cysteine sensors to confer an Nrf2 response. They further propose that whilst the Keap1 Cys-151-dependent Nrf2-inducing nitric oxide (NO) –donor, acetoxymethylated diethylamine-NONOate (DEA-NO/AM) does not form direct adducts with Cys-151, this cysteine may undergo S-nitrosylation facilitated by its flanking residues (His-129, Lys-131, Arg-135, Lys-150 and His-154) (McMahon *et al.* 2010). The concept of the S-nitrosylation of Keap1 by NO is supported by others (Fujii *et al.* 2010, Um *et al.* 2011). This study also identified the sensors of Zn²⁺ as His-225, Cys-226 and Cys-613 of Keap1, and of alkenals as Cys-288 (McMahon *et al.* 2010). Keap1 cysteine residues can also be glutathionylated by GSSG, which can cause the formation of disulphide bridges within Keap1 (Holland *et al.* 2008). This is important as under conditions of oxidative stress, the balance between oxidised and reduced glutathione (GSSG:GSH) can become altered. It is possible that increased GSSG or GSH depletion can enhance Nrf2 activation, as seen following the exposure of cells to buthionine sulfoximine (BSO), an inhibitor of the rate-limiting enzyme in the synthetic pathway of GSH, which provokes GSH depletion and the activation of Nrf2 in cells (Chia *et al.* 2010, Copple *et al.* 2008a).

These studies support the hypothesis of a “multiple sensor mechanism” within Keap1, and it is likely that the modification of a combination of cysteine residues is responsible for Nrf2 induction by discrete stimuli, as opposed to

direct adduct formation with one individual residue. See Figure 1.9 for an overview of the cysteine residues in human and/or mouse Keap1, which have been shown to be directly adducted by Nrf2-inducing electrophiles. One must bear in mind that whilst the mutation of one or many cysteine residues in Keap1 may prevent the activation of Nrf2 response by a known inducer, it is not necessarily correct that this cysteine residue is directly responsible for eliciting the Nrf2 response. Many other factors are likely to be involved, for example electrophilic compounds are likely to react with other cellular nucleophiles, which may, in turn, affect cellular homeostasis. Furthermore, there is no consensus on the precise impact that Keap1 modification has on the Keap1/Nrf2 interaction, and how this results in the activation of Nrf2 signalling. There is no direct evidence that the formation of Keap1 adducts specifically attenuates the Keap1/Nrf2 interaction, however indirect evidence supports this notion. The incubation of recombinant Keap1 protein with Nrf2 activators induces a conformational change in the secondary structure of Keap1, resulting in the dissociation of Cul3 in a Cys-151 dependent manner (Rachakonda *et al.* 2008), however its physiological relevance is currently unclear (Baird and Dinkova-Kostova 2013).

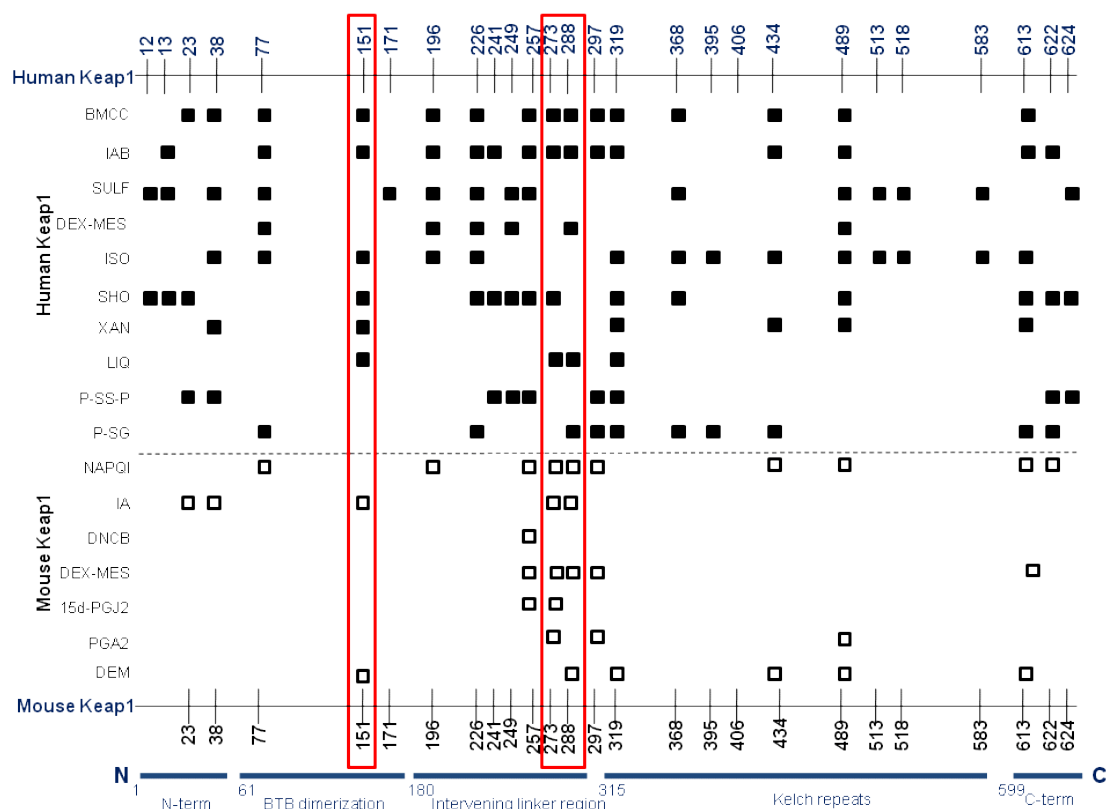


Figure 1.9 Schematic overview of Keap1 cysteine residues and their modification by electrophiles. Electrophile modification of human Keap1 cysteine residues (black box) and mouse Keap1 cysteine residues (white box). The red box outlines the three critical cysteines of Keap1 (Cys-151, Cys-273 and Cys-88). Keap1 domains are outlined at the bottom of the figure and cysteine numbers are annotated at the top and bottom. Abbreviations of the electrophiles are as follows: BMCC; 1-biotinamido-4-(4'-[maleimidodiethylcyclohexane]-carboxamido)butane (Hong *et al.* 2005b, Luo *et al.* 2007), IAB; N-iodoacetyl-N-biotinylhexylenediamine (Eggler *et al.* 2007, Hong *et al.* 2005b), SULF; sulforaphane (Hong *et al.* 2005a), DEX-MES; dexamethasone-21-mesylate (Liebler *et al.* 2006), ISO; isoliquiritigenin, SHO; 10-Shogaol, XAN; xanthohumol (Luo *et al.* 2007), LIQ; liquistilide (Dietz *et al.* 2008), P-SS-P; protein disulphide, P-SG; s-glutathionylation (Holland *et al.* 2008), NAPQI; N-acetyl-p-benzoquinoneimine, IA; iodoacetamide, DNCB; dinitrochlorobenzene (Copple *et al.* 2008a), DEX-MES (Copple *et al.* 2008a, Dinkova-Kostova *et al.* 2002), 15d-PGJ2; 15-deoxy- $\Delta^{12,14}$ -prostaglandin J2 (Copple *et al.* 2008a, Kobayashi *et al.* 2009), PGA2; prostaglandin A2, DEM; diethylmaleate (Kobayashi *et al.* 2009). Adapted from Holland *et al.* (2008), Bryan *et al.* (2013).

1.5.3 Binding partners of Keap1

Whilst Nrf2 is considered to be the only substrate for Keap1-mediated ubiquitination, a number of proteins have been shown to interact with Keap1. Some interactions with Keap1 have a functional impact on Nrf2 regulation, some tether Keap1 in a particular location within the cell to facilitate its function, whilst others have no obvious functional benefit. Nrf2 binds Keap1 via two conserved motifs (ETGE and DLG), acting as the hinge and latch. ETGE-like motifs have been noted in a number of other proteins, which have been identified as Keap1 binding partners (Fig 1.10). Recently it was shown that this motif is required for the protein to interact with Keap1. (Hast *et al.* 2013). Some known Keap1 binding partners which will be discussed in this Section are sequestosome1 (p62), phosphoglycerate mutase family member 5 (PGAM5), prothymosin α and IKK β .

hNrf2	74	L	Q	L	D	E	E	T	G	E	F	L	P	85
hPGAM5	74	R	K	R	N	V	E	S	G	E	E	E	L	85
hP62	344	K	E	V	D	P	S	T	G	E	L	Q	S	355
hIKK β	31	R	W	H	N	Q	E	T	G	E	Q	I	A	42
hProthymosin α	37	G	N	A	N	E	E	N	G	E	Q	E	A	48

Figure 1.10. Table showing the conservation of the Keap1 binding ETGE-like domain across a number of known Keap1 binding partners

p62 acts as a scaffold protein in various signalling pathways via multiple protein-protein interactions, and binds to poly-ubiquitinated proteins and the autophagic machinery, targeting proteins for degradation (Kim *et al.* 2008, Pankiv *et al.* 2007). Recently, a physical and functional relationship between Keap1 and p62 has been elucidated (Lau *et al.* 2010, Fan *et al.* 2010, Copple *et al.* 2010, Jain *et al.* 2010, Komatsu *et al.* 2010). Evidence suggests that

p62 has a role in mediating Keap1 degradation via autophagy resulting in the up-regulation of Nrf2 (Taguchi et al. 2012, Komatsu et al. 2010). The ectopic expression of p62 in cells results in reduced levels of Keap1 protein, whilst siRNA-mediated knockdown of p62 results in an increase in Keap1 half-life, and decreased Nrf2 protein (without changes in mRNA levels), concurrent with reduced levels of a number of Nrf2-regulated genes (Copples *et al.* 2010). Liver-specific autophagy-deficient mice (*Atg*^{-/-}) show p62 accumulation and the formation of p62/Keap1 aggregates as well as the development of hepatocellular carcinoma; moreover, this p62 accumulation leads to the consistent activation of Nrf2 which promotes the development of human hepatocellular carcinoma (Inami *et al.* 2011). p62 contains an STGE motif and it is proposed that under conditions of stress, Keap1 releases Nrf2 from the DLG binding site and p62 binds this site in Keap1 via this STGE motif (Komatsu et al. 2010). Additionally, p62 binds to LC3 which is associated with the autophagosome membrane, providing a link between the Keap1-Nrf2 complex and autophagic degradation, supporting the notion that autophagy is capable of degrading specific, targeted proteins (I. Kim *et al.* 2007, Sakai *et al.* 2006, Deretic 2006, Kaniuk *et al.* 2007).

PGAM5 is a member of the phosphoglycerate mutase family with a role in programmed necrosis by accumulating in the cytosol and sensitising cells to death signals (Zhuang *et al.* 2013). This protein has been shown to be ubiquitinated and targeted for proteasomal degradation via a Keap1-dependent E3 ubiquitin ligase complex, and this degradation is inhibited in the presence of oxidative stress and sulforaphane, indicating PGAM5 as a

novel substrate for Keap1 degradation(Lo and Hannink 2006). PGAM5 contains an ETGE-like motif at its N-terminus, facilitating the interaction with Keap1. Interestingly, the half-life of PGAM5 is approximately 6 hr when co-expressed with Keap1, considerably longer than the half-life of Nrf2, suggesting the affinity for PGAM5 may be lower than for Nrf2 (Lo and Hannink 2006). A follow up study showed that PGAM5 is primarily located on the outer membrane of the mitochondria via an N-terminal mitochondrial localisation sequence (Lo and Hannink 2008). As the mitochondria are a major source of ROS, it is possible that PGAM5 tethers the Keap1/Nrf2 complex in this location to facilitate the sensing of oxidative stress (Lo and Hannink 2008). This interaction provides an interesting link between oxidative stress and cell death, especially as the knockdown of Keap1 or PGAM5 activates the expression of Nrf2-dependent genes (Lo and Hannink 2008).

Prothymosin α is a ubiquitously and abundantly expressed small nuclear protein with roles in proliferation and protection against apoptosis(Manrow *et al.* 1991, Gomez-Marquez *et al.* 1989, Jiang *et al.* 2003). There is growing evidence for this proteins role in transcriptional regulation (Karetsou *et al.* 2002, Martini *et al.* 2000, Vareli *et al.* 2000). An association between prothymosin α and Keap1 was identified in a yeast two-hybrid screen, and confirmed using co-localisation studies (Karapetian *et al.* 2005). Furthermore, the interaction is via an ETGE-like motif within prothymosin α and the same region of Keap1 that binds Nrf2 (Karapetian *et al.* 2005). Additionally, the over-expression of prothymosin α in cells increases the level of HO-1 mRNA in both stressed and non-stressed cells, and vice-versa in cells transfected

with siRNA targeting prothymosin α (Karapetian *et al.* 2005). It has been suggested that the interaction with prothymosin α facilitates the localisation of the Nrf2/Keap1/Cul3/Rbx1 complex in the nucleus, which is promoted upon oxidative stress (Niture and Jaiswal 2009). It is also possible that the limited release of Nrf2 from Keap1 triggered by prothymosin α is sufficient to provide basal ARE-mediated transcription (Karapetian *et al.* 2005)

I κ B kinase β (IKK β) is a subunit of the IKK complex which phosphorylates the inhibitor protein of NF- κ B, I κ B α (Gilmore 1999). This phosphorylation results in the dissociation of I κ B α from NF- κ B, allowing the latter to translocate to the nucleus (Gilmore 1999). Once in the nucleus, NF- κ B up-regulates the expression of genes involved in immunity, inflammation, angiogenesis, cell proliferation and cell survival (Hoesel and Schmid 2013, Lee *et al.* 2009). An association between Keap1 and IKK β was first identified by Lee *et al.* (2009) who demonstrated that Keap1 acts as an IKK β E3 ubiquitin ligase and that the depletion of Keap1 leads to the stabilisation and accumulation of IKK β in cells, and the up-regulation of NF- κ B. Further studies have shown that the Kelch domain of Keap1 interacts directly with the kinase domain of IKK β through an ETGE-like motif (Kim *et al.* 2010). Additionally, it was found that the ectopic expression of Keap1 in cells reduces tumour necrosis factor α (TNF α)-mediated stimulation of NF- κ B, whilst the depletion of Keap1 up-regulates NF- κ B and the expression of its downstream genes (Kim *et al.* 2010). This study further clarified that the degradation of IKK β may not be due to proteasomal degradation, but rather via autophagy (Kim *et al.* 2010). Thus far, it is not known what effect this interaction has on the Nrf2 pathway.

1.6 KEAP1-INDEPENDENT REGULATION OF NRF2

Whilst the regulation of Nrf2 by Keap1 is a commonly investigated mechanism, there are a number of mechanisms which result in changes in Nrf2 activity and function independently of Keap1. A recent publication by Papp *et al.* (2012) highlighted that whilst Nrf2 is associated with a variety of cellular processes and functions, there are few (10-20) known Nrf2-interacting proteins in the major protein-protein interaction databases. A selection of Keap1-independent mechanisms which regulate Nrf2 activity discussed in this Section.

1.6.1 Phosphorylation of Nrf2

Protein kinase C (PKC) is a family of serine/threonine kinases, subdivided into classes (classical, novel and atypical), each requiring different co-factors for activation, with roles in cell growth, differentiation, apoptosis and survival (Numazawa *et al.* 2003). The atypical form can phosphorylate Nrf2 at Ser40 within the Neh2 domain, thus disturbing the association between Nrf2 and Keap1 (Huang *et al.* 2002, Bloom and Jaiswal 2003). Mutation of this residue to an alanine (Nrf2^{S40A}) results in reduced translocation of Nrf2 to the nucleus in comparison to WT Nrf2. Moreover, PKC enzymes are activated under similar conditions to those which induce Nrf2, such as oxidative stress (Numazawa *et al.* 2003).

Casein kinase 2 (CK2) is a protein targeting a number of substrates with functions ranging from gene transcription to cell replication and survival, and

the Nrf2 protein sequence contains approximately 13 potential CK2 phosphorylation sites (Pi *et al.* 2007). The Nrf2 transactivation domains (Neh4 and Neh5) can be phosphorylated by CK2 *in vitro*, and this post-translational modification correlates with the translocation of Nrf2 to the nucleus, and is reduced in the presence of a CK2 inhibitor (Apopa *et al.* 2008). Furthermore, the tyrosine kinase Fyn can phosphorylate Tyr-568 in Nrf2, and this correlates with the translocation of Nrf2 out of the nucleus, and its degradation following the activation of ARE-regulated gene expression (Kaspar and Jaiswal 2011). Upon mutation of Tyr-568 to alanine, Nrf2 accumulates in the nucleus, due to a loss of phosphorylation and reduced interaction with the exportin protein Crm1 (Jain and Jaiswal 2006). Glycogen synthase kinase 3 β (GSK3 β) acts upstream of Fyn, phosphorylating it and in turn, triggering its nuclear accumulation, where it is suitably positioned to phosphorylate Nrf2 (Jain and Jaiswal 2007).

A number of serine/threonine residues in Nrf2 have been shown to be phosphorylated by a panel of mitogen-activated protein kinases (MAPKs). MAP kinases respond to a variety of stimuli, including osmotic stress and heat shock to up-regulate differentiation, mitosis, cell survival and apoptosis (Cargnello and Roux 2011). Keum *et al.* (2006) showed that the classical MAPK, p38, phosphorylates Nrf2, promoting its association with Keap1, an effect reversed by the Nrf2-inducing compound sulforaphane. JNK (c-jun N-terminal kinase 1/2) and ERK (extracellular signal-regulated kinase) have also been implicated in the activation of Nrf2 as butylated hydroxyanisole (BHA) increases the phosphorylation of both ERK1/2 and

JNK1/2 and leads to Nrf2 release from Keap1 (Yuan *et al.* 2006). PERK kinase has also been shown to phosphorylate Nrf2, however the site of phosphorylation is yet to be identified (Cullinan *et al.* 2003).

Glycogen synthase kinase 3 β (GSK3 β) is a key regulator of Nrf2 protein stability, and has provided insight into the activation of Nrf2 by phosphorylation, whilst correspondingly acting as a common downstream effector for a number of Nrf2 inducers (Rojo *et al.* 2012). GSK3 β is involved in the regulation of processes including glycogen metabolism and apoptosis (Salazar *et al.* 2006). GSK3 β stabilises Nrf2 by phosphorylation of the Neh6 region which, in turn, facilitates its ubiquitination by the adaptor protein β -TrCP which forms a complex with Cullin-1 forming a complete E3 ligase (Rada *et al.* 2011). GSK3 β is a downstream target of multiple kinase cascades (Akt, MAPK), the activation of which inhibits GSK3 β through phosphorylation at multiple sites (Thornton *et al.* 2008, Moore *et al.* 2013). Furthermore, the inhibition of GSK3 β promotes Nrf2 stabilization in Keap1-deficient cells (Rojo *et al.* 2012), in Keap1^{-/-} mice and in the presence of a mutant Nrf2 lacking the ETGE motif (Rada *et al.* 2011), suggesting that GSK3 β degrades Nrf2 independently of Keap1.

1.6.2 Alternative post-translational modification of Nrf2

The transcriptional co-activators p300/CBP acetylate histones to facilitate chromatin decondensation and recruit RNA polymerase machinery (Ogryzko *et al.* 1996, Roth *et al.* 2001), and have been shown to associate with Nrf2

(Sun *et al.* 2009, Katoh *et al.* 2001). p300/CBP binds to Nrf2 in response to stress induced by arsenite and acetylates lysine residues within the Neh1 DNA binding region of Nrf2 (Sun *et al.* 2009). The mutation of these lysine residues does not affect Nrf2 protein abundance but compromises the ability of Nrf2 to bind to DNA (Sun *et al.* 2009), thus it is probable that this mechanism enhances the ability of Nrf2 to bind to DNA.

The modification of cysteine residues in Nrf2 is another possible mechanism controlling its regulation. Li *et al.* (2006) characterised a nuclear export sequence (NES) in the Neh5 domain of Nrf2 which contains a reactive cysteine residue (Cys-183). The mutation of this residue to an alanine resulted in reduced nuclear translocation of Nrf2 (compared to WT) following the activation of Nrf2 by tBHQ and H₂O₂, with no effect on Keap1. Under conditions of stress or in the presence of electrophiles, it is possible that modification at Cys-183 prevents the exportin Crm1 binding to Neh5 of Nrf2, resulting in its nuclear accumulation. Thus far, mass spectrometry has not been used to detect the formation of adducts on this residue, and there is no further evidence to support the chemical modification of Nrf2 protein itself.

More recently, caveolin-1 has been identified as an Nrf2-binding partner. Caveolin-1 is a scaffold protein component of caveolar membranes, involved in signal transduction and the uptake of lipophilic compounds (W. Li *et al.* 2012). Caveolin-1 interacts with a number of proteins including: Toll-like receptor 4 and LC3B, a constituent of the autophagy machinery, and regulates biological functions including cholesterol homeostasis and

apoptosis (W. Li *et al.* 2012, Zheng *et al.* 2012). siRNA mediated knock-down of Caveolin-1 results in the dissociation of Nrf2 and Keap1 (W. Li *et al.* 2012), which confirmed previous hypotheses of an association between this protein and the Nrf2 pathway (Zheng *et al.* 2012). On the other hand, the ectopic expression of Caveolin-1 does not result in changes in the Keap1/Nrf2 association but impedes the transcriptional activity of Nrf2 (W. Li *et al.* 2012). Nrf2 binds Caveolin-1 via a caveolin-1 binding motif in the Neh5 domain, and mutagenesis of this motif reduces the association between Caveolin-1 and Nrf2 whilst enhancing the association between Keap1 and Nrf2, indicating that Caveolin-1 competes with Keap1 to bind Nrf2 (W. Li *et al.* 2012).

Ectoderm-neural cortex protein 1 (ENC1) has a similar sequence and domain organisation to Keap1 and plays an important role in neuronal differentiation. Its ectopic expression in cells has been linked to brain tumourigenesis by augmenting cell proliferation and inhibiting apoptosis (Wang and Zhang 2009). ENC1 can form a complex with Cul3–Rbx1, as Keap1 does, and facilitates its own ubiquitination. Whilst no ubiquitination of Nrf2 has been observed with this complex, it can reduce Nrf2 protein levels and the transcription of Nrf2-dependent genes (Wang and Zhang 2009). ENC1 has no effect on Nrf2 mRNA, therefore it is proposed that it down-regulates the rate of Nrf2 protein synthesis (Wang and Zhang 2009), the mechanism of which remains to be understood.

1.6.3 MicroRNAs

MicroRNAs (miRs) are short, single-stranded non-coding RNAs, which play a role in fine-tuning the regulation of a number of proteins (Yang *et al.* 2011). A number of miRs have been associated with the Nrf2 pathway, including miR-144 (Sangokoya *et al.* 2010), miR-28 (Yang *et al.* 2011), miR-200 (Eades *et al.* 2011) and miR-34 (Li *et al.* 2011). Sangokoya *et al.* (2010) showed that an increase in miR-144 expression reduces Nrf2 protein levels, and GSH regeneration, thus altering the antioxidant capacity in erythroid cells. The abnormal expression of miR-144 has been associated with sickle cell disease, implicating a role for Nrf2 in the disease pathology (Sangokoya *et al.* 2010). A similar relationship has been seen between Nrf2 and miR-28 in breast epithelial cells (Yang *et al.* 2011). miR-28 causes the depletion of both Nrf2 mRNA and protein whilst having no effect on Keap1 or the Keap1/Nrf2 interaction (Yang *et al.* 2011). Other miRs which regulate Nrf2 include miR-200, which targets Keap1 mRNA (Eades *et al.* 2011) and miR-34, which targets Nrf2 mRNA and the mRNA of downstream genes involved in the oxidative stress response (Mgst1) (Li *et al.* 2011). The mechanism by which micro-RNAs regulate Nrf2 and other proteins requires further elucidation but some hypotheses are reviewed by Filipowicz *et al.* (2008) and more recently by Ling *et al.* (2013)

1.7 NRF2/KEAP1 IN HEALTH AND DISEASE

Due to the importance of the Nrf2 pathway for maintaining cellular homeostasis, and its role in defending the cell against numerous cell stresses, it is not surprising that it has been associated with toxicity and a number of diseases. The dysregulation of this pathway confers the cell with increased susceptibility to various pathological states, many of which are a consequence of increased oxidative stress, or are linked to changes in the cell's ability to respond to stress. Additionally, the process of drug metabolism generating reactive metabolites which are able to interact with the pathway can also lead to unfavourable outcomes. Understanding how the Nrf2 pathway can affect the onset or progression of disease, or how certain compounds which cause toxicity activate this pathway, will be vital in informing the design of safe therapeutic agents.

1.7.1 Nrf2 and cancer

Nrf2 activation has tumour suppressor functions, and is considered "*the good side of Nrf2*" in cancer (Jaramillo and Zhang 2013). Many of the genes Nrf2 up-regulates are able to inhibit chemical carcinogenesis. For example, Nqo1 catalyses the reduction of both highly reactive quinones, and lipid-soluble antioxidants maintaining them in an active state, as well as affecting cell survival decisions via a role in p53 stabilisation following DNA damage (Nioi and Hayes 2004). For this reason, many Nrf2-inducing compounds are considered to be chemo-preventative agents, including butylated

hydroxyasnisole, curcumin and dithiolethiones (Hayes and McMahon 2009, Kwak *et al.* 2001a). Studies on *Nrf2*^{-/-} mice show that Nrf2 can protect against chemical carcinogen-induced tumour formation in the stomach (Ramos-Gomez *et al.* 2001), bladder (Fahey *et al.* 2002) and skin (Xu *et al.* 2006), and this is likely to be due to Nrf2's ability to protect against oxidative stress and DNA damage. Moreover, individuals with a single-nucleotide polymorphism (SNP) in the promoter region of the Nrf2 gene have low Nrf2 mRNA levels and an increased risk of developing non-small-cell lung cancer (NSCLC), particularly in those who have smoked (Suzuki *et al.* 2013).

Conversely, high Nrf2 levels can be associated with poor prognosis in cancer (Sporn and Liby 2012), and this is considered "*the dark side of Nrf2*" in cancer (Jaramillo and Zhang 2013). In malignant cells, the constitutive activation of Nrf2 can confer cells with a growth advantage and chemo/radio-resistance in lung (Singh *et al.* 2010), breast (Wang *et al.* 2008), ovarian (Konstantinopoulos *et al.* 2011) and pancreatic (Lister *et al.* 2011) cancer. This constitutive activation increases the expression of drug metabolising enzymes and drug transport proteins, increasing the turn-over and efflux of chemotherapeutic drugs, reducing their pharmacological activity (Hayes and McMahon 2009). The ectopic expression of Nrf2 in cancer cells lines with endogenously low Nrf2 levels renders them more resistant to anti-cancer agents, whilst siRNA-mediated knock-down of Nrf2 in cancer cells with high Nrf2 activity can reduce drug resistance (Lister *et al.* 2011, Homma *et al.* 2009). Moreover, constitutive activation of Nrf2 enhances cell proliferation via metabolic reprogramming, by promoting the synthesis of

purine nucleotides, the building blocks of DNA and RNA (Mitsuishi *et al.* 2012). The constitutive activation of Nrf2 which affords cancer cells with these characteristics can be conferred by a variety of mechanisms, including: a) mutations within Keap1/Nrf2 which disrupt their ability to interact; b) epigenetic silencing (by methylation) of Keap1 expression resulting in a loss of Nrf2 repression; c) accumulation of proteins which can disrupt the Nrf2/Keap1 interaction; d) transcriptional activation of Nrf2 by oncogenes (K-Ras, c-Myc); and e) post-translational modification of Keap1 cysteines by metabolic intermediates (for more details regarding these mechanisms, see Jaramillo and Zhang (2013)).

Whilst Nrf2 activation is protective in pre-malignant cells (i.e. where the Keap1/Nrf2 interaction is maintained), when this interaction is disrupted (i.e. in cancer cells) the cells favour survival, thus Nrf2 acts as a double-edged sword in this context (Hayes and McMahon 2006).

1.7.2 Nrf2 and diseases associated with oxidative stress

Oxidative stress has been associated with a wide variety of diseases, from neurological disorders such as Alzheimer's and Parkinson's, to cardiovascular disease, asthma and chronic obstructive pulmonary disease (COPD), as well as aging. This is not surprising, as oxidative stress is tied to mitochondrial dysfunction and thus a reduction in energy generation (Cui *et al.* 2012), and has the ability to disrupt many metabolic pathways (Hybertson *et al.* 2011). As cells age, there is emerging evidence that they express

decreased cellular levels of Nrf2 protein, which reduces the cell's ability to protect itself from oxidative stress (Ungvari *et al.* 2011, Tomobe *et al.* 2012). Why this might be is not yet clear.

Neurodegenerative diseases encompass conditions whereby nerve cells of the brain and spinal cord are lost, due to a functional (ataxia) or sensory (dementia) dysfunction (Uttara *et al.* 2009). Neurodegeneration is thought to arise due to an interplay between environmental and genetic predispositions, however ROS have also been shown to play a role (Emerit *et al.* 2004). The biochemical composition of neuronal cells is particularly sensitive to ROS due to a pool of unsaturated lipids which are liable to peroxidation and oxidative modification, starting a chain reaction of damage to neighbouring fatty acids (Butterfield *et al.* 2002). Not only are neurons more sensitive to ROS, these cells also have lower antioxidant capabilities than other cells of the body, that is approximately 10 % of the livers antioxidant capabilities (Uttara *et al.* 2009). It is the oxidative stress and mitochondrial dysfunction which contributes to neuronal cell death (Calkins *et al.* 2009). The induction of Nrf2 has been shown to protect against neurotoxicity in a number of models, whilst depletion of Nrf2 increases sensitivity (Calkins *et al.* 2009). Thus, the activation of Nrf2 signalling is considered a promising therapeutic strategy in this context.

Whilst dysfunction of the Nrf2 pathway can be associated with many diseases, there are likely to be other factors at play. The accumulation of oxidative stress could be a symptom of Nrf2 dysfunction and/or other

simultaneous pathologies in the tissue. Therefore, reduced Nrf2 may be contributing to the onset and progression of these diseases, however it may not necessarily be causative.

1.7.3 Adverse drug reactions and drug-induced liver injury

Adverse drug reactions (ADRs) are briefly defined as an “undesirable effect of a drug beyond its anticipated therapeutic effect occurring during clinical use” (Pirmohamed *et al.* 1998). They constitute a major public health problem due to their contributions to patient morbidity and mortality (Park *et al.* 2005) and are often responsible for drug attrition (Jefferys *et al.* 1998). ADRs often occur due to the metabolic biotransformation of xenobiotics into potentially hazardous chemically reactive intermediates, which contribute to the onset of oxidative stress, or alter vital cellular factors via post-translational modifications (Park 1986). Drug metabolism is divided into three main phases. Phase I is a functionalisation step (via oxidation, reduction or hydrolysis), performed by cytochrome P450 enzymes (CYPs). Phase II facilitates the conjugation of the metabolite to charged species, such as glutathione (GSH) making them more hydrophilic, thus more readily excreted (Dansette 2008). Conjugation with GSH is especially important in the detoxification of electrophilic compounds (Caldwell *et al.* 1995), as conjugated metabolites are, for the most part, less toxic than the parent compounds and Phase I metabolites (Dansette 2008). Phase III is responsible for the excretion of the resultant metabolite from the cell and eventually, the body.

As the primary drug metabolising organ of the body, the liver is often exposed to reactive metabolites, and thus prone to drug-induced liver injury (DILI). In severe cases, DILI can become life-threatening and require an organ transplant, if enough of the tissue is damaged irreparably (Russo *et al.* 2004). DILI is often caused by the accumulation of a toxic drug or metabolite causing changes in the biochemistry of the cell (commonly the hepatocyte), or mediating an immune response resulting in cell death (Wang 2014).

Paracetamol (Acetaminophen/APAP) is widely used in *in vitro* and *in vivo* models of DILI due to its clinical relevance and dose-dependent toxicity (Newsome *et al.* 2000), and it has been shown *in vivo* that APAP activates the Nrf2 pathway in mouse liver (Goldring *et al.* 2004). Studies have shown that *Nrf2*^{-/-} mice are more sensitive to APAP-induced liver injury, exhibiting increased liver necrosis and decreased survival rates, due to reduced detoxification enzymes and low cellular thiol levels (Chan *et al.* 2001, Enomoto *et al.* 2001). Moreover, liver-specific Keap1-null mice are resistant to APAP doses which are lethal in WT mice, demonstrating that Keap1-mediated regulation of Nrf2 is required for protection against APAP (Okawa *et al.* 2006). The toxicity caused by APAP overdose is conferred by its reactive metabolite, N-acetyl-p-benzoquinone imine (NAPQI) (Dahlin *et al.* 1984). NAPQI is conjugated with GSH however, when that latter becomes depleted, NAPQI accumulates and can bind covalently to other cellular thiols, resulting in hepatocyte necrosis (James *et al.* 2003). NAPQI has been shown to activate Nrf2 via the direct covalent modification of Keap1 cysteine residues

(Copples *et al.* 2008a), thereby directly linking the Nrf2 pathway and the onset of DILI. DILI mimics many other diseases of the liver such as viral hepatitis, acute fatty liver and cirrhosis (Park *et al.* 2005), therefore furthering our knowledge of the pathogenesis of this disorder will improve both drug safety and the development of treatments for other liver disorders.

1.7.4 Potential therapeutic strategies related to Nrf2

Due to the association of many diseases with oxidative stress, there have been attempts to create therapeutic agents from superoxide dismutase (SOD), which can scavenge reactive oxygen (Greenwald 1990). Proteins and enzymes commonly make poor drugs due to immunogenicity, poor pharmacokinetic dynamics and non-availability by oral administration, and such issues were encountered with the SODs (Hybertson *et al.* 2011). A genetically engineered SOD was synthesised with high efficacy at low doses and slowed renal clearance (Gao *et al.* 2003). However, the problems outlined above remained, as well as issues of production costs, purification and stability (Hybertson *et al.* 2011). The direct activation of Nrf2 is a more promising approach, due to its ability to regulate the expression of a variety of cellular antioxidants (Hybertson *et al.* 2011).

The majority of known Nrf2 inducers are purported to be inhibitors of the Keap1/Nrf2 interaction, facilitated by the modification of Keap1 cysteine residues by covalent adduction (or oxidation) (Magesh *et al.* 2012). Electrophiles can be divided into two groups, hard or soft. Soft electrophiles

will react predominantly with soft nucleophiles, such as the sulphhydryl group of a cysteine, whereas hard electrophiles react with amino and hydroxyl groups on nucleic acids, which can result in carcinogenicity, thus are best to avoid with regards to developing therapeutic agent targeting Nrf2 (Magesh *et al.* 2012). The most potent inducers of Nrf2 signalling are triterpenoids (TPs), such as CDDO-Me (methyl 2-cyano-3,12-dioxooleana-1,9(11)dien-28-oate), which exhibit anti-tumour and anti-inflammatory properties, among other health benefits (Liby and Sporn 2012). The mechanism of action of these compounds with regards to Nrf2 activation will be discussed further in Chapter 3. There are a number of U.S. Food and Drug Administration (FDA)-approved Nrf2-inducing compounds, including dimethyl fumarate (DMF) (Tecfidera, Biogen Idec) for the treatment of adults with multiple sclerosis. Protandim (LifeVantage Corporation) is a patented dietary supplement which has not been evaluated by the FDA, therefore not intended for prevention, treatment or cure of any disease. The components of Protandim are known Nrf2 inducers including turmeric and green tea, and it is advertised as an “Nrf2 activator”. It been tested both *in vivo* and *in vitro* (Nelson *et al.* 2006, Velmurugan *et al.* 2009, Qureshi *et al.* 2010) and there is interest in it as a potential therapeutic agent (Hybertson *et al.* 2011). As previously alluded to, the use of Nrf2 inducers for therapeutic purposes is controversial due to its association with cancer, therefore the conditions under which Nrf2 activators are used must be tightly monitored.

The reversible disruption of the Keap1/Nrf2 complex by small peptides has recently become an avenue of investigation. Proteins that contain an ETGE-

like motif have been shown to compete with Nrf2 to bind to Keap1, and result in the up-regulation of ARE-driven gene expression (Camp *et al.* 2012, Ma *et al.* 2012). The synthesis of peptides containing ETGE-like motifs has been optimised to increase protein binding and cellular activity (Hancock *et al.* 2013), and a high throughput screening assay has been developed to discover novel small-molecule inhibitors of the Keap1/Nrf2 interaction (Inoyama *et al.* 2012). This method of manipulating Nrf2 activity will increase specificity for the pathway, and avoid the use of potentially toxic electrophiles, and is therefore a promising therapeutic strategy.

The pharmacological inhibition of Nrf2 is considered a promising therapeutic approach in cancers which show elevated levels of Nrf2. Brusatol, a plant extract from the *Brucea javanica* seed, is able to reduce Nrf2 protein levels in cells at nanomolar (nM) concentrations, reducing the expression of Nrf2 target genes and enhancing the cytotoxic effect of the chemotherapeutic agent cisplatin both *in vitro* and *in vivo* (Ren *et al.* 2011). The mechanism by which brusatol inhibits Nrf2, and its specificity for the pathway, is currently under investigation; however it appears to reduce Nrf2 protein levels independently of Keap1 and the proteasome (data presented in thesis of Adedamola Olayanju). The basal and inducible activity of Nrf2 can be suppressed by small molecules such as ascorbic acid (vitamin C) and luteolin (Magesh *et al.* 2012). Vitamin C inhibits formation of the Nrf2/DNA complex at the ARE of the GCL gene promoter and reduces peroxide levels (Tarumoto *et al.* 2004). Furthermore, the treatment of an imatinib-resistant cell line with ascorbic acid enhances sensitivity to imatinib

(Tarumoto *et al.* 2004). Luteolin inhibits ARE-dependent gene expression in a redox-independent manner, and reduces both Nrf2 protein and mRNA levels (Tang *et al.* 2011). However, as a flavonoid, it has also been shown to have Nrf2-activating properties, and can induce HO-1 expression and increase Nrf2 ARE-binding (Lin *et al.* 2010). A further inhibitor of the Nrf2 pathway is the chemo-preventative and chemotherapeutic agent *all-trans* retinoic acid (ATRA), which reduces the tBHQ-mediated induction of ARE-driven genes in cells (Wang *et al.* 2007). Additionally, ATRA can repress the basal expression of ARE-driven genes in cells, by reducing the binding of Nrf2 to the ARE region, through formation of a complex with retinoic acid receptor α (RAR α) (Wang *et al.* 2007). Retinoids are known to activate or repress gene expression by forming heterodimers with RARs and interacting with other transcription factors, such as AP-1 and NF- κ B (Shaulian and Karin 2002). A recent surge in interest in Nrf2 inhibitors will further the development of therapeutic possibilities in this area.

1.8 THESIS AIMS

In light of the critical role of the Nrf2 pathway in cell defence and its association with toxicity and many disease pathologies, furthering our understanding of the regulation of this pathway is vital to determine how these toxicities or diseases arise and develop. This thesis aims to investigate the molecular interactions with Keap1 which may play a role in the activation and/or repression of Nrf2 signalling by addressing the following questions:

- 1) Do molecules that are known to activate Nrf2 do so via the covalent or oxidative modification of cysteine residues in Keap1?
- 2) Can the most potent known inducers of Nrf2 (triterpenoids; TPs) form covalent adducts with Keap1?
- 3) Are there unidentified proteins that interact with Keap1 and which can modulate the activity of Nrf2 interaction?

By furthering our knowledge of how Nrf2-inducing compounds are able to activate the pathway via interactions with Keap1, we can aim to develop predictive toxicity screens based on the ability of a compound to modify Keap1 covalently. As the manipulation of this pathway is considered a viable therapeutic target, with regards to the prevention and/or treatment of diseases such as cancer and other pathologies associated with oxidative stress, understanding the mechanism of action of pharmacological agents towards Nrf2 should allow the synthesis of chemically-tuned compounds with increased potency and specificity towards this pathway, thus reducing the risk of off-target effects. Therefore, this thesis aims to gain further insight into the regulation of this cytoprotective pathway via molecular interactions between Keap1 and pharmacological agents or other proteins.

CHAPTER 2

COVALENT AND OXIDATIVE MODIFICATION OF KEAP1 CYSTEINE RESIDUES AS A MECHANISM OF NRF2 ACTIVATION

CONTENTS

2.1. INTRODUCTION	- 56 -
2.2 MATERIALS AND METHODS	- 60 -
2.2.1 Materials and reagents.....	- 60 -
2.2.2 Cell culture.....	- 61 -
2.2.3 Mouse Keap1-V5 plasmid purification.....	- 62 -
2.2.4 Transfection of cells with Keap1-V5.....	- 63 -
2.2.5 Cell treatment.....	- 64 -
2.2.6 Immunopurification of Keap1-V5.....	- 64 -
2.2.7 Measurement of protein content.....	- 65 -
2.2.8 Quantification of glutathione levels.....	- 65 -
2.2.9 Western Immunoblotting- whole cell lysates.....	- 67 -
2.2.10 Western Immunoblotting- immunopurified Keap1-V5.....	- 69 -
2.2.11 Preparation of Keap1-V5 for LC-ESI-MS/MS.....	- 69 -
2.2.12 MALDI-TOF mass spectrometry.....	- 70 -
2.2.13 LC-ESI-MS/MS methods.....	- 70 -
2.3 RESULTS	- 72 -
2.3.1 Optimisation of Keap1-V5 transfection in HEK293T cells.....	- 72 -
2.3.2 MALDI validation of Keap1-V5.....	- 72 -
2.3.3 LC-ESI-MS/MS validation of Keap1-V5.....	- 73 -
2.3.4 Effect of chosen compounds on Nrf2 and GSH in cells.....	- 75 -
2.3.5 Determining susceptibility of cysteine residues to modification.....	- 76 -
2.3.6 Modification of cysteines in Keap1-V5 by DNCB.....	- 77 -
2.3.7 Modification of cysteines in Keap1-V5 by Dex-mes.....	- 79 -
2.3.8 Modification of cysteines in Keap1-V5 by H ₂ O ₂	- 81 -
2.3.9 Modification of cysteines in Keap1-V5 by BSO.....	- 83 -
2.3.10 Modification of cysteines in Keap1-V5 by CDDO-Me.....	- 85 -
2.4 DISCUSSION	- 87 -

2.1. INTRODUCTION

The Nrf2 cell defence pathway regulates the basal and inducible expression of an array of genes which combat chemical and oxidative stress (Bryan *et al.* 2013). The most widely-accepted model of Nrf2 regulation describes the cysteine-rich protein Keap1 as an active repressor of Nrf2 activity, as discussed in Section 1.5. A number of studies provide compelling evidence for the direct covalent modification of cysteine residues in recombinant Keap1 by Nrf2-inducing molecules *in vitro* (Fig. 1.9) (Egglar *et al.* 2005, Hong *et al.* 2005a, Hong *et al.* 2005b, Luo *et al.* 2007, Dinkova-Kostova *et al.* 2002, He and Ma 2010). Furthermore, recent work by our group and others has shown that Keap1 can be selectively modified by reactive chemical species in a cell based model (Hong *et al.* 2005b, Rachakonda *et al.* 2008, Copple *et al.* 2008a). Moreover, it has also been shown that under conditions of substantial depletion of cellular GSH, an Nrf2 response can be elicited in the absence of Keap1 covalent modification (Chia *et al.* 2010, Copple *et al.* 2008a).

The mechanism whereby GSH depletion may induce Nrf2 activation is currently unclear, however one proposal is that when GSH levels are depleted, naturally produced ROS can no longer be scavenged and thus accumulate in the cell. This accumulation may give rise to oxidative stress and changes in the redox state of the cell, resulting in the oxidation of Keap1 cysteines, and subsequent Nrf2 activation. Currently, there is no concrete evidence to suggest that Keap1 cysteine residues are susceptible to

oxidation *in vivo* and the techniques used to confidently identify thiol oxidation states are still in their infancy (Burgoyne and Eaton 2011). Under certain experimental conditions, evidence supports the presence of modifications on recombinant or ectopically expressed Keap1, including the formation of inter- and intra-disulphide bonds, glutathionylation and nitrosylation (Wakabayashi *et al.* 2004, Holland *et al.* 2008, Fourquet *et al.* 2010, Zhang *et al.* 2010, Um *et al.* 2011). Unfortunately, modification is often substoichiometric with only a small proportion of the protein being modified, obstructing analysis of protein modification and function simultaneously, and this is only made more challenging by the low abundance of Keap1 in cells (approximately 10 parts per million) (McMahon *et al.* 2006).

As the oxidation of cysteine residues is both selective and, for the most part, reversible (Burgoyne and Eaton 2011), it can enable the function of a protein to be rapidly regulated in response to changes in cellular redox state. The thiol group of cysteine residues can form various reversible oxidative states such as sulphenic acid (S-OH) as well as the irreversible oxidative states of sulphinic (S-O₂H) and sulphonic acid (S-O₃H) (Lee *et al.* 2013) (Fig. 2.1). We have recently observed that all Keap1 cysteine residues are in a reduced state, thus are available for adduction by a common alkylating agent, and do not appear to participate in disulphide bonds under basal conditions (unpublished data). From this we conclude that, basally, all cysteine residues are available for modification following exposure to an Nrf2 inducer.

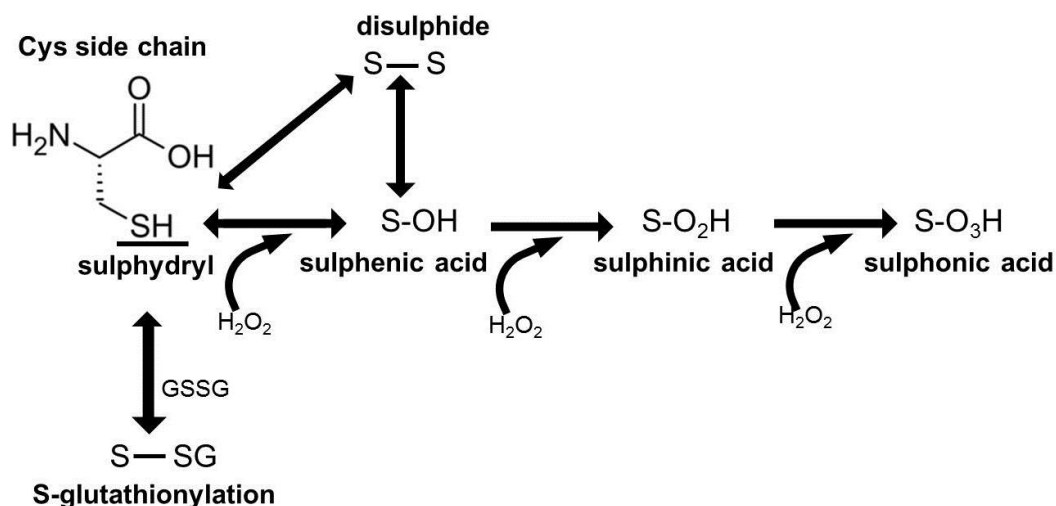


Figure 2.1. Schematic diagram of protein cysteine oxidation. Sulphydryl groups can be reversibly oxidised to sulphenic acid, which can be further irreversibly oxidised to sulphinic and sulphonic acids. Sulphydryl groups can also react with other sulphydryl groups to form disulphide linkages or be s-glutathionylated.

In order to investigate the oxidation of Keap1 cysteine residues in response to Nrf2-inducing compounds, a mass spectrometry based method (LC-ESI-MS/MS) has been developed in our lab using the alkylating agents N-ethylmaleimide (NEM) and iodoacetamide (IAA). These agents were used to investigate the susceptibility of cysteine residues in ectopically expressed Keap1-V5 in HEK293T cells to modification, following treatment with Nrf2-inducing compounds. The compounds used for this investigation were chosen based on their purported mechanism of Nrf2 induction. 2,4-Dinitrochlorobenzene (DNCB) depletes cellular GSH and has previously been shown to covalently modify Keap1 (Chia et al. 2010, Copple et al. 2008a) whilst Dexamethasone 21-mesylate (dex-mes) has been shown to covalently modify Keap1 (Dinkova-Kostova et al. 2002, Hong et al. 2005b, Copple et al. 2008a) whilst having no effect on GSH levels in the cell. Buthionine (S,R)-sulphoximine (BSO) is a GCL inhibitor which provokes the specific depletion of intracellular GSH without causing protein covalent

modification (Cople et al. 2008a). Hydrogen peroxide (H_2O_2) causes significant oxidative stress in cells and is a strong oxidiser of thiol groups, which does not form stable covalent adducts with cysteine residues, nor attenuate cellular GSH (Fourquet et al. 2010). The semi-synthetic triterpenoids (TPs), such as CDDO-Me, are extremely potent Nrf2-inducing compounds (Yates et al. 2007) with a mechanism of action that is yet to be fully resolved however these compounds do not appear to provoke oxidative stress or alter GSH in cells. See Fig 2.2 for chemical structures of the compounds used in this study. **These compounds will be used to test the hypothesis that small molecules, which activate Nrf2 in the absence of direct covalent adduction of Keap1, provoke changes in the oxidation state of Keap1 cysteine residues, which may alter the susceptibility of these residues to further modification.**

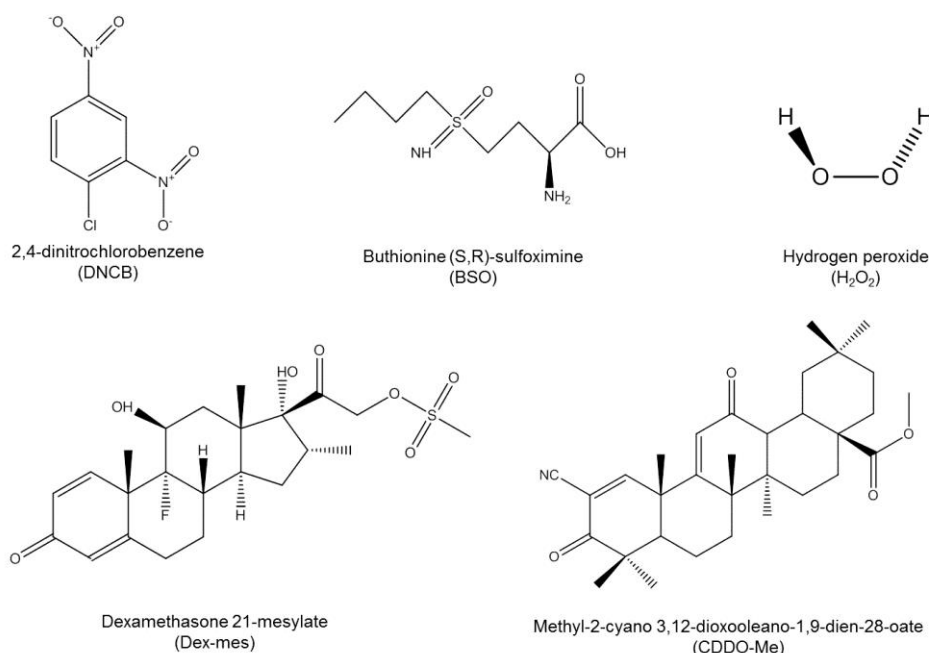


Figure 2.2 Chemical structures of the Nrf2 inducing compounds under investigation in this chapter.

2.2 MATERIALS AND METHODS

2.2.1 Materials and reagents

The human embryonic kidney cell line (HEK293T) was obtained from American Type Culture Collection (Masassas, VA, USA). The Wilovert D6330 light microscope was from Will-Wetzler (Wetzlar, Germany). Nunclon Δ cell culture flasks, dishes and multi-well plates were from Nalge-Nunc International (c/o VWR International, Lutterworth, UK). The mouse Keap1-V5 encoding plasmid was generated at the MRC Centre for Drug Safety Science, University of Liverpool, UK by Dr Ian Copple. The XL10-Gold ultra-competent *E.coli* were purchased from Agilent Technologies (Stockport, UK). Sequencing grade modified trypsin was purchased from Promega (Southampton, UK) and the QIAfilter Plasmid Maxi Kit from QIAGEN (Crawley, UK). Protein assay dye reagent, Precision Plus protein Kaleidoscope standards, non-fat dry milk, Mini Trans-Blot Cell and GS-800 calibrated image densitometer were from Bio-Rad (Hemel Hempsted, UK). FBS, NuPAGE Novex 4-12% Bis-Tris gels, NuPage LDS sample buffer, NuPAGE reducing agent and antioxidant, XCell Surelock mini-cell and Lipofectamine 2000 were from Invitrogen (Paisley, UK). The goat-anti-Keap1 antibody was obtained from Santa Cruz Biotechnology (Heidelberg, Germany) whilst the mouse-anti-beta actin and rabbit-anti-Nrf2 antibodies were from Abcam (Cambridge, UK). The anti-goat HRP-conjugated antibody was from Dako UK (Ely, UK) and, anti-mouse HRP-conjugated antibody was from Abcam (Cambridge, UK). The MRX microplate reader was from Dynatech Laboratories (Billingshurst, UK) and TotalLab 100 software was from Non-

linear Dynamics (Newcastle, UK). Western Lighting Enhanced Chemiluminescence (ECL) reagents were from Perkin-Elmer (Seer Green, UK). Hybond nitrocellulose membranes and Hyperfilm ECL were from GE Healthcare Life Sciences (Little Chalfont, UK). The Series 200 HPLC was from Perkin Elmer (Massachusetts, USA), the C18 Uptisphere column from Interchim, Cheshire Sciences Ltd (Chester, UK). The MALDI target plate, Voyager-DE PRO-MALDI-TOF Biospectrometry Workstation, APSciex API3000 triple-quadrupole mass spectrometer, API QSTAR Pulsar 1 MS/MS spectrometer, Analyst QS and ProteinPilot software packages were from Applied Biosystems (Warrington, UK). The NanoDrop 1000 UV-spectrophotometer was from Labtech International (East Sussex, UK). The concentrator 5301 and C18 ZipTips were from Eppendorf (Cambridge, UK). The DMEM, Penicillin-streptomycin solution, Trypsin, Trypan Blue solution, DNCB, DMSO, BSO, BSA, H₂O₂, MOPS, GSH, NADPH, GSH reductase, Kodak developer and fixer solution, Ponceau S solution, Tween-20, PBS tablets, sulphosalicylic acid (SSA), the goat-anti rabbit HRP-conjugated secondary antibody and anti-V5 agarose beads were from Sigma-Aldrich (Poole, UK) All other reagents were of analytical or molecular grade and from Sigma-Aldrich.

2.2.2 Cell culture

HEK293T cells were maintained at 37°C in 5% CO₂ in Dulbecco's modified Eagle's medium (DMEM) supplemented with 584 mg/L L-glutamine, 10% heat inactivated fetal bovine serum (FBS), 100 U/mL penicillin and 100 µg/

mL streptomycin. Cells were grown in 75cm² Nunclon Δ culture flasks and passaged routinely every 3-4 days at approximately 80% confluence. Following a wash with 5 mL unsupplemented DMEM, cells were returned to the incubator with 5 mL trypsin for up to 5 min to allow detachment of cells from the flask surface. Cells were resuspended in 5 mL supplemented DMEM and centrifuged at 1500 rcf for 5 min. Cells were then resuspended in 5 mL supplemented DMEM and dissociated five times using a 21-gauge needle with a 5 mL syringe. For continuation, cells were re-seeded at a cells:growth medium ratio of 1:10.

To ensure that an accurate number of cells were seeded, cells were counted using Trypan Blue solution (0.4% w/v) and a haemocytometer. Briefly, cells were detached from the surface of a culture flask as described above and 40 μ L was combined with 10 μ L of Trypan Blue solution. 10 μ L of this was transferred to the haemocytometer. Cells were visualised using the 20X objective of a Wilovert D6330 light microscope. Viable cells (those that did not take up the Trypan Blue dye) within the central 5 x 5 square were counted and the original cell density was calculated as follows:

$$\text{Number of cells counted} \times 1.25 \text{ (to correct for dilution with Trypan Blue solution)} = \text{cells per } 0.1 \text{ mm}^3 \times 10,000 = \text{cells per } 1 \text{ cm}^3 = \text{cells per } 1\text{mL}$$

2.2.3 Mouse Keap1-V5 plasmid purification

The mouse Keap1-V5-encoding plasmid (Keap1-V5) was generated by Dr. Ian Copple (Copple et al. 2008a). Briefly, the full mouse Keap1 coding

sequence lacking a stop codon in the TOPO cloning site of pcDNA3.1/V5-His-TOPO was transformed into XL10-Gold ultracompetent *E.coli*. A 15% (v/v) glycerol stock of pcDNA3.1/Keap1-V5 XL10-Gold *E.Coli* was cultured in 1 L LB broth supplemented with 100 µg/mL ampicillin and incubated for 16 hr at 37°C, 250 rpm. The pc.DNA3.1/Keap1-V5 plasmid was purified using a QIAfilter Plasmid Midi Kit and eluted into 1XTE buffer (10 mM Tris base, 1 mM EDTA, pH 7.5). The concentration and purity of the plasmid DNA was determined using a Nano Drop. The purity of the DNA was determined by reference to the 260 nm:280 nm ratio. Only samples with a ratio of above 1.8 were used for future experiments. Mouse Keap1-V5 was used instead of human Keap1 due to the high sequence identity between the two (94%) and to facilitate the translation of these data to *in vivo* and transgenic studies which have previously been performed in mice.

2.2.4 Transfection of cells with Keap1-V5

For mass spectrometry experiments, HEK293T cells were seeded onto 9cm Nunclon Δ cell culture dishes at 5×10^6 cells/dish in 10 mL growth media (3 dishes per condition) and returned to the humidified incubator. The following day, cells were transfected with pcDNA3.1/Keap1-V5-His plasmid using Lipofectamine 2000 according to the manufacturer's instructions. For each dish of cells, 3 mL OptiMEM was combined with 60 µL Lipofectamine 2000 and 20 µg of Keap1-V5 plasmid. The contents were mixed and incubated at room temperature for 20 min. The mixture was then added dropwise to the dish. Cells were then returned to the humidified incubator, at 37°C in a 5%

CO₂ atmosphere for 24 hr. All preparations were done under sterile conditions.

2.2.5 Cell treatment

For mass spectrometry experiments, following the transfection of HEK293T cells with Keap1-V5-His for 24 hr, cells were treated with various compounds. DNCB, CDDO-Me, and Dex-Mes were dissolved, at 200x the required final concentration, in dimethyl sulphoxide (DMSO). BSO was dissolved in distilled water (dH₂O) at 200x the final concentration. H₂O₂ was dissolved in cell culture media at 200x the final concentration. To the appropriate dish of cells, the vehicle control or Nrf2 inducer was added (a 1:200 dilution) giving the required final concentration. The final volume of solvent in the cell culture medium was 0.5% (volume/volume; v/v). The cells were placed back into the humidified incubator (37°C in a 5% CO₂) for the indicated period of time (1 hr or 24 hr). Following this incubation, 2mM NEM dissolved in DMSO was added as above, for 5 min.

2.2.6 Immunopurification of Keap1-V5

Following exposure to Nrf2 inducers, followed by NEM, cells were resuspended in their own media. Cells were pelleted by centrifugation for 5 min at 800rcf and washed once with 1 mL 1x PBS. The cells were then resuspended in 1 mL radioimmunoprecipitation assay (RIPA) buffer (0.15 M NaCl, 1% (v/v) NP-40, 0.5% (v/v) sodium deoxycholate, 0.1% (v/v) SDS, 25

mM Tris-Cl₂). 1 mL of lysate was incubated with 50 µL anti-V5 agarose beads on a mechanical roller for 4 hr at 4°C to facilitate immunopurification of Keap1-V5. The beads were collected by centrifugation at 14,000g for 1 min and washed 3 times in 0.5 mL 1x PBS. 20 µL samples were taken before and after immunopurification to be analysed by immunoblotting.

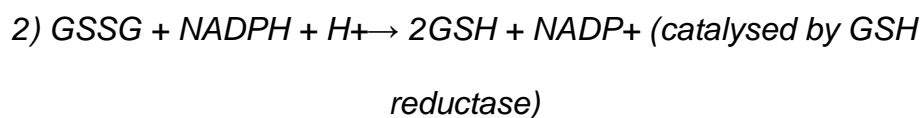
2.2.7 Measurement of protein content

For western blotting and quantification of glutathione levels, the total protein content of whole cell lysates was determined using Protein Assay Dye Reagent based on the method of Bradford (1976). This assay relies on the binding of Coomassie Brilliant Blue G-250 dye to basic and aromatic amino acids. This results in a change in the colour of the dye from red to blue, and a consequential change in absorbance maximum from 465 to 595nm. The increase in absorbance at 570 nm, measured using an MRX microplate reader, is proportional to the amount of protein present. A standard curve, ranging from 0.0125-0.25 µg bovine serum albumin (BSA) was used to calculate the protein content in the cell lysates.

2.2.8 Quantification of glutathione levels

Total glutathione (GSH) content was quantified using the 5,5'-dithiobis(2-nitrobenzoic acid) (DTNB)-GSH reductase recycling method, as previously described by Vandeputte *et al.* (1994). DTNB oxidises GSH to yield GSSG and the 5-thio-2-nitrobenzoic acid (TNB) chromophore, with an absorbance

maximum of 412 nm. The rate of formation of TNB, followed at 405 nm, is proportional to the sum of GSH and GSSG in each sample.



Briefly, 293T cells were seeded into 24-well plates at 3×10^5 cells/well before being treated with the appropriate Nrf2 inducer or vehicle control, as described in Section 2.2.5. Cells were resuspended in their own media and pelleted by centrifugation at 800 rcf for 5 min. Cells were then resuspended in 0.125 mL of 10 mM HCl. Aliquots were taken to enable the determination of total protein content as described in Section 2.2.7. Sulphosalicylic acid (SSA) was added to the remaining samples to a final concentration of 1.3 % (w/v), and samples incubated on ice for 10 min to facilitate protein precipitation. Protein was pelleted by centrifugation at 18,000 rcf for 5 min. The supernatant was removed and placed into a fresh eppendorf and a proportion of the supernatant was diluted 1:5 in assay buffer (0.143 M NaH_2PO_4 , 6.3 mM EDTA, pH 7.4). 20 μL of the diluted supernatant and the neat supernatant were transferred to a clear 96-well plate. Samples were incubated at room temperature with 0.2 mL assay reagent (1.0 mM DTNB, 0.34 mM NADPH, in 0.143 M NaH_2PO_4 , 6.3 mM EDTA, pH 7.4) for 5 min. The enzymatic reaction was initiated by the addition of 0.35 U GSH reductase and followed kinetically at 405 nm for 5 min on a MRX microplate reader. The rate of TNB formation was calculated as the change in

absorbance min^{-1} . Sample GSH concentrations were calculated via reference to a standard curve (1-50 nmol/mL GSH). The GSH concentration for each sample was normalised to total protein content and expressed as mean \pm standard deviation of the mean (SD).

2.2.9 Western Immunoblotting- whole cell lysates

Cells were seeded into 12-well Nunclon Δ cell culture plates at 3×10^5 cells/well and returned to the humidified incubator overnight. Cells were treated with Nrf2 inducers as described in Section 2.2.5. After treatment for the indicated period of time, cells were resuspended in their own media, pelleted by centrifugation for 5 min at 800 rcf and washed twice in 1 mL PBS. Cells were resuspended in 60 μL RIPA buffer and incubated on ice for 5 min before storing at -80°C . Clarification by centrifugation at 18,000 rcf for 5 min before analysis was necessary, as freeze-thaw cycles may promote the formation of protein aggregates.

Whole cell lysates (20 μg), or samples taken before and after Keap1-V5 immunopurification were denatured via the addition of 5 μL loading buffer (70 % (v/v) NuPAGE sample loading buffer, 30 % (v/v) NuPAGE reducing agent) and heated to 80°C for 5 min. Samples were loaded onto pre-cast 4-12 % NuPAGE Novex bis-tris polyacrylamide gels, alongside PrecisionPlus protein Kaleidoscope standards. Samples were resolved by electrophoresis in an XCell Surelock Mini-cell, using 3-(N-morpholino)propanesulphonic acid (MOPS) running buffer (50 mM MOPS, 50 mM Tris base, 3.5 mM sodium

dodecyl sulphate, 1 mM EDTA, 0.25 % (v/v) NuPAGE antioxidant), at 90 V for 10 min, followed by 170 V for 60 min. Separated proteins were transferred to nitrocellulose membranes using the Bio-Rad Mini Trans-Blot cell, in accordance with the manufacturer's instructions. To ensure the transfer process was successful, membranes were stained for 10 sec with Ponceau S solution. Membranes were blocked for 30 min or overnight, on an orbital shaker, in tris-buffered saline (TBS; 0.15 M NaCl, 25 mM Tris base, 3 mM KCl, pH 7.0) containing 0.1 % (v/v) Tween 20 and 10 % (weight/volume; w/v) non-fat dry milk. Blocked membranes were probed for 3 hr with a rabbit anti-human Nrf2 (1:400 in TBS-Tween containing 2 % (w/v) non-fat dry milk), or a goat anti-Keap1 (1:2000 in TBS-Tween containing 2 % (w/v) non-fat dry milk) primary antibody. Following several washes in TBS-Tween, membranes were probed for 1 h with goat anti-rabbit (1:10,000 in TBS-Tween containing 2 % (w/v) non-fat dry milk) or rabbit anti-goat (1:2000 in TBS-Tween containing 2 % (w/v) non-fat dry milk) horseradish peroxidase (HRP) -conjugated secondary antibodies. Immunoblots were visualised with Western Lightening chemiluminescence reagents and exposed to Hyperfilm ECL under darkroom conditions. Blots were developed using Kodak developer and fixer solutions. To ensure equal loading across gels, membranes were probed with rabbit anti-actin primary (1:20,000 in TBS-Tween containing 2 % (w/v) non-fat dry milk) and goat anti-rabbit HRP-conjugated secondary antibodies. Films were scanned using a GS-710 calibrated imaging densitometer, immune-reactive band volumes were quantified using TotalLab 100 software, and normalised to actin.

2.2.10 Western Immunoblotting- immunopurified Keap1-V5

To assess the immunopurification of Keap1-V5, proteins were eluted from anti-V5 agarose beads by resuspending in an equal volume of NuPAGE loading buffer. The slurry was heated at 80 °C for 10 min, the beads were pelleted by centrifugation at 5000 g for 5 min, and the supernatant loaded onto a pre-cast 4-12 % NuPAGE Novex bis-tris polyacrylamide gel as described in Section 2.2.9.

2.2.11 Preparation of Keap1-V5 for LC-ESI-MS/MS

After incubation and washing, PBS was removed from the Keap1-V5-bound anti-V5 agarose beads after centrifugation. The resulting beads (50 µL dry volume) were reduced by resuspending in 1 mL 0.1mM dithiothreitol (DTT). The mixture was incubated on a mechanical roller for 15 min at 4°C. The beads were washed three times with 0.5 mL PBS to remove residual DTT. Any unmodified cysteines were alkylated by resuspending beads in 1 mL 55mM iodoacetamide (IAA) and incubated on a mechanical roller for 15 min at 4°C. The beads were washed twice in 0.5 mL PBS to remove residual IAA. Prior to trypsin digestion, beads were washed twice with 0.5 mL 25mM ammonium bicarbonate and resuspended in 90 µL ammonium bicarbonate. A 400 µg/mL stock solution of sequence-grade modified trypsin was diluted 1:10 with 25mM ammonium bicarbonate and 10 µL (40ng) was added to the bead slurry. Trypsin digestion of the sample was performed overnight at 37°C.

2.2.12 MALDI-TOF mass spectrometry

Following overnight trypsin digestion and C18 ZipTipping according to the manufacturer's instructions, peptide mixtures (0.5 μ L) were combined with an equal volume of α -cyano-4-hydroxy-cinnamic acid (α CHCA) matrix (5 mg/mL α CHCA in 50 % (v/v) acetonitrile (ACN), 0.1 % (v/v) trifluoroacetic acid (TFA)) and spotted onto a matrix-assisted laser desorption ionization mass spectrometry (MALDI-MS) target plate alongside ProteoMass MALDI-MS standards (angiotensin II, adrenocorticotrophic hormone fragment 18-39, oxidised insulin chain B, 0.5 pmol each), using the dried-droplet method. Peptide mass fingerprints were obtained on a Voyager DE Pro MALDI time-of-flight (TOF) Biospectrometry Workstation, in positive ion reflector mode, and used in a MASCOT protein database search (<http://www.matrixscience.com>) to identify proteins present within the sample.

2.2.13 LC-ESI-MS/MS methods

Samples were delivered into a Triple TOF 5600 mass spectrometer (AB Sciex) by automated in-line reversed phase liquid chromatography (LC) using an Eksigent NanoUltra cHiPLC System mounted with microfluidic trap and analytical column (15cm x 75 μ m) packed with ChromXP C₁₈-CL 3 μ M. A NanoSpray III source was fitted with a 10 μ m inner diameter PicoTip emitter (New Objective). Samples were loaded in 0.1% formic acid onto the trap which was then washed with 2% ACN/0.1% FA for 10 min at 2 μ L/min before switching in-line with the analytical column. A gradient of 2-50 % (v/v) ACN,

0.1 % (v/v) FA over 90 min was applied to the column at a flow rate of 300 nL/min. Spectra were acquired automatically in positive ion mode using information-dependent acquisition powered by Analyst TF 1.5.1. software, using mass ranges of 400-1600 atomic mass units (amu) in MS and 1000-1400 amu in MS/MS. Up to 25 MS/MS spectra were acquired per cycle (approx. 10Hz) using a threshold of 100 counts per sec, with dynamic exclusion for 12sec and rolling collision energy. The instrument was automatically calibrated after every fifth sample using a beta-galactosidase digest. Amino acid modifications were detected with ProteinPilot software v4.0 using the Paragon™ algorithm (Shilov *et al.* 2007) and the most recent version of the SwissProt database. Carboxyamidomethyl (IAA) (+57.0 amu) or NEM (+125.0 amu) were selected as variable modifications. Adducts were confirmed by visual inspection of MS/MS spectra. Changes in the susceptibility of a cysteine to modification by NEM or IAA were deemed relevant if observed ≥ 2 out of 6 biological repeats.

2.3 RESULTS

2.3.1 Optimisation of Keap1-V5 transfection in HEK293T cells

To obtain adequate Keap1-V5 expression in HEK293T cells to give sequence coverage sufficient (>70%) to detect cysteine modification, the protocol for cell transfection was optimised. A number of batches of 293T cells were transfected with Keap1-V5 or mock transfected. Batch 3, which showed the highest level of Keap1-V5 expression (Fig. 2.3A) was used in subsequent experiments. The conditions for Keap1-V5 immunopurification (IP) were optimised by varying the volume of V5-agarose beads and incubation time. An incubation time of 4 hr yielded the highest amount of Keap1-V5 following IP, whilst altering the volume of V5-agarose beads had minimal effect (Fig. 2.3B). The loss of Keap1-V5 in some samples indicates a loss of V5 agarose beads during washing steps. For subsequent experiments, immunopurification was carried out for 4 hr with 50 μ l V5-agarose beads.

2.3.2 MALDI validation of Keap1-V5

Following transfection of HEK293T cells using optimised conditions, MALDI-TOF analysis was performed to confirm expression, IP and tryptic digestion of Keap1-V5. These data show that the most highly represented proteins in the sample were mouse and rat Keap1 (Fig. 2.4A) which share 98% sequence homology. A Mascot search showed 75% sequence coverage of mouse Keap1 (Fig. 2.4B).

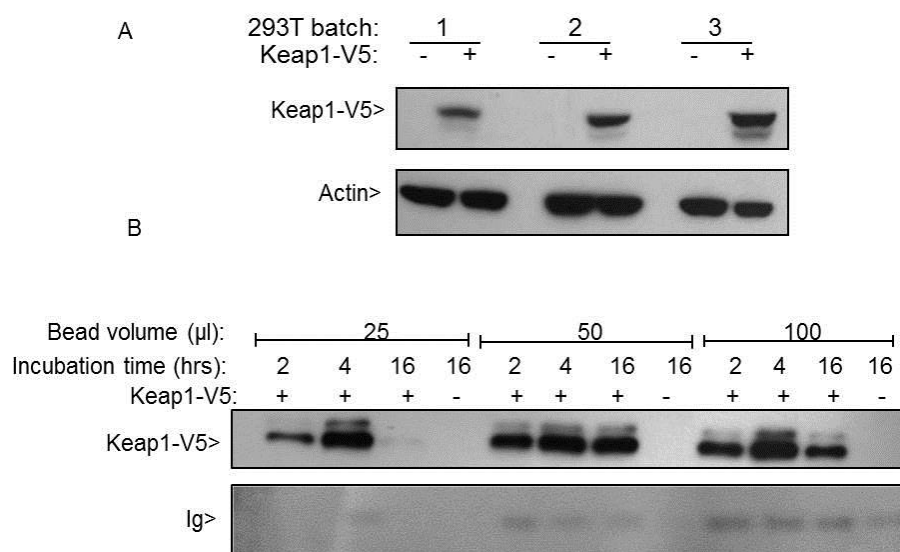


Figure 2.3. Optimisation of Keap1-V5 transfection in HEK293T cells. (A) Different batches of HEK293T cells (1,2,3) were transfected with 1xTE buffer (-) or Keap1-V5 plasmid (+) for 24 hr. (B) Cells transfected as in A were lysed, and clarified lysates incubated with differing volumes of anti-V5 agarose beads (25, 50, 100 µl) for increasing time periods (2, 4, 16 hr). The proteins eluted from the beads were resolved by SDS-PAGE. Expression levels of Keap1-V5 were assessed by western blotting using an anti-Keap1 antibody. The volume of anti-V5 agarose beads is indicated in the lower panel by a Ponceau S stain and highlights the immunoglobulin fraction of the monoclonal anti-V5 (Ig).

2.3.3 LC-ESI-MS/MS validation of Keap1-V5

The successful detection of Keap1 using MALDI-TOF mass spectrometry afforded confidence to use LC-ESI-MS/MS to detect Keap1 peptides in trypsin digests. Samples were prepared as in 2.3.2 and analysed using an AB SCIEX TripleTOF 5600 LC-ESI-MS/MS setup. A ProteinPilot search showed that mouse Keap1 was significantly represented (92.6% sequence coverage) and 188 mouse Keap1 peptides confidently detected (Fig. 2.4C). High sequence coverage is considered necessary for the reliable detection of covalent modifications of Keap1, as determined by previous users of this technique within the lab.

A Protein Summary Report

Format As	Protein Summary	Help
Significance threshold p<	0.05	Max. number of hits
		AUTO
Re-Search All	Search Unmatched	

Index

Accession	Mass	Score	Description
1. KEAP1_MOUSE	69508	100	Kelch-like ECH-associated protein 1 OS=Mus musculus GN=Keap1 PE=1 SV=1
2. KEAP1_RAT	69354	60	Kelch-like ECH-associated protein 1 OS=Rattus norvegicus GN=Keap1 PE=2 SV=1

B Mascot Search Results

Protein View

Match to: [KEAP1_MOUSE](#) Score: 100 Expect: 5.3e-05
 Kelch-like ECH-associated protein 1 OS=Mus musculus GN=Keap1 PE=1 SV=1

Nominal mass (M_r): 69508; Calculated pI value: 6.00
 NCBI BLAST search of [KEAP1_MOUSE](#) against nr
 Unformatted [sequence string](#) for pasting into other applications

Taxonomy: [Mus musculus](#)

Variable modifications: Carbamidomethyl (C)
 Cleavage by Trypsin: cuts C-term side of KR unless next residue is P
 Number of mass values searched: 359
 Number of mass values matched: 41
 Sequence Coverage: 75%

Matched peptides shown in **Bold Red**

```

1  MQPEPKLSGA PRSSQFLPLW SKCPEGAGDA VMYASTECKA EVTPSQDGNR
51  TFSYTLEDHT KQAFGVMNEL RLSQQLCDVT LQVKYEDIPA AQFMAHKVVL
101 ASSSPVFKAM FTNGLREQGM EVVSIIEGHP KVMERLIEFA YTASISVGEK
151 CVLHVMNGAV MYQIDSVVRA CSDFLVQQLD PSNAIGIANP AEQIGCTELH
201 QRAREYIYMH FGEVARQEEF FNLSHCQLAT LISRDDLNVR CESEVPHACI
251 DWVKYDCPQR RFYVQALLRA VRCHALTPRF LQTQLQKCEI LQADARCKDY
301 LVQIPQELTL HKPTQAVPCR APKVGRLIYT AGGYFRQSL S YLEAYNPSNG
351 SWLRLADLQV PRSGLAGCVV GGLLYAVGGR NNSPDGNTDS SALDCYNPMT
401 NQWSPCASMS VPRNRIGVGV IDGHIYAVGG SHGCIHSSV ERYEPERDEW
451 HLVAPMLTR IGVGVAVLNR LLYAVGGFDG TNRLNSAECY YPERNEWRFI
501 TPMNTIRSGA GVCVLHNCIY AAGGYDGDQ LNSVERYDVE TETWTFVAPM
551 RHHRSALGIT VHQGIYVVLG GYDGHTFLDS VECYDPDSDI WSEVTRMTSG
601 RSGVGVAVTM EPCRKQIDQQ NCTC
  
```

C

N	Unused	Total	% Cov	Accession #	Name	Species	Peptides(95%)
1	147.99	147.99	92.6	sp Q9Z2X8 KEAP1_MOUSE	Kelch-like ECH-associated protein 1 OS=Mus musculus GN=Keap1 PE=1 SV=1	MOUSE	188
2	60.53	60.53	79.7	sp P99024 TUBB5_MOUSE	Tubulin beta-5 chain OS=Mus musculus GN=Tubb5 PE=1 SV=1	MOUSE	57
3	49.32	49.32	83.5	sp P68373 TBA1C_MOUSE	Tubulin alpha-1C chain OS=Mus musculus GN=Tba1c PE=1 SV=1	MOUSE	44
4	38.58	38.58	65.6	sp P68480 ATP5B_MOUSE	ATP synthase subunit beta, mitochondrial OS=Mus musculus GN=Atp5b PE=1 SV=2	MOUSE	21
5	37.38	37.38	66.1	sp P11499 HSP90B_MOUSE	Heat shock protein HSP90-beta OS=Mus musculus GN=Hsp90ab1 PE=1 SV=2	MOUSE	25
6	35.96	35.96	63.3	sp P20162 VIME_MOUSE	Vimentin OS=Mus musculus GN=Vim PE=1 SV=3	MOUSE	24
7	32.20	32.20	48.9	sp P01869 IGH1M_MOUSE	Ig gamma-1 chain C region, membrane-bound form OS=Mus musculus GN=Ighg1 PE=1 S...	MOUSE	30
8	30.75	30.75	45.0	sp Q03265 ATPA_MOUSE	ATP synthase subunit alpha, mitochondrial OS=Mus musculus GN=Atp5a1 PE=1 SV=1	MOUSE	19

Protein Group 1 - Kelch-like ECH-associated protein 1 OS=Mus musculus GN=Keap1 PE=1 SV=1

Figure 2.4. Validation of Keap1-V5 Immunopurification. Following cell transfection with Keap1-V5 and immunopurification using anti-V5 beads, trypsin digestion preceded the sample analysis by mass spectrometry. (A) MALDI-TOF analysis protein summary report showed mouse Keap1 and rat Keap1 as highly represented in the immunopurified fraction. (B) A Mascot search shows 75% sequence coverage of mouse Keap1 (C) LC-ESI-MS/MS analysis confirmed the presence of mouse Keap1 with high sequence coverage.

2.3.4 Effect of chosen compounds on Nrf2 and GSH in cells

It was important to confirm that the compounds chosen for this investigation were capable of inducing Nrf2, and whether they induce changes in GSH. HEK293T cells were treated with the relevant vehicle control (DMSO, dH₂O or growth media) or Nrf2-inducing compound at the following concentrations: DNCB 100 μ M, Dex Mes 30 μ M, CDDO-Me 100 nM, BSO 300 μ M and H₂O₂ 200 μ M. The treatment conditions used in this study had previously been optimised in the lab as treatment duration is critical when investigating Nrf2 activation. Western blot analysis was performed on whole cell lysates. Nrf2 induction was seen with all compounds (Fig. 2.5A). Quantification of GSH was performed on samples prepared under the same conditions with these data showing a significant depletion of GSH by DNCB (98%) and BSO (72%) ($p \leq 0.01$ and $p \leq 0.05$, respectively) but not for other compounds (Fig. 2.5B).

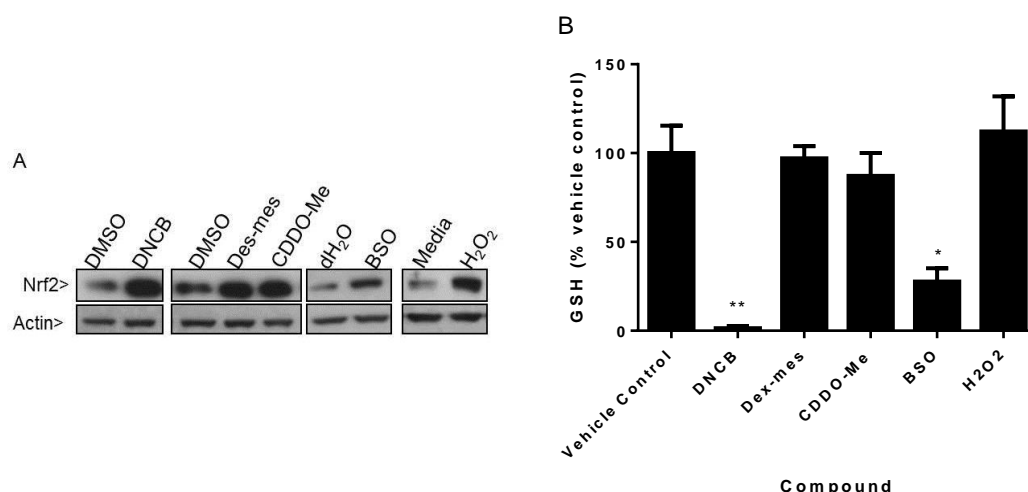


Figure 2.5. Nrf2 induction and GSH quantification by Nrf2-inducing compounds. HEK293T cells were treated with the indicated compounds. (A) Western blot analysis shows Nrf2 induction (representative blot from 3 biological repeats) (B) Levels of GSH in cell lysates following treatment. ** $p \leq 0.01$ * $p \leq 0.05$. Average GSH levels of 3 biological repeats.

2.3.5 Determining susceptibility of cysteine residues to modification

The LC-MS/MS method employed allows for the detection of differential capping of cysteine residues in proteins. Following treatment with Nrf2-inducing compounds, cells were treated with NEM which can covalently modify all reduced cysteine residues, i.e. those not involved in direct adducts with the Nrf2-inducing compound, or oxidised (Fig. 2.6). Following cell lysis and Keap1 immunopurification, DTT treatment reduces all reversibly oxidised cysteine residues (Fig. 2.6). The subsequent addition of IAA caps all newly reduced cysteine residues, whilst not affecting those previously adducted by the Nrf2-inducing compound, or NEM (Fig. 2.6). Cysteine residues less prone to forming an adduct with IAA indicate the presence of a reversible modification, such as oxidation, whilst residues more prone to IAA adduct formation indicate the presence of irreversible modifications. It has previously been determined in our lab that NEM and IAA can form adducts with all Keap1 cysteine residues, except Cys-622 and -624, which reside close to the V5 tag and are often not cleaved during trypsin digestion (data not shown).

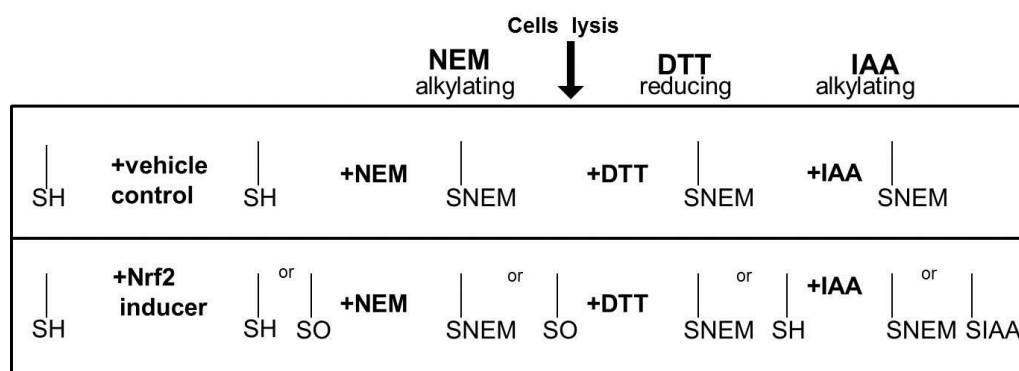


Figure 2.6. Schematic overview of the experimental protocol. Cells were treated with vehicle control or Nrf2 inducers followed by NEM. Cells were then lysed, Keap1-V5 was immunopurified and reduced with DTT prior to re-alkylation with IAA after which samples were prepared for LC-MS/MS.

2.3.6 Modification of cysteines in Keap1-V5 by DNCB

Cells expressing Keap1-V5 were treated with DNCB, which induces Nrf2 and depletes GSH (Fig. 2.5). LC-MS/MS analysis of immunopurified Keap1-V5 provided evidence for the covalent modification of cysteine residues, one of which has previously been shown to be targeted by DNCB (Cys-257) (Chia et al. 2010, Cople et al. 2008a), as well as a number not previously reported (Fig. 2.7). DNCB formed covalent adducts (detected as dinitrophenol (DNP) adducts) with the following cysteine residues: Cys-77, -226, -257, -319, -434, -489 and -622. Notably, Cys-23, -38, -151, -241, -249, -257, -297 and -319 of Keap1-V5 were found to be less prone to NEM capping following DNCB treatment compared to vehicle control (Fig. 2.7), suggesting DNCB induces modifications of these cysteines preventing NEM binding. Under the same conditions, Cys-23, -38, -241, -249, -297 and -434 of Keap1-V5 were found to be more prone to post-DTT capping by IAA following DNCB exposure. Given that amongst this subset of cysteines, only Cys-434 was covalently modified by DNCB, this datum implies that exposure to DNCB promotes reversible (potentially oxidative) modifications on specific cysteine residues in Keap1. These modifications may be responsible for the inability of NEM to bind to this group of cysteines. In addition, we noted that Cys-395 and -406 of Keap1-V5 showed decreased post-DTT capping by IAA following DNCB exposure (Fig. 2.7), suggesting an irreversible modification on these residues. These data show evidence of direct adducts between Keap1-V5 and DNCB, as well as reversible/irreversible modification of thiol groups, potentially caused by oxidation subsequent to GSH depletion.

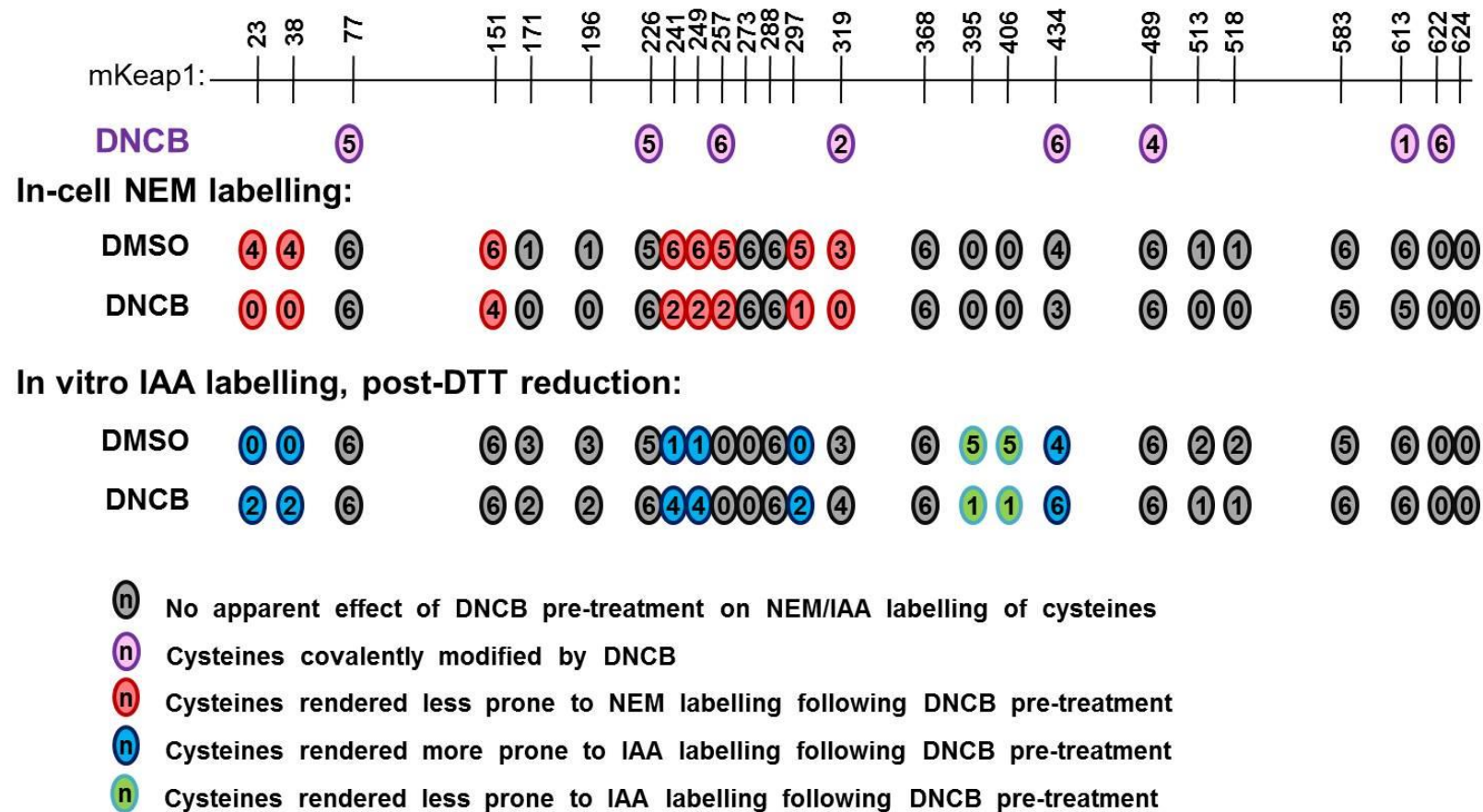


Figure 2.7. Labelling of Keap1-V5 cysteine residues by NEM and IAA following exposure of HEK293T cells to DNCB. HEK293T cells expressing Keap1-V5 were treated with DMSO or 100µM DNCB for 1hr, followed by 2mM NEM for 5 min. Keap1-V5 was immunopurified, incubated with DTT, and newly reduced cysteines capped with IAA. Trypsin digestion was performed and digests were analysed by LC-MS/MS for direct covalent modifications or NEM/IAA modifications. Numbers in circles represent number of independent experiments in which a modification was observed (n=6). Average protein coverage 84.7%.

2.3.7 Modification of cysteines in Keap1-V5 by Dex-mes

In cells expressing Keap1-V5 and treated with dex-mes, which induces Nrf2 in the absence of GSH depletion (Fig. 2.5), LC-MS/MS analysis revealed evidence for the direct covalent modification of a number of cysteine residues in Keap1-V5 by dex-mes (Cys-226, -257, -288, -434, -489 and -613) (Fig. 2.8). Whilst some of these cysteines have previously been shown to be targeted by dex-mes (Dinkova-Kostova *et al.* 2002) some of these modifications (Cys-266, -434, -489 and -613) have not previously been reported. Interestingly, one cysteine residue of Keap1-V5 (Cys-273) was found to be less prone to NEM capping following dex-mes treatment compared to vehicle control, indicating the presence of an irreversible modification (Fig. 2.8). This cysteine has previously been shown to be directly modified by dex-mes (Dinkova-Kostova *et al.* 2002) and would explain this observation. Additionally, there was an increase in the ability of IAA to cap Cys-226 and Cys-368 in Keap1-V5 following dex-mes and DTT treatment, indicating a reversible modification (Fig. 2.8). Furthermore, Cys-288 was shown to be less prone to post-DTT capping by IAA following dex-mes and DTT treatment, indicative of the irreversible modification of this residue- most likely the adduct formed between dex-mes and the thiol that we, and others (Dinkova-Kostova *et al.* 2002) have observed. These data highlight the covalent modification of cysteine residues in Keap1-V5 by dex-mes following the treatment of cells with the compound, as well as a limited number of reversible/irreversible modifications of thiol groups.

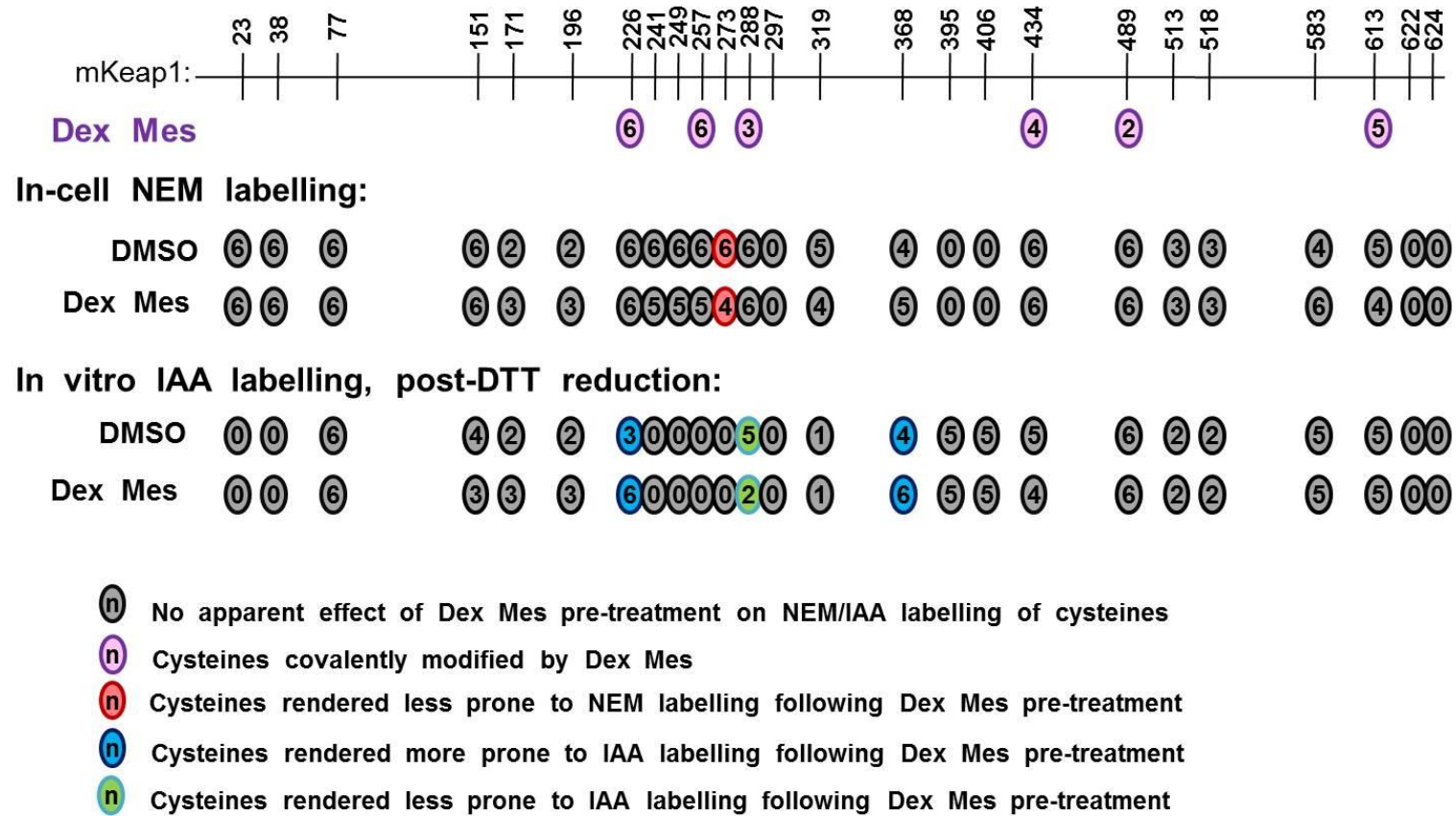


Figure 2.8. Labelling of Keap1-V5 cysteine residues by NEM and IAA following exposure of HEK293T cells to Dex Mes. HEK293T cells transiently expressing Keap1-V5 were treated with (DMSO or 30µM Dex Mes for 1hr, followed by 2mM NEM for 5 min. Keap1-V5 was immunopurified, incubated with DTT, and newly reduced cysteines capped with IAA. Trypsin digestion was performed and digests were analysed by LC-MS/MS for direct covalent modifications or NEM/ IAA modifications. Numbers in circles represent number of independent experiments in which a modification was observed (n=6). Average protein coverage 85.3%.

2.3.8 Modification of cysteines in Keap1-V5 by H₂O₂

Following treatment of Keap1-V5 expressing cells with H₂O₂, which induces Nrf2 in the absence of GSH depletion, there was no evidence for the covalent modification of cysteine residues in Keap1-V5 (Fig. 2.9). Whilst H₂O₂ does bind covalently to thiol groups, this would be rapidly degraded to form a sulphonic acid (S-O₃H), and oxygen (O₂) as a by-product. Interestingly, there were relatively few changes in the ability of NEM or IAA to modify cysteine residues in Keap1 (Fig. 2.9), indicating that the induction of Nrf2 by H₂O₂ is not associated with the substantial oxidative modification of Keap1-V5. Cys-434 was rendered more prone to IAA modification following DTT-mediated reduction (Fig. 2.9), suggesting a reversible modification on this amino acid, potentially oxidation. Additionally, Cys-513 and -518 were shown to be less prone to IAA modification following DTT treatment indicating non-reversible modification of these residues (Fig. 2.9). The protein coverage in these samples (73% average) was lower than in other experiments detailed in this chapter (all were above 80% average) which may explain why a number of cysteine containing peptides were not found to be modified by either NEM or IAA. However, of the peptides that were consistently detected, only a few residues (Cys-434, -513, 518) showed an altered susceptibility to modification by NEM or IAA following treatment with H₂O₂ that would implicate the oxidative modification of Keap1 as a mechanism of action for H₂O₂ as an inducer of Nrf2. As no covalent modification of Keap1-V5 is expected, or indeed detected, this implicates a mechanism of Nrf2 induction independent of Keap1, or changes in cell redox state.

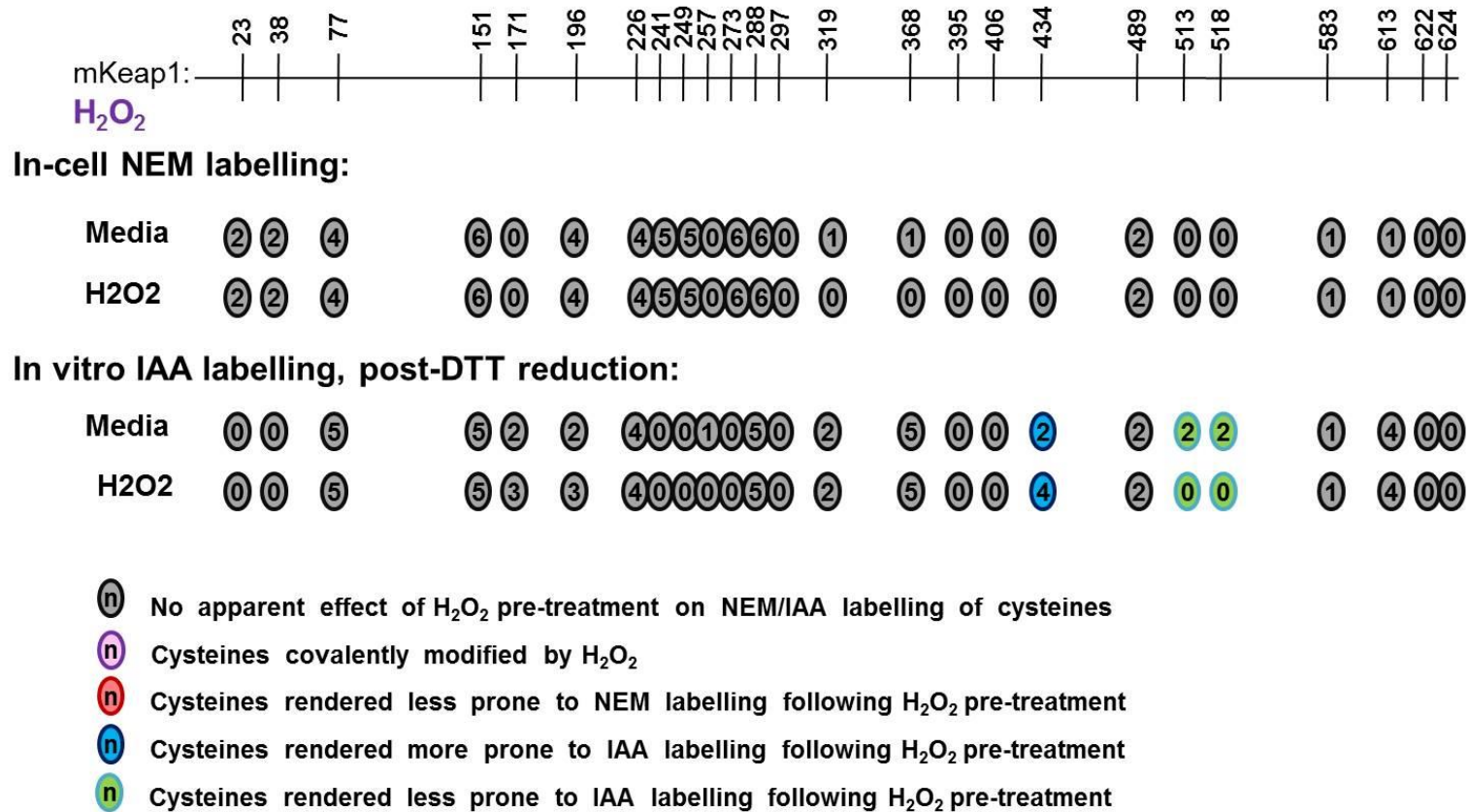


Figure 2.9. Labelling of Keap1-V5 cysteine residues by NEM and IAA following exposure of HEK293T cells to H_2O_2 . HEK293T cells transiently expressing Keap1-V5 were treated with cell growth media or 200 μM H_2O_2 for 1hr, followed by 2mM NEM for 5 min. Keap1-V5 was immunopurified, incubated with DTT, and newly reduced cysteines capped with IAA. Trypsin digestion was performed and digests were analysed by LC-MS/MS for direct covalent modifications or NEM/IAA modifications. Numbers in circles represent number of independent experiments in which a modification was observed (n=6). Average protein coverage 73.0%.

2.3.9 Modification of cysteines in Keap1-V5 by BSO

Consistent with previous published data from our group (Chia et al. 2010, Copple et al. 2008a), LC-MS/MS analysis of Keap1-V5 peptides following the treatment of cells with BSO yielded no evidence for the covalent modification of cysteines in Keap1-V5 by this compound (Fig. 2.10), which induces Nrf2 in conjunction with GSH depletion (Fig. 2.10). Interestingly, no other modifications indicative of cysteine oxidation were detected in Keap1-V5 purified from cells exposed to BSO (Fig. 2.10). This raises the possibility that the mechanism of Nrf2 induction by BSO is independent of Keap1.

Unpublished data from our lab demonstrates that BSO pre-treatment can render Keap1-V5 Cys-257 less available for DNP modification (data not shown). DNP adduction of Cys-257 was only observed in two of five experiments when cells were pre-treated with BSO, and five out of five experiments when BSO was omitted. This may indicate a change in the redox state of this residue that is beyond the limit of detection of the method employed here. This observation indicates that BSO is able to alter the sensitivity of at least one Keap1 cysteine residue to modification by an Nrf2-inducing electrophile. It is worth highlighting that, in this study, following treatment with vehicle control or BSO, Cys-257 is modified by IAA more frequently than following treatment with the other vehicle controls or Nrf2-inducing compounds (Fig. 2.10). Further work is needed to define the chemical basis of this phenomenon.

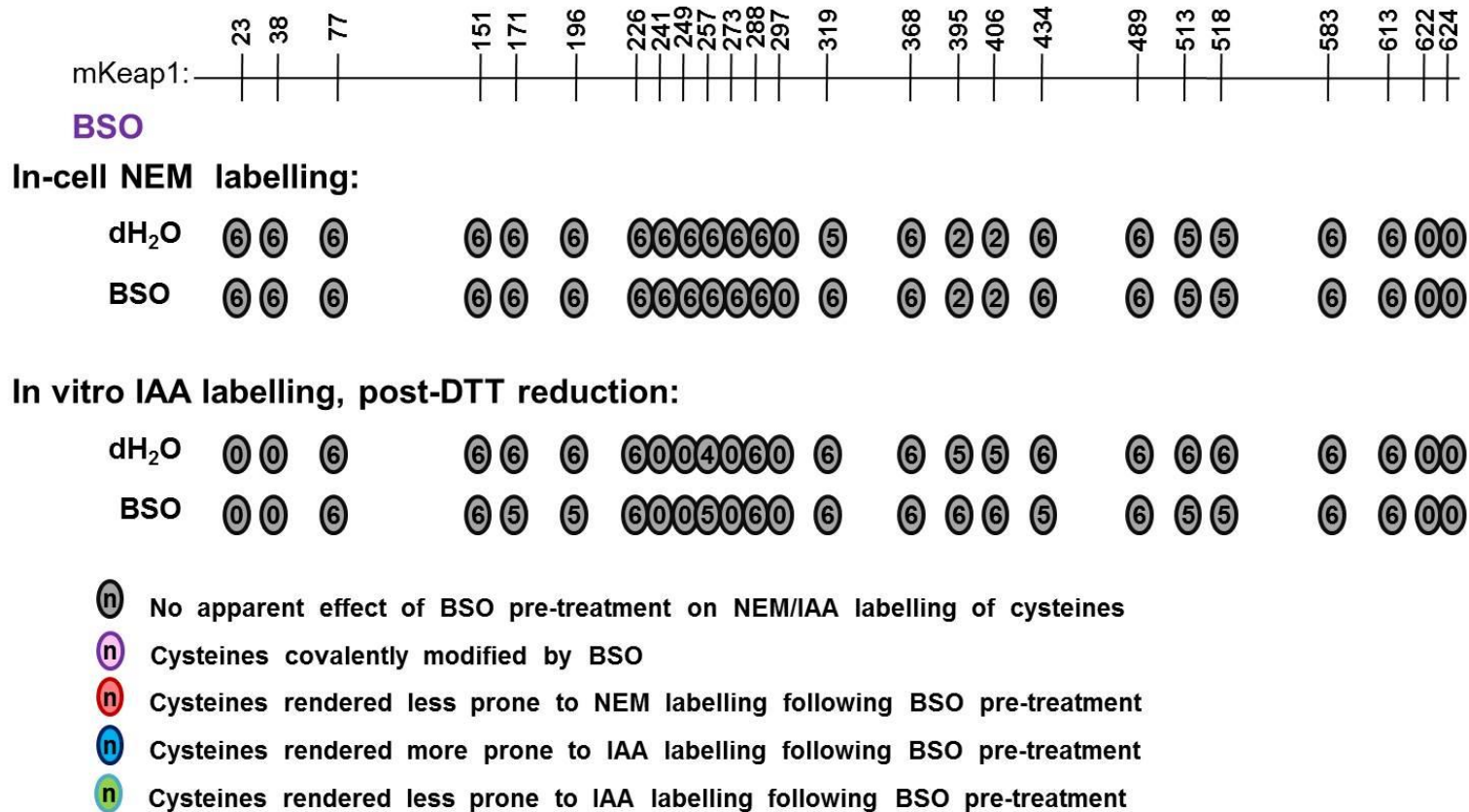


Figure 2.10. Labelling of Keap1-V5 cysteine residues by NEM and IAA following exposure of HEK293T cells to BSO. HEK293T cells transiently expressing Keap1-V5 were treated with dH₂O or 300µM BSO 1hr, followed by 2mM NEM for 5 min. Keap1-V5 was immunopurified, incubated with DTT, and newly reduced cysteines capped with IAA. Trypsin digestion was performed and digests were analysed by LC-MS/MS for direct covalent modifications or NEM/IAA modifications. Numbers in circles represent number of independent experiments in which a modification was observed (n=6). Average protein coverage 88.5%.

2.3.10 Modification of cysteines in Keap1-V5 by CDDO-Me

In cells expressing Keap1-V5 and treated with the potent Nrf2 inducer CDDO-Me, LC-MS/MS analysis provided no evidence for the direct covalent modifications of any cysteine residues in Keap1-V5 by the compound (Fig. 2.11). Additionally, there was no detectable change in the ability of NEM to modify any of the cysteine residues in immunopurified Keap1-V5 (Fig. 2.11). Interestingly, a subset of cysteine residues (Cys-151, -226 -369) were found to be more prone to IAA modification following reduction with DTT, indicating the presence of reversible modification of these residues (Fig. 2.11). Additionally, Cys-434 was rendered less prone to IAA modification following DTT treatment (Fig. 2.11), implying the presence of an irreversible modification on this residue. Cys-151 of Keap1 has been implicated in the activation of Nrf2 by TPs (Eggler *et al.* 2009, Cleasby *et al.* 2014), however, the importance of this residue in the mechanism of TP-mediated Nrf2 induction is the subject of controversy (Takaya *et al.* 2012). Our data suggests that Cys-151 may be reversibly modified by this compound, thus potentially playing a role in its chemico-biological mechanism of action. These data are also in agreement with the purported reversibility of this compound when binding thiol groups (Ahmad *et al.* 2006) and may explain the difficulty in detecting changes in modification by NEM and IAA following the treatment of cells with this compound. The chemical mechanism of action of this compound as an inducer of Nrf2 is further examined in Chapter 3.

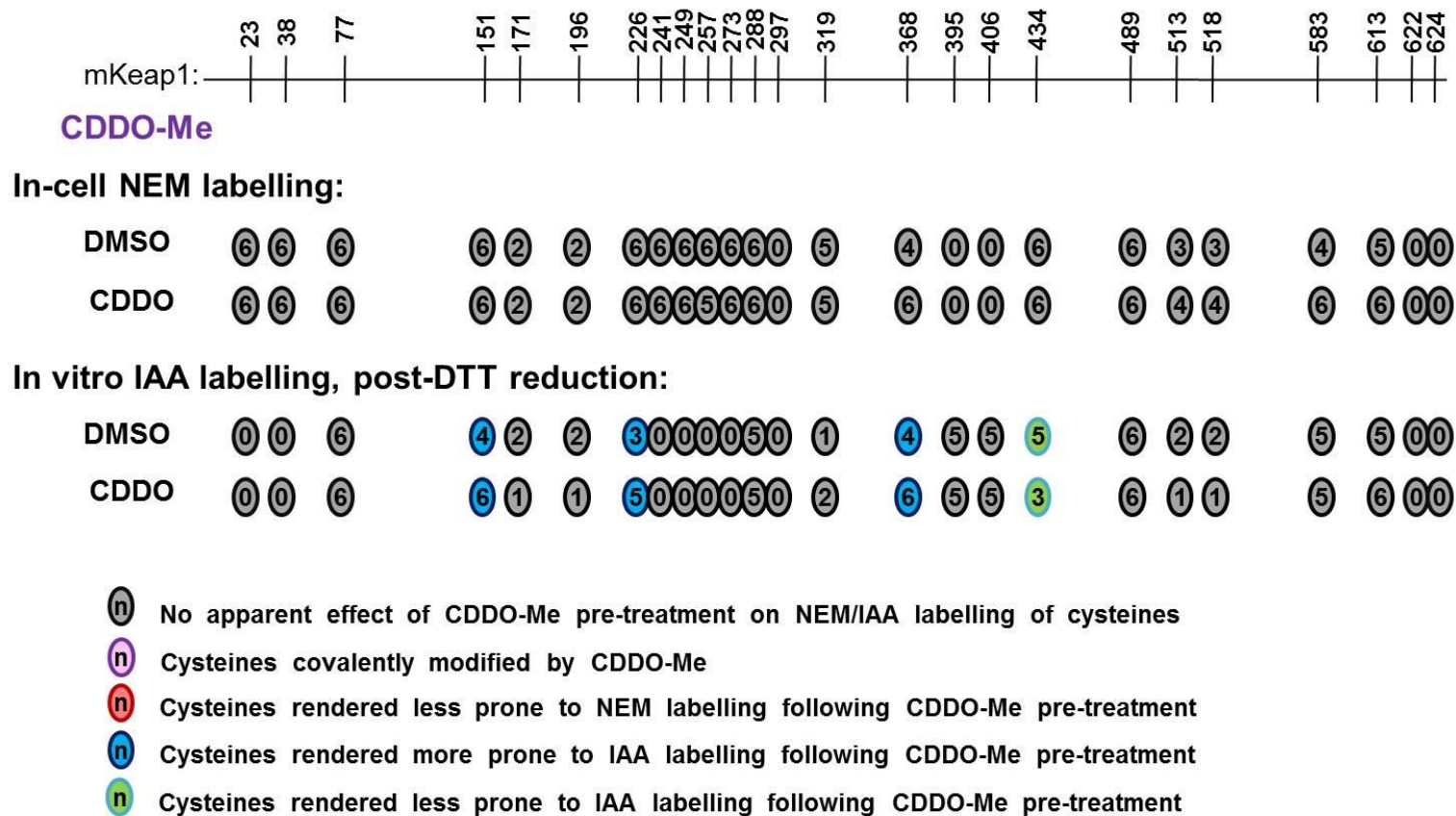


Figure 2.11. Labelling of Keap1-V5 cysteine residues by NEM and IAA following exposure of HEK293T cells to CDDO-Me. HEK293T cells transiently expressing Keap1-V5 were treated with DMSO or 100µM CDDO-Me 1hr, followed by 2mM NEM for 5 min. Keap1-V5 was immunopurified, incubated with DTT, and newly reduced cysteines capped with IAA. Trypsin digestion was performed and digests were analysed by LC-MS/MS for direct covalent modifications or NEM/IAA modifications. Numbers in circles represent number of independent experiments in which a modification was observed (n=6). Average protein coverage 84.4%.

2.4 DISCUSSION

Keap1 cysteine residues are purported to serve as sensors of both chemical and oxidative stress. The selective modification of Keap1 cysteine residues by Nrf2-inducing compounds, and Nrf2 induction in the absence of adduct formation, has inspired the hypothesis that oxidative modifications caused by changes in the redox state of the cell, for example by the depletion of GSH, may contribute to the de-regulation of Nrf2 provoked by certain chemical entities, which do not form covalent adducts with proteins.

The data presented here support the proposal that there are modifications of Keap1-V5 provoked by DNCB that may be attributed to oxidation. Previous data from our lab shows that the mutation of Cys-257 to a non-reactive amino acid does not attenuate the ability of this compound to induce Nrf2, suggesting that the direct covalent modification of Cys-257 is not involved in the mechanism by which DNCB induces Nrf2 in cells (data not shown). The importance of direct covalent modification of other cysteines identified here (Cys-77, -226, -434, -489 and -622) requires further investigation. It has been demonstrated previously that Cys-23/-38; Cys-241/-249; and Cys-257/-297 of Keap1 form disulphide bonds upon incubation of the protein with an excess of glutathione (Holland *et al.* 2008). It is plausible that exposure of cells to DNCB results in the formation of disulphide bonds within/between this subset of residues, which our data supports, although more extensive analysis would be required to confirm this. The accumulation of reversibly oxidised peroxiredoxin and thioredoxin proteins induced by DNCB has been reported,

indicating the inhibition of thioredoxin reductase (TRX-R) (Baty *et al.* 2005). As thioredoxin reductase inhibition has been shown to induce Nrf2-mediated transcription, it is possible that this is an alternative mechanism of Nrf2-activation by DNCB. It is also possible that the oxidation/covalent modification of Keap1 by DNCB may be sufficient for perturbation of the Nrf2/Keap1 interaction, leading to Nrf2 activation.

Dex-mes forms covalent adducts with Cys-288 and Cys-273. These residues are known to be required for the basal regulation of Nrf2 by Keap1 (Kobayashi *et al.* 2004), and their mutation to a less reactive residue renders Keap1 unable to suppress Nrf2 (Yamamoto *et al.* 2008). Notably, we have shown here that dex-mes provokes changes in Keap1 cysteine redox state, indicative of oxidative modification. Therefore, whilst direct modification of Keap1 cysteine residues by dex-mes may result in Nrf2 induction, the importance of the oxidative modification of cysteine residues by this compound requires further investigation. There is little experimental evidence for the ability of dex-mes to oxidise thiol groups directly, therefore it is likely that the oxidation seen in this study is due to changes in the redox state of the cell, however not dependent on GSH depletion.

Hydrogen peroxide is a strong oxidising agent which forms highly unstable adducts with thiol groups, thus it is improbable that LC-MS/MS techniques will be able to detect them directly (Luo *et al.* 2005). H₂O₂ was found to alter the susceptibility to modification of only a few cysteine residues, including Cys-434 which lies within the Nrf2 binding region of Keap1. It has been

shown that under situations of oxidative stress, glutathionylation of Keap1 Cys-434 may be sufficient for the activation of Nrf2 (Holland and Fishbein 2010). The formation of disulphide bonds between two Keap1 molecules at Cys-151 in response to H_2O_2 has previously been demonstrated (Fourquet *et al.* 2010), and it is possible that the analytical method used here was not sensitive enough to detect such a modification. Moreover, they observed that changes in oxidation state were transient (Fourquet *et al.* 2010), thus there is the potential that the disulphide bond was degraded during our 1 hr exposure of cells. As direct adducts are formed then rapidly degraded, they may play a part in Nrf2 induction, however, due to the absence of alternative modification of Keap1 observed here, our hypothesis regarding the oxidative modification by H_2O_2 does not seem to be a viable mechanism of Nrf2 induction. This is surprising as H_2O_2 is known to oxidise protein thiols and alter their function, as is the case with the oxidation of peroxiredoxins (Pillay *et al.* 2009).

The depletion of GSH by BSO did not alter the susceptibility of cysteine residues to modification by NEM/IAA, within the limits of detection of our assay. This implies that the activation of Nrf2 by BSO may be independent of Keap1. Interestingly, the GSH-depleting action of BSO can increase cellular levels of nitro-cGMP, a signalling molecule that can adduct Keap1 (Fujii *et al.* 2010). However it is not clear which residue this occurs on or whether it results in Nrf2 activation, and we do not see evidence for this modification in this study. Whilst there is evidence for the oxidation of proteins following BSO treatment of cells (Go *et al.* 2013), we do not show the oxidation of Keap1 by BSO treatment in our study.

CDDO-Me is a potent Nrf2-inducer showing promise as a therapeutic agent due to antioxidant, anti-inflammatory and pro-apoptotic properties (Wang *et al.* 2014). Whilst we saw that CDDO-Me rendered a subset of residues more (Cys-151, -226, -368), or less (Cys-434), susceptible to further modification, the inability to detect direct interactions between triterpenoids and Keap1 is not unique to our lab, due to their ability to selectively and reversibly bind thiol groups (Couch *et al.* 2005). The mechanism of action of CDDO-Me with respect of Nrf2 induction is largely unknown, and its inclusion in this investigation was to gain insight into the potential for it to modify Keap1. Published data implicates the involvement of Cys-273 and -288 (Dinkova-Kostova *et al.* 2005, Ahn *et al.* 2010) with dispute over Cys-151 (Takaya *et al.* 2012, Egger *et al.* 2009) and the data presented here further indicates a role for the latter residue. There is evidence for the oxidation of unidentified mitochondrial proteins by the TP CDDO which is potentially a mechanism of inducing apoptosis via attenuating the permeability transition pore (Brookes *et al.* 2007). Moreover, the ability to TPs to inhibit the inflammatory response mediated by NF- κ B has been shown to be facilitated by TP-mediated inhibition of I κ B α kinase β (IKK β) via a reversible modification of Cys-179 (Ahmad *et al.* 2006), which could be oxidation or reversible adduct formation. Therefore, the oxidation of Keap1 by CDDO-Me is worth investigating as a mechanism of Nrf2 induction. A more in-depth review of published data regarding CDDO-Me modification of Keap1, and further experimental investigation, is presented in Chapter 3.

Previous attempts to detect the native redox state of Keap1 cysteine residues by LC-MS/MS have not been successful as Keap1 requires alkylation of cysteine residues for efficient MS detection and analysis. If this step is omitted, a loss of protein coverage is observed (data not shown). The reversible and dynamic nature of oxidation makes detection extremely challenging. A MS method for detecting sulphinic (S-O₂H) and sulphonic acid (S-O₃H) *in vivo* and *in vitro* has recently been published (Lee *et al.* 2013). The method is a label-free, quantification method with high sensitivity (Lee *et al.* 2013), however attempts to replicate this method proved unsuccessful with our MS set-up and would require substantial method optimisation. Furthermore, methods utilising dimedone-based chemical probes to label sulphenic acid (S-OH) are common (Klomsiri *et al.* 2010) however, this method only identifies reversible oxidative states and not irreversible oxidative states of cysteines. Multiple reaction monitoring (MRM), an MS method used to detect modification involving isotope labelling and differential alkylation of residues, has been adapted to detect oxidative modifications in some enriched proteins (Held *et al.* 2010). The use of such an approach here would require the development of a method to detect each cysteine-containing peptide of Keap1, of which there are 19. Antibodies targeted towards oxidised peptides have been used successfully to detect oxidation of recombinant protein and components of cell lysates (Woo *et al.* 2003), however, the use of such an approach in this context would require the synthesis of antibodies targeted to all cysteine-containing peptides in Keap1. Non-reducing SDS-PAGE can detect oxidised Keap1 following the treatment of cells to H₂O₂ (Fourquet *et al.* 2010), however such an approach is unable

to identify specific target residues unless a mutagenesis approach is taken. As a result, there is considerable scope for the improvement of methods available for distinguishing the oxidation states of cysteine residues in proteins. Such advances would better enable the occurrence and importance of Keap1 oxidation to be determined.

The data presented here provides evidence that Keap1 cysteine residues may undergo oxidation in response to GSH depletion, and under conditions of Nrf2 induction, or that GSH-depleting compounds may alter the susceptibility of Keap1 cysteines to modification. This may represent an alternative mechanism of Nrf2 activation, as direct covalent modification of cysteines is not necessarily a pre-requisite for Nrf2 activation. To test the functional importance of the oxidative modification of Keap1 for the induction of Nrf2, it would be necessary to perform mutagenesis experiments. It is worth investigating in our cell model, whether the oxidation of one or more cysteines can lead to the formation of intra- and inter-molecular disulphide bond formation, which could render Keap1 unable to repress Nrf2 (Wakabayashi *et al.* 2004, Fourquet *et al.* 2010). In a physiological sense, the oxidation of Keap1 thiols would be preferable to their irreversible covalent modification, as the former would allow for the regeneration of fully-functional Keap1, possibility facilitated by the Nrf2-mediated induction of antioxidant proteins (e.g. TRX, TRX-R, GSH) which serve to maintain the redox state of important thiol-containing proteins. On the other hand, the irreversible inactivation of Keap1 by the formation of stable covalent adducts would require *de novo* synthesis of Keap1 to regain protein function.

CHAPTER 3

**CHARACTERISING THE COVALENT MODIFICATION OF
KEAP1 BY TRITERPENOID, POTENT INDUCERS OF NRF2
SIGNALLING**

CONTENTS

3.1 INTRODUCTION	- 95 -
3.2 MATERIALS AND METHODS	- 99 -
3.2.1. Materials and reagents	- 99 -
3.2.2. Cell culture	- 99 -
3.2.3. H4IIE ARE-reporter cell luciferase assay.....	- 100 -
3.2.4. Western blotting- whole cell lysates.....	- 101 -
3.2.5. Quantification of glutathione levels	- 101 -
3.2.6. Expression and purification of recombinant proteins	- 102 -
3.2.7. Determination of on-bead protein content.....	- 103 -
3.2.8. Treatment of recombinant protein.....	- 104 -
3.2.9. Preparation of recombinant protein for LC-ESI-MS/MS	- 105 -
3.2.10. LC-ESI-MS-MS methods	- 105 -
3.2.11. Mouse Keap1-V5 plasmid purification.....	- 106 -
3.2.12. Transfection of cells with Keap1-V5	- 106 -
3.2.13. Cell treatment.....	- 106 -
3.2.14. Immunopurification of Keap1-V5.....	- 106 -
3.2.15. Preparation of Keap1-V5 for LC-ESI-MS/MS	- 107 -
3.2.16. <i>In silico</i> modelling	- 107 -
3.2.17. Data analysis.....	- 108 -
3.3. RESULTS	- 109 -
3.3.1. Effect of chemically tuned TPs on the Nrf2 pathway in cells...	- 109 -
3.3.2. LC-ESI-MS/MS validation of recombinant protein.....	- 111 -
3.3.3. LC-ESI-MS/MS evidence for TP modification of GSTP1-His..	- 111 -
3.3.4. LC-ESI-MS/MS evidence for TP modification of Keap1-His ...	- 114 -
3.3.5. Investigating the ability of CDDO-Me to compete with CDDO-Epoxyde to covalently modify protein thiols	- 119 -
3.3.6. CDDO-Epoxyde forms covalent adducts with Keap1-V5 in cells-	123 -
3.3.7. Molecular modelling of CDDO-Epoxyde modification of Keap1-	127 -
3.3.8. Correlation of TP potency towards Nqo1 activity and Keap1 covalent binding score	- 129 -
3.3.9. Correlation of TP potency towards Nqo1 activity and Keap1 non-covalent binding score	- 132 -
3.4 DISCUSSION	- 135 -

3.1 INTRODUCTION

The Nrf2 pathway plays a vital role in defining the susceptibility of cells to chemical and oxidative insults. This, in combination with links between Nrf2 and the pathology of many diseases, has resulted in considerable interest in the manipulation of this pathway for therapeutic benefit (Copple 2012). Such manipulation may involve the pharmacological activation or inhibition of Nrf2. The activation of Nrf2 may reduce the onset of pathologies associated with oxidative stress, such as cancer, inflammation and degenerative disease (Hybertson *et al.* 2011). Alternatively, the inhibition of Nrf2 has been shown to sensitise cancer cells to treatment with chemotherapeutic agents and reduce tumour size (Ren *et al.* 2011). Whilst there are a number of known Nrf2 inducers, none are as potent as those synthesised from TPs, which are naturally produced in many plants (Phillips *et al.* 2006).

TPs exhibit anti-inflammatory and anti-tumorigenic properties *in vivo* (Nishino *et al.* 1988, Huang *et al.* 1994, Singh *et al.* 1992). In order to improve the potency of naturally occurring TPs (such as oleanolic acid), medicinal chemists have made modifications to the basic TP structure (Dzubak *et al.* 2006, Connolly and Hill 2005) giving rise to compounds such as CDDO, CDDO-Im and CDDO-Me. These are, to our knowledge, the most potent anti-inflammatory and anti-carcinogenic TPs described to date (Liby *et al.* 2007). The increase in potency is concurrent with additional health benefits including anti-viral, anti-microbial and antioxidant properties (Jung *et al.* 2004). The

diverse biological effects of TPs have been attributed to their ability to react with nucleophiles within the cell, such as the thiol group of cysteine residues (Liby *et al.* 2007, Couch *et al.* 2005). Moreover, the antioxidant and anti-inflammatory effects of these compounds is purported to be due to their ability to induce Nrf2 (Liby and Sporn 2012). CDDO-Me activates Nrf2 signalling at concentrations approximately 1000-fold lower than many other inducers (Copples *et al.* 2014). However, the chemico-biological mechanism that underlies the ability of TPs to induce Nrf2 remains largely unknown.

Due to the established role of Keap1 as a sensor of stress, and the ability of TPs to react selectively and reversibly with nucleophiles (Couch *et al.* 2005), we hypothesised that CDDO-Me induces Nrf2 via the reversible covalent modification of one or more cysteine residues in Keap1. To date, there have been no reports describing the formation of direct adducts between CDDO-Me (or other TPs), and specific cysteine residues in the full length Keap1 protein (or other proteins). We postulate that the selective and reversible nucleophilic addition between TPs and non-protein thiols (Couch *et al.* 2005) underlies the difficulty in detecting adducts between CDDO-Me and Keap1 (i.e. using standard LC-MS/MS techniques). We further hypothesised that the reversibility accounts for the potent nature of CDDO-Me as an inducer of Nrf2. For example, whilst electrophiles which irreversibly bind thiol groups will be removed by detoxification mechanisms, i.e. by conjugation with GSH, CDDO-Me can evade this, enabling each molecule of the compound to bind multiple Keap1 molecules.

To examine the above hypothesis, and through a collaboration with the Department of Chemistry at the University of Liverpool, we have synthesised novel TPs which can be used as biochemical tools to characterise the covalent modification of thiols by CDDO-Me. Indeed, through the chemical tuning of CDDO-Me, we have generated a TP capable of irreversible adduct formation with the model thiol β -mercaptoethanol (confirmed by NMR and MS; data presented in thesis of Michael Wong). The cyano (CN) group on the A ring of CDDO-Me acts as an electron withdrawing group and the double bond is rich in electrons, attracting electrons from nucleophiles and enabling soft nucleophiles to react. However, the electron withdrawing group affords the compound with a reversible nucleophilic binding property. An epoxide group is a highly strained group, making it more reactive than other ethers, and has been used as affinity probes for protein labelling (Chen *et al.* 2003). When an epoxide group is added to the A ring of CDDO-Me (yielding CDDO-Epoxy, Table 3.1), nucleophilic attack opens the epoxide ring, forming a stable, irreversible adduct.

Due to the complexity of the Keap1 protein structure, the vast number of cysteine residues, and the lack of evidence for CDDO-Me binding to protein thiols, we used recombinant glutathione-S-transferase pi (GSTP1) as a model protein to determine whether the TPs are capable of forming adducts with protein thiols. Of the four cysteine residues present in GSTP1, one of these (Cys-47) is highly reactive, and has previously been used to characterise site-specific protein modification by electrophilic compounds, including the reactive metabolite of paracetamol (NAPQI) (Jenkins *et al.*

2008), DNCB (Caccuri *et al.* 1992), and NEM (Tamai *et al.* 1990), using LC-MS/MS. We investigated the ability of TPs to bind to purified recombinant GSTP1 and Keap1 using LC-MS-MS techniques. This was further investigated by transfecting HEK293T cells with Keap1-V5 and treating with the TPs. Moreover, we use an *in silico* approach using homology modelling and the crystal structure of the Keap1 BTB domain recently published by Cleasby *et al.* (2014), to model the point of interaction between Keap1 cysteine residues and TPs. We use these data to correlate their covalent and non-covalent interactions with Keap1 thiol groups with their potency towards the Nrf2 pathway. **In this chapter we use chemically tuned TPs to test the hypothesis that CDDO-Me induces Nrf2 via the covalent modification of one or more cysteine residues in Keap1.**

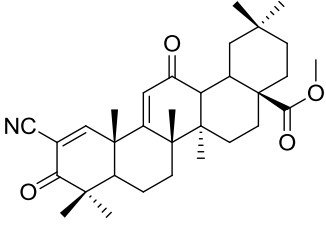
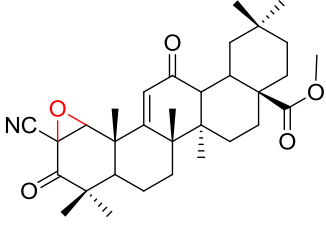
Triterpenoid	Mwt (Da)	Thiol binding properties	Chemical structure
CDDO-Me C ₃₂ H ₄₃ NO ₄	505.7	Reversible	
CDDO-Epoxyde C ₃₂ H ₄₃ NO ₅	521.3	Irreversible	

Table 3.1 Chemical structure and properties of the semi-synthetic TPs used in this study.

3.2 MATERIALS AND METHODS

3.2.1. Materials and reagents

Both pET-21a(+)/Keap1-transformed BL21 (DE3) and pET-15b(+)/GSTP1-transformed BL21 (DE3) *E.coli* stocks were generated at the CDSS, University of Liverpool. All TPs were synthesised at the Department of Chemistry, University of Liverpool, by Michael Wong. H4IIE cells stably expressing the ARE8L-reporter transgene (originally generated by Dr. Joanne Walsh, CDSS, University of Liverpool) were provided by Prof. Alex Odermatt (Department of Pharmaceutical Sciences, University of Basel, Switzerland). All antibodies used were from Abcam (Cambridge, UK). GS-800 calibrated imaging densitometer was from Bio-Rad (Hemel Hempsted, UK) and TotalLab 100 software was from Nonlinear Dynamics (Newcastle, UK). Power Broth was from Molecular Dimensions (Suffolk, UK). Bright-Glo luciferase assay system and Glo lysis buffer were from Promega (Southampton, UK). Sonication was performed in a Soni-prep 150 from MSE (London, UK). All other reagents were either described in Section 2.2.1, or of analytical or molecular grade and from Sigma-Aldridge (Poole, UK).

3.2.2. Cell culture

HEK293T cells were maintained as described in Section 2.2.2. Rat hepatoma H4IIE ARE-reporter cells were maintained in the same way but in Dulbecco's modified Eagle's medium (DMEM) supplemented with 584 mg/L L-glutamine,

10% heat inactivated fetal bovine serum (FBS), 5mL sterile filtered 100xnon-essential amino acid solution and 1mM sterile filtered HEPES solution. The culture medium was antibiotic free. Cells were counted as in Section 2.2.2.

3.2.3. H4IIE ARE-reporter cell luciferase assay

To determine the ability of the TPs to activate the expression of ARE driven genes which are commonly activated by Nrf2, we obtained a cell line which contains an ARE-driven luciferase reporter gene. Luciferases are a class of oxidative enzymes found in several species that enable the host to bioluminesce in the presence of luciferin. The emission can be read using a luminometer and is directly correlated to the level of ARE activation (Fig 3.1).

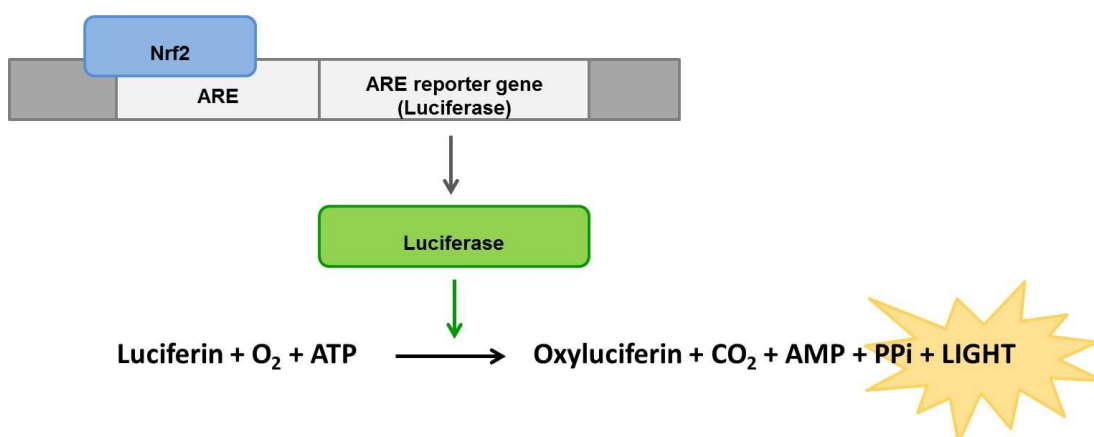


Figure 3.1. Schematic of ARE-reporter luciferase assay. Upon translocation to the nucleus, Nrf2 binds to the ARE in the promoter region of Nrf2 regulated genes. In this cell line, luciferase is under the control of an ARE promoter therefore luciferase protein is synthesised following Nrf2 activation. On addition of luciferin, in the presence of oxygen (O₂) and adenosine triphosphate (ATP), luciferase catalyses the formation of oxyluciferin, carbon dioxide (CO₂), adenoside monophosphate (AMP), inorganic pyrophosphate (PPi) and light which can be quantified using a luminometer.

Cells were plated at 2.0×10^4 cells per well in 0.2 mL media onto a sterile Nunclon Δ flat bottom 96 well plate, and returned to the incubator overnight. The cells were then treated with the compound of interest at the stated concentrations, diluted in DMSO to a final volume of 0.5% (v/v). The cells were returned to the humidified incubator for 24 hours, before adding 0.1 mL 1x Glo Lysis buffer to each well. The plate was shaken at 700 rpm for 5 min to provoke cell lysis. A proportion (80 μ L) of lysate was transferred to a flat-bottomed white 96-well microplate and 20 μ L of Bright-Glo luciferase reagent was added. The plate was shaken at 700 rpm for 15 sec prior to quantification of luminescence on a Varioskan Flash Spectra Luminometer.

3.2.4. Western blotting- whole cell lysates

For the measurement of Nrf2 activation, H4IIE ARE-reporter cells were seeded into 12-well Nunclon Δ cell culture plates at 3.0×10^5 cells/well and returned to the humidified incubator overnight. Cells were treated with increasing doses of the TPs dissolved in DMSO (final volume of 0.5 % (v/v)) for 1 or 24 hrs. Cells were washed twice with 1 mL PBS before lysis in 60 μ L RIPA buffer. Protein content was measured as described in Section 2.2.7 and western blotting for Nrf2 and Nqo1 was carried out as in Section 2.2.9.

3.2.5. Quantification of glutathione levels

H4IIE cells were treated with increasing concentrations of the compounds for up to 24hr before glutathione levels were quantified as in Section 2.2.8.

3.2.6. Expression and purification of recombinant proteins

LB broth or Power Broth (0.02 L), supplemented with 100 µg/mL ampicillin, was inoculated with 50 µL pET-21a(+)/GSTP1-transformed BL21 (DE3) or pET-21a(+)/Keap1-transformed BL21 (DE3) glycerol stock respectively and incubated at 37 °C, 220 rpm, overnight. The cultures were diluted to 1 L with the relevant broth containing 100 µg/mL ampicillin, and incubated at 37 °C, 220 rpm. At 30 minute intervals, the optical density at 600 nm (OD_{600}) was measured using a spectrophotometer, to ensure that the cultures were at the early-log phase of growth ($OD_{600} \sim 0.4$). Upon reaching this point in the growth phase, His-tagged protein expression was induced over 24 hr, at room temperature, 150 rpm, with 1 mM isopropyl- β -Dthiogalactopyranoside (IPTG). For Keap1-His only, the pH of the culture was adjusted to 7.5 with 1M Tris base. Bacteria were then pelleted at 5000 g, for 5 min, and re-suspended in 10 mL His buffer (0.5 M NaCl, 20 mM imidazole, 20mM Na_2HPO_4 , pH 8.0). This was divided into equal aliquots in 50 mL tubes and disrupted by sonication (60 sec, followed by 30 sec recovery, x 3 repeats). Disrupted bacteria were divided into 1.5 mL aliquots and cell debris was pelleted at 18,000 g for 10 min. The supernatants were then pooled and frozen at -80°C before being thawed and re-centrifuged at 18,000g for 10minutes, and re-pooled. The resulting supernatant was incubated at a ratio of 1:1 lysate (GSTP1) or 10:1 lysate (Keap1) to dry volume HIS-Select nickel (Ni^{2+}) -charged agarose beads at room temperature for 15 min. Beads were pelleted by centrifuging at 18,000 g for 1 min and were washed 3x in His buffer.

3.2.7. Determination of on-bead protein content

The on-bead content of Keap1-His or GSTP1-His was assessed with a bicinchoninic acid (BCA) Protein Assay Kit, with a slight modification of the method of Stich (Stich 1990). The BCA assay is based on the reduction of Cu^{2+} to Cu^+ by protein in an alkaline environment (the biuret reaction). Each Cu^+ formed reacts with two molecules of BCA to form a purple chromophore that has an absorbance maximum at 562 nm (Smith *et al.* 1985). For the determination of protein immobilised on agarose beads, the BCA assay is preferred to a standard Bradford protein assay, as the blue chromophore that forms when Coomassie Brilliant Blue G-250 reacts with immobilised protein remains associated with the agarose beads, which settle at the bottom of the plate/tube. Thus, constant stirring of the sample is required to enable spectrophotometric determination of protein content. The purple chromophore formed via the reaction of BCA with immobilised protein is water-soluble, and thus does not remain associated with the agarose beads, enabling spectrophotometric determination of protein content, without the need for constant stirring of the sample. Keap1-His or GSTP1-His coupled Ni^{2+} -charged agarose beads (50 μL dry volume) were washed five times with 0.5 mL PBS. A standard curve ranging from 0.01-1 mg/mL BSA was prepared in separate tubes (25 μL each). 5 μL dry beads resuspended in 20 μL of dH_2O or standards were combined with 0.2 mL BCA assay reagent and incubated in a 37 °C incubator for 30 min. Tubes were vortexed every 10 min during this incubation period. Following the incubation, the beads were pelleted by centrifugation at 18,000 g for 1 min, and 0.2 mL supernatant, or

standards were transferred to a clear 96-well plate, and the absorbance at 570 nm was read on a MRX microplate reader. A blank reading (dH₂O and BCA reagent) was subtracted from all sample/standard readings. A bead blank reading (uncoupled Ni²⁺-charged agarose beads and BCA reagent) was subtracted from the sample readings. For the calculation of molar ratios, the concentration of Keap1-His or GSTP1-His (μg/μL) was converted to molarity using the following equation:

$$\text{Protein concentration } (\mu\text{g}/\mu\text{L}) \times [1/\text{protein molecular weight (Da)}] = \text{concentration}$$

3.2.8. Treatment of recombinant protein

Following quantification of protein levels on the agarose beads, beads were incubated with a specified molar ratio of the indicated compound for the specified time points. Compounds were dissolved in DMSO to make a stock solution of 20 mM and from this; dilutions to the final concentration were made in PBS. Following all treatments, cells were pelleted by centrifugation at 18,000 g for 1 min and washed in 0.5 mL PBS x 2. For competition assays, the beads were not pelleted or washed in between the compound treatments. All Keap1-His samples were treated with 55 mM IAA, and the beads were washed in 0.5mL PBS x 3.

3.2.9. Preparation of recombinant protein for LC-ESI-MS/MS

In preparation for LC-ESI-MS/MS, beads washed in 0.5 mL PBS x 2 were then washed in 0.5mL 25 mM ammonium bicarbonate x 2 and resuspended in 90 μ L ammonium bicarbonate. A 400 μ g/mL stock solution of sequence-grade modified trypsin was diluted 1:10 with 25 mM ammonium bicarbonate and 10 μ L was added to the bead slurry. Trypsin digestion of the sample was performed overnight at 37°C.

3.2.10. LC-ESI-MS-MS methods

Samples were delivered into a Triple TOF 5600 mass spectrometer (AB Sciex) as described in Section 2.2.13. All adducts were confirmed by visual inspection of the MS/MS spectra. The presence of adducts was determined by the addition of the molecular weight of the compound to the expected molecular weight of the cysteine containing peptide. For CDDO-Me, this was an addition of 505.7 amu, for CDDO-Epoxyde 521.3 amu, for Iodoacetamide (IAA), 184.9 amu (See Appendix 1, 2 and 3 for details). Modified peptides were quantified using PeakView software to extract parent ions of the appropriate peptide plus compound m/z (extracted ion count, XIC). The area under the curve of each XIC peak was used to assess the relative quantification of individual modified peptides across samples. This was normalised to the total ion count (TIC) for the first datum point for each set of samples.

3.2.11. Mouse Keap1-V5 plasmid purification

Mouse Keap1-V5 was purified as described in Section 2.2.3.

3.2.12. Transfection of cells with Keap1-V5

HEK293T cells were transfected as described in Section 2.2.4.

3.2.13. Cell treatment

For mass spectrometry, Keap1-V5-expressing HEK293T cells were prepared as in Section 2.2.4 and 2.2.5. Cells were treated with CDDO-Epoxy dissolved in DMSO at 100 μ M for 1 hr. The final volume of DMSO in the cell culture medium was 0.5% (v/v). The cells were then returned to the humidified incubator (37 °C in 5 % CO₂) for the indicated period of time.

3.2.14. Immunopurification of Keap1-V5

After treatment for the indicated period of time, cells were lysed and Keap1-V5 was immunopurified as described in Section 2.2.6. Samples (20 μ l) were taken before and after immunopurification for immunoblot analysis to ensure sufficient Keap1-V5 expression and purification.

3.2.15. Preparation of Keap1-V5 for LC-ESI-MS/MS

After incubation and washing, the Keap1-V5-bound anti-V5 agarose beads were prepared as described in Section 2.2.11.

3.2.16. *In silico* modelling

All *in silico* modelling was performed by Jaclyn Bibby, Department of Chemistry, University of Liverpool. The mouse Keap1 protein sequence was aligned against that of KLHL11 (PDB: 4AP2) (Canning *et al.* 2013) using ClustalW and was used, alongside crystal structures of the BTB (PDB: 4CXI) (Cleasby *et al.* 2014) and DGR (PDB: 2DYH) (Lo *et al.* 2006) domains of Keap1, to generate models using Modeller 9.11 (Sali and Blundell 1993). GOLD 5.2 (CCDC Software; Jones *et al.* (1997)) was used to dock each TP ligand within the pocket surrounding a given cysteine, with the binding site defined as 10 Å around the cysteine C α . A generic algorithm with ChemPLP (Korb *et al.* 2009) as the fitness function was used to generate 50 binding modes per ligand. Default settings were retained for the “ligand flexibility”, “fitness and search options” and “GA settings”, however the “allow early termination” setting in the “fitness and search option” was turned off to retain all ligand conformations. Protons were added, and crystallographic water molecules were removed. For covalent docking to cysteines, the corresponding side chain was removed from the protein and the ligand modified to contain the side chain to allow flexibility. The site of covalent attachment was at the cysteine C α . The best score, and mean score + SD were calculated from the 50 poses generated. Quantitative structure activity

relationship data for the induction of Nqo1 by a series of TPs was taken from Dinkova-Kostova *et al.* (2005). Pearson correlation coefficients were determined using GraphPad Prism 6.01 (GraphPad Software, USA).

3.2.17. Data analysis

Where appropriate, experiments were performed at least in duplicate, all replicates performed on separate occasions. Data are expressed as mean \pm standard deviation of the mean (SD). A two-sided P value of ≤ 0.05 was considered to be statistically significant.

3.3. RESULTS

3.3.1. Effect of chemically tuned TPs on the Nrf2 pathway in cells

We hypothesised that the ability of CDDO-Me to reversibly bind thiol groups underlies the potency of this compound as an inducer of Nrf2. To investigate this, we synthesised a TP with the ability to bind thiol groups irreversibly (Table 3.1) and tested both TPs to determine their potency towards Nrf2. To measure Nrf2 activation, we used the rat hepatoma H4IIE-ARE reporter cell line, which expresses luciferase under control of the ARE and is therefore responsive to Nrf2 induction. The concentration at which the TPs caused a 200% increase in reporter activity (EC₂₀₀) show that the TPs are of similar potencies (EC₂₀₀= 0.6 nM and 2.1 nM respectively) (Fig 3.2A). We confirmed this observation by western blot analysis for Nrf2 and Nqo1, an Nrf2-regulated gene, following treatment of H4IIE-ARE cells with the TPs (Fig. 3.2 B-D). This data confirms that the TPs induce Nrf2 in cells and this translates to an induction of Nqo1 protein expression. We measured GSH levels within the cell, as GSH depletion would indicate irreversible binding of the TP to GSH molecules, reducing its potency towards Nrf2. Following exposure of H4IIE-ARE cells to the TPs for 1 hr, no substantial effect on GSH was seen (Fig 3.2E). We also show that dimethyl fumarate (DMF), an irreversible thiol modifier, and sulforaphane (Sul), a purported reversible thiol modifier cause GSH depletion, under the same conditions. The data presented suggests that the ability of these compounds to bind thiol groups reversibly does not have significant bearing on its ability to activate Nrf2.

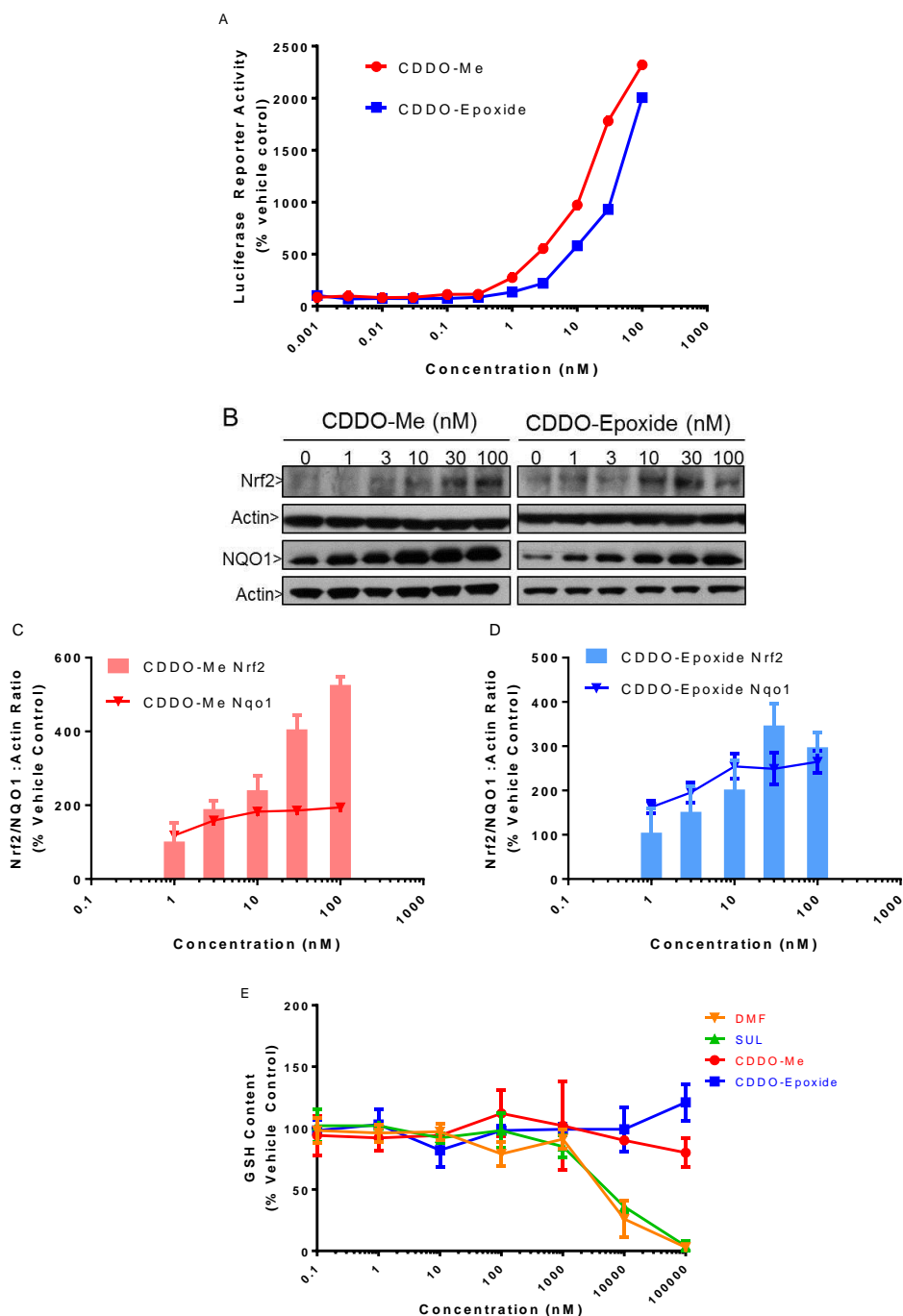


Figure 3.2.Effect of TPs on Nrf2 cell defence pathway in cells.H4IIE-ARE reporter cells were treated with CDDO-Me or CDDO-Epoxy for 24 hr before being lysed and luminescence measured (A). Western blot analysis for Nrf2 and Nqo1 was carried out after 1 hr or 24 hr treatment respectively (B) and band density quantified using TotalLab (C,D). Glutathione levels measured following 1 hr CDDO-Me, CDDO-Epoxyde, dimethyl fumarate (DMF) or sulforaphane (SUL) exposure. All data representative of 3 biological repeats.

3.3.2 LC-ESI-MS/MS validation of recombinant protein

In order to examine the ability for TPs to form covalent adducts with protein thiols, we exposed purified recombinant GSTP1 and Keap1 to novel TPs, before subjecting the protein to LC-MS/MS analysis. Sufficient (>70%) protein coverage is required in order to detect adducts between protein peptides and compounds. Following expression and purification, the recombinant protein was subjected to trypsin digestion and LC-MS/MS analysis. These data were subjected to a ProteinPilot search to identify all proteins in the sample. Sequence coverage was found to be sufficient for both proteins and would enable the detection of adducts (Table 3.2).

Protein	Coverage (%)
hGSTP1-His	98.4
mKeap1-His	86.4

Table 3.2. Sequence coverage of recombinant His tagged GSTP1 and Keap1 following LC-ESI-MS/MS, as determined by a ProteinPilot search.

3.3.3 LC-ESI-MS/MS evidence for TP modification of GSTP1-His

It was then investigated whether the TPs bind the highly reactive cysteine residue of the model protein GSTP1. The purified recombinant protein was incubated with 10 – 100- fold excess of CDDO-Me or CDDO-Epoxyde for 1-24 hr (see Figure 3.3A for an overview of the procedure undertaken). We observed that both TPs were able to covalently modify Cys-47 of GSTP1 (Fig 3.4). To our knowledge, this is the first direct evidence that CDDO-Me can form a covalent adduct with a protein thiol.

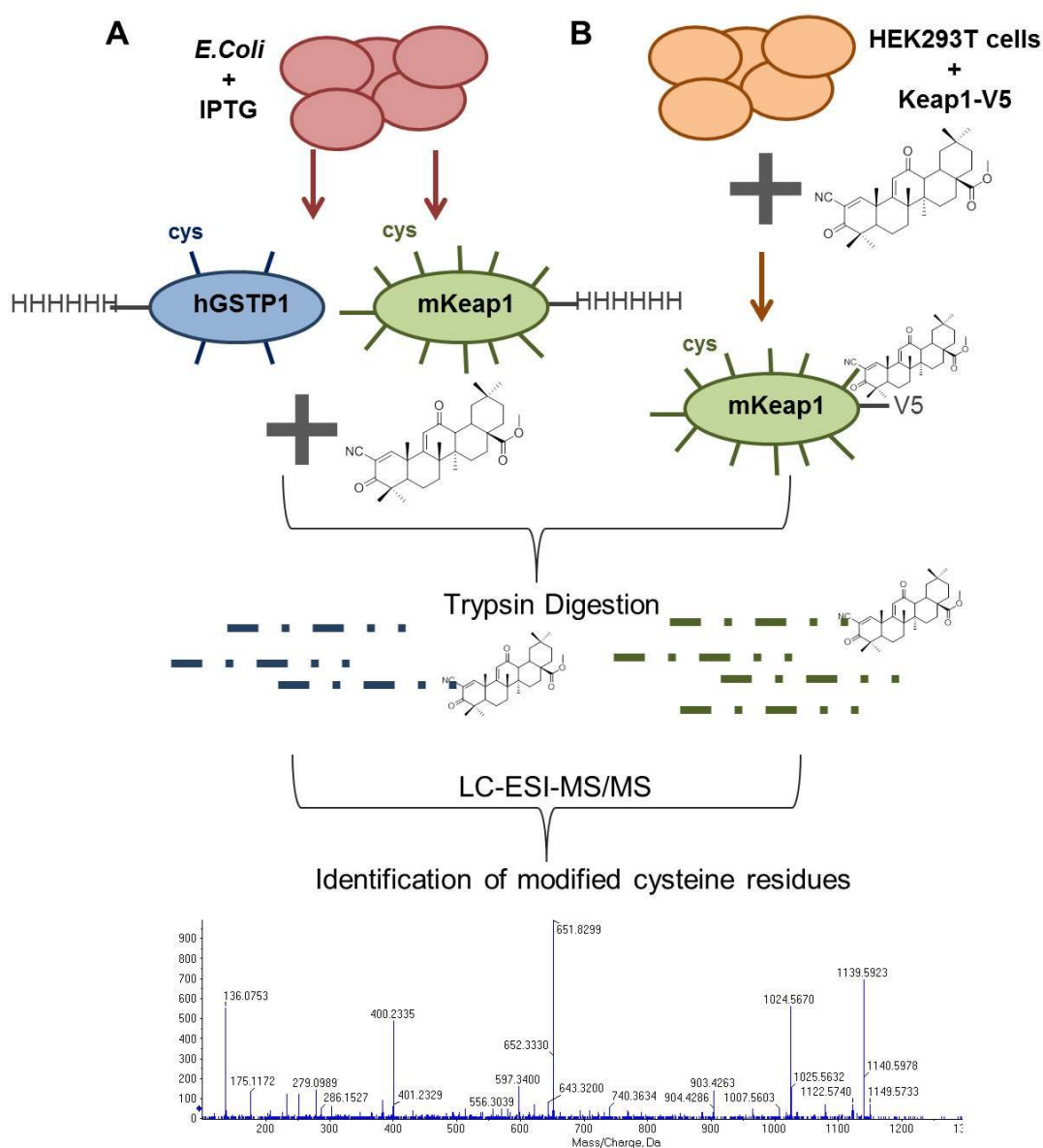


Figure 3.3. Schematic of the procedure to identify covalently modified cysteine residues. (A) *E. coli* containing vectors coding for recombinant His-tagged human GSTP1 or mouse Keap1 were cultured. Proteins were expressed using IPTG, and purified with Ni²⁺-charged agarose beads before treatment with the TPs at the specified molar excess for up to 24 hr. (B) HEK293T transfected with V5-tagged mouse Keap1 were treated with 100 μ M CDDO-Epoide for 1 hr before Keap1-V5 was purified with anti-V5 agarose beads. Proteins were then subjected to trypsin digestion and prepared for tandem mass spectrometry (LS-ESI-MS/MS). Peptides containing the addition of the molecular weight of the TP were identified.

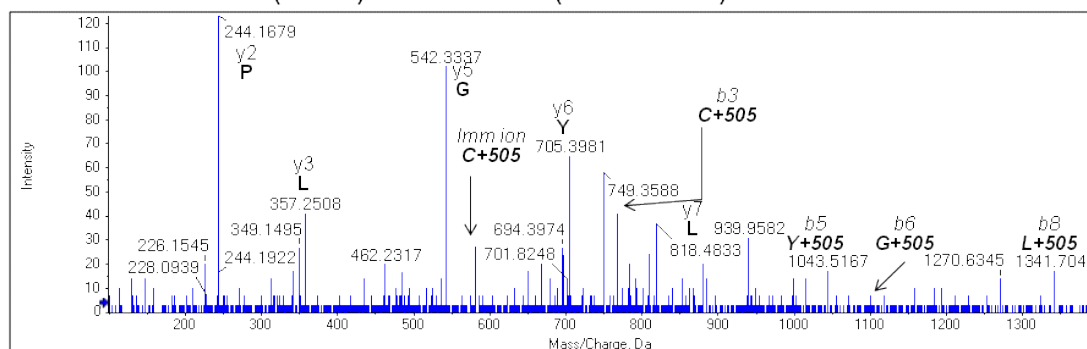
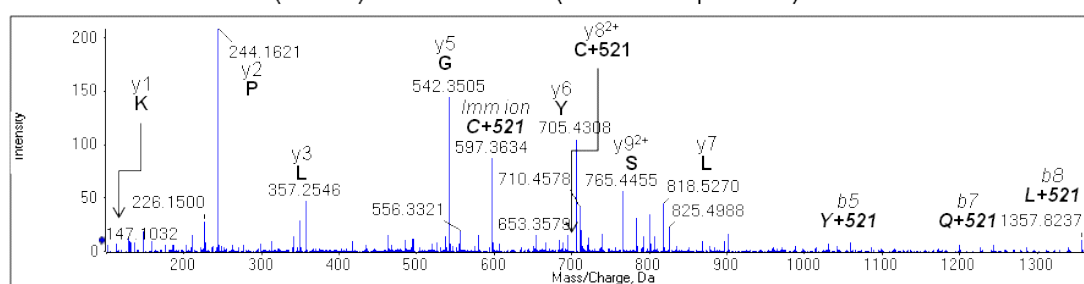
A GSTP1 ⁴⁵ASC(+505)LYGQLPK⁵⁴ (CDDO-Me)**B** GSTP1 ⁴⁵ASC(+521)LYGQLPK⁵⁴ (CDDO-Epoxyde)

Figure 3.4. Mass spectrometry spectra showing GSTP1 cysteine-47 modified by (A) CDDO-Me and (B) CDDO-Epoxyde. Purified GSTP1-His was exposed to 10 -100- fold molar excess of each compound, dissolved in DMSO and diluted in PBS (pH 8.4), at 37°C for 24 hr. LC-MS/MS was performed and mass spectra were analysed manually for cysteine containing peptides with an additional mass equivalent to the relevant compound. Representative spectra from three biological repeats.

3.3.4 LC-ESI-MS/MS evidence for TP modification of Keap1-His

Having detected modification of GSTP1 by both TPs, the procedure was repeated with recombinant Keap1-His (see Fig 3.3A for an overview). After exposure to the TPs, the protein was treated with 55 mM IAA for 15 min to alkylate all remaining cysteines and improve their detection rate, including those not modified by the TP (Table 3.3). Following incubation with a 100:1 molar excess of the TP, modification of Keap1-His cysteine residues by CDDO-Epoxyde was observed on the following residues:

Cys-257, -273, -288, -434, -489 and -613 (Fig 3.5).

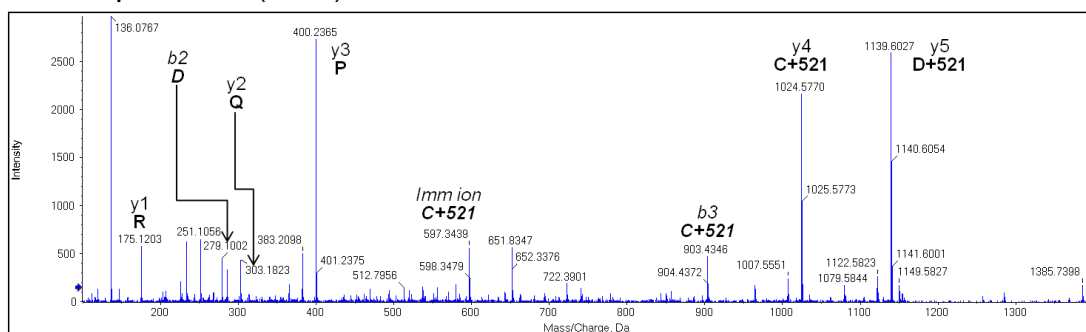
There was no evidence for modification of Keap1 by CDDO-Me. All cysteine residues were sensitive to adduction by IAA following CDDO-Epoxyde, except Cys-257 and -273 (Table 3.3) which is likely to be due to the presence of a CDDO-Epoxyde adduct on these residues, preventing IAA binding. No adducts between IAA and Cys-622 and -624 were seen (Table 3.3) which, as described in Section 2.3.5, are close to the V5 tag and often not cleaved during the trypsin digest, therefore not identified by LC-MS/MS.

Keap1-His Peptide	Cys Residue	IAA Mod
CPEGAGDAVMYASTECK	23, 38	2
LSQQLCDVTLQVK	77	4
CVLHVMNGAVMYQIDSVVR	151	4
ACSDFLVQQLDPSNAIGIANFAEQIGCTELHQR	171, 196	4
QEEFFNLSHCQLATLISR	226	4
CESEVFHACIDWVK	241, 249	1
YDCPQR	257	0
CHALTPR	273	0
CEILQADAR	288	4
CK	297	3
DYLVQIFQELTLHKPTQAVPCR	319	4
SGLAGCVVGGLLYAVGGR	368	4
NNSPDGNTDSSALDCYNPMTNQWSPCASMSVPR	395, 406	4
IGVGVIDGHIYAVGGSHGCIHHSSVER	434	4
LNSAECYPER	489	4
SGAGVCVLHNCIYAAGGYDGQDQLNSVER	513, 518	4
IYVLGGYDGHTFLDSVECYDPDSDTWSEVTR	583	4
SGVGVAVTMEPCR	613	4
QIDQQNCTC	622, 624	0

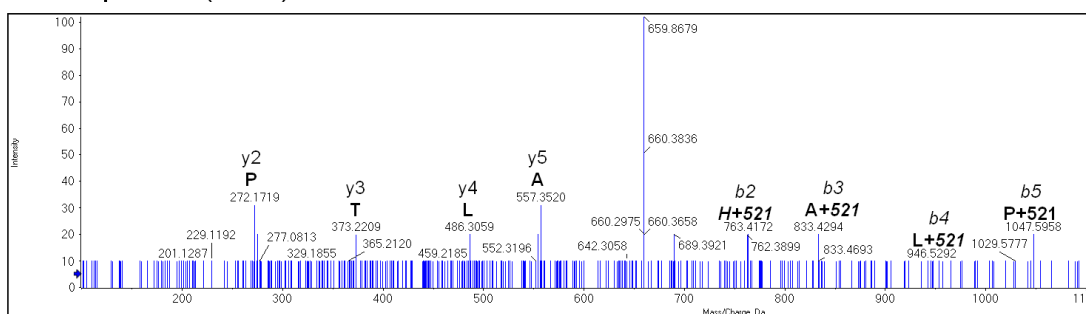
Table 3.3. Recombinant Keap1-V5 cysteines modified by IAA *in vitro*.

Purified Keap1-His was exposed to 100:1 molar ratio of CDDO-Epoxyde for 24 hr at 37°C followed by 55 mM IAA for 15 min. LC-ESI-MS/MS analysis was performed following trypsin digestion, and ProteinPilot searches identified cysteine containing peptides with an additional mass equivalent to IAA over 4 biological repeats. Average sequence coverage= 94.6%.

A Keap1²⁵⁵YDC(+521)PQR²⁶⁰



B Keap1²⁷³C(+521)HALTPR²⁷⁹



C Keap1²⁸⁸C(+521)EILQADAR²⁹⁶

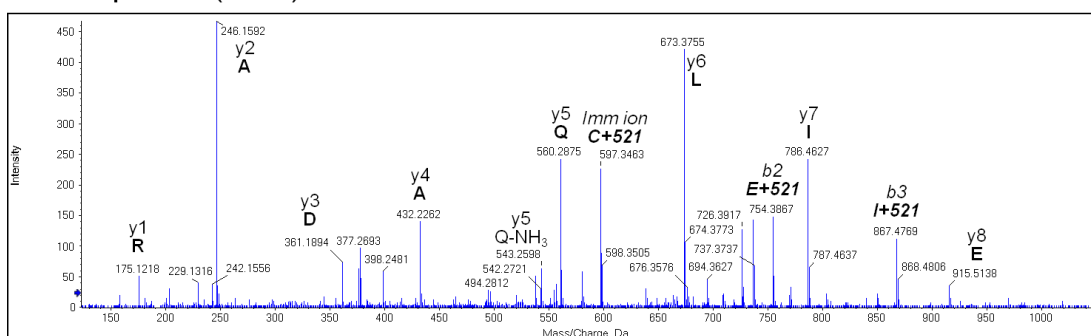
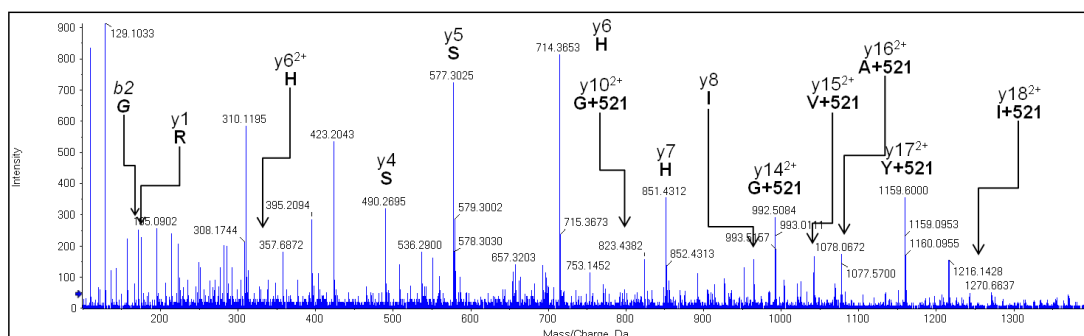
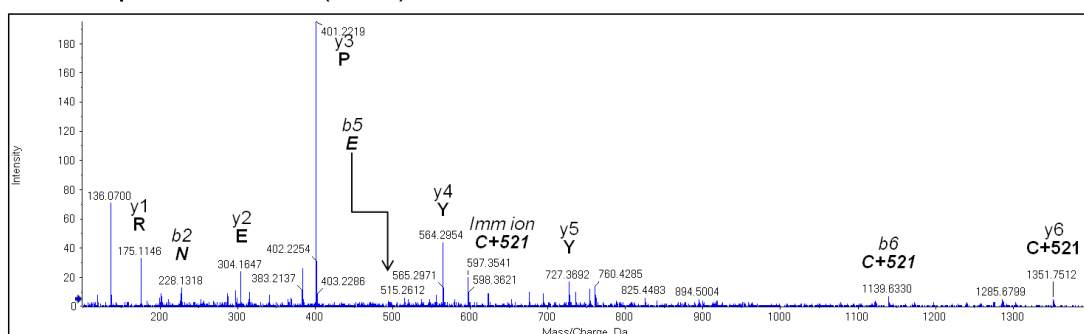


Figure 3.5. Mass spectra showing Keap1 cysteine residues modified by CDDO-Epoxyde. (A Cys-257; B Cys-273; C Cys-288). Purified Keap1-His was exposed to 100:1 molar ratio of CDDO-Epoxyde for 24 hrs at 37°C. LC-ESI-MS/MS analysis was performed following trypsin digestion, and ProteinPilot searches identified cysteine containing peptides with an additional mass equivalent to the compound (521). Showing one representative spectra from four biological repeats.

D Keap1⁴¹⁶IGVGVIDGHIYAVGGSHGC(+521)IHHSSVER⁴⁴²



E Keap1⁴⁸⁴LNSAEC(+521)YYPYR⁴⁹⁴



F Keap1⁶⁰²SGVGVAVTMEPC(+521)RK⁶¹⁵

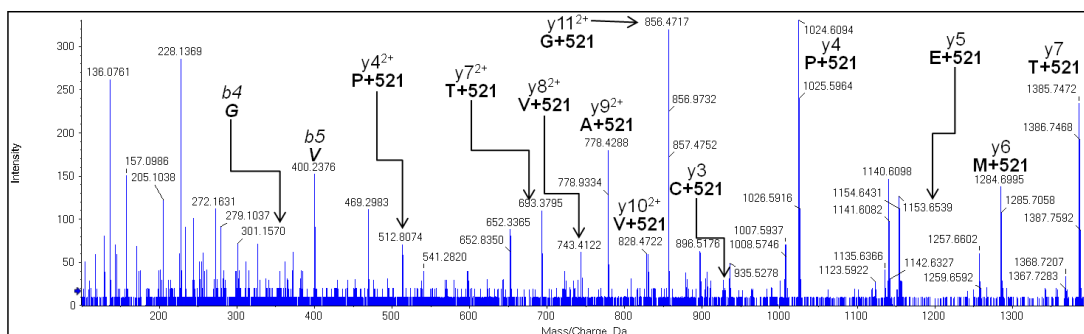


Figure 3.5 continued. Mass spectra showing Keap1 cysteine residues modified by CDDO-Epoxyde.(D Cys-434; E Cys-489; F Cys-613). Purified Keap1-His was exposed to 100:1 molar ratio of CDDO-Epoxyde for 24 hrs at 37°C. LC-ESI-MS/MS analysis was performed following trypsin digestion, and ProteinPilot searches identified cysteine containing peptides with an additional mass equivalent to the compound (521). Showing one representative spectra from four biological repeats.

Following the treatment of Keap1-His with increasing molar excesses of CDDO-Epoxyde, Cys-257 was found to be most readily modified (Fig 3.6). However, this requires further investigation, as it may be a function of the relative ability of the Cys-257-containing peptide to be ionized, lending itself better to MS detection compared to other peptides. Of the cysteine-containing peptides in Keap1 we observed to be modified by CDDO-Epoxyde, all show a concentration-dependent increase in modification (Fig 3.6). At higher molar ratios of CDDO-Epoxyde (200:1), the presence of non-tryptic peptides in the MS data suggests protein degradation is occurring, and may explain why modification levels were found to decrease.

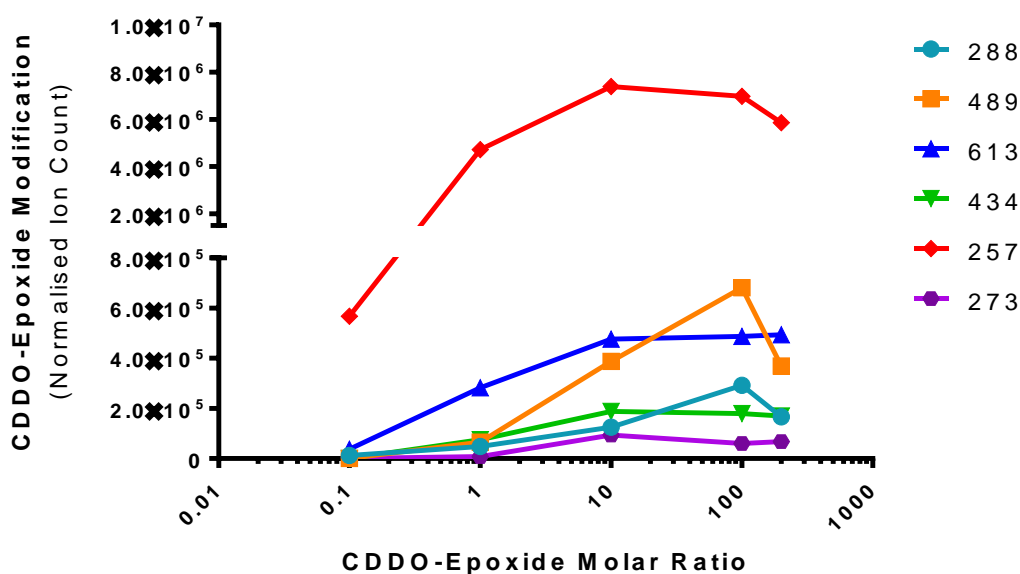


Figure 3.6. Concentration-dependent changes in Keap1-His cysteine modification by CDDO-Epoxyde. Keap1-His was treated with increasing molar ratios of CDDO-Epoxyde for 24 hrs, at pH 8.4, 37°C. Following trypsin digestion, LC-ESI-MS/MS analysis was performed, and the level of modification of each cysteine-containing peptide was compared. Showing the average level of cysteine modification of 3 biological repeats.

3.3.5 Investigating the ability of CDDO-Me to compete with CDDO-Epoxyde to covalently modify protein thiols

In light of our inability to detect modification of Keap1 cysteine residues by CDDO-Me, we examined the ability of CDDO-Me to competitively inhibit the modification of Keap1 by CDDO-Epoxyde. A reduced ability of CDDO-Epoxyde to bind a cysteine residue following pre-treatment with CDDO-Me would indicate that both TPs are capable of forming adducts with the same cysteine residues in Keap1. We focussed analyses on the modification of Cys-257, as this is the residue most readily modified by CDDO-Epoxyde, particularly at low molar ratios (1:1) of drug:protein. Keap1-His was pre-treated with CDDO-Me at increasing molar ratios for 1 hr followed by the addition of CDDO-Epoxyde, at a 1:1 molar ratio for a further 24 hrs. We observed significant variation of Cys-257 modification by CDDO-Epoxyde between biological repeats (Fig. 3.7). This pattern of variable modification was also seen on the other cysteine residues modified by CDDO-Epoxyde (data not shown). This inherent variability within the assay made it difficult to conclude whether CDDO-Me is able to compete with CDDO-Epoxyde to bind to Keap1, from this data.

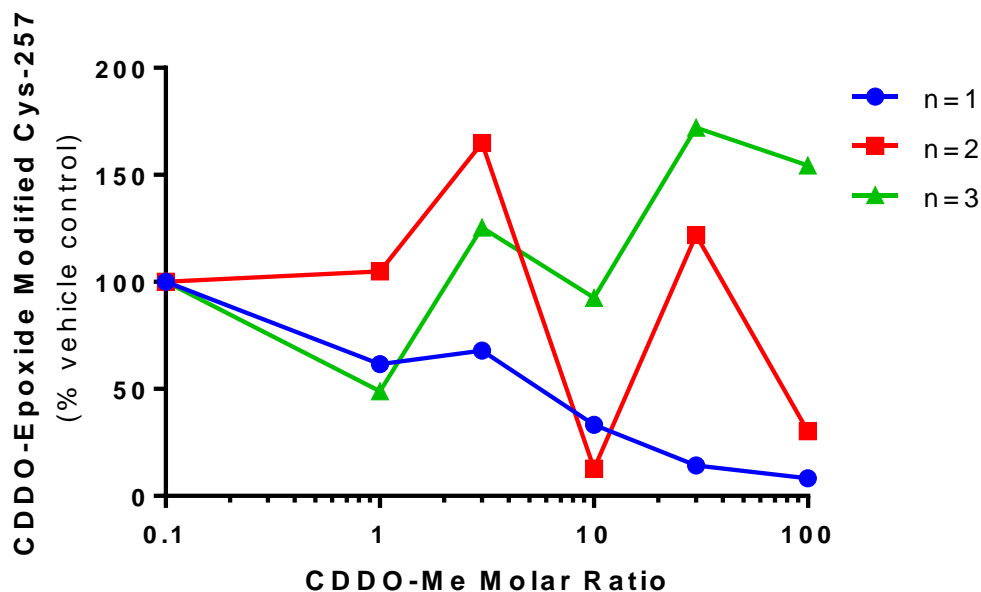


Figure 3.7. Variation in CDDO-Me competing with CDDO-Epoxyde to bind to Keap1. Keap1-His was exposed to increasing molar ratios of CDDO-Me for 1 hr, followed by a single molar ratio of CDDO-Epoxyde (1:1) for a further 24 hr, and LC-ESI-MS/MS analysis was performed following trypsin digestion. Showing the level of CDDO-Epoxyde modification of Cys-257 following normalisation to the TIC, and shown relative to vehicle control (i.e. no CDDO-Me followed by 1:1 CDDO-Epoxyde) for 3 biological repeats.

We further examined the variation by simultaneously preparing four Keap1-His samples treated with a 1:1 molar ratio of CDDO-Epoxyde. All recombinant protein was purified from the same bacterial lysate, and treated under identical conditions. We observed substantial variation between the levels of modification of the cysteine residues adducted by CDDO-Epoxyde (Fig. 3.8 A-D). This variation is unlikely to be due to discrepancies in the volume / amount of peptides loaded or the MS process as the TIC (total ion count; the sum of intensities of all MS peaks belonging to the same scan, including background noise) of each sample is consistent (Table 3.4). The source of

the variability is likely to be the multi-step process of sample preparation, whereby each step can introduce variability.

Repeat	1	2	3	4
TIC	1.22×10^{10}	8.27×10^9	1.21×10^{10}	1.16×10^{10}

Table 3.4. Total ion count (TIC) of four Keap1 samples treated with CDDO-Epoxyde. Conditions: 1:1 molar ratio, 24 hr, followed by 55 mM Iodo for 15 min, made simultaneously and prepared for LC-MS/MS by trypsin digestion

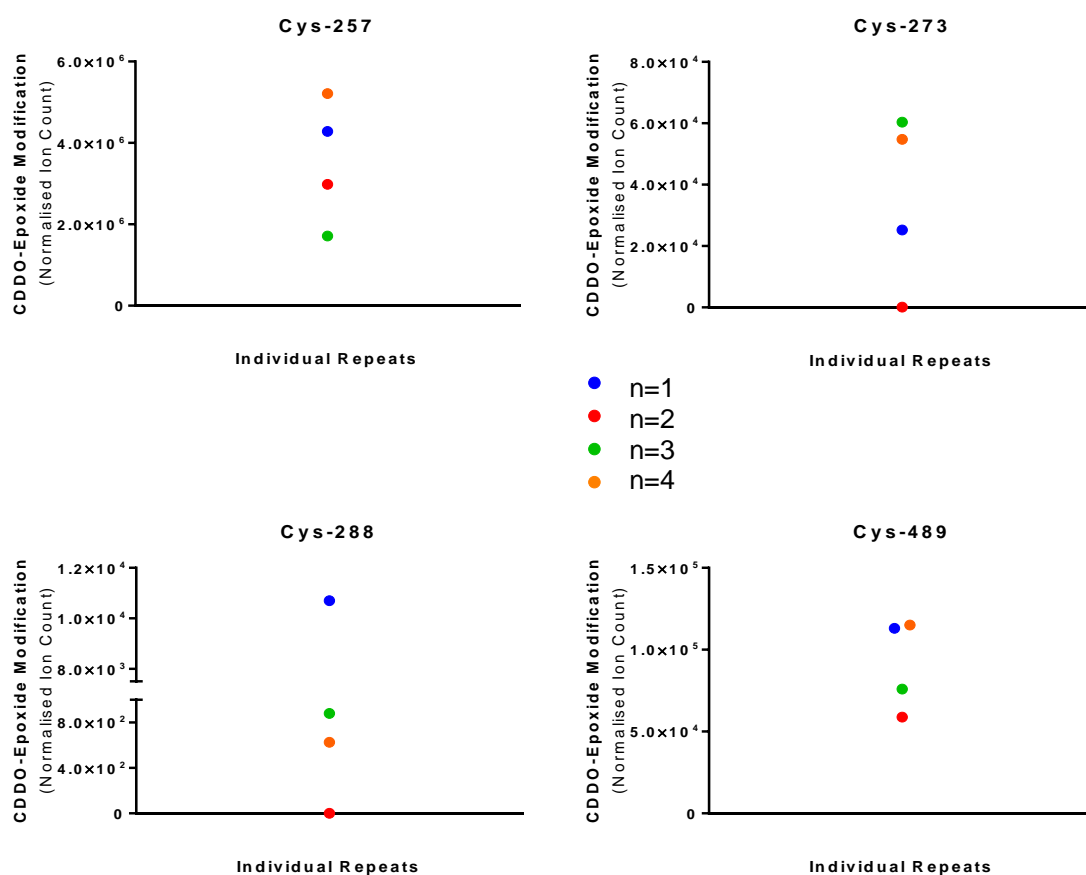


Figure 3.8. Variation in CDDO-Epoxyde modification of Keap1. Recombinant Keap1-His was exposed to a 1:1 molar ratio of CDDO-Epoxyde for 24 hr followed by 55 mM IAA for 15 min, before trypsin digestion and LC-MS/MS analysis was performed on four biological repeats prepared simultaneously.

Due to the variation seen in the modification levels of Keap1 cysteine residues by CDDO-Epoxyde, the experiment was repeated with GSTP1. We focussed on the reactive cysteine residue (Cys-47), on which we had previously detected modification by both CDDO-Me and CDDO-Epoxyde. GSTP1 was pre-treated with CDDO-Me at increasing molar ratios for 1 hr, followed by treatment with CDDO-Epoxyde at a single molar ratio (1:1) for 24 hr. The data show that there is a loss of CDDO-Epoxyde binding to GSTP1 Cys-47 with increasing molar ratios of CDDO-Me (Fig 3.9), indicating that both compounds can bind to the same cysteine residue within a protein and can compete with each other to do so.

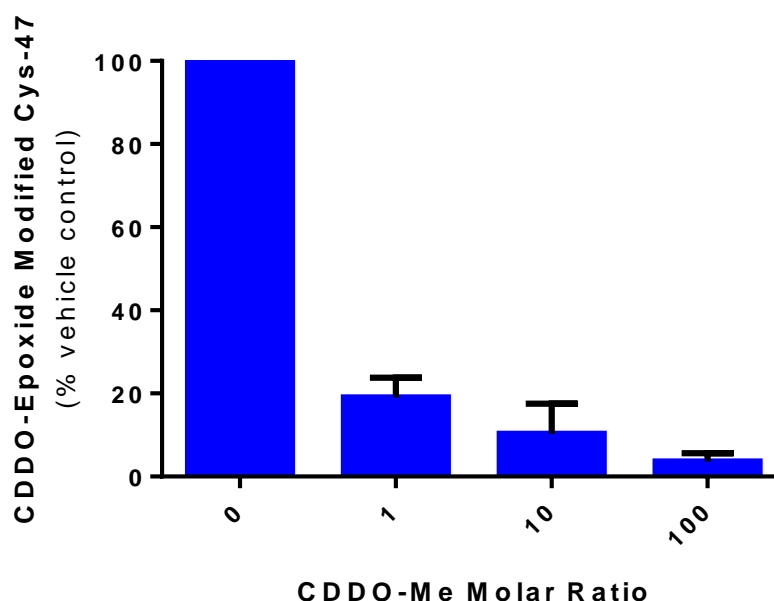


Figure 3.9. CDDO-Me competes with CDDO-Epoxyde to bind to GSTP1 Cys-47. Purified recombinant GSTP1 was pre-treated with increasing molar ratios of CDDO-Me, followed by a single molar ratio of CDDO-Epoxyde (1:1), prior to trypsin digestion and LC-MS/MS analysis. Showing CDDO-Epoxyde modified cysteine normalised to TIC and as a percentage of vehicle control (i.e. no CDDO-Me, 1:1 CDDO-Epoxyde). Average of 3 biological repeats.

3.3.6 CDDO-Epoxyde forms covalent adducts with Keap1-V5 in cells

Following the detection of adducts between CDDO-Epoxyde and six cysteine residues in recombinant Keap1 *in vitro*, we hypothesised that these adducts would also be formed in a cell based model. Using methods outlined in Section 2.2, HEK293T cells were transfected with Keap1-V5 before being treated with 100 μ M CDDO-Epoxyde for 1 hr (see Figure 3.3B for an overview of the procedure undertaken). Following immunopurification of Keap1-V5 using anti-V5 agarose beads, the protein was treated with 55 mM IAA for 15 min to cap all remaining cysteines, and improve our ability to detect the cysteine containing peptides, including those not modified by the compound (Table 3.5). LC-ESI-MS/MS analysis revealed that CDDO-Epoxyde modified the following cysteine residues in Keap1-V5: Cys-257, -273, -288 and -489 (Fig 3.10, Table 3.6), in agreement with those detected in the experiments with recombinant protein (Fig 3.11). Only Cys-434 and Cys-613 were found to be modified by CDDO-Epoxyde in recombinant Keap1 *in vitro* but not in the cell based model. Both of these residues were found to be modified by IAA (Table 3.4), therefore we conclude that they were successfully detected in the MS analysis, yet, at least in this cell based model, these residues were not modified by CDDO-Epoxyde.

Keap1-V5 Peptide	Cys Residue	IAA Mod
CPEGAGDAVMYASTECK	23, 38	4
LSQQLCDVTLQVK	77	4
CVLHVMNGAVMYQIDSVVR	151	4
ACSDFLVQQLDPSNAIGIANFAEQIGCTELHQR	171, 196	4
QEEFFNLSHCQLATLISR	226	4
CESEVFHACIDWVK	241, 249	4
YDCPQR	257	1
CHALTPR	272	0
CEILQADAR	288	4
CK	297	4
DYLVQIFQELTLHKPTQAVPCR	319	4
SGLAGCVVGGLLYAVGGR	368	4
NNSPDGNTDSSALDCYNPMTNQWSPCASMSVPR	395, 406	4
IGVGVIDGHIYAVGGSHGCIHHSSVER	434	4
LNSAECYYPER	489	4
SGAGVCVLHNCIYAAGGYDGQDQLNSVER	513, 518	4
IYVLGGYDGHTFLDSVECYDPDSDTWSEVTR	583	4
SGVGVAVTMEPCR	613	4
QIDQQNCTC	622, 624	0

Table 3.5. Keap1-V5 cysteines modified by IAA in cells. HEK293T cells expressing Keap1-V5 were treated with 100 μ M CDDO-Epoxyde (1 hr), lysed and Keap1-V5 was immunopurified. Cysteines were capped with 55 mM IAA before trypsin digestion and LC-MS/MS analysis. ProteinPilot identified the indicated peptides as modified by IAA over four biological repeats. Average sequence coverage =93.5 %

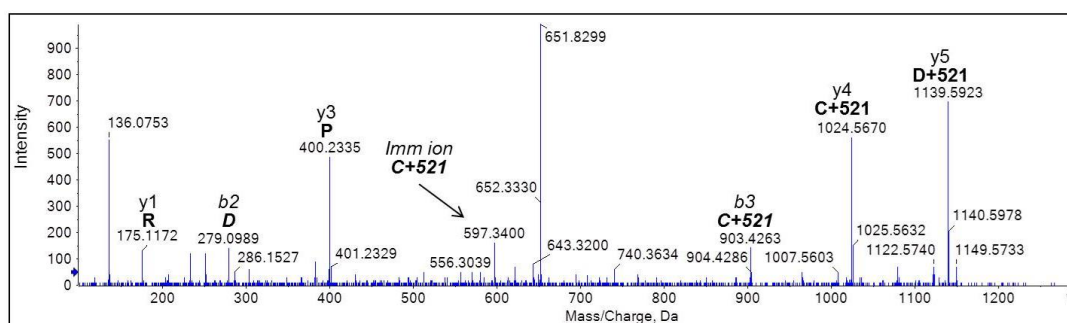
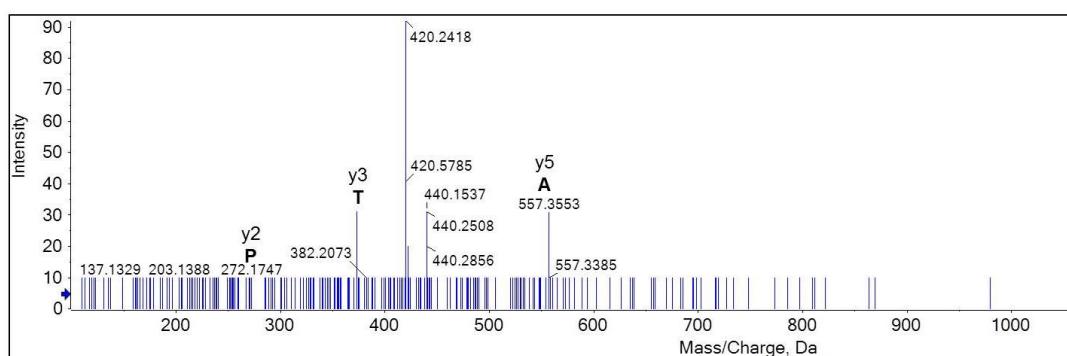
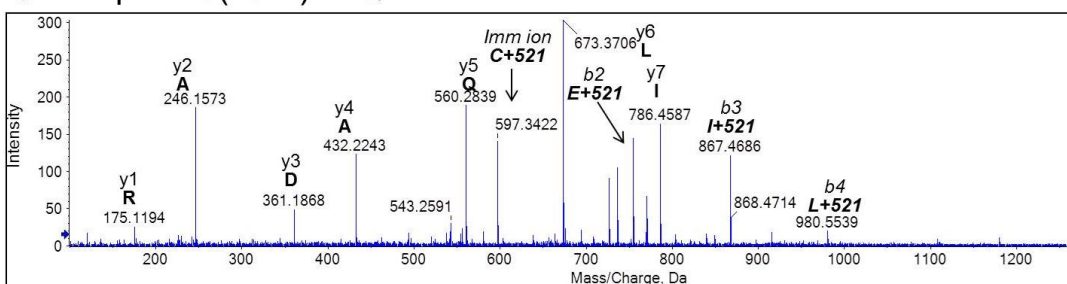
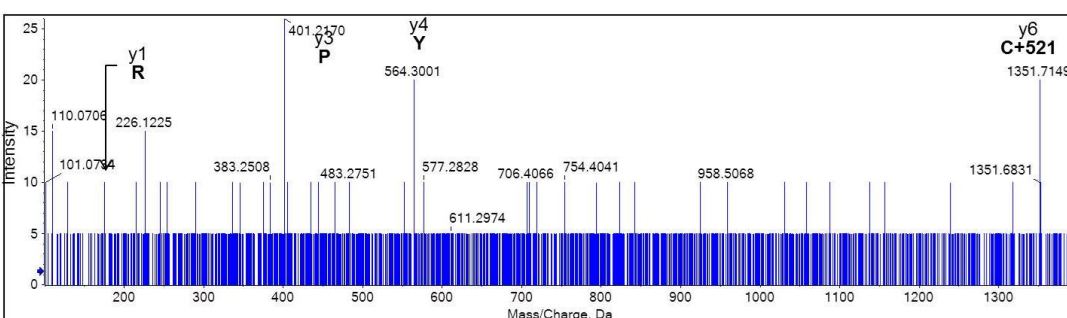
A Keap1²⁵⁵YDC(+521)PQR²⁶⁰**B** Keap1²⁷³C(+521)HALTPR²⁷⁹**C** Keap1²⁸⁸C(+521)EILQADAR²⁹⁶**D** Keap1⁴⁸⁴LNSAEC(+521)YYPER⁴⁹⁴

Figure 3.10. Mass spectra showing Keap1-V5 cysteine containing peptides modified by CDDO-Epoide in cells. (A Cys-256; B Cys-273; C Cys-288; D Cys-489) HEK293T cells transfected with Keap1-V5 were treated with 100 μ M CDDO-Epoide for 1 hr. Keap1-V5 was immunopurified, residues were capped with 55 mM IAA before undergoing trypsin digestion and LC-ESI-MS/MS analysis.

Keap1-V5 Peptide	Cys Residue	Number of times CDDO-Epox mod seen (4 repeats)
YDCPQR	257	4
CHALPTR	273	1
CEILQADAR	288	2
LNSAECYYPER	489	3

Table 3.6. Keap1-V5 cysteine residues modified by CDDO-Epoxyde in cells

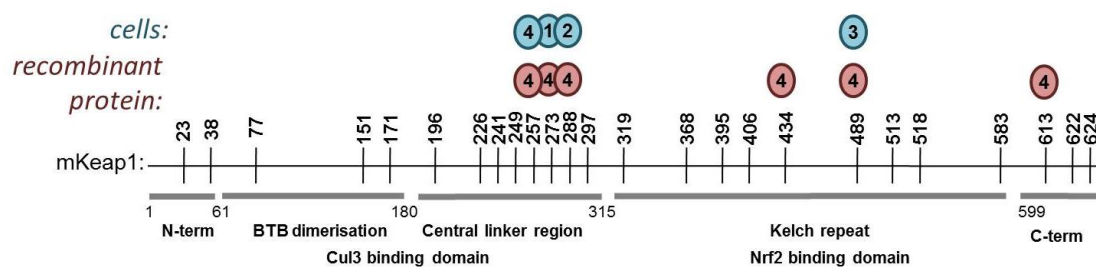


Figure. 3.11. Correlation between CDDO-Epoxyde modification of recombinant Keap1 and Keap1-V5 expressed in cells. Recombinant Keap1 was exposed to 100:1 molar ratio of CDDO-Epoxyde for 24 hr or HEK293T cells expressing Keap1-V5 were treated with 100 μ M CDDO-Epoxyde for 1 hr before Keap1 immunopurification, trypsin digestion and LC-MS/MS analysis. Number in circle represents the number of times this residues was identified as modified in 4 biological repeats.

3.3.7 Molecular modelling of CDDO-Epoxyde modification of Keap1

To further examine the nature of the chemical interaction between CDDO-Epoxyde and Keap1, we used an *in silico* approach to model the points of interaction. Using previously reported crystal structures of Keap1 domains including the BTB (PDB: 4CXI) (Cleasby *et al.* 2014) and the DGR (PDB: 2DYH) (Lo *et al.* 2006) domains, along with homology modelling based on the crystal structure of the BACK domain of KLHL11 (PDB: 4AP2) (Canning *et al.* 2013), a member of the Kelch family of proteins, we modelled the most likely docking pose or orientation in which CDDO-Epoxyde would bind covalently to the Keap1 cysteine residues found to be modified by MS. Using GOLD 5.2, CDDO-Epoxyde was docked within the pocket surrounding a given Keap1 cysteine residue. ChemPLP was used to generate 50 binding modes (poses) per ligand. The poses are grouped into those which are most similar, and we show the pose most representative of the largest group for the cysteine residues in Keap1 identified as modified by CDDO-Epoxyde (Fig. 3.12). Interestingly, Cys-257 and Cys-288 form a binding pocket in which CDDO-Epoxyde can sit (Fig 3.12A,C) In this model we show, in accordance with previously published data (McMahon *et al.* 2010), these cysteine residues are located adjacent to basic amino acids (Fig 3.11), which are known to reduce the pKa of cysteine thiols, enhancing their reactivity towards electrophilic compounds (Snyder *et al.* 1981).

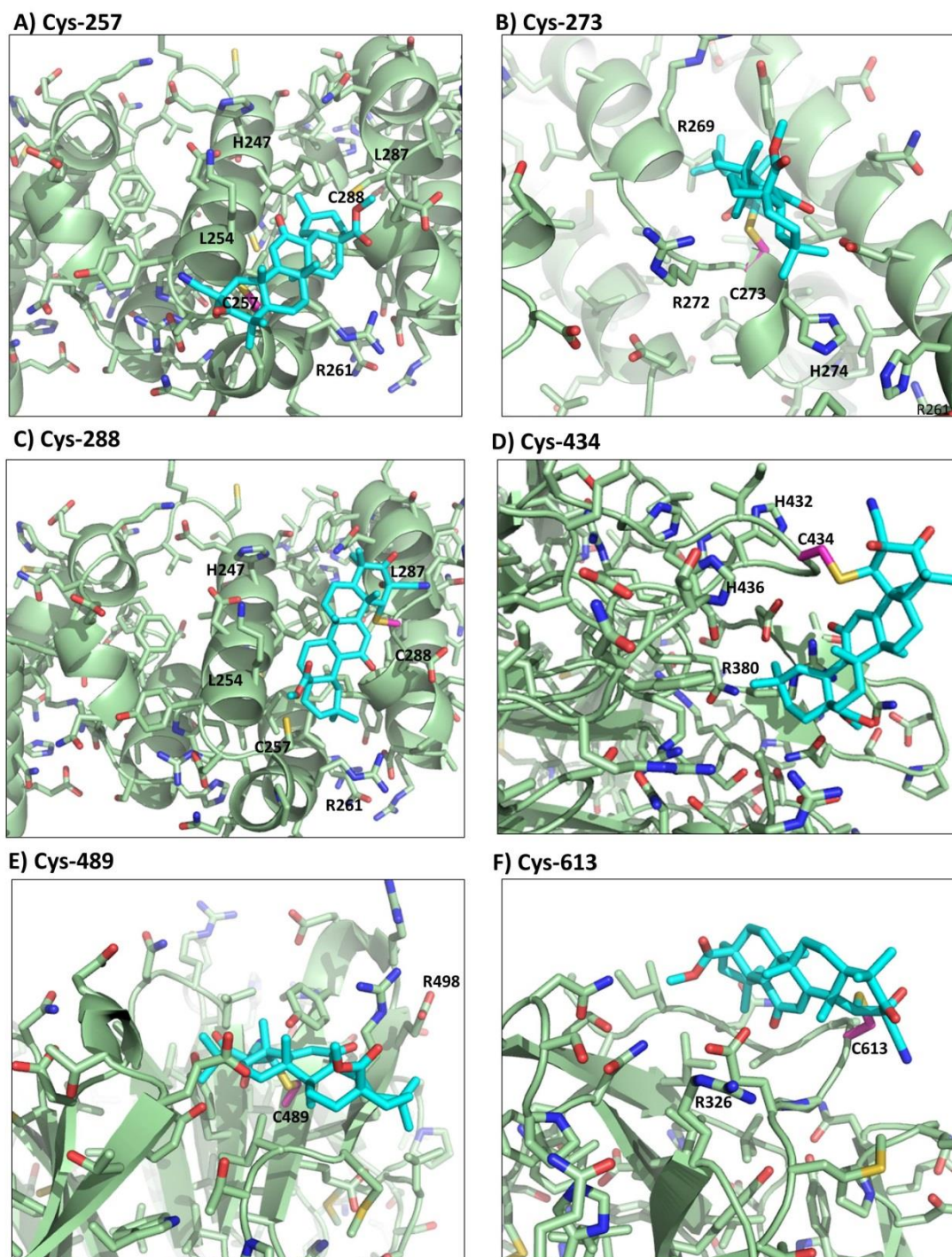


Figure 3.12. Molecular modelling of CDDO-Epoxy bound to Keap1 cysteine residues identified in this study. The depicted poses are representative of the largest group of poses from 50 pose simulations using ChemPLP. Cysteine residues and neighbouring basic amino acids are shown in bold type. The cysteine residue of interest in each panel is highlighted in magenta. CDDO-Epoxy is shown in light blue, Keap1 structure in green. Red moieties represent oxygen, blue nitrogen and yellow sulphur.

3.3.8 Correlation of TP potency towards Nqo1 activity and Keap1 covalent binding score

To investigate the importance of the ability of TPs to covalently bind to Keap1 cysteine residues Keap1, we used data for the potency of TPs as inducers of Nqo1 activity published by Dinkova-Kostova *et al.* (2005). Modifications to the A or C ring are thought to alter the potency of the TP by affecting the ability to interact with thiol groups whilst modification of the side chain between the D and E ring are thought to affect cellular permeability. From the original published data set, we took 14 compounds (Appendix 4), removing those that contained large side chains at the D/E ring. These structures were covalently docked into the models detailed in Section 3.3.7, and ChemPLP was used to generate and score 50 binding modes per ligand. The scores are generated based on a number of factors including covalent, lipophilic, hydrogen bond, clash and torsion components. These scores were correlated with \log_{10} of the CD value for each TP, where CD is the concentration required to double the activity of Nqo1. We show no correlation between the covalent binding of the TP via the A ring and the potency of these compounds towards Nqo1 activity (Fig 3.13). We show this for the six cysteine residues we have seen modified by CDDO-Epoxyde in this study. We also show this for three Keap1 cysteine residues chosen at random, one from each functional domain of Keap1 (Cys-77, -196 and -583), as well as Cys-151 which has previously been suggested to be the key molecular target of TPs such as CDDO-Me (Cleasby *et al.* 2014, Egger *et al.* 2009) (Fig 3.14). We also observed no correlation between the covalent binding of the TP via the C ring of the TPs and the

potency towards Nqo1 activity, for the same cysteine residues (data not shown).

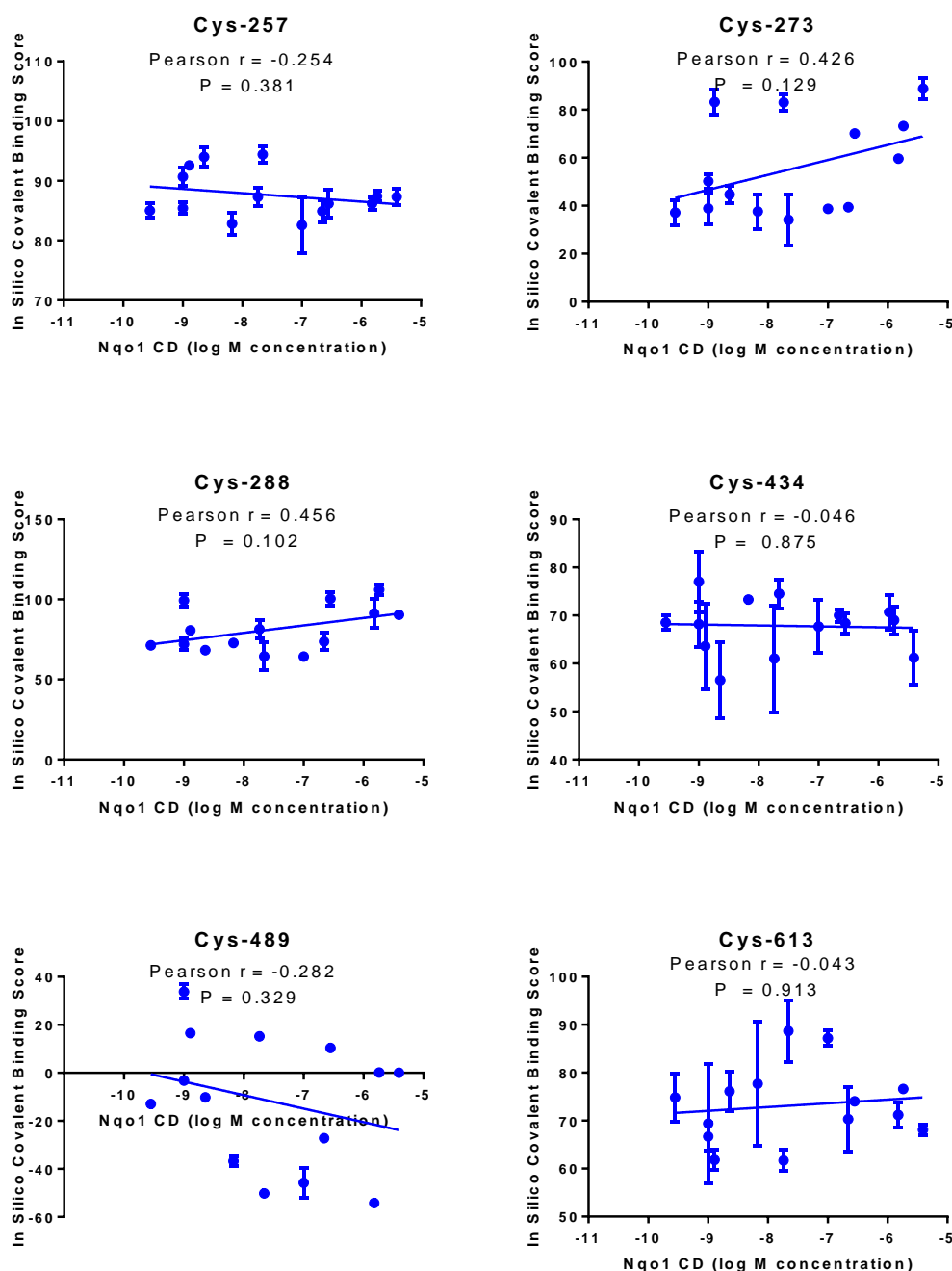


Figure. 3.13. Correlation between TP *in silico* covalent binding score and potency as inducers of Nqo1 activity. Showing \log_{10} scale of concentration at which Nqo1 activity is doubled (CD) by each TP. Average covalent binding score shown from 50 randomly generated poses for each TP, binding each cysteine residue identified as modified by CDDO-Epoide in MS studies, via the A ring. Pearson's r and p values calculated using Pearson's coefficient. Negative Pearson's r value indicates positive correlation.

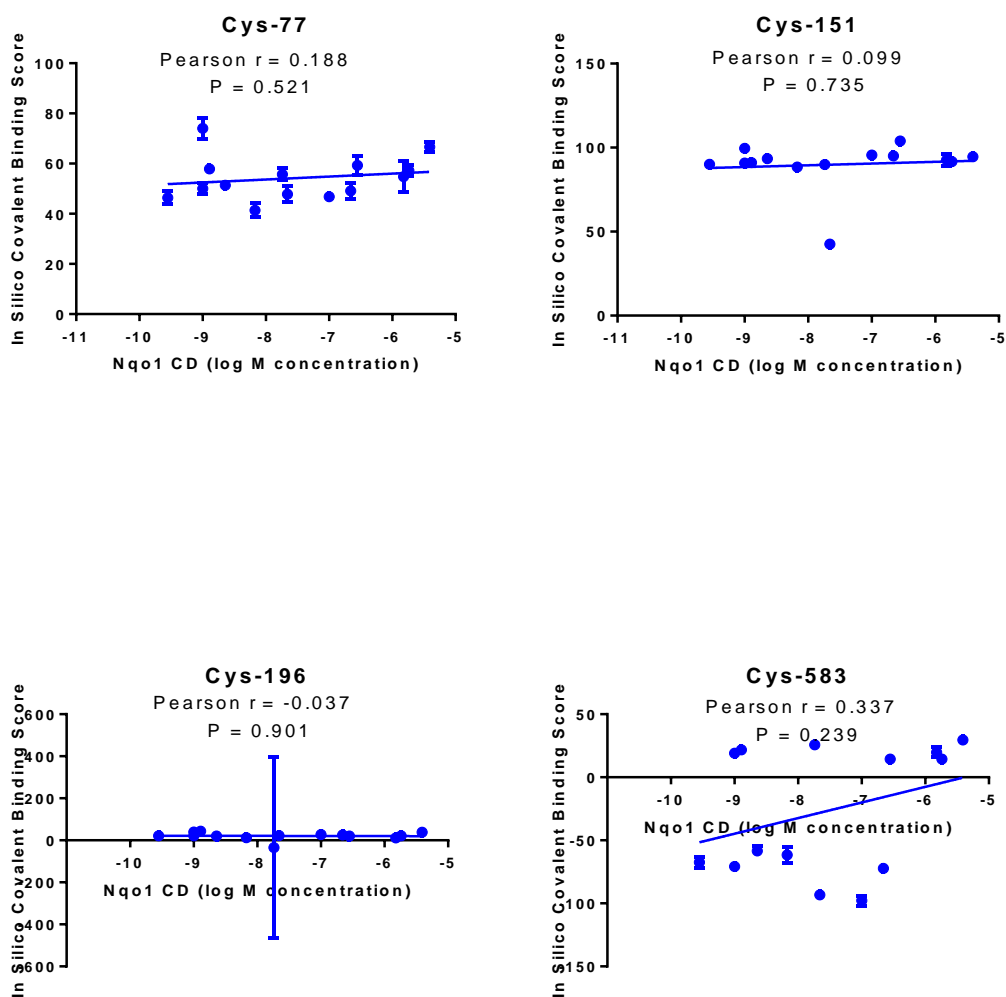


Figure. 3.14. Correlation between TP *in silico* covalent binding score and potency as inducers of Nqo1 activity. Showing \log_{10} scale of concentration at which Nqo1 activity is doubled (CD) by each TP. Average covalent binding score shown from 50 randomly generated poses, for each TP binding 4 cysteine residues within Keap1 functional domains, via the A ring. Pearson's r and p values calculated using Pearson's coefficient. Negative Pearson's r value indicates positive correlation.

3.3.9 Correlation of TP potency towards Nqo1 activity and Keap1 non-covalent binding score

As no correlation was observed between the ability of these compounds to covalently modify Keap1 cysteine residues and their potency towards Nrf2, we hypothesised that the ability of these compounds to bind Keap1 non-covalently within cysteine containing pockets may be important. We used the same approach as detailed in Section 3.3.8, and docked the structures outlined in Appendix 4 non-covalently into the models detailed in Section 3.3.7. The score generated in this case differs from the covalent binding score, as the covalent binding component is removed, and in this docking mode, the ligand is allowed to bind anywhere within a docking sphere (i.e. the cysteine containing pocket), whilst the covalent dockings are limited by the restraint of covalently binding to a specific residue. We show a significant correlation between potency towards Nqo1 activity and the average non-covalent docking score for Cys-273 ($p < 0.05$) and Cys-288 ($p \leq 0.001$) (Fig 3.15). There was no significant correlation observed with the additional Keap1 cysteine residues identified as modified by CDDO-Epoxyde (Cys-257, -434, -489, -613) (Fig 3.15), nor with those chosen from Keap1 functional domains (Cys-77, -151, -196 and -583) (Fig 3.16). This *in silico* data support the hypothesis that TPs mechanism of action may be the modification (covalent or non-covalent) of the pockets containing Cys-273 and Cys-288 in Keap1, which have previously been shown to be essential for Keap1s ability to repress Nrf2 (Zhang and Hannink 2003, Yamamoto *et al.* 2008, McMahon *et al.* 2010).

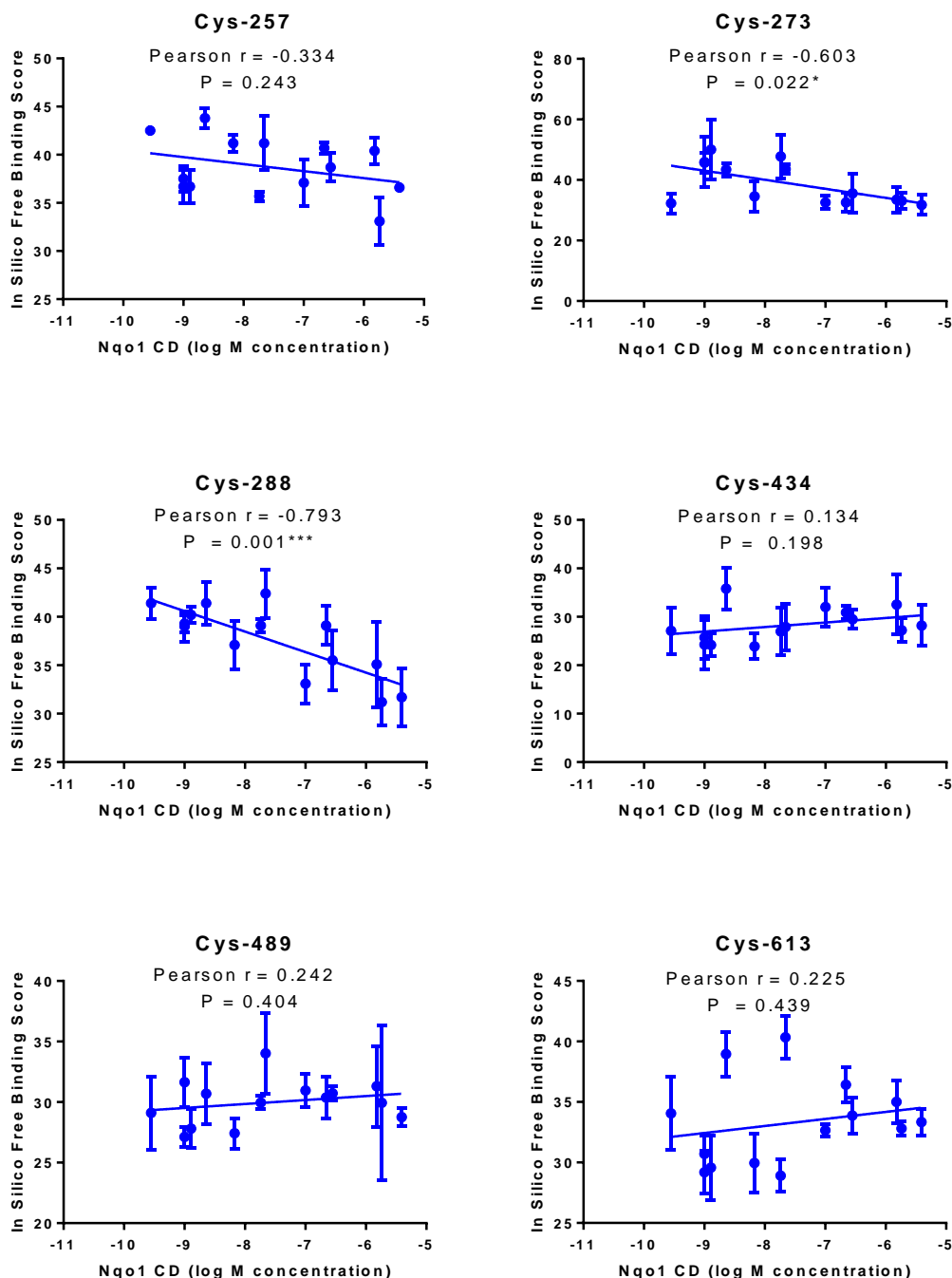


Figure. 3.15. Correlation between TP *in silico* free binding score and potency as inducers of Nqo1 activity. Showing \log_{10} scale of concentration at which Nqo1 activity is doubled (CD) by each TP. Average score shown from 50 randomly generated poses for each TP at each cysteine residue identified as modified by CDDO-Epoide in MS studies. Pearsons r and p values calculated using Pearsons coefficient. Negative Pearsons r value indicates positive correlation ($^* P \leq 0.05$, $^{***} P \leq 0.005$).

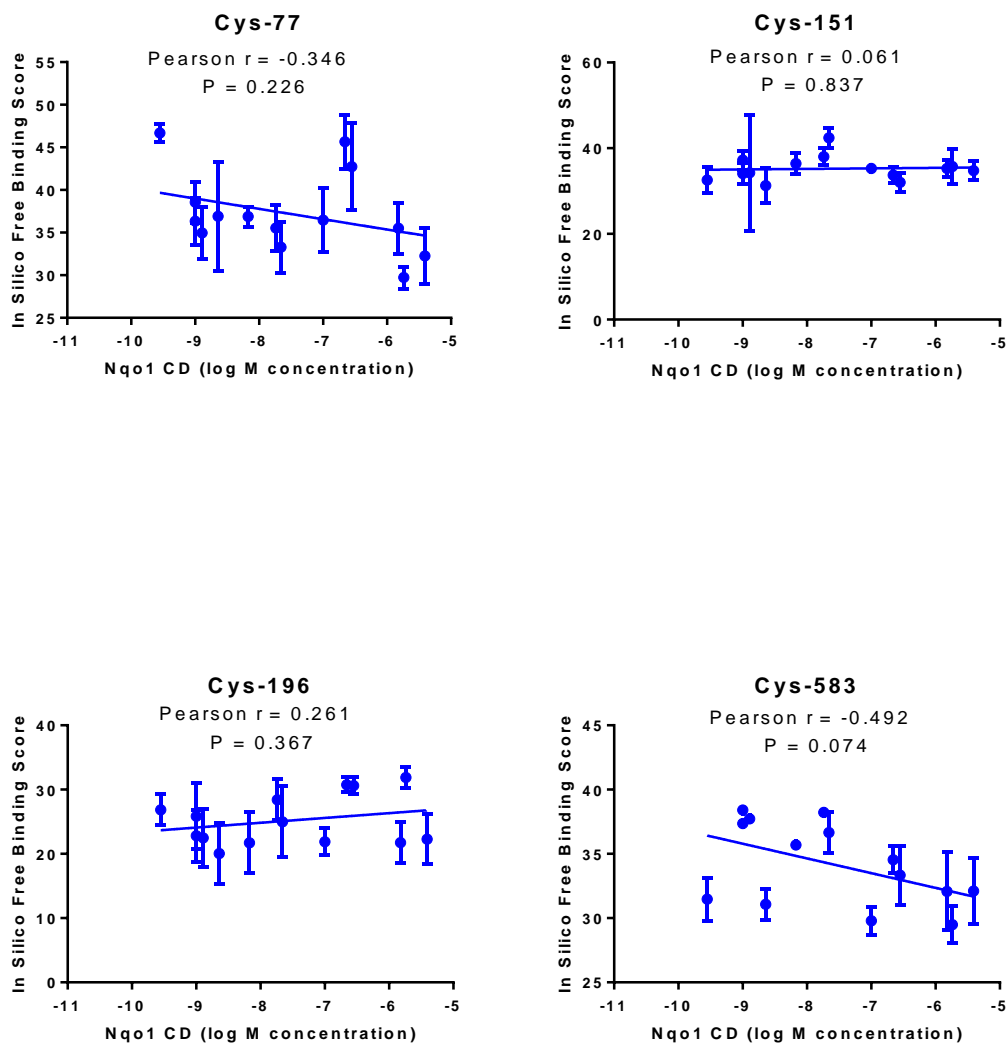


Figure. 3.16. Correlation between TP *in silico* free binding score and potency as inducers of Nqo1 activity. Showing \log_{10} scale of concentration at which Nqo1 activity is doubled (CD) by each TP. Average score shown from 50 randomly generated poses, for each TP at 4 cysteines within Keap1 functional domains. Pearson's r and p values calculated using Pearson's coefficient. Negative Pearson's r value indicates positive correlation (* $P < 0.05$, *** $P < 0.005$).

3.4 DISCUSSION

With a growing interest in Nrf2 as a potential therapeutic target, it is important to further our understanding of the molecular mechanism of action of the compounds which manipulate its activity, in order to predict or design out toxicity. TPs have potential as therapeutic agents due to their many health benefits (Dzubak *et al.* 2006) and large therapeutic index *in vitro* (Copple *et al.* 2014), however little is known about their mechanism of action with regards to Nrf2 activation. Clinical trials using CDDO-Me (Bardoxolone methyl; BM) for the treatment of solid tumours or lymphoid malignancies showed promising results. This led to further clinical trials (the BEAM trial), for the treatment of patients suffering from mid-stage chronic kidney disease (CKD) and type 2 diabetes (Pergola *et al.* 2011a, Pergola *et al.* 2011b). The subsequent Phase 3 trial in patients with end-stage CKD (the BEACON trial) was halted due to “severe adverse events and mortality”, namely cardiovascular events, in patients receiving the drug (de Zeeuw *et al.* 2013, Chin *et al.* 2014). There had been no prior indication of severe adverse events (Pergola *et al.* 2011b, Pergola *et al.* 2011a). The cardiovascular events are purported to be due to the pharmacological modulation of the endothelin pathway, promoting sodium and volume retention, thus increasing blood pressure in patients with late-stage CKD (Chin *et al.* 2014), who are known to be pre-disposed to cardiovascular disease (Locatelli *et al.* 2003). Whilst Nrf2 has been shown to protect against kidney pathologies in animal models (Shelton *et al.* 2013), a role for Nrf2 in the increased estimated glomerular filtration rate (eGFR) observed in CKD patients receiving BM is not known. It is for these reasons it is important to gain a greater

understanding of the chemico-biological triggers for Nrf2 activation by TPs, to determine whether these play a role in toxicity.

To determine whether TP-mediated Nrf2 induction occurs due to the covalent modification of Keap1 cysteine residues, we synthesised a novel TP (CDDO-Epoxyde), capable of irreversible thiol modification, as a chemical tool to characterise protein modification using LC-MS/MS. We hypothesised that the ability of CDDO-Me to bind thiol groups reversibly contributes to its potency towards Nrf2. However, as CDDO-Epoxyde is of similar potency as CDDO-Me, we conclude that reversible thiol modification does not fully explain its potency. As neither TP causes GSH depletion, we conclude that the compounds are likely to be thiol selective. The Nrf2 inducing compounds, DEM, an irreversible thiol modifier (Kobayashi *et al.* 2009, Castillo *et al.* 2002), and sulforaphane, a purported reversible thiol modifier (Dinkova-Kostova *et al.* 2002) both deplete GSH and are less potent inducers of Nrf2 than the TPs (Copple *et al.* 2014), further supporting that reversibility does not affect potency. We conclude that the TPs may be more potent towards Nrf2 than other inducers due to increased specificity for Keap1 thiol groups.

We observed that both TPs form adducts with the reactive Cys-47, in recombinant GSTP1 *in vitro*. Moreover, we detected the modification of a subset of cysteine residues by CDDO-Epoxyde on recombinant Keap1 protein (Cys-257, -273, -288, -434, -489 and -613) and in cells (Cys-257, -273, -288 and -489). This is the first direct observation of adducts formed between a TP and the full length Keap1 protein. In Section 2.3.10, we observed a reversible thiol modification on Cys-434 of Keap1-V5 following treatment of

cells with CDDO-Me, and show here that CDDO-Epoxyde is able to form adducts with this residue, therefore it is possible that this adduct explains the data in Section 2.3.10. We hypothesise, based on the ability of CDDO-Me to compete with CDDO-Epoxyde to bind GSTP1, that both TPs will bind to the same cysteine residues, or will fit in to the same cysteine containing pockets within Keap1. Performing competition assays between the TPs on Keap1 proved unsuccessful due to variation in the quantification of CDDO-Epoxyde adducts. This variation is likely to be an artefact of the multi-step process used to prepare samples for MS analysis. Often, modifications are at the lower limit of detection of the MS, thereby reducing our ability to quantify levels of modification with confidence. Furthermore, the presence of highly abundant peptides in the MS at the same time may overwhelm the less abundant proteins, affecting our ability to detect them. Multiple reaction monitoring (MRM) could reduce this issue and is discussed in Chapter 5.

Our data are consistent with work carried out by Dinkova-Kostova *et al.* (2005) who shows that TPs compete with radiolabelled dex-mes to bind to Keap1 *in vitro* which, as seen in Section 2.3.7, covalently binds Keap1 at Cys-226, -257, -288, -434, -613 and potentially Cys-489. Additionally, Ahn *et al.* (2010) show that TPs compete with a click-tagged analogue of SF in cells, which binds to Keap1 at Cys-273, -288 and -613. This data, in conjunction with the findings reported here, indicate the importance of Cys-273 and -288. These residues are important for the ability of Keap1 to repress Nrf2 (Kobayashi *et al.* 2004, Yamamoto *et al.* 2008). Whilst we show no modification of Cys-151 by TPs, there is evidence for a role of this residue in

the de-repression of Nrf2 by Keap1 (Yamamoto *et al.* 2008), and conflicting data regarding the role of this residue in relation to TP-mediated Nrf2 induction. Egger *et al.* (2009) show that the mutation of Cys-151 diminishes Nrf2 induction by the TP CDDO-Im in cells. On the other hand, experiments using embryonic fibroblasts derived from Cys-151 mutant mice have shown that the Nrf2 response to CDDO-Im is not diminished (Takaya *et al.* 2012).

The MS data shown here are supported by our *in silico* molecular modelling approach. We show no correlation between potency towards Nqo1 activity and the ability of a panel of TPs to covalently bind Keap1 cysteine residues, in our model. Conversely, we show that the potency of the TPs towards Nqo1 activity correlates with their ability to interact non-covalently with the pockets surrounding Cys-273 and -288. It is possible that whilst the other cysteine residues are covalently modified by TPs, they are not functionally relevant regarding Nrf2 induction, as Cys-273 and Cys-288 are. Indeed, there are no reports on the functional effect of mutating Cys-434, however neighbouring residues Ser-431 and Asn-414 form a hydrogen bond, stabilising Arg-415 allowing it to interact with residues located within the ETGE and DLG motifs of the Neh2 domain of Nrf2 (Padmanabhan *et al.* 2006). Therefore, it is possible that the modification of this residue could provoke a conformational change which may disrupt the Keap1/Nrf2 interaction.

The *in silico* data supports observations that Cys-151 of Keap1 is unlikely to be important in the TP mechanism of action. The recent publication which provided the crystal structure of the Keap1 BTB domain showed that CDDO

was able to bind to Cys-151 of human Keap1 (Cleasby *et al.* 2014). The protein domain used in this study contains Keap1 residues 48-180, with only 3 cysteine residues. Thus one could argue that, due to the reactivity of Cys-151 towards electrophiles, and its low pKa value, an interaction between CDDO and this residue is likely under the conditions used, however may not be reproducible with the full Keap1 protein. It is important to note that homology modelling was used, thus the location and organisation surrounding these residues in the homology model may not mirror that of the endogenous protein. Furthermore, in this study, the TP and Keap1 are modelled using rigid-docking which will not take into account whether there is a conformational change in the protein that may affect further interactions.

The investigation of whether Cys-151 of Keap1 is important for the ability of TPs to activate Nrf2 could be tackled by using a competition assay similar to that used in Section 3.3.5. Efforts should be made to identify a compound which forms an adduct with Cys-151, to a sufficient level that the loss of modification could be confidently quantified using MS. Initial attempts in our lab using monomethyl fumarate (MMF) (Linker *et al.* 2011) and DEM (Kobayashi *et al.* 2009) have not been successful (data not shown). To confirm the involvement of the residues indicated in this study, mutagenesis studies would quantify the ability of TPs to induce Nrf2 in cells expressing Keap1 mutants. Unfortunately, the mutation of residues Cys-273 and -288 causes a marked increase in Nrf2 levels under basal conditions (Yamamoto *et al.* 2008, McMahon *et al.* 2010, Zhang and Hannink 2003), thus detecting further activation of Nrf2 by TPs would be difficult.

Whilst the detection of adducts between Keap1 and TPs does not categorically confirm that the modification of Keap1 cysteines by these compounds is responsible for Nrf2 activation, there is sufficient evidence in the literature to suggest that this is a likely mechanism. The *in silico* model detailed here highlights that non-covalent modification of Keap1 by TPs may be important. Using the knowledge that increased TP potency towards Nrf2 correlates with increased safety (Copple *et al.* 2014), by screening compounds using this model there is a potential for identifying novel inducers. which may be more efficacious and less toxic, and structurally dissimilar enough to CDDO-Me to circumvent the effects on the endothelin pathways, thought to be responsible for the cardiovascular events in the BM trial in patients with CKD (Chin *et al.* 2014). This is currently ongoing in our lab. The data shown here do not explain why BM was toxic in clinical trials, and investigating the effect of these compounds of other pathways will be important. The publication of the molecular structure of the BTB region of Keap1 (Cleasby *et al.* 2014) will help determine the importance of covalent and non-covalent modification of Keap1 as a mechanism of Nrf2 induction. Complementing the existing crystal structures of the BTB and Kelch domains of Keap1 with those of the IVR domain and/or full length Keap1, will facilitate virtual screening of compound libraries to identify novel Nrf2 inducers with potential as drug candidates.

CHAPTER 4

**THE IDENTIFICATION OF NOVEL KEAP1 BINDING
PARTNERS**

CONTENTS

4.1	INTRODUCTION	- 143 -
4.2	MATERIALS AND METHODS	- 147 -
4.2.1	Materials and reagents	- 147 -
4.2.2	Cell culture	- 147 -
4.2.3	Mouse Keap1-V5 plasmid purification	- 148 -
4.2.4	Transfection of cells with Keap1-V5	- 148 -
4.2.5	Immunopurification of Keap1-V5.....	- 148 -
4.2.6	Preparation of Keap1-V5 for LC-ESI-MS/MS	- 148 -
4.2.7	LC-ESI-MS/MS methods.....	- 148 -
4.2.8	Western immunoblotting of immunopurified Keap1-V5	- 149 -
4.2.9	Network analysis.....	- 149 -
4.2.10	Amplification of PCR product from pDONR DNA plasmid	- 149 -
4.2.11	DNA electrophoresis	- 150 -
4.2.12	GAP repair of PCR product	- 151 -
4.2.13	Diagnostic yeast colony PCR (YCPCR)	- 153 -
4.2.14	Determination of auto-activating clones	- 154 -
4.2.15	Yeast 2-Hybrid (Y2H) matrix style mating.....	- 156 -
4.2.16	β -Galactosidase enzymatic assay	- 158 -
4.3	RESULTS	- 161 -
4.3.1	Validation of LC-MS/MS assay	- 161 -
4.3.2	LC-MS/MS analysis of putative Keap1-V5 binding partners ...	- 163 -
4.3.3	Identification of proteins with Keap1 binding motif	- 165 -
4.3.4	Network and pathway analysis.....	- 166 -
4.3.5	Validation of Keap1-interacting partners using Y2H	- 174 -
4.3.6	β -Galactosidase Reporter Assay	- 180 -
4.3.7	Comparison of Keap1 interactome composition following exposure of cells to selected Nrf2 inducers	- 182 -
4.4	DISCUSSION	- 189 -

4.1 INTRODUCTION

Keap1 directs the ubiquitination and subsequent proteasomal degradation of Nrf2, and is therefore a main regulator of Nrf2 activity (Bryan *et al.* 2013). The Keap1/Nrf2 complex has been shown to associate with proteins/protein complexes, in addition to the Cul3 ubiquitination system (Kobayashi *et al.* 2004, Hast *et al.* 2013). Interactions between Nrf2 and other proteins affect the localisation of Nrf2 (Theodore *et al.* 2008), its DNA binding (Itoh *et al.* 1997), and the transcription of Nrf2 target genes (Kato *et al.* 2001). Additionally, Keap1 has been shown to associate with a number of other proteins (Zhang *et al.* 2004, Kang *et al.* 2004, Furukawa and Xiong 2005, Karapetian *et al.* 2005, Lo and Hannink 2006, Kim *et al.* 2010). Functionally, protein interactions with Keap1 may impact its ability to regulate the activity of Nrf2, by affecting the sub-cellular location and stabilisation of the protein. The localisation of Keap1 is vital for its ability to sense chemical/oxidative stress and to sequester Nrf2 outside of the nucleus, and some of its known protein-protein interactions reflect this. For example, by binding to the actin cytoskeleton, Keap1 is located in the cytosol, in proximity to reactive metabolite by-products of drug metabolism (Kang *et al.* 2004). By binding to PGAM5, Keap1 is located in proximity to the mitochondria, where considerable quantities of ROS are produced (Lo and Hannink 2008). Additionally, other cytoplasmic proteins which bind to Keap1 can compete with Nrf2, including prothymosin α (Karapetian *et al.* 2005) and fetal Alz-50 clone 1 (FAC1) (Strachan *et al.* 2004), resulting in reduced Nrf2 degradation.

Due to the variety of diseases in which the dysregulation of Nrf2 activity has been shown, therapeutic strategies are evolving which aim to manipulate Nrf2 activity levels, by altering the association between Keap1 and Nrf2, or between Keap1 and the ubiquitination machinery. This can be achieved through the use of small molecular inhibitors, thus avoiding the requirement for pharmacological intervention with (potentially toxic) electrophiles (Zhuang *et al.* 2014, Magesh *et al.* 2012). Small peptides that competitively target the point of contact between Keap1 and Nrf2, or Keap1 and Cul3, have recently been shown to cause activation of Nrf2 signalling (Magesh *et al.* 2012). Based on these observations, the discovery of novel Keap1/Nrf2 binding partners, which play a role in the regulation of the Nrf2 pathway, may provide an alternative therapeutic route to exploit, as they can compete with Nrf2 to bind to Keap1.

In 2010, a novel physical and functional interaction between Keap1 and sequestosome1 (p62) was identified in our lab (Copple *et al.* 2010), and by others (Jain *et al.* 2010, Fan *et al.* 2010, Komatsu *et al.* 2010). It was observed that p62 binds Keap1 via an ETGE-like motif (Komatsu *et al.* 2010). In our lab, the identification of novel Keap1 binding partners was facilitated by MS techniques employed to characterise the proteins co-purified with Keap1-V5 ectopically expressed in HEK293T cells (Copple *et al.* 2010). Since our identification of p62 as a Keap1 binding partner, we have obtained a substantially more sensitive MS system, which may facilitate the identification of novel Keap1 binding partners that were below the limit of detection of our previous assay. In Chapter 2 of this thesis, HEK293T cells were transfected

with Keap1-V5 prior to treatment with Nrf2-inducing compounds (or vehicle controls), followed by exposure to NEM for 5 min to alkylate remaining cysteine residues, to facilitate MS analysis. The aim of this work was to examine chemical and oxidative modifications on the cysteines of immunopurified Keap1-V5, provoked by different Nrf2 inducers. Incidentally, the output from these analyses included a comprehensive list of proteins in the samples which were co-purified with Keap1. Here, this data has been analysed to identify proteins which are putative Keap1 binding partners, by comparison to a data set obtained following mock transfection of the cells. Additionally, the occurrence of changes in the Keap1 complex, following the treatment of cells with the Nrf2-inducing compounds used in Chapter 2, has been investigated. These analyses have been informed by the observation that many Keap1 binding partners have a conserved ETGE-like motif (Fig 1.10), which has been shown to be essential for the ability of numerous Keap1 binding partners to interact with Keap1 (Hast *et al.* 2013). This allowed us to concentrate the analyses on proteins with ETGE-like motifs which are predicted to directly bind to Keap1. In order to validate Keap1 interacting partners, yeast two-hybrid (Y2H) has been used (see Figure 4.1 for an overview of the methods used in this study). **Therefore, the aim of the work described in this chapter is to use our previously generated MS data sets to identify novel Keap1 binding partners which may play a role in the regulation of the Nrf2 cell defence pathway. These may, in turn, provide an alternative avenue to manipulate the activity of the Nrf2 pathway for therapeutic benefit.**

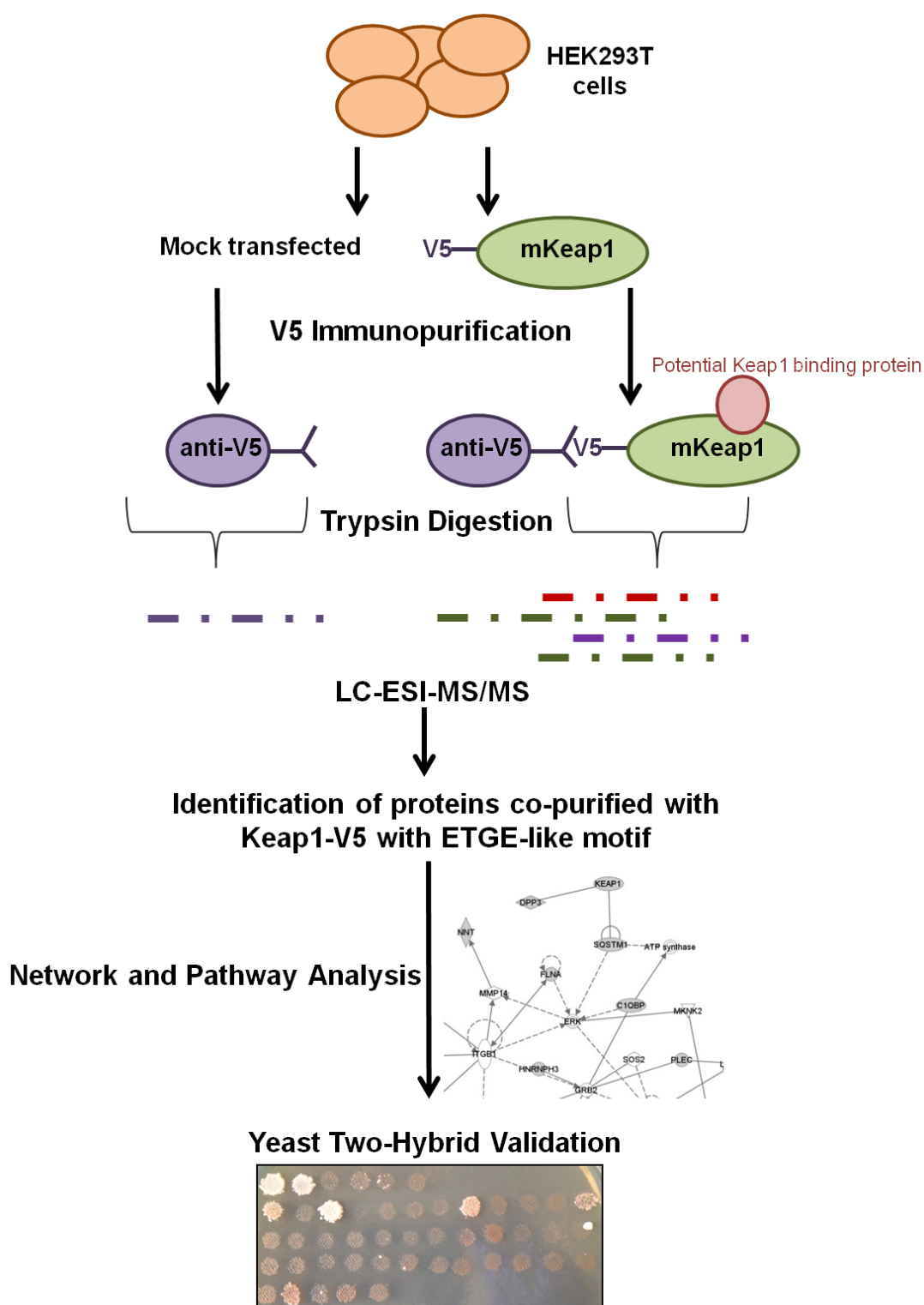


Figure 4.1. Flow diagram of the methods used in this study. HEK293T cells were transfected with Keap1-V5, or mock transfected. Using anti-V5 agarose beads, Keap1-V5 was purified following lysis. Proteins were subjected to trypsin digestion and LC-ESI-MS/MS. A list of protein co-purified with Keap1-V5 was generated using ProteinPilot. Of those identified which contained ETGE-like motifs, network and pathways analysis was performed. Validation of protein interactions was performed using yeast two-hybrid.

4.2 MATERIALS AND METHODS

4.2.1 Materials and reagents

The KOD HotStart DNA Polymerase kit was obtained from Novagen, (Hertfordshire, UK). The Biotaq DNA Polymerase, agarose and HyperLadder 1kb was obtained from Biorline (London, UK). All primers, SybrSafe were from Life Technologies (Paisley, UK). The 10x TBE buffer (Tris/borate/EDTA) and tryptone, were from Fisher Scientific (Loughborough, UK). The glucose, peptone and yeast extract were from ForMedium (Norfolk, UK), and the Bio/Agar was from Biogene (Cambridgeshire, UK). All antibodies were obtained from Abcam (unless stated otherwise in Section 2.2.1). All PCR was performed on a Tetrad PTC-225 Thermo Cycler system from MJ Research (Quebec, Canada), and agarose gels visualised on a Gene Genium Bio-Imaging System from Syngene (Cambridge, UK). All plasmids used were a kind gift from Amy Ponsford, University of Liverpool. All other reagents were either described in Section 2.2.1, 3.2.1, or of analytical or molecular grade and from Sigma-Aldridge (Poole, UK).

4.2.2 Cell culture

Cells were cultured as described in Section 2.2.2.

4.2.3 Mouse Keap1-V5 plasmid purification

The mouse Keap1-V5-encoding plasmid was cultured as in Section 2.2.3

4.2.4 Transfection of cells with Keap1-V5

Cells were transfected as described in Section 2.2.4. Control cells were transfected in the same manner, with equal volumes of 1x TE buffer replacing the Keap1-V5 plasmid.

4.2.5 Immunopurification of Keap1-V5

Keap1-V5 was immunopurified as described in Section 2.2.6.

4.2.6 Preparation of Keap1-V5 for LC-ESI-MS/MS

Keap1-V5 was prepared for LC-ESI-MS/MS as described in Section 2.2.11

4.2.7 LC-ESI-MS/MS methods

LC-ESI-MS/MS was performed as described in Section 2.2.13

4.2.8 Western immunoblotting of immunopurified Keap1-V5

Proteins bound to immunopurified Keap1-V5 were identified by western immunoblotting as described in Section 2.2.10.

4.2.9 Network analysis

Network analysis was performed using QIAGEN Ingenuity Pathway Analysis (IPA, QIAGEN Redwood City, www.qiagen.com/ingenuity). A spreadsheet containing the UniProt details of all proteins outlined in appendix 5, as well as Keap1 and Nrf2, was uploaded to the program, and network and pathway analysis were performed. Network analysis was performed in the same manner for the comparison of the Keap1-V5 complex following the treatment of cells with various Nrf2 inducers.

4.2.10 Amplification of PCR product from pDONR DNA plasmid

Sequence verified cDNA clones in pDONR plasmids containing the protein encoding sequence of a selection of potential Keap1 binding partners were a kind gift from Jonathan Woodsmith, (Max-Planck Institute for Molecular Genetics, Berlin, Germany), and were used as templates for Hot-Start KOD Polymerase amplification. Primers were designed against the appropriate pDONR plasmid as follows:

pDONR221 Forward:

5' GAATTCACAAGTTTGTACAAAAAGCAGGCTCCACCATG 3'

pDONR221 Reverse:

5' GTCGACCACTTTGTACAAGAAAGCTGGG 3'

pDONR223 Forward:

5' GAATTCACAAGTTTGTACAAAAAAGCTGGCATG 3'

pDONR223 Reverse:

5' GTCGACCACTTTGTACAAGAAAGCTGGG 3'.

PCR reactions contained 10 ng of pDONR DNA plasmid, 0.5 μ M forward and reverse primers, 2.5 μ L of 10x KOD buffer, 0.2 mM dNTPs, 15 mM MgSO₄, 0.5 μ L Hot-Start KOD enzyme and made up to a final volume of 25 μ L with dH₂O. Conditions for Hot-Start KOD PCR can be found in Table 4.1.

Step	Cycles	Temperature/Time	Process
1	1	95°C for 2 min	Pre-denaturing
2		95 °C for 30 sec	Denaturing
3	29	60 °C for 60 sec	Annealing
4		70°C for 30 sec/kb	Extension
5	1	4°C to finish	Hold

Table 4.1. Steps and cycles for Hot-Start KOD Polymerase amplification of sequence verified cDNA clones

4.2.11 DNA electrophoresis

The PCR products were resolved on a 1% agarose gel dissolved in 0.5 x Tris/borate/EDTA (TBE) buffer, supplemented with a 1:20,000 dilution of SYBR Safe DNA Gel Stain, at 120 V for approximately 30 minutes. The PCR product (5 μ L) was combined with 2 μ L of 5 % Orange G (5 % sucrose, 0.005 % Orange G) prior to loading onto the gel. PCR samples were resolved alongside a Hyperladder DNAMarker to enable estimation of DNA band sizes. Bands were visualised using a UV Transillumination system (Syngene Bioimaging system).

4.2.12 GAP repair of PCR product

If a DNA band of the correct size was obtained (Fig 4.2A), the PCR product was used for Gap Repair reactions. The yeast transformation/gap repair was performed using the lithium acetate method as previously described by Ito *et al.* (1983). Briefly, 2 mL YPAD broth (10 g/L yeast extract, 100 µg/L adenine hemisulphate, 20 g/L peptone and 20 g/L D-glucose) was inoculated with PJ69-4A (MatA) yeast and incubated for 18 hr at 30 °C shaking at 220 rpm. Following this, a further 8 mL of YPAD broth was added and incubated for an additional 5 hr at 30 °C, 220 rpm. The culture was then centrifuged at 2,300 rpm for 5 min at room temperature and the supernatant discarded. The pellet was resuspended in 5 mL 100 mM lithium acetate (LiOAC), 1.5 mL was transferred to 1.5 mL eppendorf tube and centrifuged at 2,300rpm for 5 min. The supernatant was discarded and to each pellet, the following was added: 230 µL 50% (w/v) PEG 3350, 35 µL 1M LiOAC, 9 µL of 10.5 mg/mL heat denatured (5 min at 95°C) salmon testes DNA, 45 µL dH₂O and 30 ng of *Bam*HI linearised bait destination vector (pGBAE-B). Of this solution, 34 µL was transferred to individual 0.5 mL tubes and 4 µL of the PCR product obtained in Section 4.2.10 was added. The samples were heat shocked in the following steps: 30°C for 30 min, 42°C for 25 min, 30°C for 1 min. The yeast transformation reaction was then plated onto selective drop-out media (supplemented with low adenine (ADE) to enable identification of successfully transformed yeast) and incubated at 30°C for 3-5 days (Fig. 4.2B).

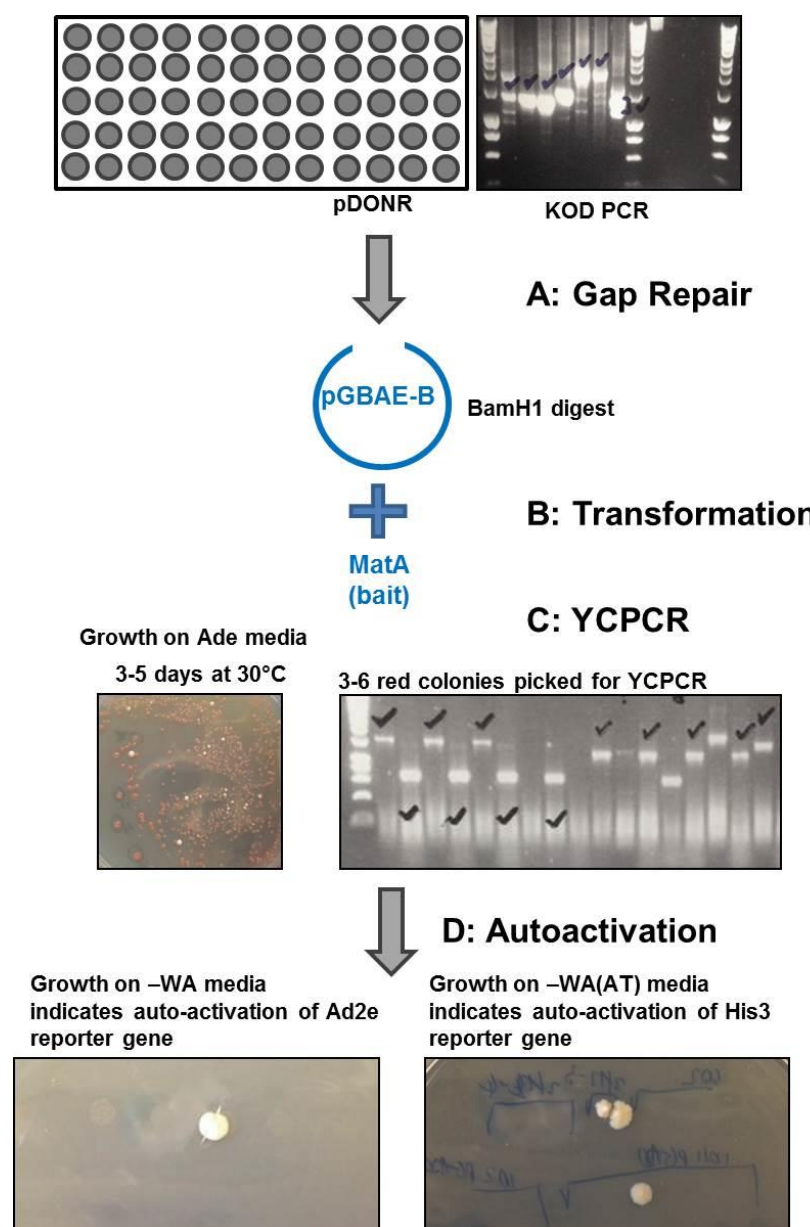


Figure 4.2. Flow diagram of the experimental procedure undertaken for Yeast 2-Hybrid. Constructs in pDONR vectors were amplified using KOD PCR and confirmed by observing PCR bands on an agarose gel. PCR products were inserted into a pGBAE-B vector (A) and MatA yeast cells were transformed (B). Yeast were left to grow for 3-5 days before 3-6 red colonies were picked and clones were checked for the correct MW insert by yeast colony PCR (YCPCR) and confirmed by observing PCR bands on an agarose gel (C). Clones were checked for auto-activation status prior to the generation of glycerol stocks by growing on -WA media and -WH(AT) media. Growth on either of these plates indicated the auto-activation of the Ade2 or the His3 reporter genes, respectively (D). Auto-activating clones were not used in the subsequent yeast 2-hybrid screen.

Successful bait transformants can be identified by the growth of red colonies on this selective drop-out media. The pGBAE-B bait vector contains both the DNA binding domain (BD) and the activation domain (AD) of the Gal4 transcription factor, separated by an in-frame linker sequence. This vector has been previously modified to introduce a stop codon at the 3' end of gene inserts following gap repair, to prevent transcription of the activation domain, thus removing the need for stop codons at the 3' end of the open reading frame (ORF) (Semple *et al.* 2005). Therefore, when the PCR product containing compatible gap repair flanking sequences is recombined in the correct reading frame into the pGBAE-B vector, the yeast cell itself cannot transcribe the Ade2 reporter gene, and grows red on media containing low adenine. Un-linearised vector will produce both the AD and BD in a single in-frame fusion and will therefore be able to activate transcription of the Ade2 gene to produce adenine, and will grow white on the same media. Colonies unable to transcribe the Ade2 reporter gene grow red due to the accumulation of P-ribosylamino imidazole (AIR) which is generated during the synthesis of adenine. In the presence of Ade2, the adenine biosynthetic pathway can continue, however in its absence, the next step of the pathway is inhibited. When AIR accumulates in yeast which grow aerobically, it is oxidised to a red pigment.

4.2.13 Diagnostic yeast colony PCR (YCPCR)

The aforementioned cloning method is directional; therefore inserts should always be introduced with the correct orientation and reading frame. However, to ensure the insert size is as expected, primers flanking the

recombination sites can be used to amplify the insert. The primers used are as follows:

Forward: 5'CCGGAATTCACAAGTTTGTAC3'

Reverse: 5' CGTTAGAGGAGGCAATTGGTTG3'

A toothpick was used to take a sample from 3-6 red colonies from each plate into 3 μ L 20mM sodium hydroxide (NaOH), and left to lyse for 20 min at room temperature. To each of the yeast NaOH suspensions, 12 μ L of the following master mix for Taq DNA PCR was added (amounts indicated are sufficient for 10 reactions): 0.7 μ M forward and reverse primers, 0.625 mM dNTPs, 15 μ L of 10x NH_4 buffer, 7.5 μ L of 2.25 mM MgCl_2 , 3 μ L DMSO, 73.5 μ M dH_2O and 1.5 μ L Taq polymerase. Conditions for Taq DNA PCR can be found in Table 4.2. PCR products were resolved on a 1% agarose gel, as described in Section 4.2.11 (Fig 4.3 C).

Step	Cycles	Temperature/Time	Process
1	1	95°C for 5 min	Pre-denaturing
2		95°C for 1 min	Denaturing
3	39	55-68 for 1 min	Annealing
4		72°C for 3 min 30 secs	Extension
5	1	72°C for 5 min	Final extension
6	1	15°C to finish	Hold

Table 4.2. Steps and cycles for Taq DNA polymerase yeast colony PCR

4.2.14 Determination of auto-activating clones

To avoid false positives, such as clones capable of activating reporter genes in haploid form (i.e. in the presence of only the BD of the Gal4 transcription factor), all clones were tested to assess their potential to self-activate either

higher (ADE) or lower (His + 3-AT) stringency Y2H reporter genes. Of the red colonies picked with the correct insert size (Fig 4.2C), the remainder of the colony on the plate was picked into 20 μL dH_2O . Of this, 3 μL was pipetted onto selective drop-out media plates for bait (MatA) yeast as described in Table 4.3, and plates incubated at 30°C for 7-14 days (Fig. 4.2 D). If colonies grew on auto-activation plates (-WA, -WH(AT)), they were not continued. Causes of auto-activation may include: spontaneous host mutations allowing yeast to grow on selective media in the absence of bait/prey interactions; bait proteins with inherent transcriptional activity or that interact with other factors with transcriptional activity, or prey proteins that bind DNA may non-specifically drive transcription of yeast reporter genes.

Of colonies showing no auto-activation, colonies were selected from the -W plate using a toothpick and resuspended in 200 μL -W media, before the addition of 80 μL 80 % glycerol and storage at -80 °C. 3 μL of each was spotted onto -W plates to grow for 3-5 days at 30 °C.

Plate	Constituents	Purpose
-WA	No tryptophan No adenine	High stringency Yeast without Ade reporter gene activation should not grow
-WH(AT)	No tryptophan No histidine With 2.5mM 3-Amino-1,2,4-triazole (3AT)	Low stringency 3-AT makes it more difficult for yeast to survive by competing to binding the His3 promoter Yeast without His reporter activation should not grow
-W	No tryptophan	Positive control for the growth of the yeast. All yeast grow in the absence of tryptophan due to the Trp1 gene

Table 4.3. Table describing media for determining auto-activation.

4.2.15 Yeast 2-Hybrid (Y2H) matrix style mating

Matrix style Y2H assays test for binary interaction between a pre-defined set of proteins (bait or prey) in a high throughput manner. The Y2H system exploits the properties of the Gal4 transcription factor which activates the transcription of an array of reporter genes within the yeast genome (Fields and Song 1989). The protein is comprised of two domains- a DNA binding domain (BD) and a transcriptional activation domain (AD). The BD binds to Gal4 specific sequences within the yeast DNA promoter regions whilst the AD recruits and activates RNA polymerase which in turn, activates transcription. The system is used to look at protein-protein interactions by dividing the two domains of the protein and fusing them each to proteins of interest. Conventionally, the BD region is fused to the N-terminus of a protein of interest (bait) whilst the AD domain is fused to the N-terminus of a second protein (prey). If the two fused proteins interact, this will bring together the two domains of the Gal4 transcription factor which can, in turn activate transcription of the reporter gene (Figure 4.3). The reporter genes used in this study are ADE2 and HIS3, which are under the control of different Gal4-induced promoters, Gal2p and Gal1p, respectively. The yeast used in this study will therefore only grow on low adenine or low histidine selective media if these reporter genes are activated, i.e. in the presence of a protein-protein interaction, bringing together the DB and the AD of Gal4.

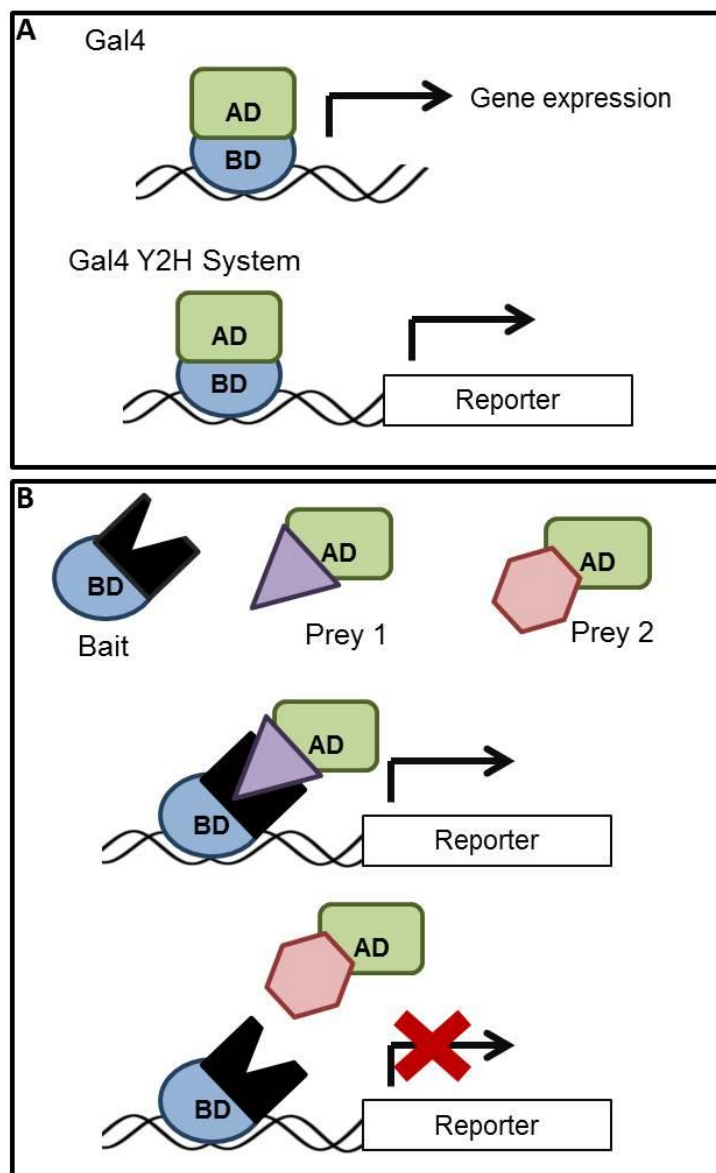


Figure 4.3. Schematic of the classical Y2H system. (A) The two domains of the Gal4 transcription factor; the DNA binding domain (BD), and the transcriptional activation domain (AD). Gal4 activates the transcription of a reporter gene. (B) In the Y2H system, Gal4 is fragmented. The DB domain is fused to a protein of interest and the AD domain to a potential binding partner. If the two proteins interact, the DB and AD domains are brought together and drive transcription of a downstream reporter gene (prey 1). If they do not interact, no reporter activation is seen (prey 2)

Using a toothpick, a small amount of prey colony was picked from an SD-L plate (Mata yeast) and resuspended in 6 μ L of sterile water. Of this, 3 μ L was spotted onto a YPAD plate and allowed to dry. The same method was used

to pick bait colonies from an SD-W plate (MatA yeast) and 3 μ L spotted on top of the prey (Fig 4.4 A). The preys screened were a gift from Amy Ponsford (University of Liverpool, UK) and include Keap1, and the known Keap1 binding partners Nrf2 and p62, as the protein co-purified with Keap1-V5 may not bind Keap1 directly, but via an interaction with other Keap1 binding partners. Once dry, the plates were incubated at 30 °C for 24 hr. Once grown, a replication block was used with a sterile velvet overlay. The YPAD plate was inverted onto the velvet and gentle, even pressure was applied using the fingertips. The YPAD plate was removed and replaced with two diploid selection plates (SD-WL). Gentle pressure was applied to the plate to transfer the colonies from the velvet and the plate was then incubated at 30 °C for 2 days (Fig 4.4 B). Incubation on this media allows the bait and prey yeast to mate, and selects for only those that have mated (i.e. diploid). The process was then repeated, transferring the colonies from one SD-WL plate into an SD-WLA plate and an SD-WHL(AT) plate and these were incubated at 30 °C for up to 14 days. The growth of yeast colonies on the plates indicates the activation of the reporter genes ADE2 and HIS3 respectively, which are under the control of the Gal4-induced promoters Gal2p and Gal1p respectively. Growth was recorded by photographing plates (Fig 4.4 C)

4.2.16 β -Galactosidase enzymatic assay

The β -galactosidase (β -gal) enzymatic assay was used as a third reporter gene assay to increase stringency. Briefly, X-Gal (5-bromo-4-chloro-3-indolyl-beta-D-galactopyranoside) is an inert chromogenic substrate for β -

galactosidase, an enzyme that promotes lactose utilisation. β -gal hydrolyses X-Gal into a colourless galactose and 4-chloro-3-brom-indigo, which forms an intense blue precipitate. Induction of the lacZ gene in yeast by the Gal4 transcription factor (i.e. by a protein-protein interaction) leads to the production of the β -galactosidase enzyme, and thus hydrolysis of X-Gal and the development of blue colonies (Fig 4.4 C).

X-gal was reconstituted in DMF to 100 mg/mL and stored away from direct light at 2 °C. The β -gal reagent was made from 6 mL sterile Z buffer (60 mM Na_2HPO_4 , 40 mM NaH_2PO_4 , 10mM KCl, 1mM MgSO_4), 100 μL of 100 mg/mL X-gal, and 11 μL β -Mercaptoethanol. Filter paper was cut to cover the colonies, laid over yeast and rubbed until the yeast was transferred onto the paper. The paper was peeled off at an angle to leave maximum yeast attached. This filter paper was submerged in liquid nitrogen for 10 sec to lyse the cells, and then allowed to thaw for 30 sec. This was repeated. Two circular pieces of filter paper were covered with the β -Gal reagent ensuring no air bubbles are present beneath either the two filters, or the bottom filter and the plastic base of the plate. The thawed filter paper with the yeast on was placed face up onto the filter paper, and sealed. The plate was incubated at 37°C for 6 hr, checking frequently to record colour change, and then left at 4 °C overnight to allow further development of the blue pigment. Colour change was recorded by photographic filter paper (Fig 4.4 C).

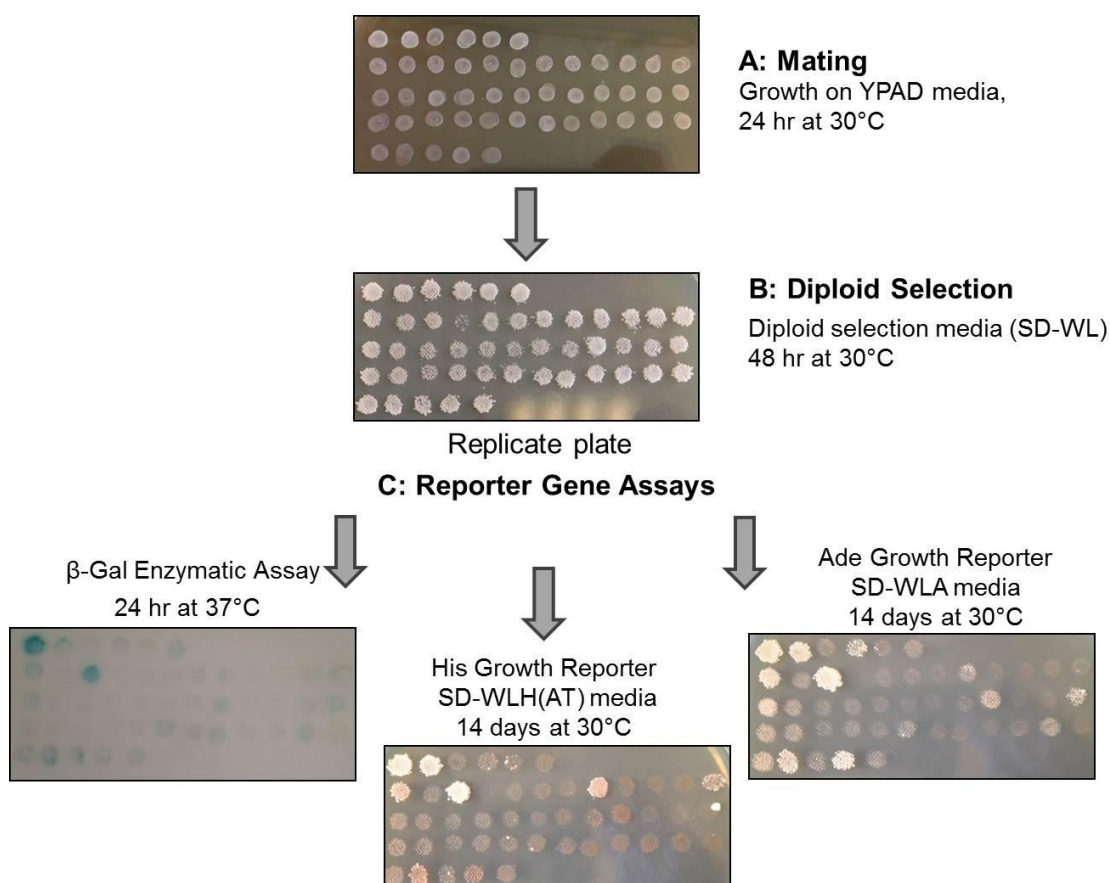


Figure 4.4. Flow diagram of the experimental procedure used for determining binary protein interactions. The prey yeast (*Mat α*) was pipetted on to the YPAD media and allowed to dry, before the bait yeast (*MatA*) was pipetted on top, and incubated at 30 °C for 24 hr. A replicate plate was created for diploid selection and grown for 48 hr at 30 °C. The yeast were then replicated for reporter gene assays onto Ade or His growth media (SD-WLA or SD-WLH)AT) respectively, and grown at 30 °C for 14 days. Yeast were also transferred onto filter paper for the β -Gal assay and grown for 6 hr at 37 °C.

4.3 RESULTS

4.3.1 Validation of LC-MS/MS assay

To identify novel Keap1 binding partners, HEK293T cells were transfected with Keap1-V5, or mock transfected. As the end-point of the original experimental set up used in this study was to identify modifications of Keap1-V5 provoked by Nrf2 inducing compounds (see Chapter 2), cells were treated with NEM (2 mM for 5 min) prior to lysis and LC-ESI/MS/MS analysis, to cap the cysteine residues in Keap1 and enhance their detection. Following lysis, Keap1-V5 was purified using anti-V5 agarose beads before trypsin digestion and LC-ESI/MS/MS analysis. A ProteinPilot search was used to identify proteins co-purified with Keap1-V5 from HEK293T cells, or co-purified following mock transfection of the cells. To validate these data, western blotting was performed for known Keap1-binding proteins, following their elution from the anti-V5 agarose beads. Of the known Keap1- interacting partners chosen for this analysis, none were purified from the mock transfected cells (Table 4.4).

Protein	Average number of peptides		Reference(s)
	Keap1-V5	Mock	
Keap1	109.3	0	Copple <i>et al.</i> (2010)
p62	3.2	0	Fan <i>et al.</i> (2010), Komatsu <i>et al.</i> (2010)
IKK β	2.6	0	Kim <i>et al.</i> (2010), Lee <i>et al.</i> (2009)
DPP3	4.2	0	Hast <i>et al.</i> (2013)

Table 4.4. Proteins chosen for validation of MS data. The average number of peptides detected across six biological repeats is shown, and references confirming their interaction with Keap1.

In a validation of the experimental approach, both Keap1-V5 and its known binding partner p62 were enriched on anti-V5 agarose beads following immunopurification of Keap1-V5 from cell lysates (Fig 4.5A, B). Additionally, IKK β has previously been shown to bind to Keap1 and therefore provides a link between the Nrf2 and NF- κ B pathways (Kim *et al.* 2010, Lee *et al.* 2009). IKK β was shown to be highly enriched on the anti-V5 agarose beads following Keap1-V5 transfection, compared to mock transfection (Fig.4.5C). DPP3 is a recently described Keap1 binding partner (Hast *et al.* 2013) that was also identified in our MS data set. Western blot analysis confirmed that this protein is considerably enriched following anti-V5 immunopurification from Keap1-V5 transfected cells, compared to mock transfected cells (Fig 4.5D). Overall, the LC-MS/MS analysis identified a number of known Keap1 binding partners which we have successfully validated by western blotting, confirming the robustness of our experimental approach. It is worth noting that following immunopurification of Keap1-V5 from cells, there is a considerable loss of Keap1 and p62 from the cell lysate (compare input (IN) with flow through (FT) following Keap1-V5 transfection, Fig 4.5A,B), due to their presence on the agarose beads. This is not the case for IKK β and DPP3 (Fig 4.5C,D), indicating that the interaction is not as substantial between these proteins and Keap1 as it is between Keap1 and p62.

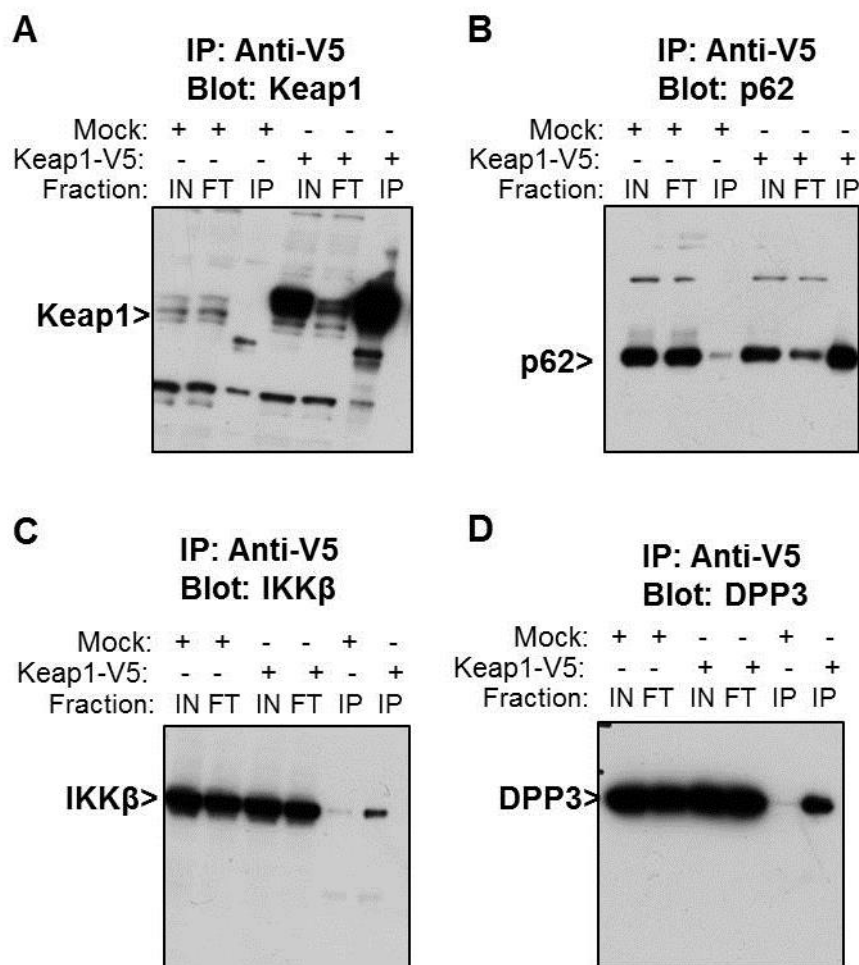


Figure 4.5. Western blot validation of Keap1 binding proteins identified by mass spectrometry. HEK293T cells transfected with Keap1-V5, or mock transfected were lysed and Keap1-V5 was immunopurified. Samples taken before immunopurification (IN; input), after immunopurification (FT; flow through) and proteins co-purified with agarose beads eluted from the beads (IP) were separated by SDS-PAGE. Western blotting was performed for a selection of known Keap1 binding partners. Representative images shown from two biological repeats.

4.3.2 LC-MS/MS analysis of putative Keap1-V5 binding partners

Using a Protein Pilot search, we were able to identify 1,449 proteins co-purified with Keap1-V5 from HEK293T cells treated with the vehicle dH₂O, which were present in at least one of six biological repeats. Proteins such as

keratins which are likely to be skin derived proteins introduced during sample preparation, were removed. The list of putative Keap1-binding proteins was further refined by excluding proteins identified in <2 of six biological repeats and by comparing the number of peptides identified for a given protein in the Keap1-V5 transfected samples with the number identified in the mock transfected control (Fig 4.6). Proteins present in the mock transfected control are likely to bind to the anti-V5 agarose beads non-specifically, as opposed to Keap1-V5. For some proteins, however, more peptides were present in Keap1-V5 transfected samples compared to mock transfected controls. These proteins were retained in the data set if the ratio of peptides in Keap1-V5 transfected samples to mock transfected controls was ≥ 1.5 (Fig 4.6).

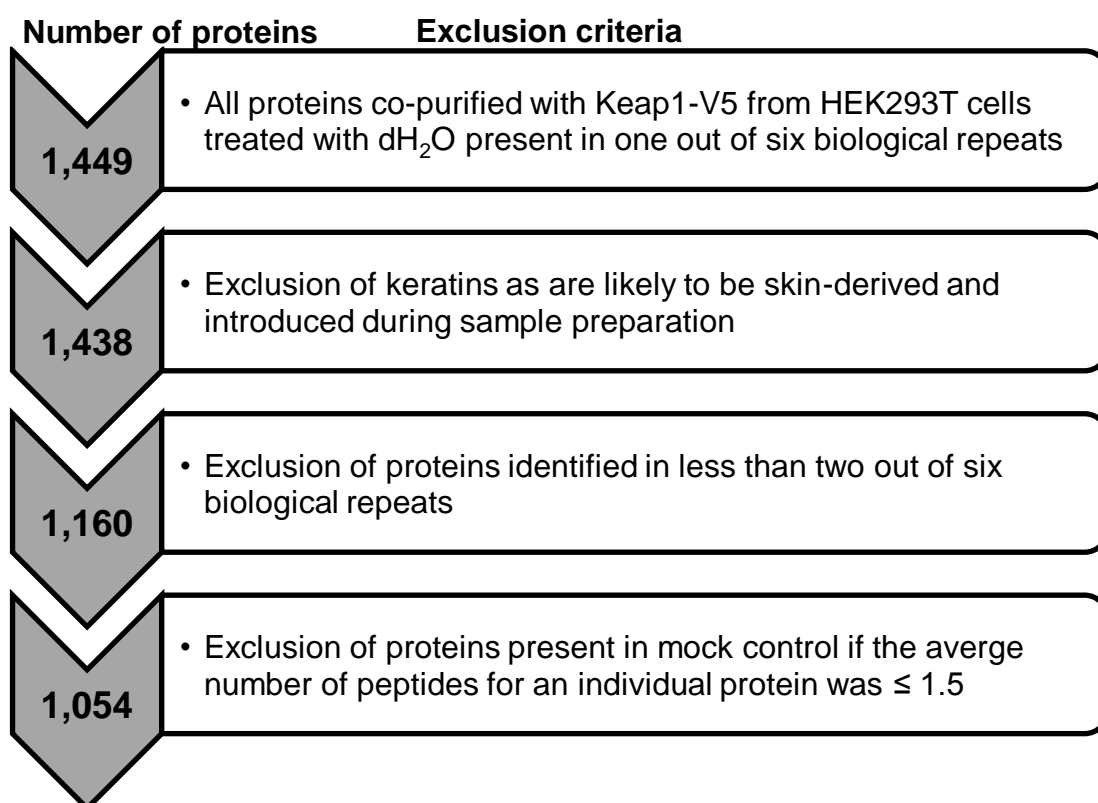


Figure 4.6. Flow diagram highlighting the number of proteins retained for further analysis of potential Keap1-interacting partners.(Following co-purification with Keap1-V5 from HEK293T cells.)

4.3.3 Identification of proteins with Keap1 binding motif

Due to the vast number (1,054) of proteins co-purified with Keap1-V5 and identified by MS, and despite our exclusion of likely false positives, it is likely that a proportion of the remaining proteins are present in the data set due to an interaction with other Keap1-binding partners. Notwithstanding the fact that such proteins may have important roles in regulating the function of Keap1, we focussed subsequent investigations on proteins that were more likely to be direct binding partners of Keap1. During the course of this investigation, Hast *et al.* (2013) published a Keap1 interactome using a similar methodology to our own, involving the transfection of HEK293T cells with Keap1-FLAG followed by affinity purification and LC-MS/MS analysis. Comparison of our data set (1,054 proteins) with that of Hast *et al.* (2013) revealed a considerable (34 %) overlap in the proteins identified (Fig 4.7A). Moreover, Hast *et al.* (2013) showed that the ETGE-like motif containing proteins that were identified and validated in their study required the ETGE-like motif to bind to Keap1. Furthermore, proteins containing ETGE-like motifs can compete with Nrf2 to bind to Keap1, resulting in up-regulation of Nrf2 signalling (Camp *et al.* 2012, Ma *et al.* 2012, Hast *et al.* 2013). Therefore, for the analysis of our data set, we focused our attention on proteins which contained an ETGE-like Keap1 binding motif (ETGE/ESGE/STGE). 44 proteins containing at least one of such motifs were commonly identified in our data set and that of Hast *et al.* (2013) (Fig 4.7B), and 11 solely in our analysis, and further analysis was focussed on these proteins (see appendix 5 for full list).

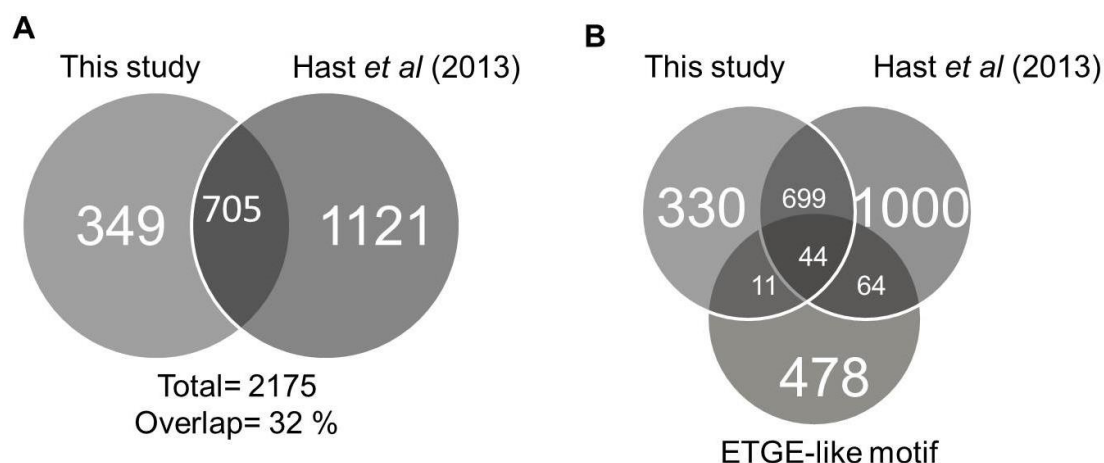


Figure 4.7. Venn diagram comparing our data with that of Hast *et al.* 2013 Comparison of total number of proteins identified in both data sets (A) and those identified containing an ETGE-like motif (ETGE/ESGE/STGE) (B). UniProt IDs were converted to DAVID gene IDs in order to facilitate comparison to the data set output of a search for proteins containing an ETGE/ESGE/STGE motif (<http://www.genome.jp/tools/motif/>). UniProt IDs taken directly from supplementary material from Hast *et al.* (2013).

To identify proteins with ETGE-like motifs, the UniProt IDs from our data set and the data set of Hast *et al.* (2013), and the gene ID output from the programme used to identify proteins with ETGE-like motifs (<http://www.genome.jp/tools/motif/>) were converted to DAVID gene IDs using DAVID Bioinformatics Resources 6.7 (Huang da *et al.* 2009b, Huang da *et al.* 2009a). Therefore, discrepancies between the total numbers of proteins in either data set are due to inconsistencies in the conversion of gene ID values.

4.3.4 Network and pathway analysis

Having identified 55 proteins containing Keap1 binding motifs in our data set, 44 of which were also identified following Keap1-FLAG IP from HEK293T cells by Hast *et al.* (2013), we subjected these proteins to network and pathway analysis using Ingenuity (see appendix 5 for details of proteins used

in this analysis). Nrf2, which was not identified in the MS dataset was also added to the list of proteins used in these analyses, as it is a well-known Keap1 binding partner, and relevant to the focus of this thesis. Additionally, Keap1 was included in these analyses, as it is the focal point of this study. Network and pathway analysis were performed to determine whether any of the 55 putative Keap1 binding partners have previously been shown to interact with Keap1, either directly or indirectly, and to identify their cellular functions.

The network analysis software identifies known interactions between proteins in the inputted data set to create a small network, and adds in molecules from a database to specifically connect two or more small networks. The functions shown (Table 4.5) are the top 3 functions associated with the proteins in the network. The top 3 represented networks (in order of their significance) are shown in Table 4.5. The score given to the network is based on a Fishers Exact Test p-value calculation which calculates the likelihood that molecules that are part of a network are found there by chance.

The 55 inputted proteins were found to be significantly associated with networks related to the cell cycle, DNA replication and repair, cell death and cell survival (Table 4.5). Network 1 does not contain Keap1, or Nrf2, but does contain PGAM5, a known Keap1 binding partner (Fig 4.8). Therefore, despite containing ETGE-like binding motifs, it is possible that some of the proteins selected for network and pathway analysis may have been co-purified with a Keap1 binding partner, such as PGAM5, and therefore not be a direct binding partner of Keap1. Further work will be needed to address this issue.

Alternatively, the proteins identified in this network could be novel Keap1-binding partners with previously unknown links to established Keap1-interacting partners. Network 2 contains Keap1, Nrf2 (NFE2L2) and p62 (SQSTM1) and a number of proteins co-purified with Keap1 in this study that have not previously been linked to Keap1 (Fig 4.9). Network 3 does not appear to contain any known Keap1 binding proteins (Fig 4.10). The focus of this network is p53, a tumour suppressor protein involved in apoptosis and cell survival, the mutation of which has been associated with numerous cancers (Muller and Vousden 2014). Identifying a direct interaction between Keap1 and a protein within this network would unequivocally link the Nrf2 cell defence pathway and the p53-mediated cell survival pathway.

Network	Functions	Focus molecules	Score
1	Cell cycle DNA replication, recombination and repair Cell death and survival	18	35
2	Cell death and survival (Cancer, Respiratory disease)	13	23
3	Cell cycle Cell growth and proliferation Connective tissue development and function	13	23

Table 4.5. Network analysis of putative Keap1 interacting proteins containing ETGE-like Keap1 binding motif. Proteins co-purified with Keap1-V5 from HEK293T cells expressing Keap1-V5 containing ETGE-like motifs, plus Nrf2 and Keap1, were subjected to Ingenuity network analysis. Showing the three most represented networks in order of significance. Focus molecules is the number of proteins from the inputted data set (55 in total) in that network, the score is generated using a right-tailed Fishers Exact Test p-value calculation, which calculates the likelihood that that inputted proteins that are part of a network are found there by chance (the higher the score, the more significant the network representation).

Network 1:

Cell cycle
DNA replication,
recombination, repair
Cell death and survival

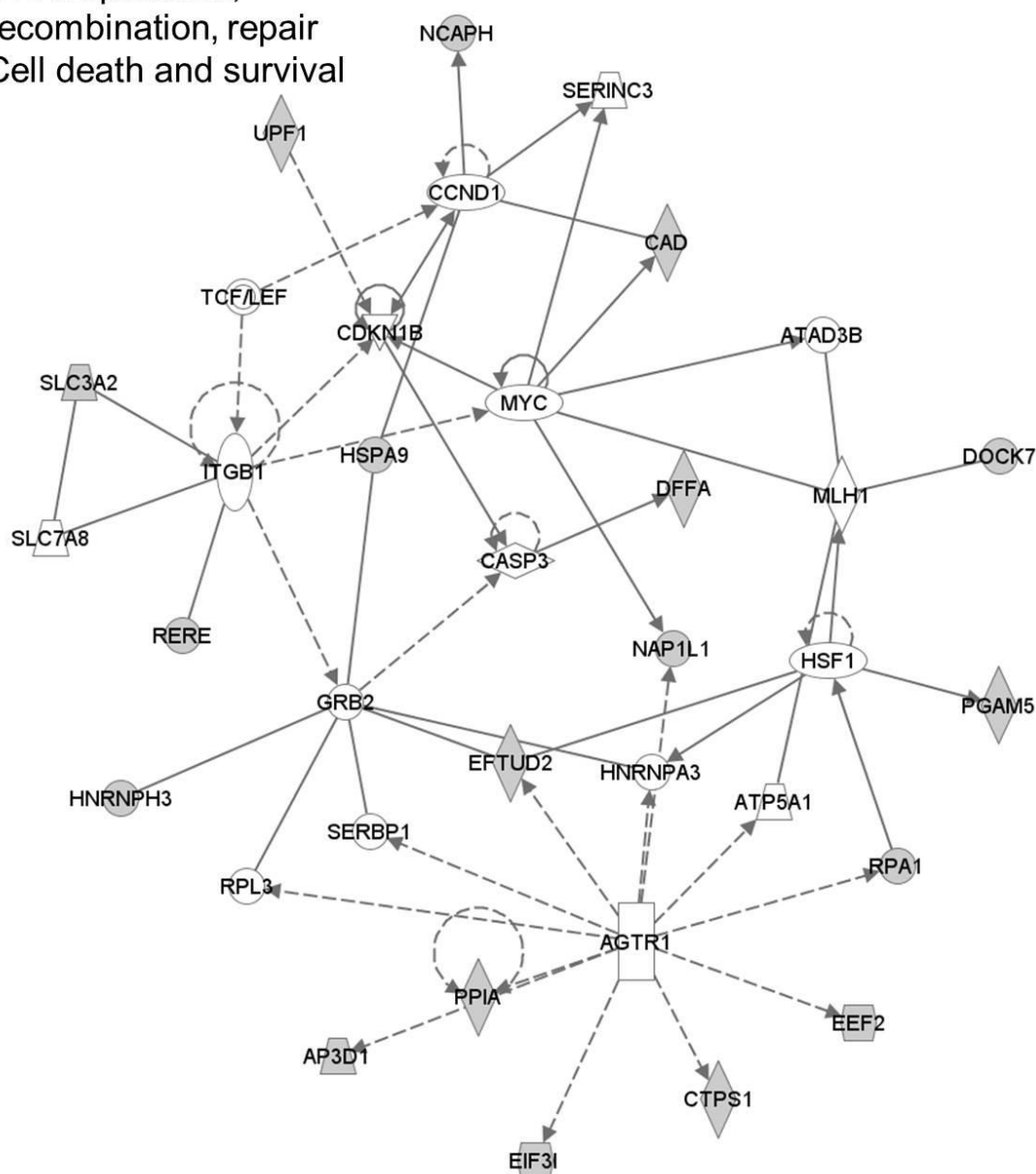


Figure 4.8. Network 1 identified through Ingenuity network analysis of putative Keap1 interacting partners. Of the proteins co-purified with Keap1-V5 from HEK293T cells, those containing ETGE-like motifs, plus Nrf2 and Keap1 and were subjected to network analysis using Ingenuity. This assigns the proteins in the data set to networks in which they are known to be involved, based on known interactions. Showing the most significantly represented network. Proteins highlighted in grey are present in the inputted data set, those in white are in the Ingenuity database in that network, but not present in the inputted data set. Solid and dotted grey lines indicate direct and indirect interactions, respectively. Arrows indicate the direction of the interaction. Different shapes indicate different molecule functions. See appendix 6 for figure legend regarding molecule shapes.

Network 2:
Cell death and survival
(cancer, respiratory disease)

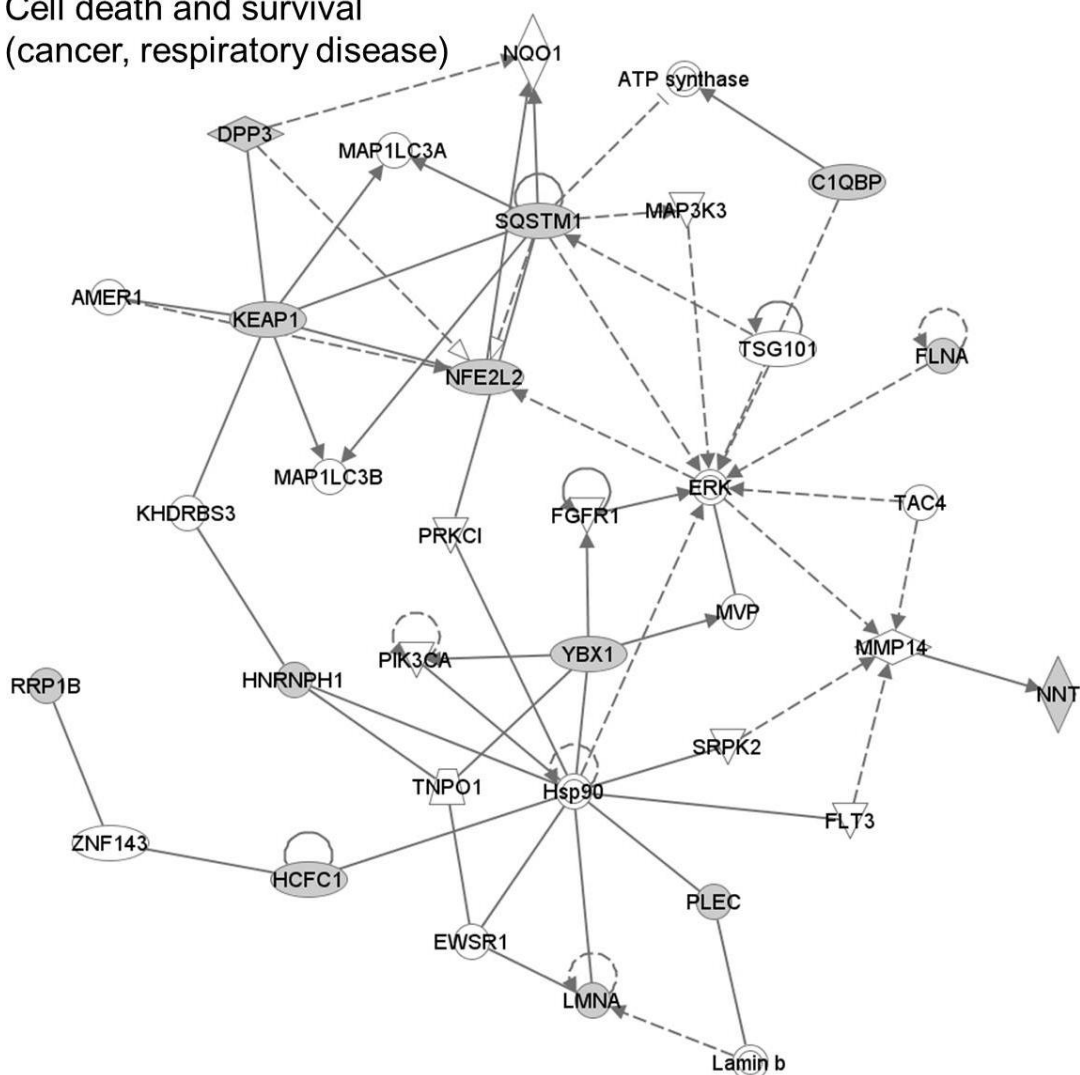


Figure 4.9. Network 2 identified through Ingenuity network analysis of putative Keap1 interacting partners. Of the proteins co-purified with Keap1-V5 from HEK293T cells, those containing ETGE-like motifs, plus Nrf2 and Keap1 and were subjected to network analysis using Ingenuity. This assigns the proteins in the data set to networks in which they are known to be involved, based on known interactions. Showing the second most significantly represented network. Proteins highlighted in grey are present in the inputted data set, those in white are in the Ingenuity database in that network, but not present in the inputted data set. Solid and dotted grey lines indicate direct and indirect interactions, respectively. Arrows indicate the direction of the interaction. Different shapes indicate different molecule functions. See appendix 6 for figure legend regarding molecule shapes.

Network 3:

Cell cycle
Connective tissue development
and function

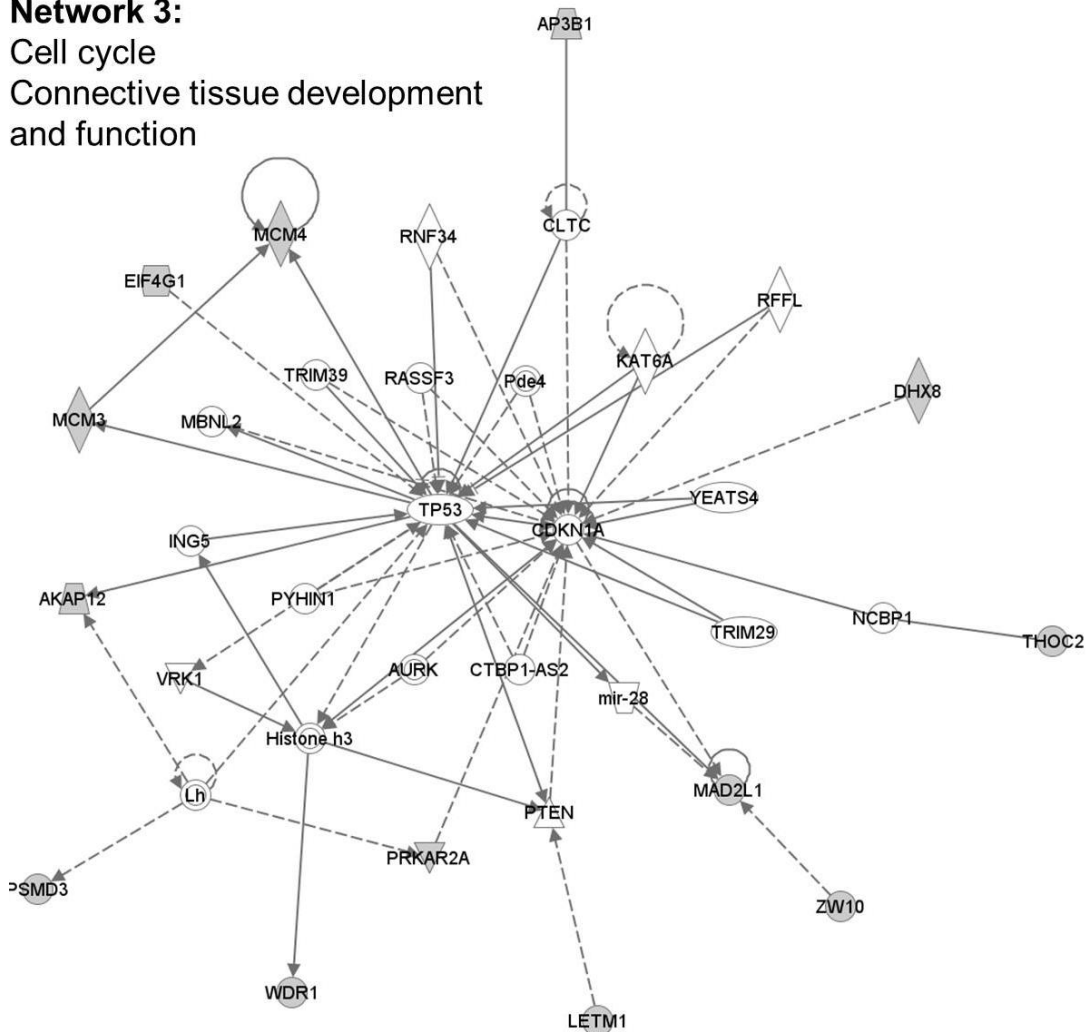


Figure 4.10. Network 3 identified through Ingenuity network analysis of putative Keap1 interacting partners. Of the proteins co-purified with Keap1-V5 from HEK293T cells, those containing ETGE-like motifs, plus Nrf2 and Keap1 and were subjected to network analysis using Ingenuity. This assigns the proteins in the data set to networks in which they are known to be involved, based on known interactions. Showing the third most significantly represented network. Proteins highlighted in grey are present in the inputted data set, those in white are in the Ingenuity base in that network, but not present in the inputted data set. Solid and dotted grey lines indicate direct and indirect interactions, respectively. Arrows indicate the direction of the interaction. Different shapes indicate different molecule functions. See appendix 6 for figure legend regarding molecule shapes.

The pathway analysis indicated that many of the proteins in this data set are not involved in similar cellular pathways (Table 4.6). The most significantly represented pathway is that of cell cycle control and chromosomal replication (pathway 1), which relates well with the network analysis (Table 4.5). However, this pathway is only represented by three proteins within the relatively small data set. As would be expected, the Nrf2-mediated oxidative stress response is represented by the presence of Keap1, Nrf2 (NFE2L2) and p62 (SQSTM1) (pathway 7). Furthermore, there is substantial representation of cell survival/apoptosis pathways (pathways 7, 8, 10, 11 and 14) and DNA repair pathways (pathways 13 and 15). Interestingly, there are a number of pathways associated with the biosynthesis of nucleic acids (pathways 2, 3 and 4), as well as transcription and translation (pathways 5, 6 and 9 respectively). In such a small data set, the number of proteins associated with each of the above pathways is low, however the analysis does highlight the diverse array of pathways that putative Keap1-interacting proteins may be associated with. In particular, it highlights the close association of Keap1 with cell defence and cell survival pathways.

	Pathway	P value	Inputted proteins represented in pathway
1	Cell Cycle Control of Chromosomal Replication	0.0001	MCM3,RPA1,MCM4
2	Pyrimidine Ribonucleotides De Novo Biosynthesis	0.0033	CAD,CTPS1
3	Uridine-5'-phosphate Biosynthesis	0.0063	CAD
4	Diphthamide Biosynthesis	0.0095	EEF2
5	Regulation of eIF4 and p70S6K Signalling	0.0102	EIF3G,EIF3I,EIF4G1
6	EIF2 Signalling	0.0170	EIF3G,EIF3I,EIF4G1
7	NRF2-mediated Oxidative Stress Response	0.0186	KEAP1,SQSTM1,NFE2L2
8	mTOR Signalling	0.0200	EIF3G,EIF3I,EIF4G1
9	NAD Phosphorylation and Dephosphorylation	0.0309	NNT
10	Apoptosis Signalling	0.0316	LMNA,DFFA
11	Death Receptor Signalling	0.0339	LMNA,DFFA
12	Cleavage and Polyadenylation of Pre-mRNA	0.0372	CPSF2
13	DNA Double-Strand Break Repair by Homologous Recombination	0.0437	RPA1
14	Granzyme B Signalling	0.0490	DFFA
15	Mismatch Repair in Eukaryotes	0.0490	RPA1

Table 4.6. Pathway analysis of putative Keap1-interacting proteins containing an ETGE-like Keap1 binding motif. Proteins co-purified with Keap1-V5 from transfected HEK293T cells containing ETGE-like Keap1 binding motifs, plus and Nrf2 and Keap1, were subjected to Ingenuity pathway analysis. This assigns the proteins to pathways in which they are known play a role. Showing the significantly represented pathways, the p-value (right-tailed Fishers Exact Test) represents the likelihood that that inputted proteins that are part of a pathway are found there by chance.

4.3.5 Validation of Keap1-interacting partners using Y2H

Having identified a number of potential Keap1 binding partners, a high-throughput method for the validation of the interactions was necessary. Y2H is a method whereby many proteins can be screened for interactions simultaneously, and with various stringencies (see Section 4.2.15 for details of how Y2H is used to identify protein-protein interactions). In order to perform Y2H, it was necessary to acquire plasmids containing the gene sequences for the proteins of interest which could be used to transform yeast. Constructs for a selection of the putative Keap1 binding proteins in pDONR gateway vectors were obtained from a collaborator (Dr. Jon Woodsmith, Max-Planck Institute for Molecular Genetics, Berlin, Germany), however not all of the 55 proteins containing ETGE-motifs were available (see appendix 7 for the details of the constructs obtained). Once KOD PCR had been performed to determine that the DNA products were of the correct molecular weight (data not shown), gap repair cloning was used to insert the constructs into vectors which would be expressed in yeast cells as bait- i.e. they would be expressed bound to the DNA binding domain of the Gal4 transcription factor. In this study, Keap1 was used as prey, due to it promoting auto-activation when used as bait (data to be presented in thesis of Amy Ponsford). Following the transformation of yeast with the appropriate vector, YCPCR was performed to further confirm the insertion of the correct construct size (data not shown). Those showing incorrect YCPCR product were not continued in the screen. Those with the correct YCPCR product size and that did not exhibit auto-activation capabilities (data not shown), were continued in the screen (see Table 4.7).

Location	Gene Name	UniProt ID	Protein Name
-*	AP3B1	O00203	AP-3 complex subunit beta-1
B7	AP3D1	O14617	AP-3 complex subunit delta-1
B3	ATP6V0A2	Q9Y487	V-type proton ATPase 116 kDa subunit a isoform 2
D3	CTPS	P17812	CTP synthase 1
-**	DFFA	O00273	DNA fragmentation factor subunit alpha
C7	DHX8	Q14562	ATP-dependent RNA helicase DHX8
B2	DPP3	Q9NY33	Dipeptidyl peptidase 3
-*	EEF2	P13639	Elongation factor 2
D6	EFTUD1	Q7Z2Z2	Elongation factor Tu GTP-binding domain-containing protein 1
B9/C2	EFTUD2	Q15029	116 kDa U5 small nuclear ribonucleoprotein component
C12/C4/D2	EIF3G	O75821	Eukaryotic translation initiation factor 3 subunit G
D2/D4	EIF3I	Q13347	Eukaryotic translation initiation factor 3 subunit I
C6	FLNA	P21333	Filamin-A
D10	GRWD1	Q9BQ67	Glutamate-rich WD repeat-containing protein 1
B12	HBS1L	Q9Y450	HBS1-like protein
D9	HCFC1	P51610	Host cell factor 1
D11/E10/D5	HNRNPH1	P31943	Heterogeneous nuclear ribonucleoprotein H1
B6/B1	HNRNPH3	P31942	Heterogeneous nuclear ribonucleoprotein H3
B11	HSPA9	P38646	Stress-70 protein, mitochondrial
C9	LETM1	O95202	LETM1 and EF-hand domain-containing protein 1, mitochondrial
C11/E8/D1	LMNA	P02545	Prelamin-A/C
B10	MAD2L1	Q13257	Mitotic spindle assembly checkpoint protein MAD2A
B5/C5	MCM3	P25205	DNA replication licensing factor MCM3
-**	NAP1L1	P55209	Nucleosome assembly protein 1-like 1
-**	NCAPH	Q15003	Condensin complex subunit 2
C3	NNT	Q13423	NAD(P) transhydrogenase, mitochondrial
B4	PPIA	P62937	Peptidyl-prolyl cis-trans isomerase A
B8	PRKAR2A	P13861	cAMP-dependent protein kinase type II-alpha regulatory subunit

D8/D7	PSMD3	O43242	26S proteasome non-ATPase regulatory subunit 3
E11/E9/C2	RIC8A	Q9NPQ8	Synembryn-A
C8	RPA1	P27694	Replication protein A 70 kDa DNA-binding subunit
-*	SLK	Q9H2G2	STE20-like serine/threonine-protein kinase
A12	SQSTM1	Q13501	Sequestosome/p62
-**	WDR1	O75083	WD repeat-containing protein 1
C10	YBX1	P67809	Nuclease-sensitive element-binding protein 1
E12	ZW10	O43264	Centromere/kinetochore protein zw10 homolog

Table 4.7. Details of clones obtained for Y2H screen against Keap1. Those in bold type were not successfully cloned into yeast bait vectors (i.e. incorrect YCPRC product size) (*), or exhibited auto-activation capabilities (**), therefore were not used in the Y2H screen. All proteins contain an ETGE-like motif (ETGE/ESGE/STGE). Location column refers to Figures 4.11 and 4.12).

Yeast containing the constructs of interest (as bait) were mated against the following preys: Keap1, Nrf2 and p62, in order to examine the potential for the proteins to interact with Keap1 directly, or indirectly through Nrf2 or p62.

Positive controls were used as follows (Fig 4.11):

Keap1 (prey) + p62 (bait), Keap1 (prey) + Cul3 (bait)

p62 (prey) + p62 (bait)

Nrf2 (prey) + MafG (bait)

The Y2H screens were carried out on two different selective medias (SD-WLA and SD-WHL(AT)). The growth of colonies on both medias indicates the activation of two different reporter genes by the Gal4 transcription factor (ADE2 and HIS3, respectively). Positive interactions identified through this Y2H screen are shown in Figure 4.11 and outlined in Table 4.8. The functions of the proteins positively identified as protein interactions are

detailed in Table 4.9. Proteins identified through activation of both ARE2 and HIS3 reporter genes, in two out of two biological repeats were considered true interactions.

Prey	Location	Bait
Keap1	A8	EIF3J
	A9	Nrf2
	A11	Cul3
	A12	p62
	B1	HNRNPH3
	B5, C5	MCM3
	B10	MAD2L1
	B12	HSB1L1
	C1, E11, E12	RIC8A
	C4	EIF3G
P62	A12	p62
	B1	HNRNPH3
	C1	RIC8A
	C4, C12, D2	EIF3G
	D2	PSMD3
Nrf2	B10	MafG

Table 4.8. Proteins identified as positive binding partners in Y2H screen from two biological repeats. Those in bold type are previously known interactions and were used as positive controls in the assay.

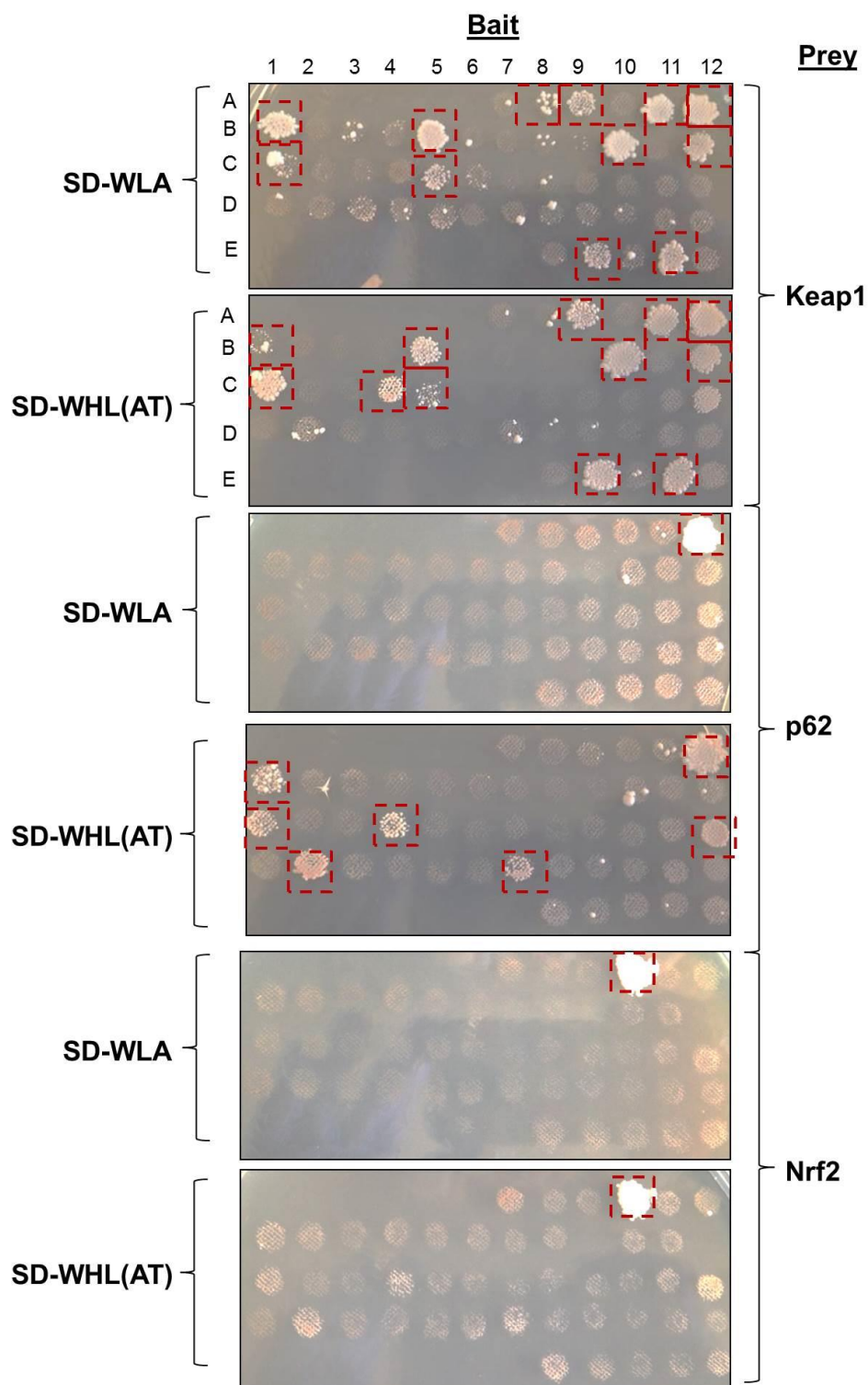


Figure 4.11. Y2H matrix style mating. Yeast were transferred onto selective media (SD-WLA and SD-WHL(AT)) and incubated at 30 °C for up to 10 days. Photographs were taken at regular intervals. The presence of yeast colonies indicates the induction of the ADE2 reporter (SD-WLA) and the HIS3 reporter (SD-WHL(AT)), each under the control of the Gal2p and Gal1pGal4 promoters respectively. A red box around yeast colonies indicates a protein interaction. The plates shown are representative of two biological repeats.

Protein	Function
EIF3J/EIF3G	Component of the eukaryotic translation initiation factor 3 (eIF-3) complex, required for the initiation of protein synthesis. EIF-3 complex associates with 40S ribosome, facilitates recruitment of subunits to form 43Spre-initiation complex (43S PIC). The complex stimulates mRNA recruitment to the 43S PIC and scanning of mRNA for AUG recognition. Complex required for disassembly and recycling of post-termination ribosomal complexes, prevents premature joining of the 40S and 60S ribosomal subunits prior to initiation.eIF-3 complex is composed of 13 subunits: EIF3A, EIF3B,EIF3C, EIF3D, EIF3E, EIF3F, EIF3G, EIF3H, EIF3I, EIF3J, EIF3K,EIF3L and EIF3M.
HBS1L	A member of the GTP-binding elongation factor family. It is expressed in multiple tissues with the highest expression in heart and skeletal muscle.
HNRNPH3	Involved in splicing process and participates in early heat shock-induced splicing arrest.
MAD2L1	Component of the spindle-assembly checkpoint that prevents the onset of anaphase until all chromosomes are properly aligned at the metaphase plate. Required for the execution of the mitotic checkpoint which monitors the process of kinetochore-spindle attachment and inhibits the activity of the anaphase promoting complex by sequestering CDC20 until all chromosomes are aligned at the metaphase plate.
MCM3	A component of MCM2-7 complex (MCM complex) which is the putative replicative helicase essential for 'once per cell cycle' DNA replication initiation and elongation in eukaryotic cells. Required for DNA replication and cell proliferation.
PSMD3	A member of the proteasome subunit S3 family that functions as one of the non-ATPase subunits of the 19S regulator lid. The 26S proteasome is a multi-catalytic proteinase complex with a highly ordered structure composed of 2 complexes, a 20S core and a 19S regulator. The 19S regulator is composed of a base, which contains 6 ATPase subunits and 2 non-ATPase subunits, and a lid, which contains up to 10 non-ATPase subunits.
RIC8A	Guanine nucleotide exchange factor (GEF), which can activate some G-alpha proteins. Involved in regulation of microtubule pulling forces during mitotic movement of chromosomes by stimulating G(i)-alpha protein, possibly leading to release G(i)-alpha-GTP and NuMA proteins from the NuMA-GPSM2-G(i)-alpha-GDP. Also acts as an

activator for G(q)-alpha (GNAQ) protein by enhancing the G(q)-coupled receptor-mediated ERK activation.

Table 4.9. Function of proteins identified as novel Keap1-binding partners in Y2H screen. Protein function descriptions are taken directly from the [NCBI Entrez Protein database](http://www.ncbi.nlm.nih.gov/sites/entrez?db=protein) (<http://www.ncbi.nlm.nih.gov/sites/entrez?db=protein>).

4.3.6 β -Galactosidase Reporter Assay

In order to further validate the interactions identified in Section 4.3.5, we used a third reporter assay, the β -Galactosidase reporter assay. Following diploid selection, the yeast are transferred onto filter paper and incubated at 37 °C in the presence of X-gal. If the Gal4 transcription factor is functional (i.e. the BD and AD are brought together), the X-gal will be catalysed into colourless galactose and 4-chloro-3-brom-indigo, which is blue on the filter paper, indicating a protein interaction. As in Section 4.3.5, all preys were screened against Keap1, p62 and Nrf2 baits. The data do not indicate any interactions that were not identified in the previous mating screen (Fig 4.11) but does confirm the novel Keap1-interacting proteins identified in Section 4.3.5, including EIF3J (A7), HNRNPH3 (B1), MAD2L1 (B10), HBS1L1 (B12) and RIC8A (E11) (Fig. 4.11, 12). In addition, strong blue colour is seen with positive control matings, such as Keap1 and p62 (top panel A12), p62 and p62 (middle panel A12) and Nrf2 with MafG (bottom panel, B10).

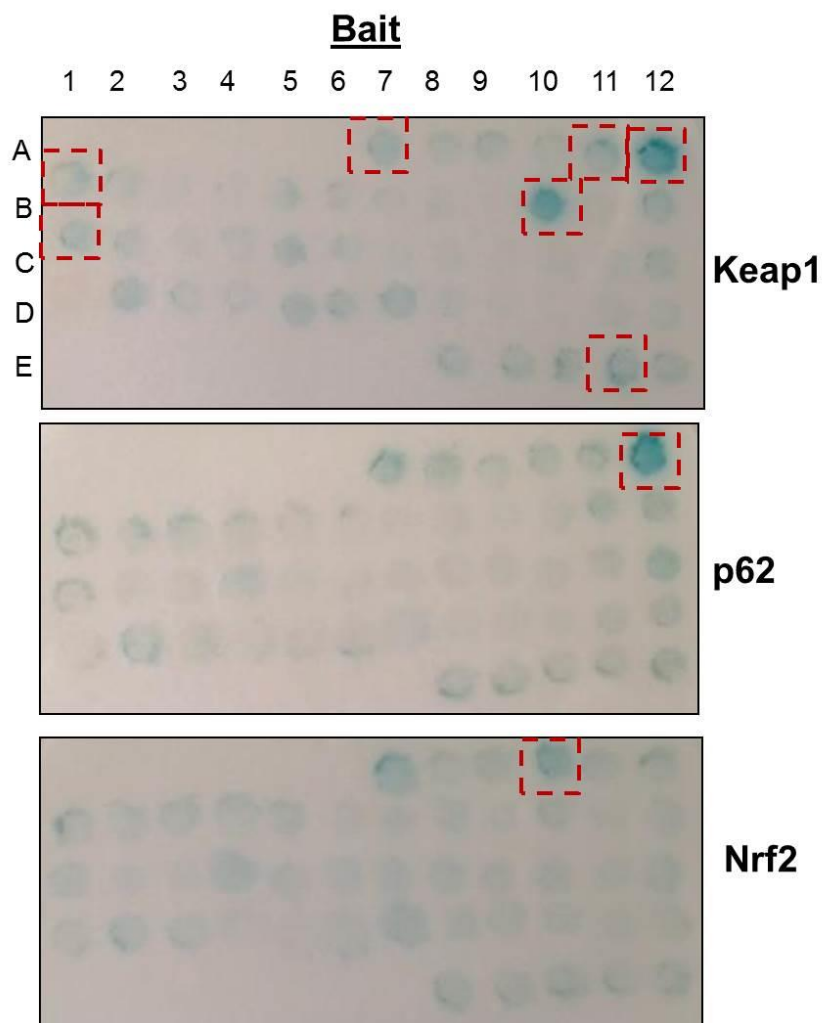


Figure 4.12. β -Gal Reporter assay. Following diploid selection, yeast were transferred onto filter paper, which was laid on top of additional filter paper covered in β -Gal reagent and incubated at 30 °C for 24 hr. Photographs were taken of the colour changes over this time period. Blue indicates the induction of the LacZ gene in yeast by the Gal4 transcription factor, catalysing the hydrolysis of X-Gal to a colourless galactose and 4-chloro-3-brom-indigo, which is blue. The red dotted box around a blue circle indicates a protein-protein interaction. One biological repeat.

4.3.7 Comparison of Keap1 interactome composition following exposure of cells to selected Nrf2 inducers

In Chapter 2, HEK293T cells were transfected with Keap1-V5 and treated with various Nrf2 inducing compounds, before Keap1 was immunopurified, subjected to trypsin digestion and LC-ESI-MS/MS analysis to identify modifications of cysteine residues. These data permit us to investigate the different proteins co-purified with Keap1-V5 following the treatment of cells with Nrf2-inducing compounds. For this, we have focussed on DNCB, CDDO-Me and Dex-mes, as they are all electrophilic compounds and exposed to cells using the same vehicle, DMSO. The other Nrf2-inducing compounds used in Chapter 2 (BSO and H₂O₂) are not electrophilic and the vehicles used were dH₂O and cell growth media respectively, therefore including these compounds in the analysis described here would have introduced additional variables. In order to compare the proteins that were co-purified with Keap1-V5 following each treatment (DMSO, DNCB, CDDO-Me, Dex-Mes), the total list of proteins co-purified with Keap1-V5 in ≥ 4 out of 6 biological repeats was compared to the list of proteins purified following mock transfection. If a protein was identified in both the mock transfected samples and those transfected with Keap1-V5, it was removed from the list if the ratio of the number of peptides in transfected:mock was ≥ 1.5 . The proteins remaining were compared using a Venn diagram (Oliveros 2007) to identify the overlap or differences in proteins co-purified with Keap1-V5 following the treatment of HEK293T cells with each Nrf2 inducing compound (Fig 4.15). Note that the proteins used in this study were not limited to only those containing ETGE-like motifs.

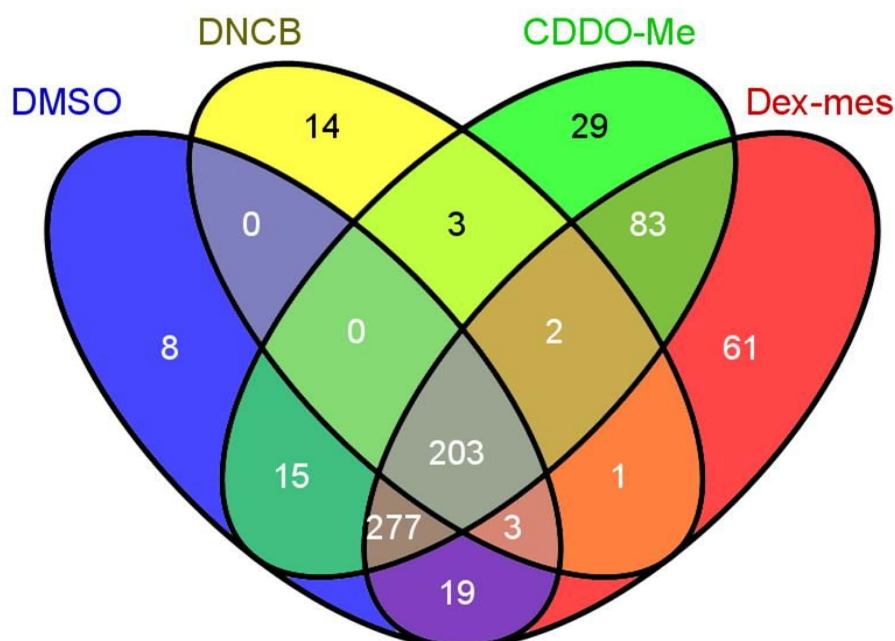


Figure 4.13. Venn diagram comparison of proteins co-purified with Keap1-V5 following treatment of cells with Nrf2 inducing electrophiles. The total list of proteins co-purified in $\geq 4/6$ biological repeats was compared to the list of proteins purified following mock transfection. If the protein was identified in both the mock transfected samples and following transfection of Keap1-V5, proteins were removed from the list if the ratio of the average number of peptides in transfected:mock was ≥ 1.5 . The proteins remaining were compared using a Venn diagram programme by Oliveros (2007).

Of these proteins, 203 of those identified following treatment with all compounds were also identified following treatment with the vehicle control (DMSO), and thus further investigation of these may reveal partners which are constitutively bound to Keap1 and unaffected by Nrf2 induction, or the presence of electrophiles (Fig 4.13) (see appendix 8 for details of proteins in each Section). Ingenuity-based pathway analysis of these 203 proteins reveals the most significantly represented pathways by these proteins (Table 4.10). The pathways represented by this data set include EIF2 signalling, mTOR signalling, the protein ubiquitination pathway, DNA double strand break repair, the Nrf2-mediated oxidative stress response, as well as nucleotide biosynthetic pathways.

Pathway	P-value	Molecules in the pathway
EIF2 Signalling	7.94E-36	RPL24,RPL22,RPL27A,RPS18,RPLP2,EIF4G1,EIF2S1,EIF2A,RPS7,RPS20,UBA52,EIF3D,RP S13,RPL23A,RPS9,EIF5,EIF3A,RPL13,PABPC1,RPL12,RPL23,RPL21,RPL9,RPL10A,EIF3F,R PL28,RPS26,RPL26L1,EIF4A3, EIF4A1,EIF3I,RPL10,RPL5,RPS 15A,RPL13A,RPSA
Regulation of eIF4 and p70S6K Signalling	2.00E-15	PABPC1,RPS18,EIF4G1,EIF2S 1,EIF2A,RPS7,EIF3F,PPP2R1A ,RPS20,EIF3D,RPS13,RPS26,E IF4A3,RPS9,EIF4A1,EIF3A,EIF 3I,RPS15A,RPSA
RAN Signalling	2.00E-10	KPNB1,CSE1L,KPNA2,TNPO1, RANGAP1,XPO1,IPO5
mTOR Signalling	2.14E-10	RPS18,EIF4G1,RPS7,EIF3F,PP P2R1A,RPS20,EIF3D,RPS13,R PS26,EIF4A3,EIF4A1,RPS9,EIF 3A,EIF3I,RPS15A,RPSA
Protein Ubiquitination Pathway	3.89E-09	USP9X,HSPA9,PSMD3,HSPD1, DNAJA1,HSPA5,PSMC5,PSMD 11,HSP90AB1,PSMD2,PSMD12 ,HSP90AA1,PSMD14,SUGT1,P SMC2,PSMC3,DNAJC7
tRNA Charging	7.59E-09	LARS,RARS,YARS,VARs,MAR S,IARS,EPRS,QARS
Caveolar-mediated Endocytosis Signalling	1.51E-04	ARCN1,FLNA,COPA,PTPN1,C OPB1,COPG1
Purine Nucleotides De Novo Biosynthesis II	2.09E-04	ADSL,GMPS,GART
Oxidized GTP and dGTP Detoxification	3.72E-04	DDX6,RUVBL2
Telomere Extension by Telomerase	5.62E-04	HNRNPA1,XRCC6,XRCC5
Tetrahydrofolate Salvage from 5,10-methenyltetrahydrofolate	1.20E-03	MTHFD1,GART
Aldosterone Signalling in Epithelial Cells	1.55E-03	HSP90AB1,HSPA9,HSP90AA1, HSPD1,DNAJA1,HSPA5,DNAJ C7
Mitotic Roles of Polo-Like Kinase	5.37E-03	PPP2R1A,HSP90AB1,HSP90A A1,CDK1
Remodelling of Epithelial Adherens Junctions	6.31E-03	TUBA1B,TUBB6,TUBB4B,TUB B
14-3-3-mediated Signalling	9.77E-03	TUBA1B,TUBB6,TUBB4B,PDC D6IP,TUBB
DNA Double-Strand Break Repair by Non-Homologous	1.02E-02	XRCC6,XRCC5

End Joining		
Acetyl-CoA Biosynthesis III (from Citrate)	1.12E-02	ACLY
Asparagine Biosynthesis I	1.12E-02	ASNS
NRF2-mediated Oxidative Stress Response	1.45E-02	PRDX1,CCT7,SQSTM1,DNAJA1,PTPLAD1,DNAJC7
Breast Cancer Regulation by Stathmin1	2.00E-02	TUBA1B,PPP2R1A,TUBB6,TUBB4B,TUBB,CDK1
Unfolded protein response	2.14E-02	HSPA9,HSPA5,EIF2A
Palmitate Biosynthesis I (Animals)	2.24E-02	FASN
Uridine-5'-phosphate Biosynthesis	2.24E-02	CAD
Fatty Acid Biosynthesis Initiation II	2.24E-02	FASN
Endoplasmic Reticulum Stress Pathway	2.24E-02	EIF2S1,HSPA5
Gap Junction Signalling	2.69E-02	DBN1,TUBA1B,TUBB6,TUBB4B,TUBB
Glycolysis I	2.88E-02	PGK1,GAPDH
Germ Cell-Sertoli Cell Junction Signalling	3.09E-02	TUBA1B,TUBB6,CFL1,TUBB4B,TUBB
Gluconeogenesis I	3.16E-02	PGK1,GAPDH
Diphthamide Biosynthesis	3.31E-02	EEF2
PRPP Biosynthesis I	3.31E-02	PRPS1
NADH Repair	3.31E-02	GAPDH
5-aminoimidazole Ribonucleotide Biosynthesis I	3.31E-02	GART
Inosine-5'-phosphate Biosynthesis II	3.31E-02	ADSL
Hypusine Biosynthesis	3.31E-02	EIF5A
Pyrimidine Ribonucleotides De Novo Biosynthesis	3.63E-02	CAD,CTPS1
PPAR α /RXR α Activation	3.72E-02	CAND1,HSP90AB1,FASN,CKA P5,HSP90AA1
Proline Biosynthesis I	4.37E-02	ALDH18A1
Sertoli Cell-Sertoli Cell Junction Signalling	4.47E-02	TUBA1B,TJP2,TUBB6,TUBB4B,TUBB
PI3K/AKT Signalling	4.68E-02	CDC37,PPP2R1A,HSP90AB1,HSP90AA1

Table 4.10. Pathway analysis proteins co-purified with Keap1-V5 following treatment of cells with Nrf2 inducers. Proteins were co-purified with Keap1-V5 from transfected HEK293T cells treated with DMSO, DNCB, Dex-mes or CDDO-Me. Those identified in $\geq 4/6$ biological repeats and with the ratio of the average number of peptides in transfected:mock ≥ 1.5 and present following treatment with all compounds or vehicle control were subjected to Ingenuity pathway analysis. Shown in order of significance.

The data demonstrate that there are proteins co-purified with Keap1 which are unique to each treatment; 14 for DNCB, 29 for CDDO-Me and 61 for Dex-Mes (Fig 4.13). Ingenuity network analysis of these individual data sets shows that the proteins are associated with diverse cellular functions. The proteins purified from HEK293T cells expressing Keap1-V5, and unique to DNCB treatment, appear to be related primarily to cell death and survival and DNA repair, indicating toxicity within the cell (Table 4.11). Proteins co-purified with Keap1-V5 unique to dex-mes treatment are also associated with networks involved in cell death and survival as well as cellular assembly and organisation, and various disease states (Table 4.12). On the other hand, proteins co-purified with Keap1-V5 from cells following treatment with CDDO-Me are associated with networks that have roles in cancer and lipid metabolism, both of which are associated with the Nrf2 signalling pathway (Table 4.13). Further investigation into these interactions may give some insight into the changes in the Keap1 complex that occur following Nrf2 induction and how this differs between electrophiles.

DNCB Network	Focus Molecules	Score
Cell death and survival Cellular compromise, DNA replication, recombination and repair	11	26
Cell cycle, Cellular movement, Cancer	1	3
Cancer, Organismal injury and abnormalities, Renal and urological disease	1	2

Table 4.11. Network analysis of proteins co-purified with Keap1-V5 from cells following DNCB treatment only. Showing the top three significantly represented networks.

Dex-mes Network	Focus Molecules	Score
Cell death and survival, Developmental disorders, Gastrointestinal disease	13	23
Cell to cell signalling and interaction, Cellular assembly and organisation, Tissue development	13	21
Dermatological conditions, Infectious disease, Inflammatory disease	10	16

Table 4.12. Network analysis of proteins co-purified with Keap1-V5 from cells following dex-mes treatment only. Showing the top three significantly represented networks.

CDDO-MeNetwork	Focus Molecules	Score
Cancer, Neurological disease, Cellular development	11	22
Lipid metabolism, Molecular transport, Small molecule biochemistry	12	22
Cellular assembly and organisation, Cellular function and maintenance	1	2

Table 4.13. Network analysis of proteins co-purified with Keap1-V5 from cells following CDDO-Me treatment only. Showing the top three significantly represented networks.

Interestingly, only two proteins were co-purified with Keap1 following treatment with all three electrophiles but not with vehicle control (Fig 4.13). These are Serine/arginine-rich splicing factor 10 (SRSF10) and heterogeneous nuclear ribonucleoprotein Q (hnRNP Q). SRSF10 is a repressor of pre-mRNA splicing during M-phase of the cell cycle and after heat shock. It is located within the cytosol and nuclear speckles, the common localisation for proteins involved in transcription and pre-mRNA processing (details from www.uniprot.org). hnRNP is also implicated in mRNA processing, and is a component of a complex which promotes mRNA

stability. Additionally, it is a component of the gamma (γ) interferon-activated inhibitor of translation (GAIT) complex which mediates interferon- γ -induced transcript-selective translation inhibition in inflammation processes. It is localised in cytoplasmic granules containing untranslated mRNAs, and in the nucleus (details from www.uniprot.org). Interestingly, another hnRNP protein (hnRNPH3) was identified as a potential Keap1 binding partner by MS and validated by the Y2H assay. It is worth noting that whilst hnRNPH3 contains an ETGE-like motif, neither hnRNP Q nor SRNF10 do. Further investigation of the Keap1-binding complex and how it changes in response to Nrf2-inducing compounds may provide insights into the mechanisms by which different inducers provoke Nrf2 activation.

4.4 DISCUSSION

As the manipulation of the Nrf2 pathway is considered a promising therapeutic strategy, furthering our understanding of its activation and regulation is vital. By investigating the proteins which are involved in the Keap1/Nrf2 complex, we can develop a more detailed picture of the molecular interactions which can be targeted to modulate Nrf2 activity, or to fine-tune Nrf2-related therapeutic interventions. As we have previously used MS methods to identify p62 as a novel Keap1 binding partner, and data obtained in Chapter 2 were available for the analysis of proteins which are co-purified with Keap1-V5 from cells, we took an unbiased approach to identify novel Keap1 binding partners and investigate the biological roles played by proteins which interact with Keap1.

The MS analysis of proteins co-purified with Keap1 from HEK293T cells identified upwards of 1,000 potential interacting partners. Further validation was concentrated on proteins which contain an ETGE-like Keap1-binding motif. Network analysis of such proteins revealed that whilst a number of the proteins identified have not been shown to bind directly to Keap1, some interact with other known Keap1 binding partners, such as PGAM5. However, the presence of an ETGE-like motif within these proteins indicates that they are likely to bind to Keap1 directly. Pathway analysis demonstrated that many of the putative Keap1-interacting proteins identified have been linked to cell survival pathways, supporting a link to p53 signalling. This supports observations of an association between p53 and Nrf2, whereby in conditions

of low ROS exposure, p53 and Nrf2 up-regulate the expression of antioxidant genes yet with extended ROS exposure, p53 is up-regulated. This mediates the expression of pro-oxidant genes augmenting p53-mediated apoptosis, whilst Nrf2 is suppressed (Chen *et al.* 2012). It is plausible that a protein interacts with p53 and Keap1, and that the interaction is altered under conditions of stress, facilitating the co-regulation of both pathways.

Y2H screening allowed the validation of a number of candidate Keap1-binding proteins. This assay verified potential Keap1-binding partners which contain ETGE-like motifs, including EIF3J/G, HBS1L, HNRNPH3, MAD2L1, MCM3, RIC8A, as well as PSMD3 as a potential p62-binding partner. PSMD3 is a non-ATPase member of the 19S regulator lid of the 26S proteasome. The lid of the 26S proteasome is responsible for the recognition of poly-ubiquitinated proteins (Thrower *et al.* 2000), therefore, it is possible that p62/Keap1 interact with the proteasome via PSMD3, to facilitate the degradation of ubiquitinated proteins, such as Nrf2. Proteins of the EIF3 complex, have been shown to interact with the 19S proteasomal lid (Sharon *et al.* 2006). In this Y2H screen, EIF3G was shown to interact with Keap1 and p62. Additionally, EIF3J, another subunit of the EIF3 complex, was screened against Keap1 as it has previously been identified as an Nrf2 binding partner using this assay (data to be presented in thesis of Amy Ponsford). EIF3J and EIF3G are subunits of the eukaryotic initiation factor 3 complex (EIF3), and participate in the initiation of transcription by aiding the recruitment of protein and mRNA to the 40S ribosome (Zhou *et al.* 2008).

HNRNPH3, verified in the Y2H screen as a Keap1-interacting partner would be worth investigating further, especially as an additional HNRNP protein (HNRPN Q) was identified as one of two proteins co-purified with Keap1, following treatment with Nrf2-inducing electrophiles. Following heat shock, pre-mRNA splicing (performed by HNRNP proteins) is transiently inhibited to prevent the synthesis of abnormal proteins (Yost and Lindquist 1986, Yost and Lindquist 1988). This is facilitated by HNRNP proteins leaving the HNRNP complex, and it is possible that under these conditions an association with Keap1 occurs, leading to concomitant activation of Nrf2 cell defence signalling.

Our Y2H validation of MCM3 as a Keap1 binding partner further supports the observations by Hast *et al.* (2013). They showed that the ETGE motif in MCM3 facilitates this interaction. As part of the MCM complex, MCM3 ensures that DNA replication occurs only once per cell cycle (Takei and Tsujimoto 1998). MCM3 is primarily a nuclear protein, its localisation facilitated via an interaction with Map80 and an NLS (Takei and Tsujimoto 1998). Therefore, due to the cytoplasmic localisation Keap1 (Watai *et al.* 2007), this interaction is only likely to occur if Keap1 enters the nucleus, perhaps under stress conditions, as it has been reported to do (Sun *et al.* 2007).

MAD2L1 was also previously identified as a Keap1-binding protein by Hast *et al.* (2013) who showed that when ectopically expressed in cells, MAD2L1 activates Nrf2-mediated transcription, dependent on the presence of its

ESGE motif. Further investigation into the functional effect this protein has on the Nrf2 pathway, and the underlying molecular mechanisms, is therefore warranted. An interaction between Keap1 and either MAD2L1 or MCM3 would directly link the Nrf2 pathway with the p53 pathway, as shown in Fig 4.9.

HBS1L is a member of the GTP-binding elongation factor family, thus is involved in protein synthesis. Polymorphisms within the HBS1L gene have been associated with fetal haemoglobin levels and sickle cell disease (Stadhouders *et al.* 2014). Interestingly, fetal haemoglobin levels have been shown to be induced by Nrf2-activating compounds (e.g. tBHQ) (Macari and Lowrey 2011), therefore it is plausible that an interaction between HBS1L and Keap1 impacts the regulation of fetal haemoglobin levels in the cell.

RIC8A is a guanine nucleotide exchange factor, which localises to the cell membrane, via an interaction with neural cell adhesion molecule (NCAM)-180 (Amoureux *et al.* 2012). As Keap1 interacts with the actin cytoskeleton, potentially tethering it adjacent to the cell membrane, it is possible that these proteins co-localise. This interaction would benefit from further investigation.

Additional proteins identified as potential Keap1 binding partners which require further investigation include those with ETGE-like motifs which were not screened using Y2H in this study. These proteins were not screened for one of three reasons. Firstly, the constructs obtained for the screen were obtained from a collaborator, and not all putative Keap1-interacting partners

were available. Secondly, some constructs were not successfully introduced into yeast bait vectors or cells. Lastly, some proteins exhibited auto-activation capabilities and thus could not be used in the screen. One example is SLK which was not used in our screen but was identified as a Keap1-binding partner by Hast *et al.* (2013), who showed that the over-expression of SLK in cells activates Nrf2-mediated transcription, independently of its ETGE motif. SLK is a kinase primarily expressed in the kidneys, which is induced during development and in recovery from acute renal failure, and which promotes apoptosis via p53 activation (Cybulsky *et al.* 2009). Therefore, further investigation of the interplay between this protein and the Keap1/Nrf2 pathway would be worthwhile

The dataset used for this analysis was not originally generated with the intention of identifying novel Keap1-binding partners. It was obtained following the treatment of Keap1-V5 expressing HEK293T cells with various Nrf2 inducers, to investigate the modification of Keap1 cysteine residues. For this reason, the data used for the studies shown in this chapter were derived from cells treated with 55 mM NEM for 5 min prior to lysis, to cap all Keap1 cysteine residues, and aid the analysis of their modification state. Although this is unlikely to affect the basal Keap1-interactome, were this experiment designed specifically to identify Keap1 binding partners, this treatment would be excluded. As for the investigation into the change in Keap1-interactome following treatment with Nrf2-inducing electrophiles, all cells used for this analysis were treated with NEM, which is a constant factor among all samples. Should this experiment be repeated, NEM would be excluded.

Analysis of the proteins that are enriched following the purification of Keap1-V5 from cells treated with different electrophilic Nrf2-inducing agents reveals distinct proteins associated with Keap1, which contribute to various cellular networks and functions. It is worth considering that the data sets used for network/pathway analyses are small, therefore pathways can appear to be significantly represented, when only one or two proteins in the data set are associated with that network/pathway. The focus of this work was to identify the type of functions associated with co-purified proteins, and not to make general conclusions regarding which pathways are significantly represented.

In conclusion, we have identified a number of proteins which may be potential Keap1-interacting partners, some of which are in agreement with previously published data. Whilst we focussed on proteins containing ETGE-like Keap1 binding motifs, a number of proteins identified did not contain this motif but would be worth investigating further. We show that Keap1-interacting proteins containing ETGE-like motifs are involved in a diverse array of cellular functions, but there appears to be a clear focus on cell survival, cell death and DNA replication. Additionally, we show that there appears to be differences in the proteins which associate with Keap1 following Nrf2 induction in cells with various electrophiles, which requires further investigation.

It will be important to validate these interactions further and determine the functional effects of the interaction of these proteins with Keap1. Further validation could be carried out as follows:

- Confirm co-purification of proteins with Keap1-V5 from cells, or of endogenous Keap1 with epitope-tagged protein of interest, by western blot
- Confirm protein co-localisation in cells using fluorescent microscopy
- Validate protein interaction in different cell lines
- siRNA-mediated knock-down, or ectopic expression of the protein of interest, and examination of the consequences for Keap1/Nrf2 protein levels and Nrf2 activity

These investigations may reveal proteins which are potential therapeutic targets to manipulate Nrf2 levels, without the use of potentially toxic electrophiles.

CHAPTER 5

CONCLUDING DISCUSSION

CONTENTS

5.1 INTRODUCTION - 198 -

5.2 SUMMARY OF THE WORK PRESENTED IN THIS THESIS - 198 -

5.3 FUTURE DIRECTIONS - 200 -

5.4 CONCLUDING REMARKS - 203 -

5.1 INTRODUCTION

Diseases associated with oxidative stress and the dysregulation of the Nrf2 pathway are a major public health concern. Additionally, ADRs, one of the prevailing reasons for drug attrition, have been associated with chemically reactive, Nrf2-inducing compounds. It is therefore important to develop novel therapeutic agents, and enhance the safety of current medicines to improve patient wellbeing. These developments will be informed by furthering our understanding of the molecular mechanisms underlying Nrf2 activation. This thesis has focused on the mechanisms whereby electrophiles and oxidants can induce Nrf2 via covalent or non-covalent interactions with Keap1. Additionally, studies presented here have aimed to reveal Keap1's interactions with other proteins, which may regulate the activity of Nrf2 and could therefore be promising therapeutic targets.

5.2 SUMMARY OF THE WORK PRESENTED IN THIS THESIS

Previous work in our lab has shown that the depletion of GSH can induce Nrf2 in the absence of covalent modification of Keap1 (Chia *et al.* 2010), thus we hypothesised that GSH depletion causes changes in the redox state of the cell, allowing ROS to accumulate and thus, the oxidation of Keap1 cysteine residues. Due to the difficulty in directly detecting oxidation states in cysteine-rich proteins such as Keap1, we developed an MS method which allowed us to detect reversible and irreversible modifications of Keap1 cysteines, following the treatment of cells with Nrf2 inducing compounds. We

showed that some Nrf2 inducers promote the formation of reversible and/or irreversible redox modifications of Keap1 which could be due to thiol oxidation, although this is not dependent on GSH depletion. Whilst we were unable to provide evidence for the direct oxidation of Keap1 cysteine residues, or that the oxidation of Keap1 cysteine residues is necessary/sufficient for the activation of Nrf2, it remains a plausible mechanism which requires further investigation.

TPs are extremely potent inducers of the Nrf2 pathway, and there is interest in these compounds as therapeutic agents, for the treatment of a variety of diseases. We hypothesised that the activation of Nrf2 by this class of compound occurs via the covalent modification of Keap1 cysteine residues. In keeping with this, we have shown that a chemically-tuned TP (CDDO-Epoxyde) can covalently modify Keap1 cysteine residues known to be important for the ability of Keap1 to repress Nrf2. We have also shown, using *in silico* modelling, that the ability of a series of TPs to interact with Keap1 non-covalently in cysteine-containing pockets correlates with their potency as inducers of Nqo1, which is regulated by Nrf2. Non-covalent modification of Keap1 by TPs is therefore a potential mechanism of Nrf2 activation, however requires further investigation before we can extrapolate this data to other Nrf2-inducing compounds.

A detailed understanding of the mechanisms that regulate the Nrf2 cell defence pathway is dependent on an appreciation of a number of molecular aspects. This includes protein-protein interactions which may affect the ability

of the pathway to function. These interactions can be examined by combining experimental work with computational pathway analysis. Using this approach, we have investigated 55 proteins containing a Keap1-binding motif that were co-purified with Keap1-V5 from HEK293T cells. Network analysis of these proteins identified links between the Keap1/Nrf2 pathway and the p53 pathway. Furthermore, we have identified potential Keap1 binding partners (HNRNPH3, EIF3G, MCM3, HBS1L, RIC8A and PSMD3) which require further validation of their functional effects on the Nrf2 pathway.

5.3 FUTURE DIRECTIONS

The experiments described here were performed on recombinant Keap1 protein and cell lines transfected with epitope-tagged Keap1. Although necessitated by the low abundance of endogenous Keap1 in most cell lines, ectopically expressing a protein may divert the cell/protein environment away from that of a physiological state, the functional consequences of which are yet to be established. Additionally, *in vitro* systems and commonly-used liver cell lines (e.g. HepG2) do not have drug metabolising capabilities (Wilkening *et al.* 2003). This makes the identification of Keap1 cysteine modifications by reactive drug metabolites difficult, in such platforms. The use of primary hepatocytes, or a transgenic animal expressing tagged Keap1, which can be purified and subjected to MS following treatment with Nrf2 inducers, would inform how we extrapolate data obtained *in vitro* and in cell models, to *in vivo* settings. Further experimental and computational assessment of the Keap1 cysteine residues located on solvent-accessible surfaces of Keap1, will be

aided by defining its full crystal structure, thus highlighting those most likely to be modified by Nrf2 activators.

As an alternative to experimentally enriching Keap1 from cells, chemically-adapted electrophiles could be used, to enable the affinity enrichment of proteins modified by such compounds (Dennehy *et al.* 2006, Shin *et al.* 2007). This is a method that has been used to identify protein targets, including IKK and JAK1, of biotin-tagged TPs (Yore *et al.* 2011). It is not presently clear what effect the affinity tag has on the reactivity of the electrophile. Additionally, low-abundance proteins such as endogenous Keap1, may still prove difficult to detect using this approach. The use of chemical probes, such as dimedone which specifically alkylates cysteine sulphenic acid (S-OH) (Nelson *et al.* 2010), would be a promising avenue to consider regarding THE investigation of oxidised cysteine residues.

The use of multiple reaction monitoring (MRM), whereby MS analysis is focussed on pre-defined target ions, such as specific peptides that are expected to be modified by a chemical entity, has permitted increased sensitivity and specificity in detecting modified proteins in cells, or tissues (Kitteringham *et al.* 2009). This approach reduces background signals, increasing the signal-to-noise ratio, giving more sensitive detection of modified peptides (Unwin *et al.* 2005), and can be guided by *in vitro* analysis to identify peptides of interest in *in vivo* assays. Further research is required to determine whether this approach will be sensitive enough to detect the modification of an endogenous protein of such low abundance as

Keap1. However, advances in sampling rate, sensitivity and the resolution of mass spectrometers are increasingly enabling the detection of modified endogenous proteins (Koen *et al.* 2006, Shin *et al.* 2007).

The importance of non-covalent interactions between Nrf2 inducers and Keap1 cysteine-containing pockets will be facilitated by detailed *in silico* molecular modelling, using the crystal structures of Keap1 domains, or the full length protein if/when it becomes available. Non-covalent interactions are more readily reversible, thus Keap1 could theoretically be recycled, and not require *de novo* synthesis in order to regenerate fully-functional protein, as would likely be the case following irreversible modification of Keap1.

The identification of novel Keap1 binding partners in this study supports, and adds, to the findings of Hast *et al.* (2013), and the Nrf2-interactome described by Papp *et al.* (2012). Further validation of the binding partners identified here is required. For example, it will be important to investigate whether these interactions are cell-type specific. The functional effect the interaction may have on the Nrf2 pathway, and its regulation, also requires investigation. This can be facilitated by over-expression or siRNA-mediated knock-down of the proteins of interest, and analysis of the effect on Keap1 protein levels and the basal/inducible activity of Nrf2.

5.4 CONCLUDING REMARKS

The main aims of this thesis were to further our understanding of the mechanisms whereby Keap1 regulates the activity of Nrf2, in particular by investigating its molecular interactions with Nrf2-inducing compounds or other cellular proteins. Such information is vital to inform the design and development of safe and efficacious Nrf2-inducing compounds, which may have therapeutic value in numerous disease contexts. As an example, the modelling approach used here could be exploited to screen compound libraries for their ability to bind non-covalently to Keap1 *in silico* and induce Nrf2 in cells, to identify novel candidate Nrf2-modulating therapeutic agents. Furthermore, determining the ability of existing and new drugs to modulate the functions of Keap1, Nrf2 and/or their interacting proteins, may reveal new pharmacological mechanisms, or explain specific off-target effects.

An increased understanding of Nrf2 signalling, in conjunction with investigations into the variation in its basal and inducible activity between individuals, will aid the stratification of medicine targeting this pathway, thereby improving patient wellbeing. Additionally, screening individuals for polymorphisms in the genes encoding Keap1 or Nrf2, which have been associated with various diseases (Wong *et al.* 2011, Hartikainen *et al.* 2012, Shimoyama *et al.* 2014), may allow the identification of at-risk patients. This could potentially allow for clinicians to develop strategies to prevent or slow the onset and/or progression of disease.

APPENDIX

Appendix 1

Table showing mass of GSTP1 cysteine-47 with addition of CDDO-Me (+ 505 amu) and CDDO-Epoxyde (+ 521 amu)

Peptide	Residue	Mass	Mass:charge ratio + TP		
			singe	double	triple
ASCLYGQLPK	47	1079.28	1584.28	793.14	529.09
ASCLYGQLPK	47	1079.28	1600.28	801.14	534.43

Appendix 2

Table showing mass of Keap1 cysteine containing peptides identified as modified with addition of CDDO-Epoxyde (+ 521 amu)

Peptide	Residue	Mass	Mass:charge ratio + TP		
			singe	double	triple
YDCPQR	257	780.32	1301.62	651.81	434.87
CHALTPR	273	796.40	1317.70	659.81	440.23
CEILQADAR	288	1017.49	1538.79	77.04	513.93
IGVGVIDGH...VER	434	2755.36	3276.66	1639.33	1093.22
LNSAECYYPER	489	1343.58	1864.88	933.44	622.63
SGVGVAVTMEPCR	613	1304.62	1825.92	913.96	609.64

Appendix 3

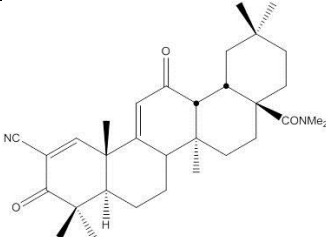
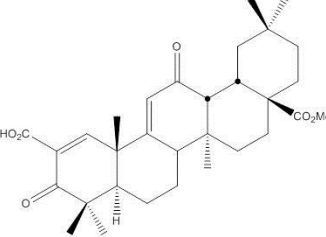
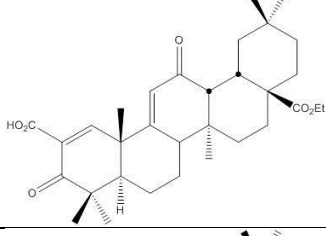
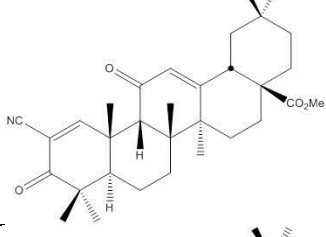
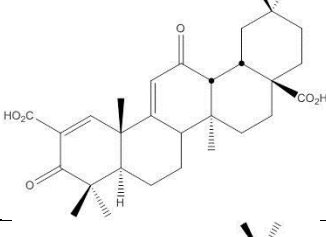
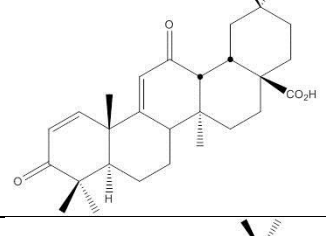
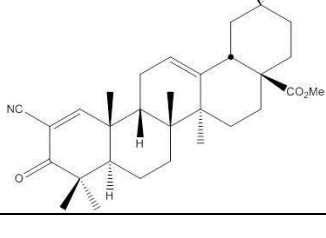
Table showing mass of Keap1 cysteine containing peptides with addition of IAA (184.9 amu)

Peptide	Residue	Mass	Mass:charge ratio + IAA		
			single	double	triple
CPEGAGDAVM...TECK	23, 38	1730.70	1915.66	958.83	639.55
LSQQLCDVTLQVK	77	1473.79	1658.75	830.37	553.92
CVLHVMNGAV...DSVVR	151	2133.05	2318.01	1160.01	773.67
ACSDFLVQQLDP...HQR	170, 196	3587.71	3957.63	1979.82	1320.21
QEEFFNLSHCQLATLISR	226	2135.05	2320.01	1161.00	774.34
CESEVFHACIDWVK	241, 249	1664.73	2034.65	1018.33	679.22
YDCPQR	257	780.32	965.28	483.64	322.76
CHALTPR	273	796.40	981.36	491.68	328.12
CEILQADAR	288	1017.49	1202.45	602.23	401.82
CK	297	2598.36	2783.32	1392.66	928.77
DYLVQIFQELTL...VPCR	319	1647.88	1832.84	917.42	611.95
SGLAGCVVGGGL...VGGR	368	3558.45	3928.37	1965.19	1310.46
NNSPDGNTDSS...VPR	395, 406	2755.36	2940.32	1471.16	981.11
IGVGVIDGHIYAV...VER	434	1343.58	1528.54	765.27	510.51
LNSAECYPER	489	2995.36	3365.28	1683.64	1122.76
SGAGVCVLHNCI...VER	513, 518	3538.55	3723.51	1862.76	1242.17
IYVLGGYDGHTFL...VTR	583	1304.62	1489.58	745.79	497.53
SGVGVAVTMEPCR	613	1051.41	1421.33	711.66	474.78
QIDQQNCTC	622, 624	1730.70	1915.66	958.83	639.55

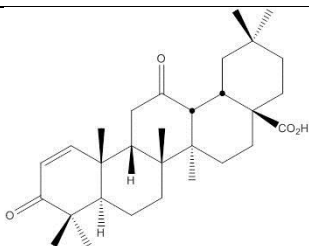
Appendix 4

Structure of TP compounds taken from published literature by Dinkova-Kostova *et al.* (2005) with concentration at which Nqo1 activity is doubled (CD) in Hepa1c1c7 cells.

Name	Structure	Nqo1 CD (nM)
TP-225		0.28
TP-224		1
TP-155		1
TP-151		2.3
TP-223		2.3

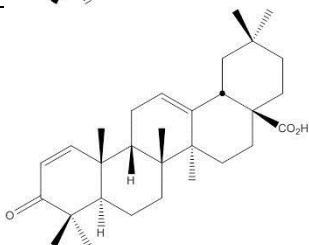
TP-226		6.9
TP-190		18
TP-222		22
TP-162		100
TP-191		220
TP-82		280
TP-156		1500

TP-69



1800

TP-46



3900

Appendix 5.


















Table of ETGE-like motif containing proteins identified in Keap1-V5 and mock transfected HEK293T cells

UniProt	Protein Name	Average peptides		Motif
		Keap1-V5	Mock	
Q15029	116 kDa U5 small nuclear ribonucleoprotein component	8.6	0	ESGE
O43242	26S proteasome non-ATPase regulatory subunit 3	9.5	4.0	STGE
P08195	4F2 cell-surface antigen heavy chain	2.8	2.0	STGE
Q02952	A-kinase anchor protein 12	2.3	0	ETGE, ESGE
Q86XL3	Ankyrin repeat and LEM domain-containing protein 2	2.0	0	ETGE
O00203	AP-3 complex subunit beta-1	1.7	0	ESGE
O14617	AP-3 complex subunit delta-1	5.3	0	STGE
Q9P2R6	Arginine-glutamic acid dipeptide repeats protein	3.4	3.0	ETGE
Q14562	ATP-dependent RNA helicase DHX8	5.3	0	ETGE
P27708	CAD protein	47.3	3.0	STGE
P13861	cAMP-dependent protein kinase type II-alpha regulatory subunit	3.2	0	ESGE
O43264	Centromere/kinetochore protein zw10 homolog	3.3	0	STGE
Q9P2I0	Cleavage and polyadenylation specificity factor subunit 2	2.0	0	ETGE
Q07021	Complement component 1 Q subcomponent-binding protein, mitochondrial	5.8	2.0	STGE
Q15003	Condensin complex subunit 2	5.2	0	STGE
P17812	CTP synthase 1	3.7	1.0	STGE
Q96N67	Dedicator of cytokinesis protein 7	4.0	0	STGE
Q9NY33	Dipeptidyl peptidase 3	4.2	0	ETGE
O00273	DNA fragmentation factor subunit alpha	1.5	0	ESGE
P25205	DNA replication licensing factor MCM3	15.5	0	ETGE
P33991	DNA replication licensing factor MCM4	5.0	1.0	STGE
P13639	Elongation factor 2	32.0	6.3	ESGE
Q7Z2Z2	Elongation factor Tu GTP-binding domain-containing protein 1	4.0	0	ETGE
O75821	Eukaryotic translation initiation factor 3 subunit G	4.2	0	STGE

Q13347	Eukaryotic translation initiation factor 3 subunit I	5.7	2.0	STGE
Q04637	Eukaryotic translation initiation factor 4 gamma 1	29.0	1.0	ESGE
P21333	Filamin-A	9.7	3.0	ETGE
Q9BQ67	Glutamate-rich WD repeat-containing protein 1	2.3	0	ETGE
Q9Y450	HBS1-like protein	9.3	0	STGE
P31943	Heterogeneous nuclear ribonucleoprotein H	14.3	7.0	STGE
P31942	Heterogeneous nuclear ribonucleoprotein H3	7.7	4.3	STGE
P51610	Host cell factor 1	1.7	0	STGE
O95202	LETM1 and EF-hand domain-containing protein 1, mitochondrial	2.2	0	ETGE
Q13257	Mitotic spindle assembly checkpoint protein MAD2A	3.0	0	ESGE
Q13423	NAD(P) transhydrogenase, mitochondrial	2.5	0	ESGE
Q96TA1	Niban-like protein 1	2.5	0	ETGE
P67809	Nuclease-sensitive element-binding protein 1	5.4	1.5	ESGE
P55209	Nucleosome assembly protein 1-like 1	6.0	2.0	ETGE
P62937	Peptidyl-prolyl cis-trans isomerase A	4.4	0	STGE
Q15149	Plectin	19.2	0	STGE
P02545	Prelamin-A/C	2.3	0	STGE
O15027	Protein transport protein Sec16A	3.0	0	ESGE
Q92900	Regulator of nonsense transcripts 1	9.2	0	ETGE
P27694	Replication protein A 70 kDa DNA-binding subunit	6.3	2.0	ESGE
Q14684	Ribosomal RNA processing protein 1 homolog B	2.0	1.5	STGE
Q13501	Sequestosome-1	3.3	0	STGE
Q96HS1	Serine/threonine-protein phosphatase PGAM5, mitochondrial	30.0	4.0	ESGE
Q9H2G2	STE20-like serine/threonine-protein kinase	2.7	0	ETGE
P38646	Stress-70 protein, mitochondrial	13.3	4.0	ETGE
Q9NPQ8	Synembryn-A	1.8	0	ETGE
Q6PGP7	Tetratricopeptide repeat protein 37	5.7	0	ETGE
Q8NI27	THO complex subunit 2	2.7	0	ETGE
Q9Y487	V-type proton ATPase 116 kDa subunit a isoform 2	10.7	0	ETGE
O75083	WD repeat-containing protein 1	2.0	0	ETGE

Appendix 6.

Figure detailing the shapes representing different molecules shown in Ingenuity pathways and what they represent. Taken directly from: http://ingenuity.force.com/ipa/articles/Feature_Description/Legend

<u>Network Shapes</u>	
	Ion Channel
	Complex/Group
	Kinase
	Chemical/Drug/Toxicant
	Ligand-dependent Nuclear Receptor
	Cytokine
	Mature microRNA
	Disease
	microRNA
	Enzyme
	Other
	Function
	Peptidase
	G-protein Coupled Receptor
	Phosphatase
	Growth Factor
	Transcription Regulator

Appendix 7.

List of constructs received from Dr Jon Woodsmith, Max-Planck Institute for Molecular Genetics, Berlin, Germany for Y2H screen. Includes details of location of construct on 96 well plate, gene symbol and ID, the pDONR vector the constructs is in and the length of the intern in nucleotides (nt)

Plate	Row	Column	Symbol	GeneID	Vector	Length(nt)
1	A	5	PPIA	5478	pDONR221	536
1	A	8	PSMD3	5709	pDONR221	1643
1	A	9	DFFA	1676	pDONR221	913
1	A	10	EFTUD2	9343	pDONR221	2957
1	A	12	HNRNPH1	3187	pDONR221	1388
1	B	1	NAP1L1	4673	pDONR221	1214
1	B	5	HNRNPH3	3189	pDONR221	686
1	B	8	EIF3G	8666	pDONR221	1001
1	B	10	EIF3I	8668	pDONR221	889
1	B	11	RIC8A	60626	pDONR221	1682
1	C	10	GRWD1	83743	pDONR221	1341
1	D	1	NCAPH	23397	pDONR221	2226
1	E	3	HNRNPH1	3187	pDONR221	1350
1	E	5	YBX1	4904	pDONR221	975
1	E	6	YBX1	4904	pDONR221	975
1	E	9	AP3B1	8546	pDONR221	3285
1	F	1	LETM1	3954	pDONR221	2220
1	F	7	MCM3	4172	pDONR221	2427
1	G	7	DFFA	1676	pDONR223	996
1	G	12	NAP1L1	4673	pDONR223	1176
1	H	2	GRWD1	83743	pDONR223	1341
1	H	5	WDR1	9948	pDONR223	1821
1	H	6	DPP3	10072	pDONR223	2214
1	H	11	WDR1	9948	pDONR223	1821
2	A	5	EFTUD2	9343	pDONR223	2919
2	A	7	MAD2L1	4085	pDONR223	618
2	B	8	PPIA	5478	pDONR223	498
2	B	9	NNT	23530	pDONR223	624
2	C	11	EIF3I	8668	pDONR223	978
2	D	4	PRKAR2A	5576	pDONR223	1149
2	E	1	HBS1L	10767	pDONR223	2055
2	E	2	LETM1	3954	pDONR223	2220
2	E	11	LMNA	4000	pDONR223	1719
2	F	1	AP3D1	8943	pDONR223	2229
2	F	2	MCM3	4172	pDONR223	2427
2	F	5	AP3B1	8546	pDONR223	3285
2	F	10	EIF3G	8666	pDONR223	963
2	G	3	PSMD3	5709	pDONR223	1605
2	G	4	HSPA9	3313	pDONR223	2040
2	G	11	DHX8	1659	pDONR223	3650

2	H	12	HCFC1	3054	pDONR223	1292
3	A	2	NCAPH	23397	pDONR223	2231
3	A	5	EFTUD1	79631	pDONR223	2609
3	B	4	LMNA	4000	pDONR223	2000
3	B	7	ATP6V0A2	23545	pDONR223	2576
3	B	8	DPP3	10072	pDONR223	2219
3	B	12	CTPS	1503	pDONR223	1781
3	C	4	FLNA	2316	pDONR223	2522
3	C	5	RPA1	6117	pDONR223	1856
3	D	1	EEF2	1938	pDONR223	2577
3	D	10	RIC8A	60626	pDONR223	1593
3	E	1	NNT	23530	pDONR223	3261
3	E	3	SLK	9748	pDONR223	3615
3	E	6	ZW10	9183	pDONR223	2019
3	E	10	HNRNPH3	3189	pDONR221	996

Appendix 8.

Details of Venn diagram comparison of proteins co-purified with Keap1-V5 following treatment of cells with Nrf2 inducing electrophiles.

DMSO (8)	DMSO, CDDO-Me (15)	DMSO, DNCB, Dex-mes (3)	DNCB (14)	DNCB, CDDO-Me (3)	CDDO-Me, Dex-mes (2)	DNCB, Dex-mes (1)
Q92667	P62191	Q7Z434	O15067	P30041	O75494	Q9NY33
Q9HAV0	Q8N163	Q16186	P12277	P49588	O60506	
Q12756	Q6P996	P67809	P55072	Q9H0U4		
P51116	P57678		Q01844			
Q99627	P35250		Q9H2G2			
O95456	Q13085		Q9Y3F4			
P62140	P06733		P05091			
P62805	Q92615		P30837			
	Q9HC35		P19338			
	Q8TD19		P22234			
	P57737		P32119			
	P09543		O00273			
	P45974		Q6PKG0			
	O75179		P62913			
	Q07866					

DMSO, Dex-mes (19)	DMSO, CDDO-Me, Dex-mes (277)				CDDO- Me (29)	Dex- mes (61)
P49207	Q02978	O43776	Q14498	Q9Y4C2	Q96J01	Q9NZB2
P06132	P61313	Q01085	Q07666	Q6NXE6	P30520	P40616
P62318	P63010	Q8TEQ6	Q13526	P56134	O14929	P61962
Q9Y4R8	O76003	P41250	Q01081	Q9BTW9	Q71DI3	Q5VT66
Q9BQ67	P46459	P55209	Q9UHD1	O15160	P62937	P11498
Q8WWM7	P20042	P10768	O96008	P16152	Q13642	Q9UN86
Q15785	Q9Y5B9	P52789	Q9UBQ7	Q92974	Q0VDF9	P61586
P62873	Q96QK1	Q86Y56	Q15185	Q9NZL4	O00159	Q9H3K6
P51148	Q8N1F7	P61619	Q14318	O43491	Q9P2R3	Q01650
P27348	O43592	Q9UQE7	P14868	P84098	Q7L5N1	P30626
P61019	P05023	Q9Y224	Q9UGI8	Q9ULC4	O75436	Q8NE71
P55265	O75694	Q14562	Q13155	P61201	Q15750	P35613
P36776	O75643	P50502	O60264	O95573	Q15424	Q9Y241
Q5BKZ1	P33993	P13489	Q9NTJ3	Q9Y263	P08133	O43347
Q9Y4L1	Q6P2Q9	O14617	Q13098	Q96L92	O43264	P42766
Q9BXW7	A5YKK6	P35573	Q9Y5L0	Q8WUM0	P46379	P52434
Q96PK6	O43390	Q14157	Q9BZE4	O95299	O14579	Q92990
P60660	Q15365	O95433	P08195	P13807	Q14C86	P35658
P46087	Q15366	Q14671	Q96EP5	Q99829	Q92905	Q15436
	O75533	Q15021	P62851	Q8TC07	Q7KZI7	P60468
	Q02878	O43143	P43686	Q01469	Q9H583	Q9ULX3
	P51991	P19525	Q8TDN6	Q8WWK9	O75369	Q13423
	P14618	Q5T4S7	A6NDG6	Q9Y295	O60488	Q7L576
	P50991	Q13595	O94906	P42677	P62333	P0C0S8
	Q9UQ35	Q9Y277	Q96FW1	O00170	Q9UHI6	P00387
	P61978	Q15813	Q00535	P41214	Q6P2E9	Q9Y3T9
	Q92734	Q08J23	P62280	P55196	P46940	Q9UJV9
	P78527	Q7L1Q6	P31040	P62266	P61353	O15027
	P22626	P61011	Q3ZCQ8	P62888	P52597	Q9Y2R9
	P35579	Q9Y450	P39748	Q9Y5M8		Q9H857
	Q9BVA1	Q92900	Q9BV20	O75569		P18077
	Q14145	P15170	P53007	P62841		Q66PJ3
	P45880	Q14697	Q15758	O75821		Q9NTK5
	P05388	O94874	Q9NZ01	Q9BRX2		Q99714
	P25705	Q15029	O95793	Q9BTT0		Q92522
	P63261	Q4VCS5	P23381	Q9BXP5		Q16795
	P17844	Q9UJS0	Q9UNM6	P04637		Q9NSD9
	P62826	P53985	Q08945	O60610		Q13523
	Q15427	O75131	Q96CS3	P63173		P61964
	P15880	O94973	O00154	P62633		P30101
	Q16891	P39656	Q14566	Q8N0X7		P49591
	P18754	P32322	P61081	Q9NVP1		Q9NRG9
	P12004	Q9Y3A5	P43487	Q9UJU6		O00165
	P11142	P52209	Q99700	Q9Y696		Q1KMD3
	Q13148	P35606	P26368	P51571		O43615
	P18621	P08240	P51114	Q9BVP2		P62879
	P50914	Q14683	O95163	P50402		Q6UB35
	Q13263	P33991	P14923	Q15738		Q96EY7

P09874	P31948	P42167	P61803	P61106
P43243	Q8N1G4	Q9Y285	Q9H307	Q6PI48
P06576	P48735	Q15555	O00264	O75439
Q9H9B4	Q9BQG0	O60678	Q9UBM7	O00425
O00571	P33992	Q15003	P21964	O15042
P14866	Q99613	Q9Y265	Q9ULT8	Q99879
P24752	P41091	P78417	O60716	P14625
Q14103	P55084	P50454	Q14160	P35580
P62899	Q99459	Q15008	Q08752	P20700
P08670	P31930	P27694	Q15056	P62917
P62701	P18085	P55884	P84103	P18124
Q96C36	Q8IYB3	Q9H078	Q9UBB6	P31942
Q08211	P78344	P22087	Q9UBX3	Q66K89
P07737	Q9UMS4	P11387	P04792	
P31943	O14979	P11172	O94979	
P11177	Q9UBF2	Q14839	Q96EY1	
Q15233	Q9NUU7	P26639	P51570	
P27824	Q07065	P41240	P00403	
Q12931	Q13838	Q9H0A0	Q02543	
Q12906	Q9BXJ9	P60228	P57088	
Q00325	P33176	Q14258	Q9Y3U8	
Q92841				

DMSO, DNCB, CDDO-Me, Dex-mes (203)				CDDO-Me, Dex-Mes (83)	
Q9Y310	P23528	P35268	Q8TEX9	P62834	Q13547
P84077	P62995	P62854	P78371	P50995	P14324
P46781	Q12904	Q16643	O14654	P14406	Q99460
P30566	P28288	O15260	P08243	Q8TCT9	P51398
P00558	Q9P035	P26196	P13010	P51648	Q9UJZ1
Q14203	Q13501	P46776	P52292	Q86X55	Q6YN16
Q92499	P06748	P62314	P53396	O43396	Q14126
P38919	Q99873	P60866	P63241	P25789	P49755
Q14152	P36542	O75964	P12956	Q96KR1	P51149
Q92973	Q9HAV4	Q9UNS2	Q9UQ80	Q16576	Q7L0Y3
Q96124	P62906	O43684	O94826	P21266	P23526
Q8WUM4	O94905	Q06830	P26641	Q8NBU5	Q96P70
Q92621	Q13200	P83731	Q9NR30	Q9UL25	Q8NCA5
Q9Y2L1	P62829	Q12769	P12236	Q8TC12	Q9UNE7
O43242	Q9BT78	Q92945	P16615	P58107	P68400
P54577	P35998	Q9UNX3	Q9NZI8	Q5SRE5	O43747
P22102	P62244	O00487	P48643	P82675	Q53GQ0
Q12905	O00299	P46778	P60842	Q14677	P51572
P26640	P40429	P30050	Q02790	Q9H0S4	P46782
P11940	Q9BY44	Q9NS69	P53618	P38606	P61026
Q9Y2Z0	Q9Y230	Q96T76	Q99832	P53992	Q9P2R6
Q9H3U1	O95373	P31689	P40227	Q14694	O95347
P49915	P62750	P17980	P35637	P52306	Q7L2H7
Q14166	P32969	P05387	Q86VP6	Q53H12	Q07955

P38646	Q99615	Q15084	Q04637	P52565	Q9Y5V3
P30153	P29692	P24534	O43175	P46783	Q86UE4
P48444	Q7Z6Z7	P62277	P54886	P37802	Q92552
O75534	Q16543	Q9UNF1	P05141	P24539	Q9P2E9
P25205	P46977	P62987	P49368	Q9NX63	Q9Y262
Q9Y487	P62081	P08559	Q9Y678	P41227	O14974
P23246	O15371	Q13347	P41252	O60762	Q7L2E3
P04844	P18031	P46777	P09651	Q5JTH9	Q5T9A4
O76094	P62195	P55010	P53621	Q09028	Q15149
Q9UHB9	Q15717	P23921	P27708	Q96AG4	P35232
P26599	O00231	P24666	P50990	P17655	P07910
P46060	O00303	Q9Y5A9	Q9P2J5	P61421	P21796
Q93008	Q7Z2W4	P62495	O00410	Q13151	P38159
P11021	Q9UBB4	Q07021	P07900	P62424	P36578
Q5VYK3	Q15393	P17812	Q7KZF4	Q07020	P40939
Q9UG63	P06493	P27635	P55060	P04843	Q13435
P11586	Q14739	P04406	Q9Y490	P62249	Q99623
P47897	P21333	P78347	Q14974	P42704	
Q14008	Q9UDY2	P46779	P17987		
P54136	Q99729	P08865	P13639		
P56192	P60891	Q71RC2	P08107		
O14980	P62269	P26373	P07814		
Q00341	O00232	P05198	P68104		
P49411	P22695	O76021	Q14204		
Q9BUF5	P68371	P10809	Q96HS1		
Q00610	P07437	P16403	P08238		
P68363	P49327		Q92616		

BIBLIOGRAPHY

- Abbas, K., Breton, J., Planson, A. G., Bouton, C., Bignon, J., Seguin, C., Riquier, S., Toledano, M. B. and Drapier, J. C. (2011) 'Nitric oxide activates an Nrf2/sulfiredoxin antioxidant pathway in macrophages', *Free Radic Biol Med*, 51(1), 107-14.
- Ahmad, R., Raina, D., Meyer, C., Kharbanda, S. and Kufe, D. (2006) 'Triterpenoid CDDO-Me blocks the NF-kappaB pathway by direct inhibition of IKKbeta on Cys-179', *J Biol Chem*, 281(47), 35764-9.
- Ahn, Y. H., Hwang, Y., Liu, H., Wang, X. J., Zhang, Y., Stephenson, K. K., Boronina, T. N., Cole, R. N., Dinkova-Kostova, A. T., Talalay, P. and Cole, P. A. (2010) 'Electrophilic tuning of the chemoprotective natural product sulforaphane', *Proc Natl Acad Sci U S A*, 107(21), 9590-5.
- Alam, J., Killeen, E., Gong, P., Naquin, R., Hu, B., Stewart, D., Ingelfinger, J. R. and Nath, K. A. (2003) 'Heme activates the heme oxygenase-1 gene in renal epithelial cells by stabilizing Nrf2', *Am J Physiol Renal Physiol*, 284(4), F743-52.
- Alam, J., Stewart, D., Touchard, C., Boinapally, S., Choi, A. M. and Cook, J. L. (1999) 'Nrf2, a Cap'n'Collar transcription factor, regulates induction of the heme oxygenase-1 gene', *J Biol Chem*, 274(37), 26071-8.
- Amoureux, M. C., Nicolas, S. and Rougon, G. (2012) 'NCAM180 regulates Ric8A membrane localization and potentiates beta-adrenergic response', *PLoS One*, 7(2), e32216.
- Aono, J., Yanagawa, T., Itoh, K., Li, B., Yoshida, H., Kumagai, Y., Yamamoto, M. and Ishii, T. (2003) 'Activation of Nrf2 and accumulation of ubiquitinated A170 by arsenic in osteoblasts', *Biochem Biophys Res Commun*, 305(2), 271-7.
- Apopa, P. L., He, X. and Ma, Q. (2008) 'Phosphorylation of Nrf2 in the transcription activation domain by casein kinase 2 (CK2) is critical for the nuclear translocation and transcription activation function of Nrf2 in IMR-32 neuroblastoma cells', *J Biochem Mol Toxicol*, 22(1), 63-76.
- Baird, L. and Dinkova-Kostova, A. T. (2013) 'Diffusion dynamics of the Keap1-Cullin3 interaction in single live cells', *Biochem Biophys Res Commun*, 433(1), 58-65.
- Banning, A., Deubel, S., Kluth, D., Zhou, Z. and Brigelius-Flohe, R. (2005) 'The GI-GPx gene is a target for Nrf2', *Mol Cell Biol*, 25(12), 4914-23.
- Baty, J. W., Hampton, M. B. and Winterbourn, C. C. (2005) 'Proteomic detection of hydrogen peroxide-sensitive thiol proteins in Jurkat cells', *Biochem J*, 389(Pt 3), 785-95.
- Bloom, D., Dhakshinamoorthy, S. and Jaiswal, A. K. (2002) 'Site-directed mutagenesis of cysteine to serine in the DNA binding region of Nrf2 decreases its capacity to upregulate antioxidant response element-mediated expression and antioxidant induction of NAD(P)H:quinone oxidoreductase1 gene', *Oncogene*, 21(14), 2191-200.
- Bloom, D. A. and Jaiswal, A. K. (2003) 'Phosphorylation of Nrf2 at Ser40 by protein kinase C in response to antioxidants leads to the release of Nrf2 from I κ Nrf2, but is not required for Nrf2 stabilization/accumulation in the nucleus and transcriptional

- activation of antioxidant response element-mediated NAD(P)H:quinone oxidoreductase-1 gene expression', *J Biol Chem*, 278(45), 44675-82.
- Bradford, M. M. (1976) 'A rapid and sensitive method for the quantitation of microgram quantities of protein utilizing the principle of protein-dye binding', *Anal Biochem*, 72, 248-54.
- Brookes, P. S., Morse, K., Ray, D., Tompkins, A., Young, S. M., Hilchey, S., Salim, S., Konopleva, M., Andreeff, M., Phipps, R. and Bernstein, S. H. (2007) 'The triterpenoid 2-cyano-3,12-dioxooleana-1,9-dien-28-oic acid and its derivatives elicit human lymphoid cell apoptosis through a novel pathway involving the unregulated mitochondrial permeability transition pore', *Cancer Res*, 67(4), 1793-802.
- Bryan, H. K., Olayanju, A., Goldring, C. E. and Park, B. K. (2013) 'The Nrf2 cell defence pathway: Keap1-dependent and -independent mechanisms of regulation', *Biochem Pharmacol*, 85(6), 705-17.
- Buckley, B. J., Marshall, Z. M. and Whorton, A. R. (2003) 'Nitric oxide stimulates Nrf2 nuclear translocation in vascular endothelium', *Biochem Biophys Res Commun*, 307(4), 973-9.
- Burgoyne, J. R. and Eaton, P. (2011) 'Contemporary techniques for detecting and identifying proteins susceptible to reversible thiol oxidation', *Biochem Soc Trans*, 39(5), 1260-7.
- Butterfield, D. A., Castegna, A., Lauderback, C. M. and Drake, J. (2002) 'Evidence that amyloid beta-peptide-induced lipid peroxidation and its sequelae in Alzheimer's disease brain contribute to neuronal death', *Neurobiol Aging*, 23(5), 655-64.
- Caccuri, A. M., Petruzzelli, R., Polizio, F., Federici, G. and Desideri, A. (1992) 'Inhibition of glutathione transferase pi from human placenta by 1-chloro-2,4-dinitrobenzene occurs because of covalent reaction with cysteine 47', *Arch Biochem Biophys*, 297(1), 119-22.
- Caldwell, J., Gardner, I. and Swales, N. (1995) 'An introduction to drug disposition: the basic principles of absorption, distribution, metabolism, and excretion', *Toxicol Pathol*, 23(2), 102-14.
- Calkins, M. J., Johnson, D. A., Townsend, J. A., Vargas, M. R., Dowell, J. A., Williamson, T. P., Kraft, A. D., Lee, J. M., Li, J. and Johnson, J. A. (2009) 'The Nrf2/ARE pathway as a potential therapeutic target in neurodegenerative disease', *Antioxid Redox Signal*, 11(3), 497-508.
- Camp, N. D., James, R. G., Dawson, D. W., Yan, F., Davison, J. M., Houck, S. A., Tang, X., Zheng, N., Major, M. B. and Moon, R. T. (2012) 'Wilms tumor gene on X chromosome (WTX) inhibits degradation of NRF2 protein through competitive binding to KEAP1 protein', *J Biol Chem*, 287(9), 6539-50.
- Canning, P., Cooper, C. D., Krojer, T., Murray, J. W., Pike, A. C., Chaikuad, A., Keates, T., Thangaratnarajah, C., Hojzan, V., Ayinampudi, V., Marsden, B. D., Gileadi, O., Knapp, S., von Delft, F. and Bullock, A. N. (2013) 'Structural basis for Cul3 protein assembly with the BTB-Kelch family of E3 ubiquitin ligases', *J Biol Chem*, 288(11), 7803-14.

- Cargnello, M. and Roux, P. P. (2011) 'Activation and function of the MAPKs and their substrates, the MAPK-activated protein kinases', *Microbiol Mol Biol Rev*, 75(1), 50-83.
- Castillo, E. A., Ayte, J., Chiva, C., Moldon, A., Carrascal, M., Abian, J., Jones, N. and Hidalgo, E. (2002) 'Diethylmaleate activates the transcription factor Pap1 by covalent modification of critical cysteine residues', *Mol Microbiol*, 45(1), 243-54.
- Chan, J. Y. and Kwong, M. (2000) 'Impaired expression of glutathione synthetic enzyme genes in mice with targeted deletion of the Nrf2 basic-leucine zipper protein', *Biochim Biophys Acta*, 1517(1), 19-26.
- Chan, K., Han, X. D. and Kan, Y. W. (2001) 'An important function of Nrf2 in combating oxidative stress: detoxification of acetaminophen', *Proc Natl Acad Sci U S A*, 98(8), 4611-6.
- Chan, K., Lu, R., Chang, J. C. and Kan, Y. W. (1996) 'NRF2, a member of the NFE2 family of transcription factors, is not essential for murine erythropoiesis, growth, and development', *Proc Natl Acad Sci U S A*, 93(24), 13943-8.
- Chanas, S. A., Jiang, Q., McMahon, M., McWalter, G. K., McLellan, L. I., Elcombe, C. R., Henderson, C. J., Wolf, C. R., Moffat, G. J., Itoh, K., Yamamoto, M. and Hayes, J. D. (2002) 'Loss of the Nrf2 transcription factor causes a marked reduction in constitutive and inducible expression of the glutathione S-transferase Gsta1, Gsta2, Gstm1, Gstm2, Gstm3 and Gstm4 genes in the livers of male and female mice', *Biochem J*, 365(Pt 2), 405-16.
- Chen, C., Pung, D., Leong, V., Hebbar, V., Shen, G., Nair, S., Li, W. and Kong, A. N. (2004) 'Induction of detoxifying enzymes by garlic organosulfur compounds through transcription factor Nrf2: effect of chemical structure and stress signals', *Free Radic Biol Med*, 37(10), 1578-90.
- Chen, G., Heim, A., Riether, D., Yee, D., Milgrom, Y., Gawinowicz, M. A. and Sames, D. (2003) 'Reactivity of functional groups on the protein surface: development of epoxide probes for protein labeling', *J Am Chem Soc*, 125(27), 8130-3.
- Chen, W., Jiang, T., Wang, H., Tao, S., Lau, A., Fang, D. and Zhang, D. D. (2012) 'Does Nrf2 contribute to p53-mediated control of cell survival and death?', *Antioxid Redox Signal*, 17(12), 1670-5.
- Chen, Z. H., Saito, Y., Yoshida, Y., Sekine, A., Noguchi, N. and Niki, E. (2005) '4-Hydroxynonenal induces adaptive response and enhances PC12 cell tolerance primarily through induction of thioredoxin reductase 1 via activation of Nrf2', *J Biol Chem*, 280(51), 41921-7.
- Chia, A. J., Goldring, C. E., Kitteringham, N. R., Wong, S. Q., Morgan, P. and Park, B. K. (2010) 'Differential effect of covalent protein modification and glutathione depletion on the transcriptional response of Nrf2 and NF-kappaB', *Biochem Pharmacol*, 80(3), 410-21.

- Chin, M. P., Reisman, S. A., Bakris, G. L., O'Grady, M., Linde, P. G., McCullough, P. A., Packham, D., Vaziri, N. D., Ward, K. W., Warnock, D. G. and Meyer, C. J. (2014) 'Mechanisms Contributing to Adverse Cardiovascular Events in Patients with Type 2 Diabetes Mellitus and Stage 4 Chronic Kidney Disease Treated with Bardoxolone Methyl', *Am J Nephrol*, 39(6), 499-508.
- Chowdhry, S., Zhang, Y., McMahon, M., Sutherland, C., Cuadrado, A. and Hayes, J. D. (2013) 'Nrf2 is controlled by two distinct beta-TrCP recognition motifs in its Neh6 domain, one of which can be modulated by GSK-3 activity', *Oncogene*, 32(32), 3765-81.
- Cleasby, A., Yon, J., Day, P. J., Richardson, C., Tickle, I. J., Williams, P. A., Callahan, J. F., Carr, R., Concha, N., Kerns, J. K., Qi, H., Sweitzer, T., Ward, P. and Davies, T. G. (2014) 'Structure of the BTB Domain of Keap1 and Its Interaction with the Triterpenoid Antagonist CDDO', *PLoS One*, 9(6), e98896.
- Collet, J. F. and Messens, J. (2010) 'Structure, function, and mechanism of thioredoxin proteins', *Antioxid Redox Signal*, 13(8), 1205-16.
- Connolly, J. D. and Hill, R. A. (2005) 'Triterpenoids', *Nat Prod Rep*, 22(4), 487-503.
- Cooper, C. E., Patel, R. P., Brookes, P. S. and Darley-Usmar, V. M. (2002) 'Nanotransducers in cellular redox signaling: modification of thiols by reactive oxygen and nitrogen species', *Trends Biochem Sci*, 27(10), 489-92.
- Copple, I. M. (2012) 'The Keap1-Nrf2 cell defense pathway--a promising therapeutic target?', *Adv Pharmacol*, 63, 43-79.
- Copple, I. M., Goldring, C. E., Jenkins, R. E., Chia, A. J., Randle, L. E., Hayes, J. D., Kitteringham, N. R. and Park, B. K. (2008a) 'The hepatotoxic metabolite of acetaminophen directly activates the Keap1-Nrf2 cell defense system', *Hepatology*, 48(4), 1292-301.
- Copple, I. M., Goldring, C. E., Kitteringham, N. R. and Park, B. K. (2008b) 'The Nrf2-Keap1 defence pathway: role in protection against drug-induced toxicity', *Toxicology*, 246(1), 24-33.
- Copple, I. M., Lister, A., Obeng, A. D., Kitteringham, N. R., Jenkins, R. E., Layfield, R., Foster, B. J., Goldring, C. E. and Park, B. K. (2010) 'Physical and functional interaction of sequestosome 1 with Keap1 regulates the Keap1-Nrf2 cell defense pathway', *Journal of Biological Chemistry*, 285(22), 16782-16788.
- Copple, I. M., Shelton, L. M., Walsh, J., Kratschmar, D. V., Lister, A., Odermatt, A., Goldring, C. E., Dinkova-Kostova, A. T., Honda, T. and Park, B. K. (2014) 'Chemical Tuning Enhances Both Potency Toward Nrf2 and In Vitro Therapeutic Index of Triterpenoids', *Toxicol Sci*.
- Couch, R. D., Browning, R. G., Honda, T., Gribble, G. W., Wright, D. L., Sporn, M. B. and Anderson, A. C. (2005) 'Studies on the reactivity of CDDO, a promising new chemopreventive and chemotherapeutic agent: implications for a molecular mechanism of action', *Bioorg Med Chem Lett*, 15(9), 2215-9.

- Cui, H., Kong, Y. and Zhang, H. (2012) 'Oxidative stress, mitochondrial dysfunction, and aging', *J Signal Transduct*, 2012, 646354.
- Cullinan, S. B., Gordan, J. D., Jin, J., Harper, J. W. and Diehl, J. A. (2004) 'The Keap1-BTB protein is an adaptor that bridges Nrf2 to a Cul3-based E3 ligase: oxidative stress sensing by a Cul3-Keap1 ligase', *Mol Cell Biol*, 24(19), 8477-86.
- Cullinan, S. B., Zhang, D., Hannink, M., Arvisais, E., Kaufman, R. J. and Diehl, J. A. (2003) 'Nrf2 is a direct PERK substrate and effector of PERK-dependent cell survival', *Mol Cell Biol*, 23(20), 7198-209.
- Cybulsky, A. V., Takano, T., Guillemette, J., Papillon, J., Volpini, R. A. and Di Battista, J. A. (2009) 'The Ste20-like kinase SLK promotes p53 transactivation and apoptosis', *Am J Physiol Renal Physiol*, 297(4), F971-80.
- Dahlin, D. C., Miwa, G. T., Lu, A. Y. and Nelson, S. D. (1984) 'N-acetyl-p-benzoquinone imine: a cytochrome P-450-mediated oxidation product of acetaminophen', *Proc Natl Acad Sci U S A*, 81(5), 1327-31.
- Dansette, A.-C. M. a. P. M. (2008) 'Biotransformations Leading to Toxic Metabolites: Chemical Aspect', *Wermuth's The Practice of Medicinal Chemistry*, 674-696.
- Davies, K. J. (2000) 'Oxidative stress, antioxidant defenses, and damage removal, repair, and replacement systems', *IUBMB Life*, 50(4-5), 279-89.
- de Zeeuw, D., Akizawa, T., Audhya, P., Bakris, G. L., Chin, M., Christ-Schmidt, H., Goldsberry, A., Houser, M., Krauth, M., Lambers Heerspink, H. J., McMurray, J. J., Meyer, C. J., Parving, H. H., Remuzzi, G., Toto, R. D., Vaziri, N. D., Wanner, C., Wittes, J., Wrolstad, D., Chertow, G. M. and Investigators, B. T. (2013) 'Bardoxolone methyl in type 2 diabetes and stage 4 chronic kidney disease', *N Engl J Med*, 369(26), 2492-503.
- DeLeve, L. D. and Kaplowitz, N. (1991) 'Glutathione metabolism and its role in hepatotoxicity', *Pharmacol Ther*, 52(3), 287-305.
- Dennehy, M. K., Richards, K. A., Wernke, G. R., Shyr, Y. and Liebler, D. C. (2006) 'Cytosolic and nuclear protein targets of thiol-reactive electrophiles', *Chem Res Toxicol*, 19(1), 20-9.
- Deretic, V. (2006) 'Autophagy as an immune defense mechanism', *Curr Opin Immunol*, 18(4), 375-82.
- Dhakshinamoorthy, S. and Jaiswal, A. K. (2001) 'Functional characterization and role of INrf2 in antioxidant response element-mediated expression and antioxidant induction of NAD(P)H:quinone oxidoreductase1 gene', *Oncogene*, 20(29), 3906-17.
- Dietz, B. M., Liu, D., Hagos, G. K., Yao, P., Schinkovitz, A., Pro, S. M., Deng, S., Farnsworth, N. R., Pauli, G. F., van Breemen, R. B. and Bolton, J. L. (2008) 'Angelica sinensis and its alkylphthalides induce the detoxification enzyme NAD(P)H: quinone oxidoreductase 1 by alkylating Keap1', *Chem Res Toxicol*, 21(10), 1939-48.

- Ding, Y., Choi, K. J., Kim, J. H., Han, X., Piao, Y., Jeong, J. H., Choe, W., Kang, I., Ha, J., Forman, H. J., Lee, J., Yoon, K. S. and Kim, S. S. (2008) 'Endogenous hydrogen peroxide regulates glutathione redox via nuclear factor erythroid 2-related factor 2 downstream of phosphatidylinositol 3-kinase during muscle differentiation', *Am J Pathol*, 172(6), 1529-41.
- Dinkova-Kostova, A. T., Holtzclaw, W. D., Cole, R. N., Itoh, K., Wakabayashi, N., Katoh, Y., Yamamoto, M. and Talalay, P. (2002) 'Direct evidence that sulfhydryl groups of Keap1 are the sensors regulating induction of phase 2 enzymes that protect against carcinogens and oxidants', *Proc Natl Acad Sci U S A*, 99(18), 11908-13.
- Dinkova-Kostova, A. T., Liby, K. T., Stephenson, K. K., Holtzclaw, W. D., Gao, X., Suh, N., Williams, C., Risingsong, R., Honda, T., Gribble, G. W., Sporn, M. B. and Talalay, P. (2005) 'Extremely potent triterpenoid inducers of the phase 2 response: correlations of protection against oxidant and inflammatory stress', *Proc Natl Acad Sci U S A*, 102(12), 4584-9.
- Dzubak, P., Hajduch, M., Vydra, D., Hustova, A., Kvasnica, M., Biedermann, D., Markova, L., Urban, M. and Sarek, J. (2006) 'Pharmacological activities of natural triterpenoids and their therapeutic implications', *Nat Prod Rep*, 23(3), 394-411.
- Eades, G., Yang, M., Yao, Y., Zhang, Y. and Zhou, Q. (2011) 'miR-200a regulates Nrf2 activation by targeting Keap1 mRNA in breast cancer cells', *J Biol Chem*, 286(47), 40725-33.
- Eggler, A. L., Liu, G., Pezzuto, J. M., van Breemen, R. B. and Mesecar, A. D. (2005) 'Modifying specific cysteines of the electrophile-sensing human Keap1 protein is insufficient to disrupt binding to the Nrf2 domain Neh2', *Proc Natl Acad Sci U S A*, 102(29), 10070-5.
- Eggler, A. L., Luo, Y., van Breemen, R. B. and Mesecar, A. D. (2007) 'Identification of the highly reactive cysteine 151 in the chemopreventive agent-sensor Keap1 protein is method-dependent', *Chem Res Toxicol*, 20(12), 1878-84.
- Eggler, A. L., Small, E., Hannink, M. and Mesecar, A. D. (2009) 'Cul3-mediated Nrf2 ubiquitination and antioxidant response element (ARE) activation are dependent on the partial molar volume at position 151 of Keap1', *Biochem J*, 422(1), 171-80.
- Elmore, S. (2007) 'Apoptosis: a review of programmed cell death', *Toxicol Pathol*, 35(4), 495-516.
- Emerit, J., Edeas, M. and Bricaire, F. (2004) 'Neurodegenerative diseases and oxidative stress', *Biomed Pharmacother*, 58(1), 39-46.
- Engin, K. N. (2009) 'Alpha-tocopherol: looking beyond an antioxidant', *Mol Vis*, 15, 855-60.
- Enomoto, A., Itoh, K., Nagayoshi, E., Haruta, J., Kimura, T., O'Connor, T., Harada, T. and Yamamoto, M. (2001) 'High sensitivity of Nrf2 knockout mice to acetaminophen hepatotoxicity associated with decreased expression of ARE-regulated drug metabolizing enzymes and antioxidant genes', *Toxicol Sci*, 59(1), 169-77.

- Fahey, J. W., Haristoy, X., Dolan, P. M., Kensler, T. W., Scholtus, I., Stephenson, K. K., Talalay, P. and Lozniewski, A. (2002) 'Sulforaphane inhibits extracellular, intracellular, and antibiotic-resistant strains of *Helicobacter pylori* and prevents benzo[a]pyrene-induced stomach tumors', *Proc Natl Acad Sci U S A*, 99(11), 7610-5.
- Fan, W., Tang, Z., Chen, D., Moughon, D., Ding, X., Chen, S., Zhu, M. and Zhong, Q. (2010) 'Keap1 facilitates p62-mediated ubiquitin aggregate clearance via autophagy', *Autophagy*, 6(5), 614-621.
- Fields, S. and Song, O. (1989) 'A novel genetic system to detect protein-protein interactions', *Nature*, 340(6230), 245-6.
- Filipowicz, W., Bhattacharyya, S. N. and Sonenberg, N. (2008) 'Mechanisms of post-transcriptional regulation by microRNAs: are the answers in sight?', *Nat Rev Genet*, 9(2), 102-14.
- Fisher, C. D., Augustine, L. M., Maher, J. M., Nelson, D. M., Slitt, A. L., Klaassen, C. D., Lehman-McKeeman, L. D. and Cherrington, N. J. (2007) 'Induction of drug-metabolizing enzymes by garlic and allyl sulfide compounds via activation of constitutive androstane receptor and nuclear factor E2-related factor 2', *Drug Metab Dispos*, 35(6), 995-1000.
- Fourquet, S., Guerois, R., Biard, D. and Toledano, M. B. (2010) 'Activation of NRF2 by nitrosative agents and H₂O₂ involves KEAP1 disulfide formation', *J Biol Chem*, 285(11), 8463-71.
- Franco, R., Sanchez-Olea, R., Reyes-Reyes, E. M. and Panayiotidis, M. I. (2009) 'Environmental toxicity, oxidative stress and apoptosis: menage a trois', *Mutat Res*, 674(1-2), 3-22.
- Fujii, S., Sawa, T., Ihara, H., Tong, K. I., Ida, T., Okamoto, T., Ahtesham, A. K., Ishima, Y., Motohashi, H., Yamamoto, M. and Akaike, T. (2010) 'The critical role of nitric oxide signaling, via protein S-guanylation and nitrated cyclic GMP, in the antioxidant adaptive response', *J Biol Chem*, 285(31), 23970-84.
- Furukawa, M. and Xiong, Y. (2005) 'BTB protein Keap1 targets antioxidant transcription factor Nrf2 for ubiquitination by the Cullin 3-Roc1 ligase', *Mol Cell Biol*, 25(1), 162-71.
- Gao, B., Flores, S. C., Leff, J. A., Bose, S. K. and McCord, J. M. (2003) 'Synthesis and anti-inflammatory activity of a chimeric recombinant superoxide dismutase: SOD2/3', *Am J Physiol Lung Cell Mol Physiol*, 284(6), L917-25.
- Gao, L., Wang, J., Sekhar, K. R., Yin, H., Yared, N. F., Schneider, S. N., Sasi, S., Dalton, T. P., Anderson, M. E., Chan, J. Y., Morrow, J. D. and Freeman, M. L. (2007) 'Novel n-3 fatty acid oxidation products activate Nrf2 by destabilizing the association between Keap1 and Cullin3', *J Biol Chem*, 282(4), 2529-37.
- Gilmore, T. D. (1999) 'The Rel/NF-kappaB signal transduction pathway: introduction', *Oncogene*, 18(49), 6842-4.

- Go, Y. M., Roede, J. R., Walker, D. I., Duong, D. M., Seyfried, N. T., Orr, M., Liang, Y., Pennell, K. D. and Jones, D. P. (2013) 'Selective targeting of the cysteine proteome by thioredoxin and glutathione redox systems', *Mol Cell Proteomics*, 12(11), 3285-96.
- Goldring, C. E., Kitteringham, N. R., Elsbey, R., Randle, L. E., Clement, Y. N., Williams, D. P., McMahon, M., Hayes, J. D., Itoh, K., Yamamoto, M. and Park, B. K. (2004) 'Activation of hepatic Nrf2 in vivo by acetaminophen in CD-1 mice', *Hepatology*, 39(5), 1267-76.
- Gomez-Marquez, J., Segade, F., Dosil, M., Pichel, J. G., Bustelo, X. R. and Freire, M. (1989) 'The expression of prothymosin alpha gene in T lymphocytes and leukemic lymphoid cells is tied to lymphocyte proliferation', *J Biol Chem*, 264(15), 8451-4.
- Greenwald, R. A. (1990) 'Superoxide dismutase and catalase as therapeutic agents for human diseases. A critical review', *Free Radic Biol Med*, 8(2), 201-9.
- Hancock, R., Schaap, M., Pfister, H. and Wells, G. (2013) 'Peptide inhibitors of the Keap1-Nrf2 protein-protein interaction with improved binding and cellular activity', *Org Biomol Chem*, 11(21), 3553-7.
- Hartikainen, J. M., Tengstrom, M., Kosma, V. M., Kinnula, V. L., Mannermaa, A. and Soini, Y. (2012) 'Genetic polymorphisms and protein expression of NRF2 and Sulfiredoxin predict survival outcomes in breast cancer', *Cancer Res*, 72(21), 5537-46.
- Hast, B. E., Goldfarb, D., Mulvaney, K. M., Hast, M. A., Siesser, P. F., Yan, F., Hayes, D. N. and Major, M. B. (2013) 'Proteomic analysis of ubiquitin ligase KEAP1 reveals associated proteins that inhibit NRF2 ubiquitination', *Cancer Res*, 73(7), 2199-210.
- Hayes, J. D., Chanas, S. A., Henderson, C. J., McMahon, M., Sun, C., Moffat, G. J., Wolf, C. R. and Yamamoto, M. (2000) 'The Nrf2 transcription factor contributes both to the basal expression of glutathione S-transferases in mouse liver and to their induction by the chemopreventive synthetic antioxidants, butylated hydroxyanisole and ethoxyquin', *Biochem Soc Trans*, 28(2), 33-41.
- Hayes, J. D. and McLellan, L. I. (1999) 'Glutathione and glutathione-dependent enzymes represent a co-ordinately regulated defence against oxidative stress', *Free Radic Res*, 31(4), 273-300.
- Hayes, J. D. and McMahon, M. (2006) 'The double-edged sword of Nrf2: subversion of redox homeostasis during the evolution of cancer', *Mol Cell*, 21(6), 732-4.
- Hayes, J. D. and McMahon, M. (2009) 'NRF2 and KEAP1 mutations: permanent activation of an adaptive response in cancer', *Trends Biochem Sci*, 34(4), 176-88.
- He, X. and Ma, Q. (2010) 'Critical cysteine residues of Kelch-like ECH-associated protein 1 in arsenic sensing and suppression of nuclear factor erythroid 2-related factor 2', *J Pharmacol Exp Ther*, 332(1), 66-75.
- Held, J. M., Danielson, S. R., Behring, J. B., Atsriku, C., Britton, D. J., Puckett, R. L., Schilling, B., Campisi, J., Benz, C. C. and Gibson, B. W. (2010) 'Targeted quantitation of site-specific cysteine oxidation in endogenous proteins using a differential alkylation

- and multiple reaction monitoring mass spectrometry approach', *Mol Cell Proteomics*, 9(7), 1400-10.
- Hirotsu, Y., Katsuoka, F., Funayama, R., Nagashima, T., Nishida, Y., Nakayama, K., Engel, J. D. and Yamamoto, M. (2012) 'Nrf2-MafG heterodimers contribute globally to antioxidant and metabolic networks', *Nucleic Acids Res*, 40(20), 10228-39.
- Hoesel, B. and Schmid, J. A. (2013) 'The complexity of NF-kappaB signaling in inflammation and cancer', *Mol Cancer*, 12, 86.
- Holland, R. and Fishbein, J. C. (2010) 'Chemistry of the cysteine sensors in Kelch-like ECH-associated protein 1', *Antioxid Redox Signal*, 13(11), 1749-61.
- Holland, R., Hawkins, A. E., Egger, A. L., Mesecar, A. D., Fabris, D. and Fishbein, J. C. (2008) 'Prospective type 1 and type 2 disulfides of Keap1 protein', *Chem Res Toxicol*, 21(10), 2051-60.
- Homma, S., Ishii, Y., Morishima, Y., Yamadori, T., Matsuno, Y., Haraguchi, N., Kikuchi, N., Satoh, H., Sakamoto, T., Hizawa, N., Itoh, K. and Yamamoto, M. (2009) 'Nrf2 enhances cell proliferation and resistance to anticancer drugs in human lung cancer', *Clin Cancer Res*, 15(10), 3423-32.
- Hong, F., Freeman, M. L. and Liebler, D. C. (2005a) 'Identification of sensor cysteines in human Keap1 modified by the cancer chemopreventive agent sulforaphane', *Chem Res Toxicol*, 18(12), 1917-26.
- Hong, F., Sekhar, K. R., Freeman, M. L. and Liebler, D. C. (2005b) 'Specific patterns of electrophile adduction trigger Keap1 ubiquitination and Nrf2 activation', *J Biol Chem*, 280(36), 31768-75.
- Huang da, W., Sherman, B. T. and Lempicki, R. A. (2009a) 'Bioinformatics enrichment tools: paths toward the comprehensive functional analysis of large gene lists', *Nucleic Acids Res*, 37(1), 1-13.
- Huang da, W., Sherman, B. T. and Lempicki, R. A. (2009b) 'Systematic and integrative analysis of large gene lists using DAVID bioinformatics resources', *Nat Protoc*, 4(1), 44-57.
- Huang, H. C., Nguyen, T. and Pickett, C. B. (2002) 'Phosphorylation of Nrf2 at Ser-40 by protein kinase C regulates antioxidant response element-mediated transcription', *J Biol Chem*, 277(45), 42769-74.
- Huang, M. T., Ho, C. T., Wang, Z. Y., Ferraro, T., Lou, Y. R., Stauber, K., Ma, W., Georgiadis, C., Laskin, J. D. and Conney, A. H. (1994) 'Inhibition of skin tumorigenesis by rosemary and its constituents carnosol and ursolic acid', *Cancer Res*, 54(3), 701-8.
- Hubbs, A. F., Benkovic, S. A., Miller, D. B., O'Callaghan, J. P., Battelli, L., Schwegler-Berry, D. and Ma, Q. (2007) 'Vacuolar leukoencephalopathy with widespread astrogliosis in mice lacking transcription factor Nrf2', *Am J Pathol*, 170(6), 2068-76.

- Hybertson, B. M., Gao, B., Bose, S. K. and McCord, J. M. (2011) 'Oxidative stress in health and disease: the therapeutic potential of Nrf2 activation', *Mol Aspects Med*, 32(4-6), 234-46.
- Inami, Y., Waguri, S., Sakamoto, A., Kouno, T., Nakada, K., Hino, O., Watanabe, S., Ando, J., Iwadate, M., Yamamoto, M., Lee, M. S., Tanaka, K. and Komatsu, M. (2011) 'Persistent activation of Nrf2 through p62 in hepatocellular carcinoma cells', *J Cell Biol*, 193(2), 275-84.
- Inoyama, D., Chen, Y., Huang, X., Beamer, L. J., Kong, A. N. and Hu, L. (2012) 'Optimization of fluorescently labeled Nrf2 peptide probes and the development of a fluorescence polarization assay for the discovery of inhibitors of Keap1-Nrf2 interaction', *J Biomol Screen*, 17(4), 435-47.
- Ishii, T., Itoh, K., Ruiz, E., Leake, D. S., Unoki, H., Yamamoto, M. and Mann, G. E. (2004) 'Role of Nrf2 in the regulation of CD36 and stress protein expression in murine macrophages: activation by oxidatively modified LDL and 4-hydroxynonenal', *Circ Res*, 94(5), 609-16.
- Ishii, T., Itoh, K., Takahashi, S., Sato, H., Yanagawa, T., Katoh, Y., Bannai, S. and Yamamoto, M. (2000) 'Transcription factor Nrf2 coordinately regulates a group of oxidative stress-inducible genes in macrophages', *J Biol Chem*, 275(21), 16023-9.
- Ito, H., Fukuda, Y., Murata, K. and Kimura, A. (1983) 'Transformation of intact yeast cells treated with alkali cations', *J Bacteriol*, 153(1), 163-8.
- Itoh, K., Chiba, T., Takahashi, S., Ishii, T., Igarashi, K., Katoh, Y., Oyake, T., Hayashi, N., Satoh, K., Hatayama, I., Yamamoto, M. and Nabeshima, Y. (1997) 'An Nrf2/small Maf heterodimer mediates the induction of phase II detoxifying enzyme genes through antioxidant response elements', *Biochem Biophys Res Commun*, 236(2), 313-22.
- Itoh, K., Wakabayashi, N., Katoh, Y., Ishii, T., Igarashi, K., Engel, J. D. and Yamamoto, M. (1999) 'Keap1 represses nuclear activation of antioxidant responsive elements by Nrf2 through binding to the amino-terminal Neh2 domain', *Genes Dev*, 13(1), 76-86.
- Itoh, K., Wakabayashi, N., Katoh, Y., Ishii, T., O'Connor, T. and Yamamoto, M. (2003) 'Keap1 regulates both cytoplasmic-nuclear shuttling and degradation of Nrf2 in response to electrophiles', *Genes Cells*, 8(4), 379-91.
- Jain, A., Lamark, T., Sjøttem, E., Larsen, K. B., Awuh, J. A., Overvatn, A., McMahon, M., Hayes, J. D. and Johansen, T. (2010) 'p62/SQSTM1 is a target gene for transcription factor NRF2 and creates a positive feedback loop by inducing antioxidant response element-driven gene transcription', *J Biol Chem*, 285(29), 22576-91.
- Jain, A. K. and Jaiswal, A. K. (2006) 'Phosphorylation of tyrosine 568 controls nuclear export of Nrf2', *J Biol Chem*, 281(17), 12132-42.
- Jain, A. K. and Jaiswal, A. K. (2007) 'GSK-3beta acts upstream of Fyn kinase in regulation of nuclear export and degradation of NF-E2 related factor 2', *J Biol Chem*, 282(22), 16502-10.

- Jakubikova, J., Sedlak, J., Bod'o, J. and Bao, Y. (2006) 'Effect of isothiocyanates on nuclear accumulation of NF-kappaB, Nrf2, and thioredoxin in caco-2 cells', *J Agric Food Chem*, 54(5), 1656-62.
- James, L. P., Mayeux, P. R. and Hinson, J. A. (2003) 'Acetaminophen-induced hepatotoxicity', *Drug Metab Dispos*, 31(12), 1499-506.
- Jaramillo, M. C. and Zhang, D. D. (2013) 'The emerging role of the Nrf2-Keap1 signaling pathway in cancer', *Genes Dev*, 27(20), 2179-91.
- Jefferys, D. B., Leakey, D., Lewis, J. A., Payne, S. and Rawlins, M. D. (1998) 'New active substances authorized in the United Kingdom between 1972 and 1994', *Br J Clin Pharmacol*, 45(2), 151-6.
- Jenkins, R. E., Kitteringham, N. R., Goldring, C. E., Dowdall, S. M., Hamlett, J., Lane, C. S., Boerma, J. S., Vermeulen, N. P. and Park, B. K. (2008) 'Glutathione-S-transferase pi as a model protein for the characterisation of chemically reactive metabolites', *Proteomics*, 8(2), 301-15.
- Jeong, W., Bae, S. H., Toledano, M. B. and Rhee, S. G. (2012) 'Role of sulfiredoxin as a regulator of peroxiredoxin function and regulation of its expression', *Free Radic Biol Med*, 53(3), 447-56.
- Jeyapaul, J. and Jaiswal, A. K. (2000) 'Nrf2 and c-Jun regulation of antioxidant response element (ARE)-mediated expression and induction of gamma-glutamylcysteine synthetase heavy subunit gene', *Biochem Pharmacol*, 59(11), 1433-9.
- Jiang, X., Kim, H. E., Shu, H., Zhao, Y., Zhang, H., Kofron, J., Donnelly, J., Burns, D., Ng, S. C., Rosenberg, S. and Wang, X. (2003) 'Distinctive roles of PHAP proteins and prothymosin-alpha in a death regulatory pathway', *Science*, 299(5604), 223-6.
- Jones, G., Willett, P., Glen, R. C., Leach, A. R. and Taylor, R. (1997) 'Development and validation of a genetic algorithm for flexible docking', *J Mol Biol*, 267(3), 727-48.
- Jung, H. J., Lee, C. O., Lee, K. T., Choi, J. and Park, H. J. (2004) 'Structure-activity relationship of oleanane disaccharides isolated from *Akebia quinata* versus cytotoxicity against cancer cells and NO inhibition', *Biol Pharm Bull*, 27(5), 744-7.
- Kalkhoven, E. (2004) 'CBP and p300: HATs for different occasions', *Biochem Pharmacol*, 68(6), 1145-55.
- Kang, M. I., Kobayashi, A., Wakabayashi, N., Kim, S. G. and Yamamoto, M. (2004) 'Scaffolding of Keap1 to the actin cytoskeleton controls the function of Nrf2 as key regulator of cytoprotective phase 2 genes', *Proc Natl Acad Sci U S A*, 101(7), 2046-51.
- Kaniuk, N. A., Kiraly, M., Bates, H., Vranic, M., Volchuk, A. and Brumell, J. H. (2007) 'Ubiquitinated-protein aggregates form in pancreatic beta-cells during diabetes-induced oxidative stress and are regulated by autophagy', *Diabetes*, 56(4), 930-9.
- Kaplowitz, N., Aw, T. Y. and Ookhtens, M. (1985) 'The regulation of hepatic glutathione', *Annu Rev Pharmacol Toxicol*, 25, 715-44.

- Karapetian, R. N., Evstafieva, A. G., Abaeva, I. S., Chichkova, N. V., Filonov, G. S., Rubtsov, Y. P., Sukhacheva, E. A., Melnikov, S. V., Schneider, U., Wanker, E. E. and Vartapetian, A. B. (2005) 'Nuclear oncoprotein prothymosin alpha is a partner of Keap1: implications for expression of oxidative stress-protecting genes', *Mol Cell Biol*, 25(3), 1089-99.
- Karetsou, Z., Kretsovali, A., Murphy, C., Tsolas, O. and Papamarcaki, T. (2002) 'Prothymosin alpha interacts with the CREB-binding protein and potentiates transcription', *EMBO Rep*, 3(4), 361-6.
- Kaspar, J. W. and Jaiswal, A. K. (2011) 'Tyrosine phosphorylation controls nuclear export of Fyn, allowing Nrf2 activation of cytoprotective gene expression', *FASEB J*, 25(3), 1076-87.
- Kataoka, K., Nishizawa, M. and Kawai, S. (1993) 'Structure-function analysis of the maf oncogene product, a member of the b-Zip protein family', *J Virol*, 67(4), 2133-41.
- Katoh, Y., Iida, K., Kang, M. I., Kobayashi, A., Mizukami, M., Tong, K. I., McMahon, M., Hayes, J. D., Itoh, K. and Yamamoto, M. (2005) 'Evolutionary conserved N-terminal domain of Nrf2 is essential for the Keap1-mediated degradation of the protein by proteasome', *Arch Biochem Biophys*, 433(2), 342-50.
- Katoh, Y., Itoh, K., Yoshida, E., Miyagishi, M., Fukamizu, A. and Yamamoto, M. (2001) 'Two domains of Nrf2 cooperatively bind CBP, a CREB binding protein, and synergistically activate transcription', *Genes Cells*, 6(10), 857-68.
- Kensler, T. W., Curphey, T. J., Maxiutenko, Y. and Roebuck, B. D. (2000) 'Chemoprotection by organosulfur inducers of phase 2 enzymes: dithiolethiones and dithiols', *Drug Metabol Drug Interact*, 17(1-4), 3-22.
- Keum, Y. S., Yu, S., Chang, P. P., Yuan, X., Kim, J. H., Xu, C., Han, J., Agarwal, A. and Kong, A. N. (2006) 'Mechanism of action of sulforaphane: inhibition of p38 mitogen-activated protein kinase isoforms contributing to the induction of antioxidant response element-mediated heme oxygenase-1 in human hepatoma HepG2 cells', *Cancer Res*, 66(17), 8804-13.
- Kiang, J. G. and Tsokos, G. C. (1998) 'Heat shock protein 70 kDa: molecular biology, biochemistry, and physiology', *Pharmacol Ther*, 80(2), 183-201.
- Kim, I., Rodriguez-Enriquez, S. and Lemasters, J. J. (2007) 'Selective degradation of mitochondria by mitophagy', *Arch Biochem Biophys*, 462(2), 245-53.
- Kim, J. E., You, D. J., Lee, C., Ahn, C., Seong, J. Y. and Hwang, J. I. (2010) 'Suppression of NF-kappaB signaling by KEAP1 regulation of IKKbeta activity through autophagic degradation and inhibition of phosphorylation', *Cell Signal*, 22(11), 1645-54.
- Kim, P. K., Hailey, D. W., Mullen, R. T. and Lippincott-Schwartz, J. (2008) 'Ubiquitin signals autophagic degradation of cytosolic proteins and peroxisomes', *Proc Natl Acad Sci U S A*, 105(52), 20567-74.

- Kim, Y. C., Masutani, H., Yamaguchi, Y., Itoh, K., Yamamoto, M. and Yodoi, J. (2001) 'Hemin-induced activation of the thioredoxin gene by Nrf2. A differential regulation of the antioxidant responsive element by a switch of its binding factors', *J Biol Chem*, 276(21), 18399-406.
- Kim, Y. C., Yamaguchi, Y., Kondo, N., Masutani, H. and Yodoi, J. (2003) 'Thioredoxin-dependent redox regulation of the antioxidant responsive element (ARE) in electrophile response', *Oncogene*, 22(12), 1860-5.
- Kim, Y. J., Ahn, J. Y., Liang, P., Ip, C., Zhang, Y. and Park, Y. M. (2007) 'Human prx1 gene is a target of Nrf2 and is up-regulated by hypoxia/reoxygenation: implication to tumor biology', *Cancer Res*, 67(2), 546-54.
- Kitteringham, N. R., Abdullah, A., Walsh, J., Randle, L., Jenkins, R. E., Sison, R., Goldring, C. E., Powell, H., Sanderson, C., Williams, S., Higgins, L., Yamamoto, M., Hayes, J. and Park, B. K. (2010) 'Proteomic analysis of Nrf2 deficient transgenic mice reveals cellular defence and lipid metabolism as primary Nrf2-dependent pathways in the liver', *J Proteomics*, 73(8), 1612-31.
- Kitteringham, N. R., Jenkins, R. E., Lane, C. S., Elliott, V. L. and Park, B. K. (2009) 'Multiple reaction monitoring for quantitative biomarker analysis in proteomics and metabolomics', *J Chromatogr B Analyt Technol Biomed Life Sci*, 877(13), 1229-39.
- Klomsiri, C., Nelson, K. J., Bechtold, E., Soito, L., Johnson, L. C., Lowther, W. T., Ryu, S. E., King, S. B., Furdui, C. M. and Poole, L. B. (2010) 'Use of dimedone-based chemical probes for sulfenic acid detection evaluation of conditions affecting probe incorporation into redox-sensitive proteins', *Methods Enzymol*, 473, 77-94.
- Kobayashi, A., Kang, M. I., Okawa, H., Ohtsuji, M., Zenke, Y., Chiba, T., Igarashi, K. and Yamamoto, M. (2004) 'Oxidative stress sensor Keap1 functions as an adaptor for Cul3-based E3 ligase to regulate proteasomal degradation of Nrf2', *Mol Cell Biol*, 24(16), 7130-9.
- Kobayashi, M., Li, L., Iwamoto, N., Nakajima-Takagi, Y., Kaneko, H., Nakayama, Y., Eguchi, M., Wada, Y., Kumagai, Y. and Yamamoto, M. (2009) 'The antioxidant defense system Keap1-Nrf2 comprises a multiple sensing mechanism for responding to a wide range of chemical compounds', *Mol Cell Biol*, 29(2), 493-502.
- Koen, Y. M., Yue, W., Galeva, N. A., Williams, T. D. and Hanzlik, R. P. (2006) 'Site-specific arylation of rat glutathione s-transferase A1 and A2 by bromobenzene metabolites in vivo', *Chem Res Toxicol*, 19(11), 1426-34.
- Komatsu, M., Kurokawa, H., Waguri, S., Taguchi, K., Kobayashi, A., Ichimura, Y., Sou, Y. S., Ueno, I., Sakamoto, A., Tong, K. I., Kim, M., Nishito, Y., Iemura, S., Natsume, T., Ueno, T., Kominami, E., Motohashi, H., Tanaka, K. and Yamamoto, M. (2010) 'The selective autophagy substrate p62 activates the stress responsive transcription factor Nrf2 through inactivation of Keap1', *Nat Cell Biol*, 12(3), 213-23.
- Konstantinopoulos, P. A., Spentzos, D., Fountzilas, E., Francoeur, N., Sanisetty, S., Grammatikos, A. P., Hecht, J. L. and Cannistra, S. A. (2011) 'Keap1 mutations and Nrf2 pathway activation in epithelial ovarian cancer', *Cancer Res*, 71(15), 5081-9.

- Korb, O., Stutzle, T. and Exner, T. E. (2009) 'Empirical scoring functions for advanced protein-ligand docking with PLANTS', *J Chem Inf Model*, 49(1), 84-96.
- Kumar, V., Kumar, S., Hassan, M., Wu, H., Thimmulappa, R. K., Kumar, A., Sharma, S. K., Parmar, V. S., Biswal, S. and Malhotra, S. V. (2011) 'Novel chalcone derivatives as potent Nrf2 activators in mice and human lung epithelial cells', *J Med Chem*, 54(12), 4147-59.
- Kwak, M. K., Egner, P. A., Dolan, P. M., Ramos-Gomez, M., Groopman, J. D., Itoh, K., Yamamoto, M. and Kensler, T. W. (2001a) 'Role of phase 2 enzyme induction in chemoprotection by dithiolethiones', *Mutat Res*, 480-481, 305-15.
- Kwak, M. K., Itoh, K., Yamamoto, M. and Kensler, T. W. (2002) 'Enhanced expression of the transcription factor Nrf2 by cancer chemopreventive agents: role of antioxidant response element-like sequences in the nrf2 promoter', *Mol Cell Biol*, 22(9), 2883-92.
- Kwak, M. K., Itoh, K., Yamamoto, M., Sutter, T. R. and Kensler, T. W. (2001b) 'Role of transcription factor Nrf2 in the induction of hepatic phase 2 and antioxidative enzymes in vivo by the cancer chemoprotective agent, 3H-1, 2-dimethiole-3-thione', *Mol Med*, 7(2), 135-45.
- Lau, A., Wang, X. J., Zhao, F., Villeneuve, N. F., Wu, T., Jiang, T., Sun, Z., White, E. and Zhang, D. D. (2010) 'A noncanonical mechanism of Nrf2 activation by autophagy deficiency: Direct interaction between keap1 and p62', *Molecular and Cellular Biology*, 30(13), 3275-3285.
- Lee, C. F., Paull, T. T. and Person, M. D. (2013) 'Proteome-wide detection and quantitative analysis of irreversible cysteine oxidation using long column UPLC-pSRM', *J Proteome Res*, 12(10), 4302-15.
- Lee, D. F., Kuo, H. P., Liu, M., Chou, C. K., Xia, W., Du, Y., Shen, J., Chen, C. T., Huo, L., Hsu, M. C., Li, C. W., Ding, Q., Liao, T. L., Lai, C. C., Lin, A. C., Chang, Y. H., Tsai, S. F., Li, L. Y. and Hung, M. C. (2009) 'KEAP1 E3 ligase-mediated downregulation of NF-kappaB signaling by targeting IKKbeta', *Mol Cell*, 36(1), 131-40.
- Lee, J. M., Li, J., Johnson, D. A., Stein, T. D., Kraft, A. D., Calkins, M. J., Jakel, R. J. and Johnson, J. A. (2005) 'Nrf2, a multi-organ protector?', *FASEB J*, 19(9), 1061-6.
- Lee, J. M., Moehlenkamp, J. D., Hanson, J. M. and Johnson, J. A. (2001) 'Nrf2-dependent activation of the antioxidant responsive element by tert-butylhydroquinone is independent of oxidative stress in IMR-32 human neuroblastoma cells', *Biochem Biophys Res Commun*, 280(1), 286-92.
- Lee, T. D., Yang, H., Whang, J. and Lu, S. C. (2005) 'Cloning and characterization of the human glutathione synthetase 5'-flanking region', *Biochem J*, 390(Pt 2), 521-8.
- Levonen, A. L., Landar, A., Ramachandran, A., Ceaser, E. K., Dickinson, D. A., Zanoni, G., Morrow, J. D. and Darley-Usmar, V. M. (2004) 'Cellular mechanisms of redox cell signalling: role of cysteine modification in controlling antioxidant defences in response to electrophilic lipid oxidation products', *Biochem J*, 378(Pt 2), 373-82.

- Lewis, K. N., Mele, J., Hayes, J. D. and Buffenstein, R. (2010) 'Nrf2, a guardian of healthspan and gatekeeper of species longevity', *Integr Comp Biol*, 50(5), 829-43.
- Li, J., Johnson, D., Calkins, M., Wright, L., Svendsen, C. and Johnson, J. (2005) 'Stabilization of Nrf2 by tBHQ confers protection against oxidative stress-induced cell death in human neural stem cells', *Toxicol Sci*, 83(2), 313-28.
- Li, N., Muthusamy, S., Liang, R., Sarojini, H. and Wang, E. (2011) 'Increased expression of miR-34a and miR-93 in rat liver during aging, and their impact on the expression of Mgst1 and Sirt1', *Mech Ageing Dev*, 132(3), 75-85.
- Li, W., Liu, H., Zhou, J. S., Cao, J. F., Zhou, X. B., Choi, A. M., Chen, Z. H. and Shen, H. H. (2012) 'Caveolin-1 inhibits expression of antioxidant enzymes through direct interaction with nuclear erythroid 2 p45-related factor-2 (Nrf2)', *J Biol Chem*, 287(25), 20922-30.
- Li, W., Yu, S. W. and Kong, A. N. (2006) 'Nrf2 possesses a redox-sensitive nuclear exporting signal in the Neh5 transactivation domain', *J Biol Chem*, 281(37), 27251-63.
- Li, Y., Paonessa, J. D. and Zhang, Y. (2012) 'Mechanism of chemical activation of Nrf2', *PLoS One*, 7(4), e35122.
- Liby, K. T. and Sporn, M. B. (2012) 'Synthetic oleanane triterpenoids: multifunctional drugs with a broad range of applications for prevention and treatment of chronic disease', *Pharmacol Rev*, 64(4), 972-1003.
- Liby, K. T., Yore, M. M. and Sporn, M. B. (2007) 'Triterpenoids and rexinoids as multifunctional agents for the prevention and treatment of cancer', *Nat Rev Cancer*, 7(5), 357-69.
- Liebler, D. C., Hong, F., Sekhar, K. R., Freeman, M. L. and James, C. F. (2006) 'Chapter 3 Site-Specific Modification of the Electrophile Sensor Protein Keap1 and Activation of Nrf2-Dependent Gene Expression' in *Advances in Molecular Toxicology*, Elsevier, 65-83.
- Lin, C. W., Wu, M. J., Liu, I. Y., Su, J. D. and Yen, J. H. (2010) 'Neurotrophic and cytoprotective action of luteolin in PC12 cells through ERK-dependent induction of Nrf2-driven HO-1 expression', *J Agric Food Chem*, 58(7), 4477-86.
- Ling, H., Fabbri, M. and Calin, G. A. (2013) 'MicroRNAs and other non-coding RNAs as targets for anticancer drug development', *Nat Rev Drug Discov*, 12(11), 847-65.
- Linker, R. A., Lee, D. H., Ryan, S., van Dam, A. M., Conrad, R., Bista, P., Zeng, W., Hronowsky, X., Buko, A., Chollate, S., Ellrichmann, G., Bruck, W., Dawson, K., Goelz, S., Wiese, S., Scannevin, R. H., Lukashev, M. and Gold, R. (2011) 'Fumaric acid esters exert neuroprotective effects in neuroinflammation via activation of the Nrf2 antioxidant pathway', *Brain*, 134(Pt 3), 678-92.
- Lister, A., Nedjadi, T., Kitteringham, N. R., Campbell, F., Costello, E., Lloyd, B., Copple, I. M., Williams, S., Owen, A., Neoptolemos, J. P., Goldring, C. E. and Park, B. K. (2011) 'Nrf2 is overexpressed in pancreatic cancer: implications for cell proliferation and therapy', *Mol Cancer*, 10, 37.

- Lo, S. C. and Hannink, M. (2006) 'PGAM5, a Bcl-XL-interacting protein, is a novel substrate for the redox-regulated Keap1-dependent ubiquitin ligase complex', *J Biol Chem*, 281(49), 37893-903.
- Lo, S. C. and Hannink, M. (2008) 'PGAM5 tethers a ternary complex containing Keap1 and Nrf2 to mitochondria', *Exp Cell Res*, 314(8), 1789-803.
- Lo, S. C., Li, X., Henzl, M. T., Beamer, L. J. and Hannink, M. (2006) 'Structure of the Keap1:Nrf2 interface provides mechanistic insight into Nrf2 signaling', *EMBO J*, 25(15), 3605-17.
- Locatelli, F., Pozzoni, P., Tentori, F. and del Vecchio, L. (2003) 'Epidemiology of cardiovascular risk in patients with chronic kidney disease', *Nephrol Dial Transplant*, 18 Suppl 7, vii2-9.
- Lou, H., Du, S., Ji, Q. and Stolz, A. (2006) 'Induction of AKR1C2 by phase II inducers: identification of a distal consensus antioxidant response element regulated by NRF2', *Mol Pharmacol*, 69(5), 1662-72.
- Luo, D., Smith, S. W. and Anderson, B. D. (2005) 'Kinetics and mechanism of the reaction of cysteine and hydrogen peroxide in aqueous solution', *J Pharm Sci*, 94(2), 304-16.
- Luo, Y., Egger, A. L., Liu, D., Liu, G., Mesecar, A. D. and van Breemen, R. B. (2007) 'Sites of alkylation of human Keap1 by natural chemoprevention agents', *J Am Soc Mass Spectrom*, 18(12), 2226-32.
- Ma, J., Cai, H., Wu, T., Sobhian, B., Huo, Y., Alcivar, A., Mehta, M., Cheung, K. L., Ganesan, S., Kong, A. N., Zhang, D. D. and Xia, B. (2012) 'PALB2 interacts with KEAP1 to promote NRF2 nuclear accumulation and function', *Mol Cell Biol*, 32(8), 1506-17.
- Macari, E. R. and Lowrey, C. H. (2011) 'Induction of human fetal hemoglobin via the NRF2 antioxidant response signaling pathway', *Blood*, 117(22), 5987-97.
- Magesh, S., Chen, Y. and Hu, L. (2012) 'Small molecule modulators of Keap1-Nrf2-ARE pathway as potential preventive and therapeutic agents', *Med Res Rev*, 32(4), 687-726.
- Maher, J. M., Dieter, M. Z., Aleksunes, L. M., Slitt, A. L., Guo, G., Tanaka, Y., Scheffer, G. L., Chan, J. Y., Manautou, J. E., Chen, Y., Dalton, T. P., Yamamoto, M. and Klaassen, C. D. (2007) 'Oxidative and electrophilic stress induces multidrug resistance-associated protein transporters via the nuclear factor-E2-related factor-2 transcriptional pathway', *Hepatology*, 46(5), 1597-610.
- Malhotra, D., Portales-Casamar, E., Singh, A., Srivastava, S., Arenillas, D., Happel, C., Shyr, C., Wakabayashi, N., Kensler, T. W., Wasserman, W. W. and Biswal, S. (2010) 'Global mapping of binding sites for Nrf2 identifies novel targets in cell survival response through ChIP-Seq profiling and network analysis', *Nucleic Acids Res*, 38(17), 5718-34.
- Manrow, R. E., Sburlati, A. R., Hanover, J. A. and Berger, S. L. (1991) 'Nuclear targeting of prothymosin alpha', *J Biol Chem*, 266(6), 3916-24.

- Marino, S. M. and Gladyshev, V. N. (2012) 'Analysis and functional prediction of reactive cysteine residues', *J Biol Chem*, 287(7), 4419-25.
- Martini, P. G., Delage-Mourroux, R., Kraichely, D. M. and Katzenellenbogen, B. S. (2000) 'Prothymosin alpha selectively enhances estrogen receptor transcriptional activity by interacting with a repressor of estrogen receptor activity', *Mol Cell Biol*, 20(17), 6224-32.
- McMahon, M., Itoh, K., Yamamoto, M., Chanas, S. A., Henderson, C. J., McLellan, L. I., Wolf, C. R., Cavin, C. and Hayes, J. D. (2001) 'The Cap'n'Collar basic leucine zipper transcription factor Nrf2 (NF-E2 p45-related factor 2) controls both constitutive and inducible expression of intestinal detoxification and glutathione biosynthetic enzymes', *Cancer Res*, 61(8), 3299-307.
- McMahon, M., Itoh, K., Yamamoto, M. and Hayes, J. D. (2003) 'Keap1-dependent proteasomal degradation of transcription factor Nrf2 contributes to the negative regulation of antioxidant response element-driven gene expression', *J Biol Chem*, 278(24), 21592-600.
- McMahon, M., Lamont, D. J., Beattie, K. A. and Hayes, J. D. (2010) 'Keap1 perceives stress via three sensors for the endogenous signaling molecules nitric oxide, zinc, and alkenals', *Proc Natl Acad Sci U S A*, 107(44), 18838-43.
- McMahon, M., Thomas, N., Itoh, K., Yamamoto, M. and Hayes, J. D. (2004) 'Redox-regulated turnover of Nrf2 is determined by at least two separate protein domains, the redox-sensitive Neh2 degron and the redox-insensitive Neh6 degron', *J Biol Chem*, 279(30), 31556-67.
- McMahon, M., Thomas, N., Itoh, K., Yamamoto, M. and Hayes, J. D. (2006) 'Dimerization of substrate adaptors can facilitate cullin-mediated ubiquitylation of proteins by a "tethering" mechanism: a two-site interaction model for the Nrf2-Keap1 complex', *J Biol Chem*, 281(34), 24756-68.
- Miao, W., Hu, L., Scrivens, P. J. and Batist, G. (2005) 'Transcriptional regulation of NF-E2 p45-related factor (NRF2) expression by the aryl hydrocarbon receptor-xenobiotic response element signaling pathway: direct cross-talk between phase I and II drug-metabolizing enzymes', *J Biol Chem*, 280(21), 20340-8.
- Miseta, A. and Csutora, P. (2000) 'Relationship between the occurrence of cysteine in proteins and the complexity of organisms', *Mol Biol Evol*, 17(8), 1232-9.
- Mitsuishi, Y., Taguchi, K., Kawatani, Y., Shibata, T., Nukiwa, T., Aburatani, H., Yamamoto, M. and Motohashi, H. (2012) 'Nrf2 redirects glucose and glutamine into anabolic pathways in metabolic reprogramming', *Cancer Cell*, 22(1), 66-79.
- Moi, P., Chan, K., Asunis, I., Cao, A. and Kan, Y. W. (1994) 'Isolation of NF-E2-related factor 2 (Nrf2), a NF-E2-like basic leucine zipper transcriptional activator that binds to the tandem NF-E2/AP1 repeat of the beta-globin locus control region', *Proc Natl Acad Sci U S A*, 91(21), 9926-30.

- Moinova, H. R. and Mulcahy, R. T. (1999) 'Up-regulation of the human gamma-glutamylcysteine synthetase regulatory subunit gene involves binding of Nrf-2 to an electrophile responsive element', *Biochem Biophys Res Commun*, 261(3), 661-8.
- Moore, S. F., van den Bosch, M. T., Hunter, R. W., Sakamoto, K., Poole, A. W. and Hers, I. (2013) 'Dual regulation of glycogen synthase kinase 3 (GSK3)alpha/beta by protein kinase C (PKC)alpha and Akt promotes thrombin-mediated integrin alphaIIb beta3 activation and granule secretion in platelets', *J Biol Chem*, 288(6), 3918-28.
- Motohashi, H., O'Connor, T., Katsuoka, F., Engel, J. D. and Yamamoto, M. (2002) 'Integration and diversity of the regulatory network composed of Maf and CNC families of transcription factors', *Gene*, 294(1-2), 1-12.
- Motohashi, H. and Yamamoto, M. (2004) 'Nrf2-Keap1 defines a physiologically important stress response mechanism', *Trends Mol Med*, 10(11), 549-57.
- Muller, P. A. and Vousden, K. H. (2014) 'Mutant p53 in cancer: new functions and therapeutic opportunities', *Cancer Cell*, 25(3), 304-17.
- Nel, A., Xia, T., Madler, L. and Li, N. (2006) 'Toxic potential of materials at the nanolevel', *Science*, 311(5761), 622-7.
- Nelson, K. J., Klomsiri, C., Codreanu, S. G., Soito, L., Liebler, D. C., Rogers, L. C., Daniel, L. W. and Poole, L. B. (2010) 'Use of dimedone-based chemical probes for sulfenic acid detection methods to visualize and identify labeled proteins', *Methods Enzymol*, 473, 95-115.
- Nelson, S. K., Bose, S. K., Grunwald, G. K., Myhill, P. and McCord, J. M. (2006) 'The induction of human superoxide dismutase and catalase in vivo: a fundamentally new approach to antioxidant therapy', *Free Radic Biol Med*, 40(2), 341-7.
- Newsome, P. N., Plevris, J. N., Nelson, L. J. and Hayes, P. C. (2000) 'Animal models of fulminant hepatic failure: a critical evaluation', *Liver Transpl*, 6(1), 21-31.
- Nguyen, T., Huang, H. C. and Pickett, C. B. (2000) 'Transcriptional regulation of the antioxidant response element. Activation by Nrf2 and repression by MafK', *J Biol Chem*, 275(20), 15466-73.
- Nguyen, T., Sherratt, P. J., Huang, H. C., Yang, C. S. and Pickett, C. B. (2003a) 'Increased protein stability as a mechanism that enhances Nrf2-mediated transcriptional activation of the antioxidant response element. Degradation of Nrf2 by the 26 S proteasome', *J Biol Chem*, 278(7), 4536-41.
- Nguyen, T., Sherratt, P. J. and Pickett, C. B. (2003b) 'Regulatory mechanisms controlling gene expression mediated by the antioxidant response element', *Annu Rev Pharmacol Toxicol*, 43, 233-60.
- Nioi, P. and Hayes, J. D. (2004) 'Contribution of NAD(P)H:quinone oxidoreductase 1 to protection against carcinogenesis, and regulation of its gene by the Nrf2 basic-region leucine zipper and the arylhydrocarbon receptor basic helix-loop-helix transcription factors', *Mutat Res*, 555(1-2), 149-71.

- Nioi, P., McMahon, M., Itoh, K., Yamamoto, M. and Hayes, J. D. (2003) 'Identification of a novel Nrf2-regulated antioxidant response element (ARE) in the mouse NAD(P)H:quinone oxidoreductase 1 gene: reassessment of the ARE consensus sequence', *Biochem J*, 374(Pt 2), 337-48.
- Nioi, P., Nguyen, T., Sherratt, P. J. and Pickett, C. B. (2005) 'The carboxy-terminal Neh3 domain of Nrf2 is required for transcriptional activation', *Mol Cell Biol*, 25(24), 10895-906.
- Nishinaka, T. and Yabe-Nishimura, C. (2005) 'Transcription factor Nrf2 regulates promoter activity of mouse aldose reductase (AKR1B3) gene', *J Pharmacol Sci*, 97(1), 43-51.
- Nishino, H., Nishino, A., Takayasu, J., Hasegawa, T., Iwashima, A., Hirabayashi, K., Iwata, S. and Shibata, S. (1988) 'Inhibition of the tumor-promoting action of 12-O-tetradecanoylphorbol-13-acetate by some oleanane-type triterpenoid compounds', *Cancer Res*, 48(18), 5210-5.
- Niture, S. K., Jain, A. K. and Jaiswal, A. K. (2009) 'Antioxidant-induced modification of INrf2 cysteine 151 and PKC-delta-mediated phosphorylation of Nrf2 serine 40 are both required for stabilization and nuclear translocation of Nrf2 and increased drug resistance', *J Cell Sci*, 122(Pt 24), 4452-64.
- Niture, S. K. and Jaiswal, A. K. (2009) 'Prothymosin-alpha mediates nuclear import of the INrf2/Cul3 Rbx1 complex to degrade nuclear Nrf2', *J Biol Chem*, 284(20), 13856-68.
- Nordberg, J. and Arner, E. S. (2001) 'Reactive oxygen species, antioxidants, and the mammalian thioredoxin system', *Free Radic Biol Med*, 31(11), 1287-312.
- Numazawa, S., Ishikawa, M., Yoshida, A., Tanaka, S. and Yoshida, T. (2003) 'Atypical protein kinase C mediates activation of NF-E2-related factor 2 in response to oxidative stress', *Am J Physiol Cell Physiol*, 285(2), C334-42.
- Ogryzko, V. V., Schiltz, R. L., Russanova, V., Howard, B. H. and Nakatani, Y. (1996) 'The transcriptional coactivators p300 and CBP are histone acetyltransferases', *Cell*, 87(5), 953-9.
- Okawa, H., Motohashi, H., Kobayashi, A., Aburatani, H., Kensler, T. W. and Yamamoto, M. (2006) 'Hepatocyte-specific deletion of the keap1 gene activates Nrf2 and confers potent resistance against acute drug toxicity', *Biochem Biophys Res Commun*, 339(1), 79-88.
- Oliveros, J. C. (2007) 'VENNY. An interactive tool for comparing lists with Venn Diagrams', [online], available: [accessed
- Padmanabhan, B., Tong, K. I., Ohta, T., Nakamura, Y., Scharlock, M., Ohtsuji, M., Kang, M. I., Kobayashi, A., Yokoyama, S. and Yamamoto, M. (2006) 'Structural basis for defects of Keap1 activity provoked by its point mutations in lung cancer', *Mol Cell*, 21(5), 689-700.
- Paget, M. S. and Buttner, M. J. (2003) 'Thiol-based regulatory switches', *Annu Rev Genet*, 37, 91-121.

- Pankiv, S., Clausen, T. H., Lamark, T., Brech, A., Bruun, J. A., Outzen, H., Overvatn, A., Bjorkoy, G. and Johansen, T. (2007) 'p62/SQSTM1 binds directly to Atg8/LC3 to facilitate degradation of ubiquitinated protein aggregates by autophagy', *J Biol Chem*, 282(33), 24131-45.
- Papp, D., Lenti, K., Modos, D., Fazekas, D., Dul, Z., Turei, D., Foldvari-Nagy, L., Nussinov, R., Csermely, P. and Korcsmaros, T. (2012) 'The NRF2-related interactome and regulome contain multifunctional proteins and fine-tuned autoregulatory loops', *FEBS Lett*, 586(13), 1795-802.
- Park, B. K. (1986) 'Metabolic basis of adverse drug reactions', *Journal of the Royal College of Physicians of London*, 20(3), 195-200.
- Park, B. K., Copple, I. M., Goldring, C. E. and Kitteringham, N. R. (2010) 'The Keap-Nrf2 Cellular Defence Pathway: Mechanisms of Regulation and Role in Protection Against Drug-Induced Toxicity', *Handbook of Experimental Pharmacology- Adverse Drug Reactions*, 196, 233-266.
- Park, B. K., Kitteringham, N. R., Maggs, J. L., Pirmohamed, M. and Williams, D. P. (2005) 'The role of metabolic activation in drug-induced hepatotoxicity', *Annu Rev Pharmacol Toxicol*, 45, 177-202.
- Park, E. Y. and Rho, H. M. (2002) 'The transcriptional activation of the human copper/zinc superoxide dismutase gene by 2,3,7,8-tetrachlorodibenzo-p-dioxin through two different regulator sites, the antioxidant responsive element and xenobiotic responsive element', *Mol Cell Biochem*, 240(1-2), 47-55.
- Pergola, P. E., Krauth, M., Huff, J. W., Ferguson, D. A., Ruiz, S., Meyer, C. J. and Warnock, D. G. (2011a) 'Effect of bardoxolone methyl on kidney function in patients with T2D and Stage 3b-4 CKD', *Am J Nephrol*, 33(5), 469-76.
- Pergola, P. E., Raskin, P., Toto, R. D., Meyer, C. J., Huff, J. W., Grossman, E. B., Krauth, M., Ruiz, S., Audhya, P., Christ-Schmidt, H., Wittes, J., Warnock, D. G. and Investigators, B. S. (2011b) 'Bardoxolone methyl and kidney function in CKD with type 2 diabetes', *N Engl J Med*, 365(4), 327-36.
- Petzer, J. P., Navamal, M., Johnson, J. K., Kwak, M. K., Kensler, T. W. and Fishbein, J. C. (2003) 'Phase 2 enzyme induction by the major metabolite of oltipraz', *Chem Res Toxicol*, 16(11), 1463-9.
- Phillips, D. R., Rasbery, J. M., Bartel, B. and Matsuda, S. P. (2006) 'Biosynthetic diversity in plant triterpene cyclization', *Curr Opin Plant Biol*, 9(3), 305-14.
- Pi, J., Bai, Y., Reece, J. M., Williams, J., Liu, D., Freeman, M. L., Fahl, W. E., Shugar, D., Liu, J., Qu, W., Collins, S. and Waalkes, M. P. (2007) 'Molecular mechanism of human Nrf2 activation and degradation: role of sequential phosphorylation by protein kinase CK2', *Free Radic Biol Med*, 42(12), 1797-806.
- Pi, J., Qu, W., Reece, J. M., Kumagai, Y. and Waalkes, M. P. (2003) 'Transcription factor Nrf2 activation by inorganic arsenic in cultured keratinocytes: involvement of hydrogen peroxide', *Exp Cell Res*, 290(2), 234-45.

- Pillay, C. S., Hofmeyr, J. H., Olivier, B. G., Snoep, J. L. and Rohwer, J. M. (2009) 'Enzymes or redox couples? The kinetics of thioredoxin and glutaredoxin reactions in a systems biology context', *Biochem J*, 417(1), 269-75.
- Pirmohamed, M., Breckenridge, A. M., Kitteringham, N. R. and Park, B. K. (1998) 'Adverse drug reactions', *BMJ*, 316(7140), 1295-8.
- Pompella, A., Visvikis, A., Paolicchi, A., De Tata, V. and Casini, A. F. (2003) 'The changing faces of glutathione, a cellular protagonist', *Biochem Pharmacol*, 66(8), 1499-503.
- Prester, T., Holtzclaw, W. D., Zhang, Y. and Talalay, P. (1993) 'Chemical and molecular regulation of enzymes that detoxify carcinogens', *Proc Natl Acad Sci U S A*, 90(7), 2965-9.
- Qureshi, M. M., McClure, W. C., Arevalo, N. L., Rabon, R. E., Mohr, B., Bose, S. K., McCord, J. M. and Tseng, B. S. (2010) 'The Dietary Supplement Protandim Decreases Plasma Osteopontin and Improves Markers of Oxidative Stress in Muscular Dystrophy Mdx Mice', *J Diet Suppl*, 7(2), 159-178.
- Rachakonda, G., Xiong, Y., Sekhar, K. R., Stamer, S. L., Liebler, D. C. and Freeman, M. L. (2008) 'Covalent modification at Cys151 dissociates the electrophile sensor Keap1 from the ubiquitin ligase CUL3', *Chem Res Toxicol*, 21(3), 705-10.
- Rada, P., Rojo, A. I., Chowdhry, S., McMahon, M., Hayes, J. D. and Cuadrado, A. (2011) 'SCF/ β -TrCP promotes glycogen synthase kinase 3-dependent degradation of the Nrf2 transcription factor in a Keap1-independent manner', *Mol Cell Biol*, 31(6), 1121-33.
- Ramos-Gomez, M., Kwak, M. K., Dolan, P. M., Itoh, K., Yamamoto, M., Talalay, P. and Kensler, T. W. (2001) 'Sensitivity to carcinogenesis is increased and chemoprotective efficacy of enzyme inducers is lost in nrf2 transcription factor-deficient mice', *Proc Natl Acad Sci U S A*, 98(6), 3410-5.
- Ramsey, C. P., Glass, C. A., Montgomery, M. B., Lindl, K. A., Ritson, G. P., Chia, L. A., Hamilton, R. L., Chu, C. T. and Jordan-Sciutto, K. L. (2007) 'Expression of Nrf2 in neurodegenerative diseases', *J Neuropathol Exp Neurol*, 66(1), 75-85.
- Rangasamy, T., Guo, J., Mitzner, W. A., Roman, J., Singh, A., Fryer, A. D., Yamamoto, M., Kensler, T. W., Tuder, R. M., Georas, S. N. and Biswal, S. (2005) 'Disruption of Nrf2 enhances susceptibility to severe airway inflammation and asthma in mice', *J Exp Med*, 202(1), 47-59.
- Ren, D., Villeneuve, N. F., Jiang, T., Wu, T., Lau, A., Toppin, H. A. and Zhang, D. D. (2011) 'Brusatol enhances the efficacy of chemotherapy by inhibiting the Nrf2-mediated defense mechanism', *Proc Natl Acad Sci U S A*, 108(4), 1433-8.
- Rojo, A. I., Medina-Campos, O. N., Rada, P., Zuniga-Toala, A., Lopez-Gazcon, A., Espada, S., Pedraza-Chaverri, J. and Cuadrado, A. (2012) 'Signaling pathways activated by the phytochemical nordihydroguaiaretic acid contribute to a Keap1-independent regulation of Nrf2 stability: Role of glycogen synthase kinase-3', *Free Radic Biol Med*, 52(2), 473-87.

- Roth, S. Y., Denu, J. M. and Allis, C. D. (2001) 'Histone acetyltransferases', *Annu Rev Biochem*, 70, 81-120.
- Russo, M. W., Galanko, J. A., Shrestha, R., Fried, M. W. and Watkins, P. (2004) 'Liver transplantation for acute liver failure from drug induced liver injury in the United States', *Liver Transpl*, 10(8), 1018-23.
- Sakai, Y., Oku, M., van der Klei, I. J. and Kiel, J. A. (2006) 'Pexophagy: autophagic degradation of peroxisomes', *Biochim Biophys Acta*, 1763(12), 1767-75.
- Salazar, M., Rojo, A. I., Velasco, D., de Sagarra, R. M. and Cuadrado, A. (2006) 'Glycogen synthase kinase-3beta inhibits the xenobiotic and antioxidant cell response by direct phosphorylation and nuclear exclusion of the transcription factor Nrf2', *J Biol Chem*, 281(21), 14841-51.
- Sali, A. and Blundell, T. L. (1993) 'Comparative protein modelling by satisfaction of spatial restraints', *J Mol Biol*, 234(3), 779-815.
- Sangokoya, C., Telen, M. J. and Chi, J. T. (2010) 'microRNA miR-144 modulates oxidative stress tolerance and associates with anemia severity in sickle cell disease', *Blood*, 116(20), 4338-48.
- Sedlak, T. W., Saleh, M., Higginson, D. S., Paul, B. D., Juluri, K. R. and Snyder, S. H. (2009) 'Bilirubin and glutathione have complementary antioxidant and cytoprotective roles', *Proc Natl Acad Sci U S A*, 106(13), 5171-6.
- Sekhar, K. R., Soltaninassab, S. R., Borrelli, M. J., Xu, Z. Q., Meredith, M. J., Domann, F. E. and Freeman, M. L. (2000) 'Inhibition of the 26S proteasome induces expression of GLCLC, the catalytic subunit for gamma-glutamylcysteine synthetase', *Biochem Biophys Res Commun*, 270(1), 311-7.
- Semple, J. I., Prime, G., Wallis, L. J., Sanderson, C. M. and Markie, D. (2005) 'Two-hybrid reporter vectors for gap repair cloning', *Biotechniques*, 38(6), 927-34.
- Sharon, M., Taverner, T., Ambroggio, X. I., Deshaies, R. J. and Robinson, C. V. (2006) 'Structural organization of the 19S proteasome lid: insights from MS of intact complexes', *PLoS Biol*, 4(8), e267.
- Shaulian, E. and Karin, M. (2002) 'AP-1 as a regulator of cell life and death', *Nat Cell Biol*, 4(5), E131-6.
- Shelton, L. M., Park, B. K. and Copple, I. M. (2013) 'Role of Nrf2 in protection against acute kidney injury', *Kidney Int*, 84(6), 1090-5.
- Shilov, I. V., Seymour, S. L., Patel, A. A., Loboda, A., Tang, W. H., Keating, S. P., Hunter, C. L., Nuwaysir, L. M. and Schaeffer, D. A. (2007) 'The Paragon Algorithm, a next generation search engine that uses sequence temperature values and feature probabilities to identify peptides from tandem mass spectra', *Mol Cell Proteomics*, 6(9), 1638-55.

- Shimoyama, Y., Mitsuda, Y., Tsuruta, Y., Hamajima, N. and Niwa, T. (2014) 'Polymorphism of Nrf2, an antioxidative gene, is associated with blood pressure and cardiovascular mortality in hemodialysis patients', *Int J Med Sci*, 11(7), 726-31.
- Shin, N. Y., Liu, Q., Stamer, S. L. and Liebler, D. C. (2007) 'Protein targets of reactive electrophiles in human liver microsomes', *Chem Res Toxicol*, 20(6), 859-67.
- Singh, A., Bodas, M., Wakabayashi, N., Bunz, F. and Biswal, S. (2010) 'Gain of Nrf2 function in non-small-cell lung cancer cells confers radioresistance', *Antioxid Redox Signal*, 13(11), 1627-37.
- Singh, A., Rangasamy, T., Thimmulappa, R. K., Lee, H., Osburn, W. O., Brigelius-Flohe, R., Kensler, T. W., Yamamoto, M. and Biswal, S. (2006) 'Glutathione peroxidase 2, the major cigarette smoke-inducible isoform of GPX in lungs, is regulated by Nrf2', *Am J Respir Cell Mol Biol*, 35(6), 639-50.
- Singh, G. B., Singh, S., Bani, S., Gupta, B. D. and Banerjee, S. K. (1992) 'Anti-inflammatory activity of oleanolic acid in rats and mice', *J Pharm Pharmacol*, 44(5), 456-8.
- Smith, P. K., Krohn, R. I., Hermanson, G. T., Mallia, A. K., Gartner, F. H., Provenzano, M. D., Fujimoto, E. K., Goeke, N. M., Olson, B. J. and Klenk, D. C. (1985) 'Measurement of protein using bicinchoninic acid', *Anal Biochem*, 150(1), 76-85.
- Snyder, G. H., Cennerazzo, M. J., Karalis, A. J. and Field, D. (1981) 'Electrostatic influence of local cysteine environments on disulfide exchange kinetics', *Biochemistry*, 20(23), 6509-19.
- Sporn, M. B. and Liby, K. T. (2012) 'NRF2 and cancer: the good, the bad and the importance of context', *Nat Rev Cancer*, 12(8), 564-71.
- Stadhouders, R., Aktuna, S., Thongjuea, S., Aghajani-refah, A., Pourfarzad, F., van Ijcken, W., Lenhard, B., Rooks, H., Best, S., Menzel, S., Grosveld, F., Thein, S. L. and Soler, E. (2014) 'HBS1L-MYB intergenic variants modulate fetal hemoglobin via long-range MYB enhancers', *J Clin Invest*, 124(4), 1699-710.
- Stich, T. M. (1990) 'Determination of protein covalently bound to agarose supports using bicinchoninic acid', *Anal Biochem*, 191(2), 343-6.
- Strachan, G. D., Morgan, K. L., Otis, L. L., Caltagarone, J., Gittis, A., Bowser, R. and Jordan-Sciutto, K. L. (2004) 'Fetal Alz-50 clone 1 interacts with the human orthologue of the Kelch-like ECH-associated protein', *Biochemistry*, 43(38), 12113-22.
- Sun, Z., Chin, Y. E. and Zhang, D. D. (2009) 'Acetylation of Nrf2 by p300/CBP augments promoter-specific DNA binding of Nrf2 during the antioxidant response', *Mol Cell Biol*, 29(10), 2658-72.
- Sun, Z., Zhang, S., Chan, J. Y. and Zhang, D. D. (2007) 'Keap1 controls postinduction repression of the Nrf2-mediated antioxidant response by escorting nuclear export of Nrf2', *Mol Cell Biol*, 27(18), 6334-49.
- Suzuki, T., Shibata, T., Takaya, K., Shiraiishi, K., Kohno, T., Kunitoh, H., Tsuta, K., Furuta, K., Goto, K., Hosoda, F., Sakamoto, H., Motohashi, H. and Yamamoto, M. (2013)

- 'Regulatory nexus of synthesis and degradation deciphers cellular Nrf2 expression levels', *Mol Cell Biol*, 33(12), 2402-12.
- Taguchi, K., Fujikawa, N., Komatsu, M., Ishii, T., Unno, M., Akaike, T., Motohashi, H. and Yamamoto, M. (2012) 'Keap1 degradation by autophagy for the maintenance of redox homeostasis', *Proc Natl Acad Sci U S A*, 109(34), 13561-6.
- Takaya, K., Suzuki, T., Motohashi, H., Onodera, K., Satomi, S., Kensler, T. W. and Yamamoto, M. (2012) 'Validation of the multiple sensor mechanism of the Keap1-Nrf2 system', *Free Radic Biol Med*, 53(4), 817-27.
- Takei, Y. and Tsujimoto, G. (1998) 'Identification of a novel MCM3-associated protein that facilitates MCM3 nuclear localization', *J Biol Chem*, 273(35), 22177-80.
- Tamai, K., Satoh, K., Tsuchida, S., Hatayama, I., Maki, T. and Sato, K. (1990) 'Specific inactivation of glutathione S-transferases in class Pi by SH-modifiers', *Biochem Biophys Res Commun*, 167(1), 331-8.
- Tang, X., Wang, H., Fan, L., Wu, X., Xin, A., Ren, H. and Wang, X. J. (2011) 'Luteolin inhibits Nrf2 leading to negative regulation of the Nrf2/ARE pathway and sensitization of human lung carcinoma A549 cells to therapeutic drugs', *Free Radic Biol Med*, 50(11), 1599-609.
- Tarumoto, T., Nagai, T., Ohmine, K., Miyoshi, T., Nakamura, M., Kondo, T., Mitsugi, K., Nakano, S., Muroi, K., Komatsu, N. and Ozawa, K. (2004) 'Ascorbic acid restores sensitivity to imatinib via suppression of Nrf2-dependent gene expression in the imatinib-resistant cell line', *Exp Hematol*, 32(4), 375-81.
- Theodore, M., Kawai, Y., Yang, J., Kleshchenko, Y., Reddy, S. P., Villalta, F. and Arinze, I. J. (2008) 'Multiple nuclear localization signals function in the nuclear import of the transcription factor Nrf2', *J Biol Chem*, 283(14), 8984-94.
- Thimmulappa, R. K., Mai, K. H., Srisuma, S., Kensler, T. W., Yamamoto, M. and Biswal, S. (2002) 'Identification of Nrf2-regulated genes induced by the chemopreventive agent sulforaphane by oligonucleotide microarray', *Cancer Res*, 62(18), 5196-203.
- Thornton, T. M., Pedraza-Alva, G., Deng, B., Wood, C. D., Aronshtam, A., Clements, J. L., Sabio, G., Davis, R. J., Matthews, D. E., Doble, B. and Rincon, M. (2008) 'Phosphorylation by p38 MAPK as an alternative pathway for GSK3beta inactivation', *Science*, 320(5876), 667-70.
- Thrower, J. S., Hoffman, L., Rechsteiner, M. and Pickart, C. M. (2000) 'Recognition of the polyubiquitin proteolytic signal', *EMBO J*, 19(1), 94-102.
- Tirumalai, R., Rajesh Kumar, T., Mai, K. H. and Biswal, S. (2002) 'Acrolein causes transcriptional induction of phase II genes by activation of Nrf2 in human lung type II epithelial (A549) cells', *Toxicol Lett*, 132(1), 27-36.
- Tomobe, K., Shinozuka, T., Kuroiwa, M. and Nomura, Y. (2012) 'Age-related changes of Nrf2 and phosphorylated GSK-3beta in a mouse model of accelerated aging (SAMP8)', *Arch Gerontol Geriatr*, 54(2), e1-7.

- Tong, K. I., Kobayashi, A., Katsuoka, F. and Yamamoto, M. (2006) 'Two-site substrate recognition model for the Keap1-Nrf2 system: a hinge and latch mechanism', *Biol Chem*, 387(10-11), 1311-20.
- Trachootham, D., Lu, W., Ogasawara, M. A., Nilsa, R. D. and Huang, P. (2008) 'Redox regulation of cell survival', *Antioxid Redox Signal*, 10(8), 1343-74.
- Um, H. C., Jang, J. H., Kim, D. H., Lee, C. and Surh, Y. J. (2011) 'Nitric oxide activates Nrf2 through S-nitrosylation of Keap1 in PC12 cells', *Nitric Oxide*, 25(2), 161-8.
- Ungvari, Z., Bailey-Downs, L., Sosnowska, D., Gautam, T., Koncz, P., Losonczy, G., Ballabh, P., de Cabo, R., Sonntag, W. E. and Csiszar, A. (2011) 'Vascular oxidative stress in aging: a homeostatic failure due to dysregulation of NRF2-mediated antioxidant response', *Am J Physiol Heart Circ Physiol*, 301(2), H363-72.
- Unwin, R. D., Griffiths, J. R., Leverentz, M. K., Grallert, A., Hagan, I. M. and Whetton, A. D. (2005) 'Multiple reaction monitoring to identify sites of protein phosphorylation with high sensitivity', *Mol Cell Proteomics*, 4(8), 1134-44.
- Uttara, B., Singh, A. V., Zamboni, P. and Mahajan, R. T. (2009) 'Oxidative stress and neurodegenerative diseases: a review of upstream and downstream antioxidant therapeutic options', *Curr Neuropharmacol*, 7(1), 65-74.
- Vareli, K., Frangou-Lazaridis, M., van der Kraan, I., Tsolas, O. and van Driel, R. (2000) 'Nuclear distribution of prothymosin alpha and parathymosin: evidence that prothymosin alpha is associated with RNA synthesis processing and parathymosin with early DNA replication', *Exp Cell Res*, 257(1), 152-61.
- Velmurugan, K., Alam, J., McCord, J. M. and Pugazhenthii, S. (2009) 'Synergistic induction of heme oxygenase-1 by the components of the antioxidant supplement Protandim', *Free Radic Biol Med*, 46(3), 430-40.
- Venugopal, R. and Jaiswal, A. K. (1996) 'Nrf1 and Nrf2 positively and c-Fos and Fra1 negatively regulate the human antioxidant response element-mediated expression of NAD(P)H:quinone oxidoreductase1 gene', *Proc Natl Acad Sci U S A*, 93(25), 14960-5.
- Wakabayashi, N., Dinkova-Kostova, A. T., Holtzclaw, W. D., Kang, M. I., Kobayashi, A., Yamamoto, M., Kensler, T. W. and Talalay, P. (2004) 'Protection against electrophile and oxidant stress by induction of the phase 2 response: fate of cysteines of the Keap1 sensor modified by inducers', *Proc Natl Acad Sci U S A*, 101(7), 2040-5.
- Wakabayashi, N., Itoh, K., Wakabayashi, J., Motohashi, H., Noda, S., Takahashi, S., Imakado, S., Kotsuji, T., Otsuka, F., Roop, D. R., Harada, T., Engel, J. D. and Yamamoto, M. (2003) 'Keap1-null mutation leads to postnatal lethality due to constitutive Nrf2 activation', *Nat Genet*, 35(3), 238-45.
- Walsh, J., Jenkins, R. E., Wong, M., Olayanju, A., Powell, H., Copple, I., O'Neill, P. M., Goldring, C. E., Kitteringham, N. R. and Park, B. K. (2014) 'Identification and quantification of the basal and inducible Nrf2-dependent proteomes in mouse liver: biochemical, pharmacological and toxicological implications', *J Proteomics*, 108, 171-87.

- Wang, K. (2014) 'Molecular mechanisms of hepatic apoptosis', *Cell Death Dis*, 5, e996.
- Wang, W. and Jaiswal, A. K. (2006) 'Nuclear factor Nrf2 and antioxidant response element regulate NRH:quinone oxidoreductase 2 (NQO2) gene expression and antioxidant induction', *Free Radic Biol Med*, 40(7), 1119-30.
- Wang, X. J., Hayes, J. D., Henderson, C. J. and Wolf, C. R. (2007) 'Identification of retinoic acid as an inhibitor of transcription factor Nrf2 through activation of retinoic acid receptor alpha', *Proc Natl Acad Sci U S A*, 104(49), 19589-94.
- Wang, X. J., Sun, Z., Villeneuve, N. F., Zhang, S., Zhao, F., Li, Y., Chen, W., Yi, X., Zheng, W., Wondrak, G. T., Wong, P. K. and Zhang, D. D. (2008) 'Nrf2 enhances resistance of cancer cells to chemotherapeutic drugs, the dark side of Nrf2', *Carcinogenesis*, 29(6), 1235-43.
- Wang, X. J. and Zhang, D. D. (2009) 'Ectodermal-neural cortex 1 down-regulates Nrf2 at the translational level', *PLoS One*, 4(5), e5492.
- Wang, Y. Y., Zhe, H. and Zhao, R. (2014) 'Preclinical evidences toward the use of triterpenoid CDDO-Me for solid cancer prevention and treatment', *Mol Cancer*, 13, 30.
- Watai, Y., Kobayashi, A., Nagase, H., Mizukami, M., McEvoy, J., Singer, J. D., Itoh, K. and Yamamoto, M. (2007) 'Subcellular localization and cytoplasmic complex status of endogenous Keap1', *Genes Cells*, 12(10), 1163-78.
- Wilkening, S., Stahl, F. and Bader, A. (2003) 'Comparison of primary human hepatocytes and hepatoma cell line Hepg2 with regard to their biotransformation properties', *Drug Metab Dispos*, 31(8), 1035-42.
- Williamson, T. P., Johnson, D. A. and Johnson, J. A. (2012) 'Activation of the Nrf2-ARE pathway by siRNA knockdown of Keap1 reduces oxidative stress and provides partial protection from MPTP-mediated neurotoxicity', *Neurotoxicology*, 33(3), 272-9.
- Wong, T. F., Yoshinaga, K., Monma, Y., Ito, K., Niikura, H., Nagase, S., Yamamoto, M. and Yaegashi, N. (2011) 'Association of keap1 and nrf2 genetic mutations and polymorphisms with endometrioid endometrial adenocarcinoma survival', *Int J Gynecol Cancer*, 21(8), 1428-35.
- Woo, H. A., Kang, S. W., Kim, H. K., Yang, K. S., Chae, H. Z. and Rhee, S. G. (2003) 'Reversible oxidation of the active site cysteine of peroxiredoxins to cysteine sulfinic acid. Immunoblot detection with antibodies specific for the hyperoxidized cysteine-containing sequence', *J Biol Chem*, 278(48), 47361-4.
- Wood, Z. A., Schroder, E., Robin Harris, J. and Poole, L. B. (2003) 'Structure, mechanism and regulation of peroxiredoxins', *Trends Biochem Sci*, 28(1), 32-40.
- Xu, C., Huang, M. T., Shen, G., Yuan, X., Lin, W., Khor, T. O., Conney, A. H. and Kong, A. N. (2006) 'Inhibition of 7,12-dimethylbenz(a)anthracene-induced skin tumorigenesis in

- C57BL/6 mice by sulforaphane is mediated by nuclear factor E2-related factor 2', *Cancer Res*, 66(16), 8293-6.
- Yamamoto, N., Sawada, H., Izumi, Y., Kume, T., Katsuki, H., Shimohama, S. and Akaike, A. (2007) 'Proteasome inhibition induces glutathione synthesis and protects cells from oxidative stress: relevance to Parkinson disease', *J Biol Chem*, 282(7), 4364-72.
- Yamamoto, T., Suzuki, T., Kobayashi, A., Wakabayashi, J., Maher, J., Motohashi, H. and Yamamoto, M. (2008) 'Physiological significance of reactive cysteine residues of Keap1 in determining Nrf2 activity', *Mol Cell Biol*, 28(8), 2758-70.
- Yang, M., Yao, Y., Eades, G., Zhang, Y. and Zhou, Q. (2011) 'MiR-28 regulates Nrf2 expression through a Keap1-independent mechanism', *Breast Cancer Res Treat*, 129(3), 983-91.
- Yates, M. S., Tauchi, M., Katsuoka, F., Flanders, K. C., Liby, K. T., Honda, T., Gribble, G. W., Johnson, D. A., Johnson, J. A., Burton, N. C., Guilarte, T. R., Yamamoto, M., Sporn, M. B. and Kensler, T. W. (2007) 'Pharmacodynamic characterization of chemopreventive triterpenoids as exceptionally potent inducers of Nrf2-regulated genes', *Mol Cancer Ther*, 6(1), 154-62.
- Yates, M. S., Tran, Q. T., Dolan, P. M., Osburn, W. O., Shin, S., McCulloch, C. C., Silkworth, J. B., Taguchi, K., Yamamoto, M., Williams, C. R., Liby, K. T., Sporn, M. B., Sutter, T. R. and Kensler, T. W. (2009) 'Genetic versus chemoprotective activation of Nrf2 signaling: overlapping yet distinct gene expression profiles between Keap1 knockout and triterpenoid-treated mice', *Carcinogenesis*, 30(6), 1024-31.
- Yoh, K., Itoh, K., Enomoto, A., Hirayama, A., Yamaguchi, N., Kobayashi, M., Morito, N., Koyama, A., Yamamoto, M. and Takahashi, S. (2001) 'Nrf2-deficient female mice develop lupus-like autoimmune nephritis', *Kidney Int*, 60(4), 1343-53.
- Yore, M. M., Kettenbach, A. N., Sporn, M. B., Gerber, S. A. and Liby, K. T. (2011) 'Proteomic analysis shows synthetic oleanane triterpenoid binds to mTOR', *PLoS One*, 6(7), e22862.
- Yost, H. J. and Lindquist, S. (1986) 'RNA splicing is interrupted by heat shock and is rescued by heat shock protein synthesis', *Cell*, 45(2), 185-93.
- Yost, H. J. and Lindquist, S. (1988) 'Translation of unspliced transcripts after heat shock', *Science*, 242(4885), 1544-8.
- Yu, B. P. (1994) 'Cellular defenses against damage from reactive oxygen species', *Physiol Rev*, 74(1), 139-62.
- Yuan, X., Xu, C., Pan, Z., Keum, Y. S., Kim, J. H., Shen, G., Yu, S., Oo, K. T., Ma, J. and Kong, A. N. (2006) 'Butylated hydroxyanisole regulates ARE-mediated gene expression via Nrf2 coupled with ERK and JNK signaling pathway in HepG2 cells', *Mol Carcinog*, 45(11), 841-50.
- Zhang, D. D. and Hannink, M. (2003) 'Distinct cysteine residues in Keap1 are required for Keap1-dependent ubiquitination of Nrf2 and for stabilization of Nrf2 by chemopreventive agents and oxidative stress', *Mol Cell Biol*, 23(22), 8137-51.

- Zhang, D. D., Lo, S. C., Cross, J. V., Templeton, D. J. and Hannink, M. (2004) 'Keap1 is a redox-regulated substrate adaptor protein for a Cul3-dependent ubiquitin ligase complex', *Mol Cell Biol*, 24(24), 10941-53.
- Zhang, H., Liu, H., Dickinson, D. A., Liu, R. M., Postlethwait, E. M., Laperche, Y. and Forman, H. J. (2006) 'gamma-Glutamyl transpeptidase is induced by 4-hydroxynonenal via EpRE/Nrf2 signaling in rat epithelial type II cells', *Free Radic Biol Med*, 40(8), 1281-92.
- Zhang, J., Hosoya, T., Maruyama, A., Nishikawa, K., Maher, J. M., Ohta, T., Motohashi, H., Fukamizu, A., Shibahara, S., Itoh, K. and Yamamoto, M. (2007) 'Nrf2 Neh5 domain is differentially utilized in the transactivation of cytoprotective genes', *Biochem J*, 404(3), 459-66.
- Zhang, X., Zhao, X. and Ma, Z. (2010) 'PYDDT, a novel phase 2 enzymes inducer, activates Keap1-Nrf2 pathway via depleting the cellular level of glutathione', *Toxicol Lett*, 199(1), 93-101.
- Zheng, Y., Morris, A., Sunkara, M., Layne, J., Toborek, M. and Hennig, B. (2012) 'Epigallocatechin-gallate stimulates NF-E2-related factor and heme oxygenase-1 via caveolin-1 displacement', *J Nutr Biochem*, 23(2), 163-8.
- Zhou, M., Sandercock, A. M., Fraser, C. S., Ridlova, G., Stephens, E., Schenauer, M. R., Yokoi-Fong, T., Barsky, D., Leary, J. A., Hershey, J. W., Doudna, J. A. and Robinson, C. V. (2008) 'Mass spectrometry reveals modularity and a complete subunit interaction map of the eukaryotic translation factor eIF3', *Proc Natl Acad Sci U S A*, 105(47), 18139-44.
- Zhuang, C., Miao, Z., Sheng, C. and Zhang, W. (2014) 'Updated Research and Applications of Small Molecule Inhibitors of Keap1-Nrf2 Protein-Protein Interaction: a Review', *Curr Med Chem*.
- Zhuang, M., Guan, S., Wang, H., Burlingame, A. L. and Wells, J. A. (2013) 'Substrates of IAP ubiquitin ligases identified with a designed orthogonal E3 ligase, the NEDDylator', *Mol Cell*, 49(2), 273-82.
- Zipper, L. M. and Mulcahy, R. T. (2002) 'The Keap1 BTB/POZ dimerization function is required to sequester Nrf2 in cytoplasm', *J Biol Chem*, 277(39), 36544-52.